DURBAN UNIVERSITY OF TECHNOLOGY
INYUVESI YASETHEKWINI YEZOBUCHWEPHESHE

Metabolomic profiling, computational and experimental validation of sunflower seeds as therapeutics against type-2 diabetes mellitus

Submitted in fulfilment of the requirements for the award of degree of Master of Applied Science in Biotechnology

Department of Biotechnology and Food Science

Faculty of Applied Sciences

Durban University of Technology

Durban, South Africa

Athika Rampadarath (21817581)

Supervisor: Prof. Saheed Sabiu

Co-supervisor: Prof. Nokwanda Makunga

November 2024

Declaration

I hereby declare that this dissertation is my own work and is being submitted for the fulfillment of Master of Appiled Science in Biotechnology under the supervision of Prof. Saheed Sabiu at the Department of Biotechnology and Food Science, Faculty of Applied Sciences, Durban University of Technology. This dissertation was not previously submitted to any other academic insitutions in any form for any degree. To the best of our knowledge, no other dissertation of similar nature exists. The usage of other work or knowledege was duly refereneced where applicable.

	27 November 2024
Student	**Date**
	27.11.2024
Supervisor	**Date**
	29 November 2024
Co-supervisor	**Date**

Acknowledgements

I would like to wholeheartedly express my gratitude to my esteemed supervisor, Prof. Saheed Sabiu. Thank you for laying the foundation, allowing me to conduct research of high quality and standard. At every step of this academic journey, your support, knowledge and expertise have proven to be a strong pillar for this project and me. Thank you for sharing your knowledge, your kindness, your criticism and words of encouragement.

I would like to thank and acknowledge Prof. Nokwanda Makunga of the Department of Botany and Zoology, Stellenbosch University, for sharing and educating me in the field of "Metabolomics". The knowledge you have shared is extremely valuable to me.

The assistance of Dr. Terisha Ghazi and Prof. Anil Chuturgoon of the Department of Medical Biochemistry, University of KwaZulu-Natal in providing an enabling environment and guidance to meet my cell culture objectives, is sincerely acknowledged.

I want to also acknowledge the National Research Foundation (NRF) for providing me with funding, allowing me to embark on this journey.

The Centre for High Performance Computing (CHPC), Cape Town, deserves a special acknowledgement for housing the Programme HEAL1361 under the leadership of Prof. Saheed Sabiu, in providing a platform for my computational analyses.

I would like to sincerely thank Mr. Jamiu for sharing his knowledge with me and constantly providing me with assistance every step of the way. Your support has been crucial to me and most especially in my development as a writer.

To my energetic supportive Computational and Systems Biology Research Group at the Department of Biotechnology and Food Science, Durban University of Technology, thank you guys for creating such a supportive and motivating environment, making this journey quite a memorable one. Every single person in the group has shared nothing but positivity with me. I could not ask for a better research group.

I would also like to thank my family for their support during my MSc journey but most importantly my late mother and grandmother, Zeenat Rampadarath and Shanti Rampadarath. Every step towards accomplishing my dreams such as this is done in both of your honour.

My biggest support system, my amazing partner Kaelyn Thavarin, thank you for keeping me sane and believing in me more than I believe in myself. Your undying support and love are my biggest strength, I am forever grateful to you.

Research Outputs

Primary publications

Article(s)

- **Rampadarath, A.**, Aribisala, J. O., Makunga, N. P., Mazibuko-Mbeje, S., and Sabiu, S. (2023). Molecular bioprospection of *Helianthus annuus* L.(sunflower) cypsela for antidiabetic therapeutics through network pharmacology, density functional theory and molecular dynamics simulation. *South African Journal of Botany*, 162, 72-95.
- **Rampadarath, A.**, Balogun, F. O., and Sabiu, S. (2023). Insights into the mechanism of action of *Helianthus annuus* (sunflower) seed essential oil in the management of type-2 diabetes mellitus using network pharmacology and molecular docking approaches. *Endocrines*, *4*(2), 327-349.

Secondary publications

- Balogun, F. O., Singh, K., **Rampadarath, A.**, Akoonjee, A., Naidoo, K., and Sabiu, S. (2023). Cheminformatics identification of modulators of key carbohydrate-metabolizing enzymes from *C. cujete* for type-2 diabetes mellitus intervention. *Journal of Diabetes and Metabolic Disorders*, *22*(2), 1299-1317.
- Akoonjee, A., **Rampadarath, A.**, Aruwa, C. E., Ajiboye, T. A., Ajao, A. A. N., and Sabiu, S. (2022). Network pharmacology-and molecular dynamics simulation-based bioprospection of *Aspalathus linearis* for type-2 diabetes care. *Metabolites*, 12(11), 1013.

Conference presentations

- **Rampadarath A** and Sabiu S. Exploring *Helianthus annuus* L. (sunflower) seeds as potential antidiabetics through network pharmacology, molecular dynamic simulations and *in vitro* validation in HepG2 cells. Computational and Systems Biology Conference 2024. Coastlands Hotel, Musgrave, Durban, South Africa. 24 – 26 June 2024
- **Rampadarath A** and Sabiu S. Snack to therapeutics: Sunflower seeds as antidiabetics. Three Minutes Flash Fact Competition 2023. Durban University of Technology, South Africa. 12 October 2023.
- **Rampadarath A**, Sabiu S and Makunga N.P (2022). Network Pharmacology analysis of *Helianthus annuus* seeds as therapeutics against Type Two Diabetes mellitus. 55th Annual Conference of the South African Society for Basic and Clinical Pharmacology. South Africa, 26 October 2022.
- **Rampadarath A,** Sabiu S and Makunga N.P (2022). Metabolomic profiling and network pharmacology analysis of sunflower seeds as therapeutics in type 2 diabetes

care. Durban University of Technology, Faculty of Applied Sciences Annual Research Day. Coastlands, Musgrave, South Africa. 15 November 2022.

Awards and recognitions

- Master's student of the year (2024), 6th Annual State of the Faculty Address (SOFA6) Awards Ceremony.
- People's Choice winner at the Computational and Systems Biology Annual Conference 2024 held at Coastlands Hotel, Musgrave, Durban, South Africa.
- Third place at the Computational and Systems Biology Annual Conference 2024, held at Coastlands Hotel, Musgrave, Durban, South Africa.
- Top master's student (Gold category) at Durban University of Technology's Annual Research and Innovation Awards 2023.
- People's Choice winner (Master's) at the 2023 Departmental Three Minutes Flash Fact competition.
- Third place (Master's) at the 2023 Departmental Three Minutes Flash Fact competition.

List of abbreviations

- 3D – Three dimensional
- ΔG – Gibbs free energy
- AAMY – α-amylase
- AGLU – α-glucosidase
- AR – Aldose reductase
- CADD – Computer aided drug discovery
- CGA – Chlorogenic acid
- DDD – Drug discovery and development
- DPP4 – Dipeptidyl-peptidase 4
- GIT – Gastrointestinal tract
- GLP-1 – Glucagon-like peptide 1
- IR – Insulin resistance
- IRS – Insulin receptor substrate
- HTVS – High-throughput virtual screening
- KEGG -Kyoto Encyclopaedia of Genes and Genomes
- MDS – Molecular dynamic simulations
- MMP1 – Matrix metalloproteinase-1
- MTT – -(4, 5-dimethyl 2 thiazolyl)-2,5-diphenyl 2 tetrazolium bromide
- OD – Optical density
- PPAR – Peroxisome proliferator-activated receptor
- PTP1B – Protein tyrosine phosphatase 1B
- PYR – 4α,6S,7α)-6α-[6-O-(4-Hydroxybenzoyl)-β-D-glucopyranosyloxy]-7β-methyloctahydrocyclopenta[c]pyran-1-one)
- SAC A – Sacranoside A
- SDH – Sorbitol dehydrogenase
- SON I – Sonchuside I
- T2DM – Type 2 diabetes mellitus
- TIC – Total ion chromatogram
- VIP – Variable Importance in Projection (VIP)
- WHO – World Health Organization

General abstract

Type 2 diabetes mellitus (T2DM) is a chronic metabolic disorder characterized by impaired glucose metabolism due to insufficient insulin secretion or insulin resistance. This global health crisis is projected to affect an estimated 7079 individuals per 100,000 by 2030. While medications like metformin are effective, accessibility and affordability are issues consistent with low-income populations alongside potential side effects like hypoglycaemia, nausea and gastrointestinal issues that have limited their use in clinical practice. More importantly, uncontrolled T2DM can lead to serious complications like retinopathy, nephropathy, neuropathy, and delayed wound healing. Therefore, this prompts the search for alternative management options that are safer, easily accessible, affordable and with minimal side effects.

Plants and their products are becoming increasingly important due to their relative ease of accessibility, affordability and potential health benefits. Sunflower seed, a popular dietary snack, has rich nutritional profile and has found significant health benefits as an anti-inflammatory, antioxidant, anticancer, antimicrobial, and antidiabetic agent. While the antidiabetic potential of sunflower seeds has been explored, there remains a lack of understanding on its mechanism of action. This study addressed this knowledge gap by establishing the comprehensive metabolite profiles and investigating the antidiabetic efficacy of sunflower seed extracts through a two-pronged approach: targeted enzyme inhibition and network pharmacology analyses complemented with experimental validation *in vitro*.

Metabolomic profiling of six cultivars of sunflower seeds commonly consumed in South Africa, namely, AGSUN 8251, 5270, 5101 CLP, 5103 CLP, 5106 CLP and 5108 CLP was performed using Liquid chromatography – mass spectrometry (LC-MS) and Gas chromatography – mass spectrometry (GC-MS) techniques. A total of 94 metabolites were identified, with LC-MS analysis revealing 44 phenolic compounds across the six cultivars with a minor variance of 39.7%, while GC-MS analysis revealed the presence of volatile compounds such as organic acids, alkanes, alcohols, terpenes, heterocyclic compounds and hydrocarbons in all the cultivars in similar abundance. Noteworthily, 84 of the 94 metabolites profiled passed Lipinski's rule of five and were selected for further analysis.

For the enzyme inhibition study, molecular docking analysis was initially used to screen the profiled metabolites against the key enzymes [α-amylase (AAMY), α-glucosidase (AGLU), aldose reductase (AR), sorbitol dehydrogenase (SDH), dipeptidyl peptidase 4 (DPP-4) and

protein tyrosine phosphatase 1B (PTP1B)] implicated in T2DM pathogenesis and its secondary complications. The top-ranked metabolites against each enzyme were further subjected to molecular dynamics (MD) simulation to identify putative leads with the strongest binding affinity, and unperturbed structural integrity through evaluation of their stability, compactness and intermolecular interactions. This aspect of the study identified sonchuside I (SON I) - AAMY (–47.26 kcal/mol), sacranoside A (SAC A) - α-glucosidase (–40.10 kcal/mol), pelatoside A (PLT) - AR (–58.84 kcal/mol), sacranoside A (SAC A) - SDH (–48.03 kcal/mol), 4α,6S,7α)-6α-[6-O-(4-Hydroxybenzoyl)-β-D-glucopyranosyloxy]-7β-methyloctahydrocyclopenta[c]pyran-1-one) (PYR) -DPP-4 (–37.93 kcal/mol) and chlorogenic acid (CGA)-PTP1B (–24.32 kcal/mol) as potential lead inhibitors of the respective enzyme relative to their respective reference standards. This was further supported by their improved thermodynamic properties and favourable post-dynamic simulation parameters such as improved stability and compactness of their resulting complexes. These observations are suggestive of multiple mechanisms by which sunflower seed may exert its antidiabetic effects such as anti-hyperglycaemia (α-amylase and α-glucosidase), prevention and management of diabetic complications (AR and SDH), increasing insulin signalling (DPP-4) and sensitivity (PTP1B) by the respective putative leads.

For network pharmacology analysis, the filtered sunflower seed metabolites were used to create a gene-compound library that was subsequently used to identify genes commonly associated with both the metabolites and T2DM. Thereafter, Kyoto Encyclopaedia of Genes and Genomes (KEGG) pathway enrichment analysis was performed to identify the most significantly enriched pathways with key target genes for molecular docking and MD simulations to identify lead metabolites. Finally, the antidiabetic activity of sunflower seed extracts and the findings from the network pharmacology analysis were validated using insulin-resistant HepG2 cells where glucose consumption assay and gene expression analysis were performed. The network pharmacology analysis revealed a total of 87 genes common to sunflower seeds metabolites and T2DM, whereas KEGG enrichment analysis highlighted 35 signalling pathways potentially influenced by the metabolites. Of these, the Peroxisome proliferator-activated receptor (PPAR) signalling pathway and its hub receptors, Matrix metalloproteinase-1(*MMPI*) and peroxisome proliferator-activated receptor alpha (*PPAR*) were selected as the most significant. These receptors interacted mostly with the identified metabolites, with CGA (–43.74 kcal/mol), GPA (–41.62 kcal/mol), and CFG (–45.36 kcal/mol) having lower binding free energy than both reference standards, rosiglitazone (ROS) and metformin (MET) against

MMP1 after 100 000 ps MD simulation. In contrast, ROS (–46.98 kcal/mol) had better affinity against *PPARA* compared to the top-hits derived from sunflower seeds. However, against both genes, the top-hits had significant thermodynamic stability, flexibility, and compactness, which are attributable to their bond interactions and molecular orbital properties. These findings are suggestive of the essential role of the top-hits in the antidiabetic potential of sunflower seeds through activation of the PPAR signalling pathway and most especially *MMP1*. In this regard, the modulation of *MMP1* and *PPARA* genes by the identified metabolites of sunflower seeds may enhance insulin sensitivity and glucose homeostasis in the management of T2DM. Finally, the *in vitro* validation using insulin-resistant HepG2 cells revealed cultivar-specific effects on cell viability, with each cultivar having a unique optimal concentration. Overall, all cultivars demonstrated the ability to stimulate glucose consumption, suggesting their potential antihyperglycemic activity. Among the cultivars, AGSUN 5103 CLP (14.4 mmol/L), 8251 (14.6 mmol/L), and 5101 CLP (13.7 mmol/L) exhibited the most pronounced glucose lowering action compared to the untreated cells (23.3 mmol/L) after 24 h, highlighting their promising antidiabetic effects. These three cultivars also modulate the PPAR signalling pathway, as evidenced by the upregulation of *MMP1* and *PPARA* expression. Specifically, AGSUN 5101 CLP emerged as a particularly promising candidate based on its superior glucose lowering potential and higher fold increase expression of *MMP1* (1.88) and *PPARA* (4.59) compared to the effect observed with the untreated cells (1.00).

In conclusion, this study provides compelling evidence for the antidiabetic potential of sunflower seeds. The observed effects on enzyme inhibition, activation of the PPAR signalling pathway, and stimulation of glucose uptake in HepG2 cells suggest a multifaceted approach by the seeds in regulating blood sugar levels. The identification of cultivar-specific effects and promising lead compounds warrants further investigation to explore the therapeutic potential of sunflower seeds in managing T2DM.

Keywords: Metabolomic profiling; Molecular dynamics simulation; Network pharmacology; Sunflower seeds; Type-2 diabetes mellitus

Table of Contents

Chapter One

1.1 Introduction

Diabetes mellitus (DM) is a complex metabolic disorder characterized by hyperglycaemia due to deficiency in insulin secretion and/or insulin activity (Kharroubi and Darwish, 2015). Diabetes mellitus is primarily classified into type 1 and type 2 (Tan *et al*., 2019). While type 1 DM (T1DM) is a result of autoimmune destruction of β--cells in the pancreas, which contributes to inadequate insulin secretion, and subsequently leading to hyperglycaemia (Paschou *et al.,* 2018), type 2 DM (T2DM) is characterized by insulin resistance or insufficient insulin that culminates in decreased rate of glucose transportation into adipose tissue, skeletal muscle cells and the liver, and ultimately leading to hyperglycaemic conditions (Berbudi *et al*., 2020). Besides hyperglycaemia, the onset of the T2DM is most often accompanied by complications such as cardiovascular diseases, neuropathy, nephropathy, hypertension, obesity, cataracts, and retinopathy which affect the quality of life of the individual and in some drastic cases the complications may lead to death (Ekoru *et al*., 2019). Other factors such as genetics, unhealthy diet, sedentary lifestyle and obesity have also been implicated in the pathogenesis of T2DM (DeFronzo *et al.,* 2015).

In 2021, the International Diabetes Federation (IDF) reported a global 537 million active diabetic cases, and this number is expected to increase to 643 million by 2030, if no practical solution is offered (IDF, 2021). In addition, T2DM is responsible for approximately 6.7 million patient deaths. Within Africa, there are 24 million T2DM cases, with more than 54% being undiagnosed (World Health Organization, 2023). However, a large proportion of that number is attributed to the sub-Saharan African region, retaining the largest number of diabetic cases with an approximate 14.2 million adults aged 20 – 79 diagnosed with T2DM. This number is predicted to increase to 34.2 million by 2040 (Zwane *et al*., 2023). Moreover in South Africa, the increasing prevalence of T2DM is emphasized by the 12.7% increase in 2019 from 4.5% in 2010. South Africa has the second largest record of T2DM cases in the sub-Saharan Africa (Sifunda *et al*., 2023). This burden of T2DM in South Africa is reflected in incurring 12% of the national health budget to treat the prevalent cases. This economical strain of T2DM in South Africa was approximated to be around R2.8 billion (both diagnosed and undiagnosed cases) in 2018, with a foreseeable increase to R35.1 billion by 2030 (Erzse *et al*., 2019). Fifty-one percent of this budget was devoted to the management of T2DM, while the remaining 49% was spent the secondary complications of T2DM like diabetic nephropathy, neuropathy, retinopathy and cardiovascular concerns. (Erzse *et al*., 2019). Oral antidiabetic drugs such as sulfonylureas, biguanides, thiazolidinediones, alpha-glucosidase inhibitors and dipeptidyl peptidase IV

inhibitors are currently being prescribed to patients. However, long-term application of these drugs is usually accompanied with adverse effects including nausea, skin rashes/irritation, liver damage, chronic heart failure, genital and urinary infections and pharyngitis (Kerru *et al*., 2018). The attendant burden of these side effects highlights the urgent need for a safer, more affordable therapeutic agent with minimal side effects.

Medicinal plants have long served a key role in traditional medicine due to their therapeutic properties (Süntar, 2020). Their significance as therapeutics has a core foundation as currently at least one-quarter of modern commercially available medicines were derived from medicinal plants (Awuchi, 2019). Therefore, the use of medicinal plants as therapeutics is encouraged due to their accessibility, affordability and relative safety profiles. Interestingly, many of these medicinal plants also form part of the human staple diets, with *Helianthus annuus* (sunflower) being one of such plants. Sunflower is an economically important crop and remains the fourth most demanded oilseed crop worldwide and the third most important crop in South Africa (Puttha *et al.,* 2023). In South Africa, the demand for sunflower is due to its role in the food industry for oil production, sunflower seed consumption and livestock feed (Adeleke and Babalola, 2020). In addition, sunflower production is significant to the economy of South Africa as it ranks first on the African continent and tenth globally for sunflower oil production (Nungula *et al.,* 2023). Presently, AGSUN (5101 CLP, 5103 CLP, 5106 CLP, 5108 CLP, 5270 and 8251), AGUARA6, LG (5678 CLP and 5710), P65L (L02, L14, P54, P65), PAN (7100, 7102 CLP, 7160 CLP, 7170 and 7180 CLP) and SY3970 CLP are the major cultivars of sunflower in South Africa. Besides their oil-producing significance, the sunflower seeds also have health benefits due to their rich phytochemical and nutritional constituents (Adeleke and Babalola, 2020; Anjum *et al.,* 2012).

To comprehensively ascertain the metabolites of medicinal plants, analysis such as metabolomics, a high-throughput approach employing liquid chromatography -mass spectrometry (LC-MS), gas chromatography- mass spectrometry (GC-MS) and capillary electrophoresis–mass spectrometry (CE–MS) etc, is normally used (Tuyiringire *et al*., 2018). Also, the application of metabolomics in the drug discovery process aids in measuring response to treatments, classifying phenotypes within a large group of test samples, as well as the discovery of biomarkers (Martinelli, 2023). Following identification/characterization of the metabolites, approaches such as the Computer-Aided-Drug-Discovery (CADD) which include network pharmacology, molecular docking and molecular dynamics (MD) simulation are now currently being employed in fast-tracking the identification, discovery and development of

novel therapeutics (Singh *et al*., 2019). Network pharmacology integrates pharmacology and information networks often known as poly-pharmacology. It is applied to address the low efficacy of highly selective single target drugs, by directly screening large therapeutic data to provide a precise output such as specific disease targets and metabolic pathways (Zhou *et al*., 2020). Molecular docking on the other hand, predicts the interaction between a protein and small molecule or between two proteins, based on the intermolecular forces between them. This provides information on the binding orientation of the small molecule to protein which in turn, provides vital information on the biological activity of the protein (Sethi *et al*., 2019). Unlike docking, MD simulation allows for the study of protein-ligand interactions over a period, on an atomic level. It provides conformational and structural information on the protein-ligand (metabolite) system which subsequently gives an indication of the effect the ligand may have on the protein (enzyme) as a drug target (Wu *et al*., 2022). Interestingly, previous studies (Guo *et al*., 2023; Umar *et al*., 2023; Adnan *et al*., 2022; Wu and Zhang, 2022 and He *et al*., 2019), have adopted the integrated strategies of metabolomics, network pharmacology, molecular docking and MD simulations in profiling and identifying novel antidiabetic therapeutics. Furthermore, to complement and further substantiate the findings from the integrated computational analyses, appropriate cell line studies alongside other *in vitro* models are normally employed. The HepG2 cells are commonly used in pharmaco-toxicological and drug metabolism studies and remain a popular choice to investigate hyperglycaemia *in vitro* as an alternative to primary human hepatocytes (Yarahmadi *et al*., 2018). The HepG2 model play a vital role in T2DM research due to its ability to mimic the human liver, the primary organ for glucose metabolism and regulation. Furthermore, as insulin resistance, a hallmark of T2DM, is particularly prominent in the liver, HepG2 cells provide a valuable platform to express and study the pathogenesis of T2DM in drug discovery (Yang *et al*., 2019). The proficiency of HepG2 cells in T2DM studies employing plant and plant-derived products as therapeutics has been extensively demonstrated (Azimian *et al*., 2023; Azam et al., 2022; Kheirollahzadeh et al., 2022; Bourebaba *et al*., 2021; Wangkiri *et al*., 2021; Odeyemi *et al*., 2019), thus affirming its position as an appropriate cell line for diabetic studies. Together, the integrated approaches of metabolomics, network pharmacology, molecular docking and MD simulations coupled with experimental validation in an appropriate *in vitro* model appears to be a viable method being currently adopted in the drug discovery process.

Although, previous studies (Saeed *et al*., 2022; Richmond *et al*., 2013 and Shivani and Sunil, 2013) have lent scientific credence to the antidiabetic potential of *H. annuus* (sunflower) seeds,

there is a lack of information on their exact mechanism of action to date. Furthermore, there is also a dearth of information on the metabolites and specific antidiabetic potential of the different cultivars of sunflower seeds commonly consumed in South Africa. It is on this background that, the current study adopted an integrated systems approach in profiling the metabolites of six South African cultivars of sunflower seeds and evaluate their possible molecular mechanism of antidiabetic action using advanced computational approaches and experimental validation.

1.2 Research problem

Type-2 diabetes mellitus (T2DM) is a worldwide epidemic with its prevalence growing particularly due to the aging population and poor-lifestyle choices. While existing drugs manage T2DM, their side effects limit patients' well-being. *H. annuus* (sunflower) seeds have been reported to possess antidiabetic properties due to their phytochemical composition. Despite the promising antidiabetic properties of sunflower seeds, the underlying mechanisms remain unknown, hindering their potential integration into therapeutic strategies for T2DM.

1.3 Aim

This study aimed to elucidate the mechanisms linked to the antidiabetic potential of *Helianthus annuus* (sunflower) seed cultivars using integrated computational and experimental approaches.

1.4 Objectives

The specific objectives were:

i. To determine the metabolite profiles of six cultivars (AGSUN 5270, AGSUN 8251, AGSUN 5108 CLP, AGSUN 5106 CLP, AGSUN 5103 CLP and AGSUN 5101 CLP) of *H. annuus* seeds using chromatographic techniques (LC-MS and GC-MS) and principal component analysis.

ii. To establish the structural mechanism of interaction between the metabolites of *H. annuus* seeds and the key enzymes (alpha-amylase (AAMY), alpha-glucosidase (AGLU), protein tyrosine phosphatase 1B (PTP1B), dipeptidyl peptidase-4 (DPP-4), aldose reductase (AR) and sorbitol dehydrogenase (SDH)) implicated in the pathogenesis of T2DM and its secondary complications through molecular docking and molecular dynamics simulation study.

iii. To identify the metabolic pathways implicated in T2DM and their association with *H. annuus* seeds metabolites using network pharmacology approach.

iv. To validate the *in vitro* antidiabetic effect of *H. annuus* cultivars in insulin-resistant HepG2 cells.

1.5 Structure of dissertation

The dissertation is organized into six distinct chapters as follows.

- Chapter one: This chapter introduces the study by providing overall background to the identified research problem, aim and objectives, and a concise structure of the dissertation.
- Chapter two: The literature review is presented in this chapter. This presents an intensive review of literature pertaining to sunflower seeds and their nutritional, phytochemical and antidiabetic profiles. Overviews on metabolomic profiling, network pharmacology, molecular docking and dynamic simulation and *in vitro* works in HepG2 cells, as the selected methodologies adopted in this study, are also presented in this chapter.
- Chapter three: Objectives one and two of this study are presented in this chapter. The chapter presents metabolomic profiling of sunflower seeds and molecular dynamics simulation of their lead metabolites against the key enzymes implicated in T2DM pathogenesis.
- Chapter four: Objective three of the study is featured in this chapter. The chapter contains detailed information on the molecular bioprospection of *Helianthus annuus* L. (sunflower) seeds for antidiabetic therapeutics through network pharmacology, MD simulation, and density functional theory.
- Chapter five: This chapter presents the findings on the last objective (four) of the study. It validates and showcases the effect of sunflower seeds on the expression of *MMP1* and *PPARA* genes in insulin-resistant HepG2 cells as profiled from objective three.
- Chapter six: This is the last chapter of the dissertation, and it featured the general discussion, conclusions, and recommendations from the study.

References

Abafe, E. A., Oduniyi, O. S., and Tekana, S. S. (2022). Beyond least squares assumptions: quantile regression estimates of the heterogeneity in commercialization–The case of sunflower-producing households in North-West province, South Africa. *Frontiers in Sustainable Food Systems*, *5*, 758399.

Adama. (2023). Sunflower Farming in South Africa. *ADAMA South Africa*. [online] Available at: https://www.adama.com/south-africa/en/sunflower-farming/sunflower-farming-south-africa.

Adnan, M., Jeon, B. B., Chowdhury, M. H. U., Oh, K. K., Das, T., Chy, M. N. U., and Cho, D. H. (2022). Network pharmacology study to reveal the potentiality of a methanol extract of *Caesalpinia sappan* L. wood against type-2 diabetes mellitus. *Life*, 12(2), 277.

Adeleke, B. S., and Babalola, O. O. (2020). Oilseed crop sunflower (*Helianthus annuus*) as a source of food: Nutritional and health benefits. *Food Science and Nutrition*, 8, 4666-4684.

Anjum, F. M., Nadeem, M., Khan, M. I., and Hussain, S. (2012). Nutritional and therapeutic potential of sunflower seeds: A review. *British Food Journal*, 114, 544-552.

Awuchi, C. G. (2019). Medicinal plants: the medical, food, and nutritional biochemistry and uses. *International Journal of Advanced Academic Research*, 5, 220-241.

Azam, S., Latif, A., Hussain, K., Shahbaz, H., Perveen, S., Ashfaq, I., and Tayyeb, A. (2022). Anti-diabetic and anti-lipidemic effect of *Albizia lebbeck* seeds against HepG2 cells. *Pakistan Journal of Pharmaceutical Sciences*, 35(3).

Azimian, L., Weerasuriya, N. M., Munasinghe, R., Song, S., Lin, C. Y., and You, L. (2023). Investigating the effects of Ceylon cinnamon water extract on HepG2 cells for type 2 diabetes therapy. *Cell Biochemistry and Function*, 41(2), 254-267.

Berbudi, A., Rahmadika, N., Tjahjadi, A. I., and Ruslami, R. (2020). Type 2 diabetes and its impact on the immune system. *Current Diabetes Reviews*, 16(5), 442-449.

Bourebaba, N., Kornicka-Garbowska, K., Marycz, K., Bourebaba, L., and Kowalczuk, A. (2021). *Laurus nobilis* ethanolic extract attenuates hyperglycaemia and hyperinsulinemia-induced insulin resistance in HepG2 cell line through the reduction of oxidative stress and improvement of mitochondrial biogenesis–implication in pharmacotherapy. *Mitochondrion*, 59, 190-213.

DeFronzo, R. A., Ferrannini, E., Groop, L., Henry, R. R., Herman, W. H., Holst, J. J., and Weiss, R. (2015). Type 2 diabetes mellitus. *Nature Reviews Disease Primers*, 1, 1-22

Ekoru, K., Doumatey, A., Bentley, A. R., Chen, G., Zhou, J., Shriner, D., ... and Rotimi, C. (2019). Type 2 diabetes complications and comorbidity in sub-Saharan Africans. *EClinicalMedicine*, 16, 30-41.

Erzse, A., Stacey, N., Chola, L., Tugendhaft, A., Freeman, M., and Hofman, K. (2019). The direct medical cost of type 2 diabetes mellitus in South Africa: A cost of illness study. *Global Health Action*, 12(1), 1636611.

Guo, X., Wang, F., Zheng, M., Li, L., Li, L., Wang, J., ... and Shi, X. (2023). Network pharmacology and molecular docking to study the potential molecular mechanism of Qi Fu Yin for diabetic encephalopathy. *Journal of Biomolecular Structure and Dynamics*, 1-15.

He, D., Huang, J. H., Zhang, Z. Y., Du, Q., Peng, W. J., Yu, R., ... and Qin, Y. H. (2019). A network pharmacology-based strategy for predicting active ingredients and potential targets of LiuWei DiHuang pill in treating type 2 diabetes mellitus. *Drug Design, Development and Therapy*, 3989-4005.

Kerru, N., Singh-Pillay, A., Awolade, P., and Singh, P. (2018). Current anti-diabetic agents and their molecular targets: A review. *European Journal of Medicinal Chemistry*, 152, 436-488.

Kharroubi, A. T., and Darwish, H. M. (2015). Diabetes mellitus: The epidemic of the century. *World Journal of Diabetes*, 6, 850.

Kheirollahzadeh, F., Eftekhari, E., Ghollasi, M., and Behzadi, P. (2022). Anti-hyperglycaemic effects of *Eryngium billardierei F. Delaroche* extract on insulin-resistance HepG2 cells *in vitro*. *Molecular Biology Reports*, 49(5), 3401-3411.

Martinelli, D. D. (2023). Machine learning for metabolomics research in drug discovery. *Intelligence-Based Medicine*, 100101.

Nungula, E. Z., Mugwe, J., Nasar, J., Massawe, B. H., Karuma, A. N., Maitra, S., ... and Gitari, H. I. (2023). Land degradation unmasked as the key constraint in sunflower (*Helianthus annus*) production: Role of GIS in revitalizing this vital sector. *Cogent Food and Agriculture*, 9(2), 2267863.

Odeyemi, S., and Dewar, J. (2019). *In vitro* antidiabetic activity affecting glucose uptake in HepG2 cells following their exposure to extracts of *Lauridia tetragona* (Lf) RH Archer. *Processes*, 8(1), 33.

Paschou, S. A., Papadopoulou-Marketou, N., Chrousos, G. P., and Kanaka-Gantenbein, C. (2018). On type 1 diabetes mellitus pathogenesis. *Endocrine Connections*, 7, 38-46.

Puttha, R., Venkatachalam, K., Hanpakdeesakul, S., Wongsa, J., Parametthanuwat, T., Srean, P., ... and Charoenphun, N. (2023). Exploring the potential of sunflowers: agronomy, applications, and opportunities within bio-circular-green economy. *Horticulturae*, 9(10), 1079.

Richmond, K., Williams, S., Mann, J., Brown, R., and Chisholm, A. (2013). Markers of cardiovascular risk in postmenopausal women with type 2 diabetes are improved by the daily consumption of almonds or sunflower kernels: a feeding study. *International Scholarly Research Notices*, 2013, 1-9.

Saeed, N. A. H., Israa, H. H., and Ghasemian, A. (2022). *Helianthus annuus* seed hydro-alcoholic extract chemical composition and effects on body weight and blood parameters among Iraqi patients suffering from type 2 diabetes mellitus. *Journal of Advanced Biomedical Sciences*, 12(2), 223-228.

Sethi, A., Joshi, K., Sasikala, K., and Alvala, M. (2019). Molecular docking in modern drug discovery: Principles and recent applications. *Drug Discovery and Development-New Advances*, 2, 1-21

Shivani, S., and Sunil, S. (2013). Antidiabetic effect of *Helianthus annuus* L., seeds ethanolic extract in streptozotocinnicotinamide induced Type 2 diabetes mellitus. *International Journal of Pharmacy and Pharmaceutical Sciences*, 5, 382-387.

Sifunda, S., Mbewu, A. D., Mabaso, M., Manyaapelo, T., Sewpaul, R., Morgan, J. W., ... and Reddy, S. P. (2023). Prevalence and psychosocial correlates of diabetes mellitus in South Africa: Results from the South African National Health and Nutrition Examination Survey (SANHANES-1). *International Journal of Environmental Research and Public Health*, 20(10), 5798.

Singh, P., Singh, V. K., and Singh, A. K. (2019). Molecular docking analysis of candidate compounds derived from medicinal plants with type 2 diabetes mellitus targets. *Bioinformation*, 15, 179.

Singh, B., Mal, G., Gautam, S. K., Mukesh, M., Singh, B., Mal, G., ... and Mukesh, M. (2019). Computer-aided drug discovery. *Advances in Animal Biotechnology*, 471-481.

Süntar, I. (2020). Importance of ethnopharmacological studies in drug discovery: Role of medicinal plants. *Phytochemistry Reviews*, 19(5), 1199-1209.

Tan, S. Y., Wong, J. L. M., Sim, Y. J., Wong, S. S., Elhassan, S. A. M., Tan, S. H., ... and Candasamy, M. (2019). Type 1 and 2 diabetes mellitus: A review on current treatment approach and gene therapy as potential intervention. *Diabetes and Metabolic Syndrome: Clinical Research and Reviews*, 13(1), 364-372.

Torimiro, D. O., Yusuf, O. J., Subair, S. K., Amujoyegbe, B. J., Tselaesele, N., and Ayinde, J. O. (2014). Utilisation of sunflower crop among smallholder farmers in sub-Saharan Africa: evidence from Nigeria and Botswana. Journal of Agricultural Extension and Rural Development. 6, 298–304.

Tuyiringire, N., Tusubira, D., Munyampundu, J. P., Tolo, C. U., Muvunyi, C. M., and Ogwang, P. E. (2018). Application of metabolomics to drug discovery and understanding the mechanisms of action of medicinal plants with anti-tuberculosis activity. *Clinical and Translational Medicine*, *7*(1), 1-12.

Umar, A. H., Ratnadewi, D., Rafi, M., Sulistyaningsih, Y. C., Hamim, H., and Kusuma, W. A. (2023). Drug candidates and potential targets of *Curculigo* spp. compounds for treating diabetes mellitus based on network pharmacology, molecular docking and molecular dynamics simulation. *Journal of Biomolecular Structure and Dynamics*, 41(17), 8544-8560.

Wangkiri, N., Sarnsri, T., Thongkanjana, T., and Sae-tan, S. (2021). Antioxidant potentials and inhibitory activities against α-amylase and α-glucosidase, and glucose uptake activity in insulin-resistance HepG2 cells of some medicinal plants. *Agriculture and Natural Resources*, *55*(1), 98-104.

Wang, G. S., and Hoyte, C. (2019). Review of biguanide (metformin) toxicity. *Journal of intensive care medicine*, 34(11-12), 863-876.

World Health Organisation. (2023). Diabetes, a silent killer in Africa. *Integrated African Health Observatory: Analytical Fact Sheet.*

Wu, M., and Zhang, Y. (2022). Combining bioinformatics, network pharmacology and artificial intelligence to predict the mechanism of celastrol in the treatment of type 2 diabetes. *Frontiers in Endocrinology*, *13*, 1030278.

Wu, X., Xu, L. Y., Li, E. M., and Dong, G. (2022). Application of molecular dynamics simulation in biomedicine. *Chemical Biology and Drug Design*, *99*(5), 789-800.

Yang, Z., Huang, W., Zhang, J., Xie, M., and Wang, X. (2019). Baicalein improves glucose metabolism in insulin resistant HepG2 cells. *European Journal of Pharmacology*, *854*, 187-193.

Yarahmadi, A., Khademi, F., Mostafavi-Pour, Z., and Zal, F. (2018). *In-vitro* analysis of glucose and quercetin effects on m-TOR and Nrf-2 expression in HepG2 cell line (diabetes and cancer connection). *Nutrition and Cancer*, *70*(5), 770-775.

Zhou, Z., Chen, B., Chen, S., Lin, M., Chen, Y., Jin, S., ... and Zhang, Y. (2020). Applications of network pharmacology in traditional Chinese medicine research. *Evidence-Based Complementary and Alternative Medicine*, *2020*.

Zwane, J., Modjadji, P., Madiba, S., Moropeng, L., Mokgalaboni, K., Mphekgwana, P. M., ... and Mchiza, Z. J. R. (2023). Self-Management of diabetes and associated factors among patients seeking chronic care in Tshwane, South Africa: A facility-based study. *International Journal of Environmental Research and Public Health*, *20*(10), 5887.

Chapter Two

Literature Review

2.1 Introduction

Diabetes mellitus (DM) also known as the global metabolic epidemic of the century is characterized as the occurrence of abnormally high blood glucose levels, resulting from insufficient insulin production or insulin resistance (Schleicher *et al.,* 2022). Diabetes mellitus can be subclassed into type-one known as insulin dependent (T1DM), type-two known as insulin independent (T2DM), gestational DM (GDM), neonatal DM (NDM), and maturity-onset diabetes of the young (MODY). T1DM is an endocrine disorder which results from destruction of β-pancreatic cells resulting in its inability to produce insulin, the outcome of which is hyperglycaemia (Syed, 2022). T1DM makes up approximately 5 – 10% of all diabetic cases and its incidence is common among children and adolescents (Mobasseri *et al.,* 2020). GDM is the occurrence of glucose intolerance caused by insulin insensitivity primarily during pregnancy leading to hyperglycaemic conditions, this affects at least 25% of pregnancies globally (Choudhury *et al.,* 2021). The risk factors for GDM include pregnancy at an advanced maternal age, obesity/ being overweight (maternal), ethnicity, history of GDM and a genetic history of T2DM (McIntyre *et al.,* 2019). This disorder is reported to pose short-term risk to the mother and offspring as blood glucose levels return to normal post-pregnancy. However recently it has been claimed to potentially affect the cardiometabolic health of the mother and offspring (Saravanan *et al.,* 2020). Treatments include dietary intervention, increased physical activity, insulin, metformin etc, (McIntyre *et al.,* 2019). Neonatal DM is a rare genetic disorder caused by a single gene mutation affecting about 1 in 90000 livebirths (Lemelman *et a*l., 2018). Additionally, it occurs in infants younger than 6 months and in some cases (rare) among infants aged 6-12 months. Alarming hyperglycaemic conditions occur due to insufficient, or no insulin being produced as a result of impairment of the pancreatic β-cell with distorted insulin secreting cells having developed or malfunctioning of gestational existing β-cells (Beltrand *et al.,* 2020). Due to the persistent hyperglycaemia, insulin therapy is often applied/administrated (Dahl and Kumar, 2020). Maturity onset diabetes of the young (MODY), on the other hand is a monogenic endocrine disorder occurring due to a single gene mutation adversely affecting the function of the pancreatic β-cell and subsequently affecting insulin secretion (Aarthy *et al*., 2021). The onset of this disorder includes persistent hyperglycaemia in individuals under the age of 30 year (Nkonge *et al*., 2020). The incidence of MODY usually targets children and young adults before the age of 25 years, and it accounts for 1-5% of all DM cases (Nkonge *et*

al., 2020). Treatment for hyperglycaemia due to MODY includes oral diabetics such as sulfonylureas (Urakami, 2019).

Type-two diabetes mellitus is the most prevalent form of DM responsible for more than 90% of all diabetic cases (Rehman *et al.*, 2021). The pathophysiology of T2DM is related to insufficient insulin production and or insulin resistance. Impairment in insulin secretion results in the failure of maintaining glucose homeostasis causing glycaemia. While in the case of insulin resistance, the cells do not respond to the amount of insulin secreted and thus also fail to maintain glucose homeostasis. However, in the occurrence of both insufficient insulin secretion and insulin resistance, hyperglycaemic persists leading to the emergence of T2DM. Type-two diabetes mellitus continues to increase annually with growing population. The prevalence of this disorder is currently 463 million active cases reported in 2019 worldwide with an estimated 50% increase expected by 2045, if no viable solution is provided (IDF, 2019). During this period, the African continent was estimated to have nineteen million cases, and among all African countries, South Africa was the hotspot with 4.6 million diabetic cases (IDF, 2019). The mortality rate associated with T2DM is also high, according to the World Health Organization (WHO) in 2019, approximately 1.5 million deaths were because of T2DM. While in 2012, 2.2 million deaths associated with high blood glucose levels was recorded and with reports suggesting that this will proceed to be one of the top seven leading causes of death by 2030 (WHO, 2020).

Type-two diabetes mellitus is a multifactorial metabolic disorder, a sedentary lifestyle, nutritionally unbalanced/unhealthy diet are some of the popular causative factors among the adult population, and in some cases even children (Olokoba *et al*., 2012). Oher factors may include genetic predisposition, obesity, hypertension, smoking, polycystic ovarian syndrome (PCOS) in women etc, (Artasensi *et al.*, 2020). Individuals who are at a risk developing T2DM, may adhere to strict and disciplined lifestyle practices as a preventative measure, while for those with T2DM it may aid in the management of the disease. The lifestyle changes may include, the maintenance of a normal body weight, healthy diet, sufficient physical activity, disuse of tobacco, as well as regular health check-ups and intake of prescribed medication (Olokoba *et al.*, 2012). Prolonged or unmanaged T2DM may result in secondary health complications such as kidney failure, heart attacks, loss of limbs/amputation, blindness, strokes, nephropathy and neuropathy (Gunathilaka *et al.*, 2020). Additionally, it has been reported that the onset of T2DM may be a result of a compromised immune system, thus, increasing the susceptibility to microbial infections as well (AL-Ishaq *et al.*, 2019). Therefore,

effective and safe T2DM therapeutic strategies are of utmost importance to ensure the abolition or control of this disease.

Currently there are several commercially available classes of drugs to manage T2DM including biguanides, sulfonylureas, thiazolidinediones and alpha-glucosidase inhibitors to name a few (Artasensi *et al.,* 2020). Biguanides such as metformin and phenformin, exhibit antidiabetic action through their blood glucose lowering abilities (Di *et al.,* 2022). Metformin has established itself as first line therapy for T2DM and is the most popular orally prescribed antidiabetic drug (He *et al.,* 2019). With long-term use, these drugs are accompanied with side effects comprising kidney failure, hypoglycaemia, heart failure, hepatotoxicity, etc (Wang and Hoyte, 2019).

Dietary intervention through the inclusion of natural antidiabetic agents such as plants and/or plant products to aid in the management of T2DM is a highly favourable due to the ease of accessibility and relative affordability (Süntar, 2020). One such dietary component is "nuts and seeds" which are an abundant source of both monounsaturated fatty acids (MUFAs) and polyunsaturated fatty acids (PUFAs) as well as proteins and fibres (Woźniak et al., 2022). Consumption of these nuts and seeds have also been associated with a decreased risk of cardiovascular diseases (Balakrishna *et al*., 2022). *Helianthus annuus* seeds/kernels (sunflower seeds) particularly, have captured attention as a health food due to their composition that include PUFAs, minerals, amino acids/proteins, phytochemicals and vitamins (Anjum *et al*., 2012). Sunflower seeds have a higher fatty acid profile of up to 31% in comparison to other oil-seed crops such as flaxseed, peanut, soybean and sesame seeds (Petraru *et al*., 2021).

Computer aided drug discovery (CADD) is the use of bioinformatics tools in the drug discovery process. Within the paradigm of CADD, structure-based drug discovery (SBDD) outperforms as the most formidable and efficient approach to drug discovery (Batool *et a*l., 2019). SBDD considers target specificity, in terms of 3D crystallography of the target structure as well as binding cavity of the target (Vemula *et al.,* 2023). Based on those key principles, these techniques involve screening ligands based on their structural compatibility for the target structure. Molecular docking and molecular dynamic simulations are techniques that are the foundation of SBDD. The use of CADD in comparison to *in vitro* studies, prevents the loss of money and may potentially decrease the amount of time spent in drug development due to precise predictions (Sajal *et al*., 2022). Molecular docking is a virtual screening of small molecules against specific targets. This rigid form of analysis determines the affinity of small molecules (drugs) in terms of its conformation and binding orientation within the binding

cavity of the protein (target) (Adelusi *et al*., 2022). Molecular dynamics simulation on the other hand, is a more flexible approach to study protein's behaviour. Using Newton's equation of motion with respect to interatomic interactions, position of atoms within the molecular system may be forewarn in terms of stability, compactness and flexibility to determine the binding affinity of the bound ligand-protein complex and the subsequent impact on the biological activity of the drug target. Hence, this is currently a well-established and popular approach for small molecule drug discovery, allowing screening and predictions of mechanism of actions complemented by experimental validation.

Metabolomics is the comprehensive phenotypical analysis of small molecules at a molecular scale. This approach permits a systematic understanding of biological activities such as response to treatment, diversity among organisms as well as identification of small molecules (Zhang *et al*., 2022). Blending with the theme of CADD, metabolomics requires minimal sample preparation and is time efficient. Network pharmacology is an advanced bioinformatic tool of analysis, that directly identifies and hypothesizes the potential mechanism of action of a small molecule against a disease (Umar *et al*., 2023). This *in silico* analysis considers the synergistic activity of ethnomedicine and lays the groundwork for drug discovery for a particular disease, such a compound-gene network and disease-gene network interactions (Noor *et al*, 2022). This approach enforces a change in approach to drug discovery from a "one-target-one-drug" to a multi-faceted network of compound-target-poly-pharmacological approach. This approach eliminates and saves time, shortening the pre-clinical stage and advancing towards development. There is an exponential growth in diabetes research, that have successfully employed these techniques leading to the discovery of lead-like compounds. A few of these studies include Balogun *et al*., 2023; Adnan *et al*., 2022; Ahmed *et al*., 2022; Sajal *et al*., 2022; Akoonjee *et al*., 2022; Rampadarath *et al*., 2022; Di *et al*., 2021; Sabiu *et al*., 2021 and Oh *et al*., 2020. Hence, this can be considered a promising avenue for small-molecule drug discovery complemented by experimental validation.

With sunflower parts and/ or products such as seeds and oil increasingly being viewed as a health foods, providing more information on its nutritional and pharmacological potentials including antidiabetic attribute, is eminent. Therefore, this chapter aims to provide an overview on sunflowers and its seeds for consideration as T2DM therapeutics. This is performed by exploring its nutritional and phytochemical compositions as well as pharmacological potentials. In addition to through constricting the ATP sensitive K+ channels and its efforts to improve the insulin resistant peripheral tissue, in this manner insulin secretion is glucose-

independent (Tomlinson *et al*., 2022). This chapter delves into the current classes of antidiabetics (drugs) available, while exploring the antidiabetic potential of sunflower and its seeds and lastly, the role of computational techniques in the T2DM drug discovery.

2.2 Classes of antidiabetic drugs

At present, there are several classes of oral antidiabetics to manage T2DM, these include biguanides, sulfonylureas, meglitinides, thiazolidinediones, DPP-4 inhibitors and alpha glucosidase inhibitors, as well as intravenous treatments such as glucagon-like peptide 1 agonists (incretin mimetics) listed in Table 1 (Mohajan and Mohajan, 2024). The first line of treatment and most prescribed and safest oral drug "metformin" falls under the class of biguanides. Biguanides function as insulin sensitizers, by decreasing gluconeogenesis action and increasing insulin sensitivity within hepatic and peripheral tissue, while inhibiting glucose absorption from the gastrointestinal tract (GIT) (Di *et al*., 2022). Despite its popularity this class of drugs are not void of side effects and drug interactions. Side effects of biguanides oral supplementation include lactic acidosis, nausea, and diarrhoea. Contraindications in relation to biguanides intake, specifically metformin range from cardiac distress, hypoxia, alcohol abuse, and drugs such as cimetidine. Similarly, thiazolidinediones (TZD) also behave as insulin sensitizers, but through the amelioration of insulin resistance. This is performed by sensitizing the muscle, liver, adipose and peripheral tissue leading to a decrease in hepatic glucose secretion and overall hyperglycaemia. Thiazolidinediones such as pioglitazone are popularly prescribed to T2DM patients. These drugs act through activating the peroxisome proliferator activated receptor gamma (PPARγ), improving the insulin secretion of the β-pancreatic cells and thereby augmenting insulin sensitivity (Charbonneau and Capoccia, 2022). Nonetheless, these drugs are accompanied with side effects which may include cardiac failure, weight gain, fluid retention and hepatic toxicity. Drug-drug interactions with gemfibrozil and rifampicin may lead to the inefficiency in the glucose reducing ability of thiazolidinediones (Jaakkola *et al*., 2006). Insulin secretagogues, on the other hand are antidiabetic agents that aim to increase the amount of insulin produced by the pancreas, this group of drugs includes the latter three classes: sulfonylureas, meglitinides and incretin mimetics (Dowarah and Singh 2020). Sulfonylureas function by promoting insulin secretion through the pancreatic β--cells. This is by the constriction of the ATP sensitive K^+ channels, while simultaneously improving the insulin resistant peripheral tissue, as a result insulin secretion in this manner is glucose-independent (Tomlinson *et al*., 2022). This class of oral antidiabetics is often the second line of treatment for T2DM and subcategorized into two groups: first generation sulfonylureas such

as tolbutamide, acetohexamide tolazamide and chlorpropamide, while the second-generation sulfonylureas compromise of glipizide, glyburide (glibenclamide) and glimepiride. The common side effects associated with sulfonylureas range from hypoglycaemia to hyperinsulinmia. This class of drugs may not be consumed by pregnant or lactating women as well as hepatic and renal compromised patients (Mohajan and Mohajan, 2024). Meglitinides (repaglinide and nateglinide) has a similar mechanism of action to sulfonylureas but are structurally different and are thus prescribes to patients allergic to the latter. Meglitinides, however causes an increased reduction in post-prandial blood glucose level and the side effect is most commonly weight gain and/or hyperglycaemia. Administration of meglitinides before the consumption of food, stimulates postprandial insulin secretion to maintain glucose homeostasis. This occurs by the binding action of meglitinides to the β-cells in the pancreas, though each meglitinide has a unique binding site than sulfonylureas (Tomlinson *et al*., 2022). Despite its efficacy this class is susceptible to drug-drug interactions with gemfibrozil, rifampicin, barbiturates, and carbamazepine and may result in voiding the glucose-reducing ability of meglitinides.

Lastly for insulin secretagogues, the class of incretin mimetics such glucagon-like peptide1 (GLP-1) is a hormone secreted by the GI for the maintenance of post-prandial glucose homeostasis, this hormone is inhibited by the DPP-4. GLP-1 levels are decreased in T2DM patients. Stimulating GLP-1 would trigger a cascade reaction, stimulating the β- pancreatic cells to secret insulin, thereby maintaining glucose homeostasis (Cornell, 2020). Exenatide, an GLP-1 agonist mimicking the human GLP-1, stimulates glucose-dependent insulin secretion while simultaneously inhibiting glucagon production. Its side effect usually include nausea. DPP-4 inhibitors, on the other hand such as sitagliptin and valdegliptin directly function to inhibit the enzymatic activity of DPP-4, which prevents the reduction of incretin hormone levels (GLP-1 and gastric inhibitory polypeptide (GIP)), limiting glucagon production (Florentin *et al*., 2022). An increase in DPP-4 enzymatic activity leads to a degradation of incretin hormones GLP-1 and GIP, which interrupts the cascade of reactions, preventing adequate glucose-dependent insulin secretion. Common side effects of DPP-4 inhibitors include diarrhoea, nausea, abdominal pain and nasopharyngitis. Finally, alpha glucosidase is a vital enzyme to carbohydrate metabolism located at the small intestine lumen, converting the carbohydrates to monosaccharides thereby contributing to the increasing blood glucose levels. Inhibition of alpha glucosidase limits the release of glucose preventing the onset of post-prandial hyperglycaemia (Usman *et al*., 2019). The most popular alpha glucosidase inhibitor is

acarbose, which is structurally like carbohydrates thereby promoting its binding to the enzyme (Altay, 2022). The profile of acarbose for T2DM management has been favourable with its weight-loss potential, positive effect on lipid profile and associated reduced risk of cardiovascular diseases. However, a risk for side effects such as bloating, and diarrhoea is recurrent. Of these classes of drugs, sodium-glucose cotransporter-2 (SGLT-2) inhibitors, a much newer class of drugs, appear to show promising antidiabetic action. SGLT-2 are responsible for glucose reabsorption within the kidneys, reabsorbing approximately 90% of the filtered glucose. The SGLT-2 inhibitors prevent the reabsorption of glucose within the kidney and elevate urinary glucose excretion, as a result ameliorating hyperglycaemia (Saisho *et al*., 2020). At present, there are six SGLT-2 inhibitors; pragliflozin, dapagliflozin, canagliflozin, empagliflozin, luseogliflozin, and tofogliflozin as T2DM medication. However, this class of drugs are also accompanied with side effects such as genitourinary infections and acute kidney injury (Lupsa and Inzucchi, 2018). Due to the limitations of these drugs, the search for more effective antidiabetic agents with less severe side effects is highly emphasised.

Table 1: Different classes of conventional oral antidiabetic drugs, their examples and 2D chemical structures.

Class	**Example**	**Chemical structure**	**Reference**
Biguanides	Metformin	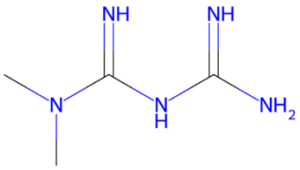	PubChem Identifier: CID 4091 [URL: https://PubChem.ncbi.nlm.nih.gov/compound/4091#section=2D-Structure]

Thiazolidinediones	Pioglitazone	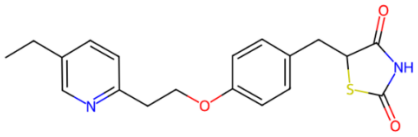	PubChem identifier: CID 4829 [URL: https://PubChem.ncbi.nlm.nih.gov/compound/4829#section=2D-Structure]
Sulfonylureas	Glipizide	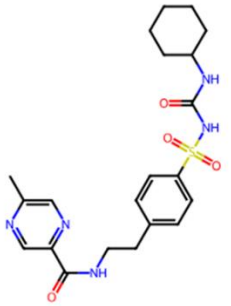	PubChem identifier: CID 3478 [URL: https://PubChem.ncbi.nlm.nih.gov/compound/3478#section=2D-Structureht tps]
Meglitinides	Repaglinide	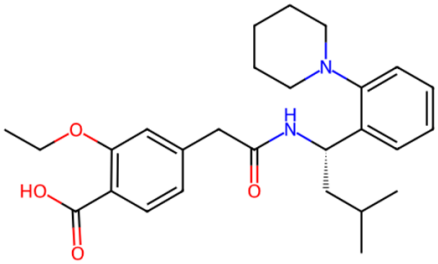	PubChem identifier: CID 65981 [URL: https://PubChem.ncbi.nlm.nih.gov/compound/65981#se

			ction=2D-Structure]
Incretin mimetics (GLP-1)	Exenatide	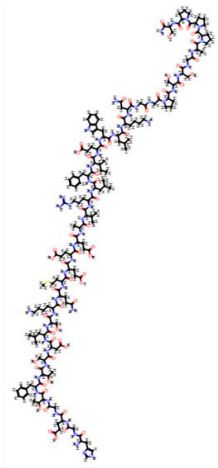	PubChem identifier: CID 53396299 [URL: https://PubChem.ncbi.nlm.nih.gov/compound/53396299#section=2D-Structure]
DPP-4 inhibitor	Sitagliptin	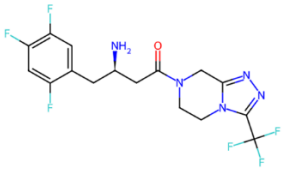	PubChem identifier: CID 4369359 [URL: https://PubChem.ncbi.nlm.nih.gov/compound/4369359#section=2D-Structure]
Alpha glucosidase inhibitor	Acarbose	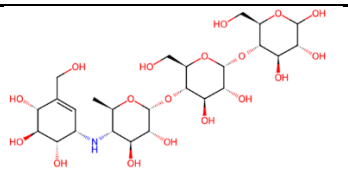	PubChem identifier: CID 41774

			[URL: https://PubChem.ncbi.nlm.nih.gov/compound/41774#section=2D-Structure]
Sodium-glucose cotransporter-2 inhibitors	Dapagliflozin	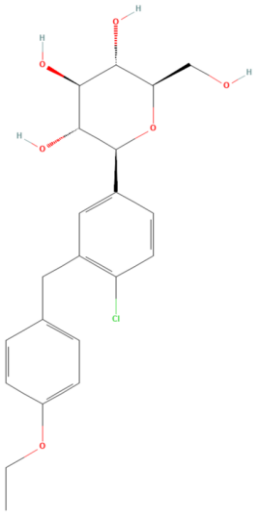	PubChem identifier: 9887712 [URL: https://pubchem.ncbi.nlm.nih.gov/compound/9887712#section=2D-Structure]

2.3 Computer-aided drug discovery (CADD) for T2DM

Drug discovery and development (DDD) is a tedious, expensive, and lengthy journey with many challenges which more than often results in failure of the drug to be approved during clinical trial stages for market release. On average it takes around 13 years and an estimate of 21.3 billion dollars to produce a drug (Kolluri *et al*., 2022). Clinical trials currently have a high failure rate of up to 90%, the factors accounting for that failure usually present during the early drug discovery/preclinical stage, which is reported to be responsible for at least 43% of the expenses during drug discovery (Sadybekov and Katritch, 2023). Issues usually include the need for more in-depth target validation, and failure to establish optimization of ligand properties. Hence prioritizing the vital preclinical stage of drug discovery would lessen the temporal and economic strain of the DDD process. The DDD process involves screening for

potential side effects and ensuring they are at a minimum, high bioavailability of the cost-effectiveness for both development, production and consumers, resources and skills required, and lastly the period for the development of the drug (Sinha and Vohora, 2018). These factors need to be extensively researched and evaluated before considering the launch of a drug.

Computational drug discovery provides a more time-effective approach to be performed at the pre-clinical stage of drug discovery, screening compounds (potential drugs) against disease targets, based on their molecular properties. This ensures that only compounds, i.e., lead compounds with suitable characteristics, minimal risk of side effects and higher probability of behaving as potential drug may be selected for further screening. The application of these techniques eliminates compounds that may not be suitable at preliminary stage of the drug discovery process reducing the waste of valuable resources such as time, labor, and money, and ultimately leading to drug candi. The application of CADD accelerates the identification of the number of clinical drug candidates. Denoting a target-lead relationship as accelerated as two months or even a target-clinical trial within 12 months (Sadybekov and Katritch, 2023).

High-throughput virtual screening (HTVS) is one of the dominant cores of CADD and has seen success as a contender to experimental techniques regarding the high-through put screening and optimization of lead compounds (Stumpfe *et al*., 2012). It is the coupled approach of physics-based docking analysis and data-based scoring function, this synergy enriched the caliber of leads identified and potentially lowers the probability of a false positive. HTVS includes the screening of small molecules against drug candidates most specifically through determination of its binding activity, which in turn may provide an indication towards its mechanism of action (Gautam *et al*., 2023). This screening analysis often leads to the identification of lead compounds against the target drug, there after heading to *in vitro* and *in vivo* testing to decipher the prospective drug candidates. The popular computational techniques that fall with HTVS include molecular docking and dynamic simulations.

2.3.1. Molecular docking and dynamic simulations

Molecular docking is the screening of two molecules against each other either, a small molecule (ligand) and a protein or protein-protein for the identification of the optimal binding mode of the ligand to a specific and ridge binding cavity (Sethi *et al*., 2019). Molecular docking is dependent on the availability of data regarding the three-dimensional (3D) structure of the protein (drug target) and on the basis of the intermolecular interaction between the ligand and protein, such as the formation of electrostatic interactions, hydrogen bonds (H-bonds), van der

Waal forces which serve to stabilize the docked complex. Once the most stable ligand-protein complex has be established the prediction of the lead compound will be successful (Stanzione *et al*., 2021). Furthermore, using biological scoring system software, the ligand-target affinity can be measured by the "docking score" which is in presented as a negative value of ΔG (kcal/mol) (Panday and Ghosh, 2019). This score is calculated based on the molecular interactions between the ligand and protein as well as the binding pose of the complex at the binding site (Menchaca *et al*., 2020). The limitation of molecular docking lies within the fact that this form analysis is based on a rigid protein rather than a flexible protein, as protein structures fluctuate in relation to the system energy. Furthermore, that conformation adopted within molecular docking may not be the most stable conformation of the protein (Menchaca *et al*., 2020). Hence, molecular docking is most effective as a preliminary screening tool preceding MD simulation, which addresses the limitations of molecular docking. MD simulations consider the flexibility of protein, which affects the differing conformation that it may undergo, impacting the binding of the ligand and overall stability of the complex (Salo-Ahen *et al*., 2020).

The current trend in pre-clinical T2DM research involves molecular docking and MD simulations as a combination to establish the mechanism of antidiabetic action. As seen in a recent study by Kahksha *et al.* (2023) that employed molecular docking and MD simulation techniques, the authors discovered that "luteolin" was able to exhibit antidiabetic action. The findings were then validated by *in vitro* and *in vivo* experiments. Similarly, another study by Salim *et al.* (2020) which implemented molecular docking techniques identified "secoisolariciresinol" present in nettle, as a potential inhibitor against the enzymes dipeptidyl peptidase 4 (DPP-4) (-7.05 kcal/mol); α-amylase (AAMY) (-3.83 kcal/mol) and α-glucosidase (AGLU) (-4.16 kcal/mol). These studies enrich the narrative regarding the predictive potential of molecular docking and MD simulations for the discovery of lead compounds and stress the importance of these screening techniques during the early drug discovery phases. Drug discovery studies carrying out MD simulations (Ranade *et al*., 2024; Zare *et al*., 2024; Chenafa *et al*., 2022 and Ahmed *et al*., 2021) have also seen the application of density function theory (DFT) to provide more insight into the molecular structure and mechanism of the target drug. DFT is an emerging computational method in virtual screening, accounting for only 0.02% of applications during the six-year study period (Sabe *et al*., 2021). The application of DFT is usually limited to studies that require a thorough understanding of intermolecular interactions and mechanisms. DFT can accurately predict molecular properties such as determination of

optimal 3D structure of molecules, calculation of binding energies, reaction energies, as well as activation energies (Artyushkova *et al*., 2013). Despite the limited frequency of DFT applications, its accuracy remains invaluable in CADD.

2.3.2. Metabolomic profiling

Metabolomic profiling is the comprehensive analysis of a biological sample to unravel the identity of small molecular metabolites present and the possible variances amongst them (Hasanpour *et al*., 2020). These metabolites are often regarded as biomarkers and used for target recognition in drug discovery. The analysis is performed using techniques such as mass spectrometry coupled with either gas chromatography (GC-MS) or liquid chromatography (LC-MS) and proton nuclear magnetic resonance (NMR) spectroscopy (de Falco and Lanzotti, 2018). A key role of metabolomic profiling in drug discovery is its ability to screen complex natural products, mixtures, and groups of compounds to culminate in the identification of potential lead small-molecule metabolites, while also distinguishing and highlighting the differences between these complex groups of compounds (Harvey *et al*., 2015). The advantages associated with metabolomic profiling are that it allows for the reduction of costs in the drug discovery and development process, by refining clinical trial design, and shorting the overall development process for a drug (Wishart, 2016). Several studies (Sehaki *et al*., 2023; Jan *et al*., 2022; Younis *et al*., 2022; Raza *et al*., 2020; Chandra *et al*., 2018) have been conducted using metabolomic profiling as foundation technique to identify novel metabolites which were subsequently recognized to have potential antidiabetic activity owing to the presence of these identified metabolites.

2.3.3. Network pharmacology

Network pharmacology is an enhanced drug discovery tool that adopts a multi-target drugs approach to complex diseases such as diabetes and cancer, forsaking the one-drug one-target and one-disease approach to drug discovery. This approach was implemented by Hopkins in 2007, who believed that numerous drugs work on numerous targets rather than just one (Xin *et al*., 2021). Using integrative systems biology and poly-pharmacology, network pharmacology can establish a compound-target (gene)-pathway network for a particular disease which ultimately predicts the underlying mechanism of synergistic therapeutic action of a potential drug (Noor *et al*., 2022). The construction of these network pathways allows for the study of associated pathways that lead drugs may be implicated in or modulates. The approach warrants a higher success rate of drug discovery by limiting side effects, enhancing therapeutic effect,

thus simultaneously reducing the costs and time included in the discovery process (Zhao *et al*., 2023). Network pharmacology has played a significant role in traditional medicine, deciphering the complex system of plant therapeutics, and the role of key phytocompounds in medicine. This includes various studies (Halayal *et al*., 2024; Luo *et al*., 2023; Adnan *et al*., 2022; Di *et al*., 2021 and Dwivedi *et al*., 2021) evaluating plants as antidiabetics.

Though the advantages of decreased economic strain, duration, more precise drug candidates associated with CADD such as molecular docking, MD simulation, metabolomic profiling and network pharmacology presents itself, it is essential to note that these are prediction studies and still require experimental validation. Nonetheless, these techniques play a vital role in improving and adding to scientific databases, updating the current pool of knowledge regarding drug candidates.

2.4 Botanical description of *H. annuus*

Helianthus annuus (commonly known as sunflower) is a fast-growing plant native to North America and remained one of seventy species belonging to the family, Asteraceae (Bashir *et al.,* 2021). It is one of the most important and popular oilseed crops that has a cosmopolitan distribution from North America throughout South America, Europe, and Africa due to its adaption to varying climatic and soil conditions globally (Spring, 2019). Within South Africa, majority of sunflower production occurs in the Free State and North West province, with the annual sowing and harvesting seasons occurring around November to January, and April to May, respectively (ADAMA, 2023). This high adaptability characteristic of sunflower is due to its ability to withstand varying weather and soil conditions such as high salt tolerance among others (Kalenska *et al.,* 2020). At the primary stage, the plant has a tap root system however upon maturation a larger, fibrous and lateral root system can be observed. Aesthetically, *H. annuus* has coarse and hairy stem and leaves with a height range of 1.5 – 3 metres (Rehman *et al.,* 2021). The stem of the sunflower is rough, unbranched and hispid, and the height dependant on the number of nodes may range from 1 – 6 ft. The leaves are ovate shaped, around 4 – 20 cm long with width of 3 – 15 cm. The height of the plant ranges up to twelve feet forming the large sunflower-head (capitulum) known as "inflorescence" as seen in Figure 1A. The flower of the plant is composed of florets, the outer ray florets are a bright yellow while the inner disc florets are a darker yellow or marron in colour (Figure 1B and 1C) (Sharma, 2019). The seeds/kernels of the plant are formed by the enclosure of the endosperm and embryo forming the hull which is composed of cellulolytic material and lignin (Petraru *et al*., 2021). These seeds filled with oil globules and protein corpuscles (Brătfălean *et al.,* 2018), are then trapped with a

"shell" called achene. Upon maturation the seeds can be found at the apical region of the plant and are made up of three layers namely the epicarp, mesocarp and endocarp which is the outer, middle, and inner layers respectively (Bashir *et al.*, 2021). While sunflower is widely cultivated and grows during summer or even early spring, in fact, in warmer climates, a higher oil content can be anticipated from the seeds (Aboelkassem, 2021). However, there are many factors that influence the sunflower seed yield, such as temperature, sowing date, precipitation and rainfall (Demir, 2019). The harvesting period of the plant commences upon physiological maturation with a moisture content ranging between 10 – 13%. The raw sunflower seeds are estimated to contain around 25% oil, however due to success of varying plant breeding techniques the quantity has increased to approximately 40% oil while retaining the quality of the oil (Adeleke and Babalola, 2020).

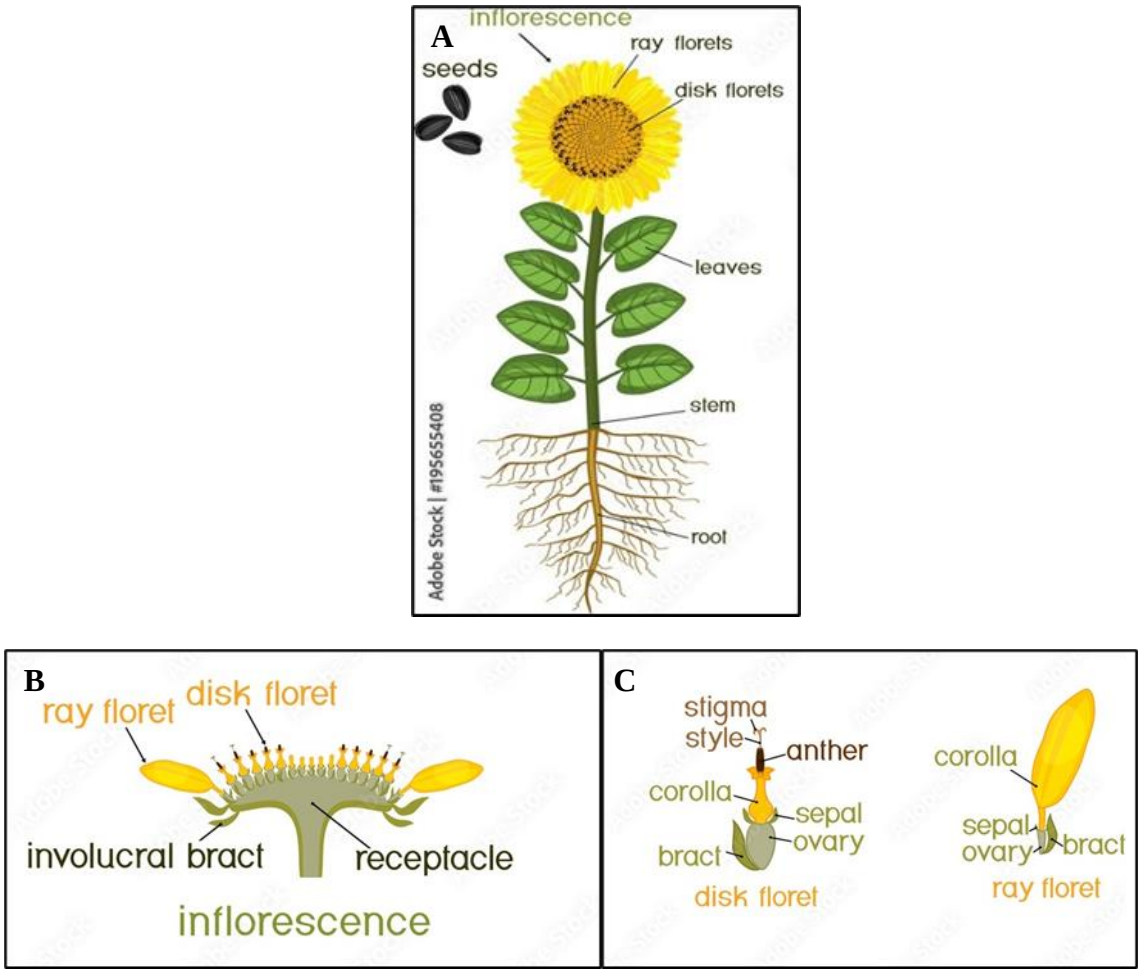

Figure 1: Schematic representation of (A) *Helianthus annuus* L. flower, (B) its inflorescence and, (C) disk floret and ray floret (Maryia, 2023).

2.5 Nutritional composition of sunflower

Though sunflowers are primarily cultivated for oil production, it has been associated with various health benefits due to its nutritional composition. Table 2 showcases the nutritional profile of one cup of sunflowers seeds. These include antioxidants which play a vital role in maintenance of a healthy diet as they neutralize free radicals thereby preventing oxidative damage to the body's cells or tissues. Sunflower oil particularly is reported to contain carotenoids and tocopherols which are antioxidants (Xu *et al.*, 2017). Conversely, the seeds of the sunflower contain phytosterol in high concentrations ranging up to 289 mg/100 g of seeds (Phillips *et al*., 2005). Independently, both the seeds and oil have a highly beneficial nutritional profile due to its fatty acid composition; high content of linoleic acid (55-70%) and oleic acid (20-25%), while the seeds are abundant in omega-6 fatty acids (Nandha *et al.,* 2014). In addition to their abundant fatty acid profile, the seeds and oil are copious in vitamins E and B (Ungurianu *et al.,* 2021).

Amino acids are the building blocks of proteins. Figure 2 illustrates the amino acid profile of one cup of sunflowers seeds. Importantly, there are essential amino acids such as histidine, isoleucine, leucine, methionine, phenylalanine, valine, threonine and tryptophan present which need to be provided to the body (because the body cannot produce them) to ensure normal cell activities. These amino acids were also reported for in as seeds, oils and cake meals have reported the presence of (Karangwa *et al.,* 2015). Other nutrients include dietary fibres and magnesium which is an essential co-factor to more than three hundred enzymes, and vital for the maintenance of a healthy body emphasizing the importance of dietary supplementation (Pinotti *et al.,* 2021). Niacin n is a precursor for co-factors, nicotinamide adenine dinucleotide (NAD) and nicotinamide adenine dinucleotide phosphate (NADP), important for energy metabolism is also present in sunflower seeds.

Table 2: Estimated nutritional profile of one cup of dry sunflower seeds (NutritionValue.org, 2023).

Forty-six grams (one cup) of dry sunflower seeds	
Energy	269 calories
Dietary fibres	4g
Protein	9.6g
Vitamins	

Alpha-tocopherol (vitamin E)	16.18 mg
Niacin (vitamin B)	3.83 mg
Thiamin (vitamin B1)	0,681 mg
Vitamin B6	0.619 mg
Pantothenic acid (vitamin B5)	0.52 mg
Folate (vitamin B9)	104.42 mcg

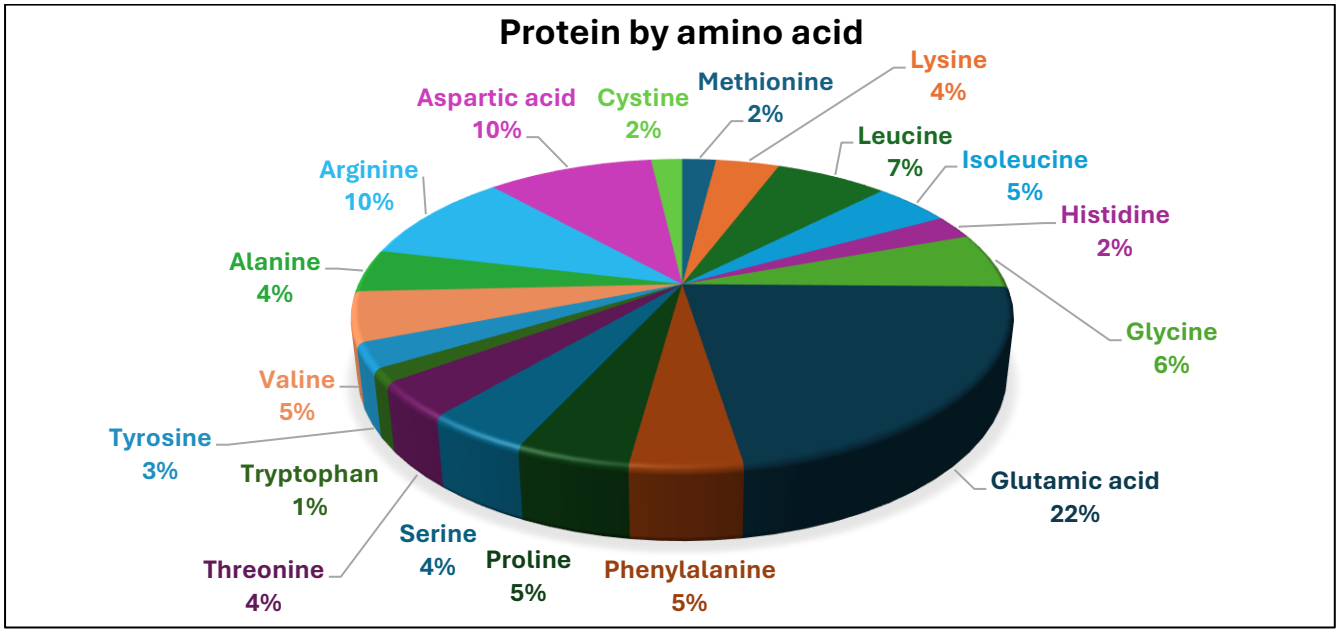

Figure 2: The figure illustrates the amino acid profile of 46 g of sunflower seeds containing a high yield of glutamic acid, followed by aspartic acid and arginine. (NutritionValue.org, 2023).

2.6 Phytochemical composition of sunflower

Sunflowers plants are said to contain various phytoconstituents including monoterpenes, diterpenes, oleic acid, triacyl glycerol, alkaloids, cyanogenic glycosides, saponins, cardiac glycosides, tannins, flavonoids, sesquiterpenes lactones (Brătfălean *et al.*, 2018). Table 3 presents diverse phytocompounds in sunflowers. Fascinatingly, many of these bioactive compounds are said to serve as a benefit to human health such as chlorogenic acid, glycosides, caffeic acid, quinic acid and phytosterols (de Carvalho *et al.*, 2021). The seeds are noted to

contain isomers of conjugated linolenic acids (cis-9 and trans-10) and oleic acid (Rehman *et al.*, 2021). While chlorogenic acid appears to be the most dominant phenolic compound present in the sunflower seeds (Li *et al.*, 2018), other identified ones include caffeoylquinic acid, gallic acid, protocatechuic, caffeic acid, chlorogenic acid, coumaric, gallic acid, ferulic acid, and sinapic acids (Adeleke and Babalola, 2020). Seeds have also been reported to contain flavonoids such as heliannone, luteolin, quercetin, kaempferol and apigenin (Adeleke and Babalola, 2020). Additionally, the presence of alkaloids, cardiac glycosides, saponins, tannins, flavonoids, balsam, phenols, resins and terpenoids and steroids sunflower leaf has been established in the sunflower leaf (Luka *et al.*, 2013). Ye *et al.* (2015) reported caffeic acid hexose I, caffeic acid hexose II, p-coumaric acid hexose, chlorogenic acid, isoquercitrin, 3,4-Di-O-caffeoylquinic acid, 1,5-Di-O-caffeoylquinic acid, 3,5-Di-O-caffeoylquinic acid, and 4,5-Di-O-caffeoylquinic acid as principal phenolic contents in sunflower florets.

Table 3: Phytoconstituents present in various parts of the sunflower. The seeds and their oils mainly comprise phytosterols, phenolic acids, flavonoids and fatty acids.

Phytoconstituent	**Class**	**Plant part**	**Reference**
Cinnamic acid	Phenolic acid	Seed and hull	Egea *et al*. (2021)
Campesterol	Phytosterol	Seed oil	García-González *et al*. (2021) and Ayerdi Gotor *et al*. (2015).
Stigmasterol	Phytosterol	Seed oil	García-González *et al*. (2021) and Ayerdi Gotor *et al*. (2015).
B−Sitosterol	Phytosterol	Seed oil	García-González *et al.* (2021) and Ayerdi Gotor *et al*. (2015)
Avenasterol	Phytosterol	Seed oil	García-González *et al*. (2021)
Pyrocatechol	Phenolic	Seed (methanolic extract)	Abdalla *et al*. (2021)
Vanillin	Phenolic	Seed (methanolic extract), seeds and hulls	Abdalla *et al*. (2021) and Egea *et al*. (2021)

3-hydroxytyrosol	Phenolic	Seed (methanolic extract)	Abdalla *et al*. (2021)
Gallic acid	Phenolic	Seed (methanolic extract), seeds, and hulls	Abdalla *et al*. (2021) and Egea *et al*. (2021)
Protocatechuic acid	Phenolic	Seed (methanolic extract), seeds and hulls	Abdalla *et al*. (2021) and Egea *et al.* (2021)
Syringic acid	Phenolic	Seed (methanolic extract), seed, seed hulls	Abdalla *et al*. (2021) and Egea *et al*. (2021)
Rosmarinic acid	Phenolic	Seed (methanolic extract)	Abdalla *et al*. (2021).
Sinapic acid	Phenolic	Seed (methanolic extract)	Abdalla *et al*. (2021).
Salicylic acid	Phenolic acid	Seed and hull	Egea *et al*. (2021) and Abdalla *et al.* (2021).
Ferulic acid	Phenolic	Seed (methanolic extract), seed and hulls	Abdalla *et al*. (2021) and Egea *et al*. (2021).
Epicatechin	Flavonoids	Seed (methanolic extract)	Abdalla *et al.* (2021).
Hesperidin	Flavonoids	Seed (methanolic extract)	Abdalla *et al*. (2021).
Hyperoside	Flavonoids	Seed (methanolic extract)	Abdalla *et al*. (2021)
Apigenin 7-glucoside	Flavonoids	Seed (methanolic extract)	Abdalla *et al*. (2021)
Luteolin	Flavonoids	Seed (methanolic extract), seed and hull	Abdalla *et al*. (2021) and Egea *et al.* (2021)

Pinoresinol	Flavonoids	Seed (methanolic extract), seed and hull	Abdalla *et al*. (2021) and Egea *et al*. (2021)
Eriodictyol	Flavonoid	Seed and hull	Egea *et al*. (2021)
Oleic acid	Fatty acids	Seed oil	Mahalik *et al.* (2022); Petraru *et al.* (2021); De *et al.* (2020); Ayerdi Gotor *et al*. (2015) and Nandha *et al.* (2014).
Linoleic acid	Fatty acid	Seed oil	Mahalik *et al.* (2022) ; Petraru *et al.* (2021); De *et al.* (2020) and Ayerdi Gotor *et al*. (2015)
Palmitic acid	Fatty acid	Seed oil	Ayerdi Gotor *et al*. (2015)
P-coumaric acid	Phenolic	Seed and hulls	Egea *et al*. (2021)
Rutin	Flavonoid	Hulls	Egea *et al*. (2021)
Stearic acid	Fatty acid	Seed oil	Ayerdi Gotor *et al*. (2015)
Omega 6	Fatty acid	Seeds	Mahalik *et al.* (2022)
Caffeic acid	Phenolic acid	Seed (methanolic extract), seeds and hulls	Abdalla *et al*. (2021); Egea *et al*. (2021) and Rehman *et al.* (2021)
Chlorogenic acid	Phenolic acid	Seeds and hulls	Abdalla *et al*. (2021); Egea *et al*. (2021) and Rehman *et al.* (2021)
Genistic acid	Phenolic acid	Hulls	Egea *et al*. (2021)

2.7 Pharmacological potential of sunflower

As popularly theorized, phytoconstituents are often responsible for the pharmacological action that is witnessed from plants. In this case as well, oils, seeds and extracts of sunflower have also exhibited substantial pharmacological effects. Sunflower seeds contain a high concentration of oleic acid (20-25%) and linoleic acid (55-70%) (Saunders *et al.,* 2013). Consequently, the consumption of sunflower oil has led to lower probability of high cholesterol, total cholesterol, and coronary artery related diseases (Saunders *et al.,* 2013). A study by Odabasoglu *et al.* (2008) evaluated the anti-inflammatory activity and gastrointestinal profile of indomethacin -induced inflammatory rats supplemented with vegetable oils including sunflower oil among corn and olive oil alongside α-tocopherol. The results showed that sunflower oil (79.5%) compared to corn (74.0%) and olive oil (60.5%) was most effective for reduction of paw edema induced by carrageenan. Ethanolic extracts of sunflowers also had promising anti-bacterial activity against multi-drug-resistant clinical isolates such as *Escherichia coli* and *Pseudomonas aeruginosa* with minimum inhibitory concentrations of 4 mg/ml and 2.5 mg/ml, respectively (Chandramoorthy, 2016). This promising activity could potentially aid in abolishment of multi-drug resistant (MDR) isolates due to the abuse of antibiotics. Furthermore, an *ex-vivo* study conducted on 200 individuals with Athlete's foot observed positive outcomes from application of ozonised *H. annuus* oil also known as "Oleozon" (Menendez *et al*., 2002). The antimicrobial potential of *H. annuus*, and its seeds (individually) was studied by Nuzha Bint Mahdi Bin Ali and Hossain (2019). The results from the study observed significant inhibition of Gram-positive and Gram-negative bacteria namely, *Streptococcus spp*, *S. aureus, E. coli* and *Klebsiella spp* . The chemo-preventative potential of sunflower seeds was also investigated by Smith *et al.* (2016), and their findings reported that high phenolic and flavonoid contents of the seeds is said to be responsible for the resultant cytotoxic and antioxidant activities.

2.8 The significance of *H. annuus* as antidiabetic therapy

2.8.1 Experimental evidence of *H. annuus* as an antidiabetic agent

A study by Shivani and Sunil (2013) evaluated the antidiabetic effects of ethanolic extracts of *H. annuus* seeds on streptozotocin-nicotinamide-induced diabetic rats. Administration of 250 mg/kg and 500 mg/kg bodyweight (b.w.) of the ethanolic extract of the seeds to the diabetic mice revealed a reduction in plasma glucose levels by 23.03% and 27.31%, respectively, as compared to non-diabetic mice at 17.78% and 24.83% indicating the antidiabetic properties of

the seed. A clinical study conducted by Richmond *et al.* (2013) evaluated the inclusion of sunflower and almonds seeds into the diets of post-menopausal women with T2DM and found significant 11% decrease in blood glucose levels from the baseline to the end of treatment. In addition, a study performed by Cheenam and Leena (2016) involving 60 diabetic patients witnessed a favourable decrease in fasting blood glucose (FBG) levels from 186.2 mg/dl to 109.9 mg/dl after the consumption of sunflower seeds, as compared to the control group experiencing a reduction from 163.3 mg/dl to 119.2 mg/dl. This reiterates the role of both dietary intervention and specifically the inclusion of sunflower seeds for the management of T2DM.

Nnadi *et al.* (2020) identified pectolinarigenin, a bioactive compound found in *H. annuus* to be a potential component responsible for the antidiabetic effect of the plant. Pectolinarigenin is a flavone which belongs to the subclass of flavonoids. Pectolinarigenin (10 mg/kg) resulted in significant ($p < 0.05$) improvement in the reduction of FBG levels in alloxan -induced diabetic albino mice relative to the control group. The suggested mechanism of action for this phytoconstituent is reported to be extra-pancreatic; the implication of which is improved insulin sensitivity, enhanced utilization of glucose via skeletal muscles and reduction in hepatic glucose production. Comparable results were also reported by Onoja *et al.* (2015) that witnessed significant reduction ($p < 0.05$) in FBG levels in a time-dependant manner. The study evaluated the effect of a crude extract of *H. annuus* leaves (600 mg/kg b.w.) as well as fractions (60 mg/kg b.w.) of the plant on alloxan -induced diabetic Wistar mice. A 50% reduction in FBG level after 6 h of treatment with the crude extract and fractions were observed and was more significant than the reduction observed by mice treated with glibenclamide (a known antidiabetic). Furthermore, this study was able to deduce that the purification of the crude extract enhanced the anti-hyperglycaemic effects. The most active fractions were found to contain triterpenoid-saponins, which are known for its associated pharmacological benefits including its anti-inflammatory, antifungal, antioxidant activity etc. The antidiabetic effects of triterpenoid-saponin however may be due to antioxidant and pancreatic/extra-pancreatic action. Another study by Saeed *et al.* (2022) investigated the effect of 500 mg/kg per day hydro-alcoholic extract of *H. annuus* seeds, rich in chlorogenic acid (40%) as revealed by GC-MS analysis on three hundred type-2 diabetic patients. The FBG levels, cholesterol, high-density lipoprotein (HDL), low density lipoprotein (LDL) and triglycerides levels was evaluated after treatment. The findings revealed a decrease in FBG levels from 196.2 mg/dL to 119.5 mg/dL as compared to the control group (from 99.2 mg/dL to 89.5 mg/dL). Cholesterol (159.2 mg/dL

to 148 mg/dL), triglyceride (129 mg/dL into 122 mg/dL) and HDL levels (36 mg/dL to 44 mg/dL) were also significantly modulated ($p < 0.05$) compared to the control.

Alpha-amylase (AAMY) and alpha-glucosidase (AGLU) are key enzymes involved in the continuous digestion of carbohydrates (Luka *et al.*, 2013). Inhibition of these enzymes prolongs the digestion of carbohydrates by reducing the rate of glucose absorption from the small intestinal tract, resulting in a reduction of postprandial blood glucose levels. An *in vitro* study conducted by Ojo *et al.* (2016) evaluated the antihyperglycemic activity of *H. annuus* leaf on the carbohydrate-digesting enzymes. The hexane extract of the leaf exhibited the best inhibition against both α-amylase and α-glucosidase at 3.92 and 3.29 mg/mL, respectively. The antidiabetic action observed in this experiment was attributed to the presence of alkaloids, tannins, cardiac glycosides and saponins in the *H. annuus* extract.

Advanced glycation end products (AGEs) are a by-product of non-enzymatic glycation between protein and sugar, and when these products pile up it induces a risk for diabetes in the presence of hyperglycaemic conditions (Spagnuolo *et al*., 2021). Four popular Chinese sprouts were investigated for antioxidant and anti-glycative activity by Sun *et al.* (2012). The results of the study demonstrated *H. annuus* sprouts as a potential antiglycative agent. The sprout performed better than the control, aminoguanidine (synthetic antiglycative) with an inhibitory rate of 83.29% at 1 mg/ml, while the control had an inhibitory rate of 80.88%. This experimental analysis *in vitro*, *in vivo* and *ex-vivo*, provided substantial evidence of the antidiabetic potential of *H. annuus*, however there is lack of understanding regarding the mechanism of antidiabetic action.

2.9 Ameliorative potential of *H. annuus* for diabetes-related health complications

Helianthus annuus is composed of many phytochemicals that may contribute towards the antihyperglycemic activity associated with the plant. Saponins derived from the roots of *H. annuus* has been reported to display potential as an hepatoprotective agent in alloxan-induced diabetic mice. The study conducted by Ojo *et al.* (2016) witnessed reduced serum levels and activities of the enzymes alanine transaminase (ALT), and alkaline phosphatase (ALP) activities as well as a decrease in urea levels in the diabetic albino mice treated with 100, 200 300 and 500 mg/kg b.w. of saponin extract suggesting the protection of the liver since increased ALT and ALP activities are indication of potential liver damage. The study further stated that the potential of the derived saponins to be able to repair or revive the liver damage in alloxan induced (diabetic) mice may be an indication of its antioxidant activity.

Onoja *et al.* (2018) evaluated the anti-dyslipidaemia, hepatoprotective and antidiabetic potential of *H. annuus* leaf extract in alloxan-induced diabetic Wistar rats. Treatment with hydro-methanol leaf extract of *H. annuus* was performed at three concentrations, 150, 300 and 600 mg/kg. The three concentrations induced a significant ($p< 0.05$) decrease in the FBG levels and overall lipid profile. Additionally, these treatments were also able to reverse the alloxan-induced deterioration in the pancreas and liver, significantly ($p < 0.05$) reduced of glycosylated haemoglobin concentration (Hba1c) and serum levels of AST, ALT and ALP observed this, respectively. These findings confirm the antidiabetic activity, anti-dyslipidemic and hepatoprotective potential of *H. annuus*. Obesity is the excessive accumulation of fat that negatively impacts human health. It is a major risk factor for T2DM (Heber, 2010). The World Health Organisation (WHO) have reported that obesity was the underlying issue for at least 44% of diabetes cases in 2014 (Malone and Hansen, 2019). Therefore, it can be assumed that treating obesity may in turn prevent or reduce the risk of developing T2DM. A pilot study by Leverrier *et al.* (2019) evaluated the effect of sunflower seeds as an anti-obesity agent due to the presence and dominance of the phenolic compound "chlorogenic acid" established with anti-diabetic, anti-hyperglycaemic and hypolipidemic properties. The subjects of the study after treatment with sunflower seeds witnessed a significant ($p < 0.05$) reduction in body mass index (BMI) (-2.60 cm) and waist circumference (-8.44 cm) compared to the placebo group, BMI (-1.88 cm) and waist circumference (-4.75 cm). Additionally, the body weight of the sunflower seed-treated group reduced by 6.90 kg in comparison to the placebo group (5.53 kg). Significant improvement was observed regarding the lipid profiles of the sunflower-treated group, cholesterol values decreased by – 18.43 mg/dL in comparison to the placebo (−8.72 mg/dL). Sunflower seeds therefore have potential as an anti-obesity agent due to its hypolipidemic properties, which would in turn reduce the risk of T2DM development and its pathogenesis. Hence, in addition to *H. annuus* antidiabetic activity, it may also harbour the potential to ameliorate T2DM -induced complications such as high cholesterol, obesity and hepatoxicity.

Generally, *Helianthus annuus*, or the common sunflower, has long been recognized for its nutritional benefits. This review underscores its potential antihyperglycemic and antidiabetic properties, primarily attributed to its rich phytochemical composition and antioxidant activity. Sunflower seeds particularly exhibit promising therapeutic potential against type 2 diabetes mellitus (T2DM) due to their unique phytochemical profile. To the best of our knowledge at

the time of conducting this study, there has been little to no *in silico* antidiabetic studies performed on sunflower seeds. The application of *in silico* methods in drug discovery could significantly accelerate the identification and characterization of bioactive compounds. Therefore, leveraging computational approaches in diabetic research offers a promising avenue for further exploration and that informed the present investigation into the comprehensive metabolomic profiling, computational and experimental validation of sunflower seeds as therapeutics against type-2 diabetes mellitus.

References

Abdalla, A. A., Yagi, S., Abdallah, A. H., Abdalla, M., Sinan, K. I., and Zengin, G. (2021). Phenolic profile, antioxidant and enzyme inhibition properties of seed methanolic extract of seven new Sunflower lines: From fields to industrial applications. *Process Biochemistry*, 111, 53-61.

Aboelkassem, K. M. (2021). Effect of growing season on yield and its components and oil quality of some Sunflower (*Helianthus annuus* L.) genotypes. *SVU-International Journal of Agricultural Sciences*, 3(4), 1-9.

Adelusi, T. I., Oyedele, A. Q. K., Boyenle, I. D., Ogunlana, A. T., Adeyemi, R. O., Ukachi, C. D., ... and Abdul-Hammed, M. (2022). Molecular modeling in drug discovery. *Informatics in Medicine Unlocked*, 29, 100-880.

Adnan, M., Jeon, B. B., Chowdhury, M. H. U., Oh, K. K., Das, T., Chy, M. N. U., and Cho, D. H. (2022). Network pharmacology study to reveal the potentiality of a methanol extract of *Caesalpinia sappan* L. Wood against type-2 diabetes mellitus. *Life*, 12(2), 277.

Adeleke, B. S., and Babalola, O. O. (2020). Oilseed crop sunflower (*Helianthus annuus*) as a source of food: Nutritional and health benefits. *Food Science and Nutrition*, 8(9), 4666-4684.

Ahmed, S., Ali, M. C., Ruma, R. A., Mahmud, S., Paul, G. K., Saleh, M. A., ... and Islam, M. R. (2022). Molecular docking and dynamics simulation of natural compounds from betel leaves (*Piper betle* L.) for investigating the potential inhibition of alpha-amylase and alpha-glucosidase of type 2 diabetes. *Molecules*, 27(14), 4526.

Ahmed, S., Islam, N., Shahinozzaman, M., Fakayode, S. O., Afrin, N., and Halim, M. A. (2021). Virtual screening, molecular dynamics, density functional theory and quantitative structure activity relationship studies to design peroxisome proliferator-activated receptor-γ

agonists as anti-diabetic drugs. *Journal of Biomolecular Structure and Dynamics*, *39*(2), 728-742.

AL-Ishaq, R.K., Abotaleb, M., Kubatka, P., Kajo, K. and Büsselberg, D. (2019). Flavonoids and their anti-diabetic effects: Cellular mechanisms and effects to improve blood sugar levels. *Biomolecules*, *9*(9).

Altay, M. (2022). Acarbose is again on the stage. *World Journal of Diabetes*, 13(1), 1.

Artasensi, A., Pedretti, A., Vistoli, G., and Fumagalli, L. (2020). Type 2 diabetes mellitus: a review of multi-target drugs. *Molecules*, 25(8), 1987.

Artyushkova, K., Kiefer, B., Halevi, B., Knop-Gericke, A., Schlogl, R., and Atanassov, P. (2013). Density functional theory calculations of XPS binding energy shift for nitrogen-containing graphene-like structures. *Chemical Communications*, 49(25), 2539-2541.

Awad, A. B., Chinnam, M. F. C. S., Fink, C. S., and Bradford, P. G. (2007). β-Sitosterol activates Fas signaling in human breast cancer cells. *Phytomedicine*, 14(11), 747-754.

Ayerdi Gotor, A., Berger, M., Labalette, F., Centis, S., Daydé, J., and Décriaud-Calmon, A. (2015). Comparative analysis of fatty acids, tocopherols and phytosterols content in sunflower cultivars (*Helianthus annuus*) from a three-year multi-local study. *Phyton*, 84(1), 14-25.

Austin, D. and Hayford, T (2021). Research and development in the pharmaceutical industry. *CBO*.

Balakrishna, R., Bjørnerud, T., Bemanian, M., Aune, D., and Fadnes, L. T. (2022). Consumption of nuts and seeds and health outcomes including cardiovascular disease, diabetes and metabolic disease, cancer, and mortality: an umbrella review. *Advances in Nutrition*, 13(6), 2136-2148.

Balogun, F. O., Singh, K., Rampadarath, A., Akoonjee, A., Naidoo, K., and Sabiu, S. (2023). Cheminformatics identification of modulators of key carbohydrate-metabolizing enzymes from *C. cujete* for type-2 diabetes mellitus intervention. *Journal of Diabetes and Metabolic Disorders*, 22(2), 1299-1317.

Bashir, T., Zia-Ur-Rehman Mashwani, K. Z., Haider, S., and Shaista Tabassum, M. (2021). 02. Chemistry, pharmacology and ethnomedicinal uses of *Helianthus annuus* (Sunflower): A review. *Pure and Applied Biology (PAB)*, 4(2), 226-235.

Batool, M., Ahmad, B., and Choi, S. (2019). A structure-based drug discovery paradigm. *International Journal of Molecular Sciences*, 20(11), 2783.

Brătfălean, D., Cristea, V. M., Agachi, P. Ş., and Irimie, D. F. (2008). Improvement of sunflower oil extraction by modelling and simulation. *Revue Roumaine de Chimie*, 53(9), 881-888.

Chandramoorthy, H. C. (2016). Antibacterial activity of *Sphaeranthus indicus* and *Helianthus annuus* against multi-drug resistant (MDR) clinical isolates. *International Journal of Advanced Applied Science*, 3, 1-8.

Chandra, K., Khan, W., Jetley, S., Ahmad, S., and Jain, S. K. (2018). Antidiabetic, toxicological, and metabolomic profiling of aqueous extract of *Cichorium intybus* seeds. *Pharmacognosy Magazine*, 14(57s).

Charbonneau, M. S., and Capoccia, K. L. (2022). Pioglitazone: Reviewed and renewed. *ADCES in Practice*, 10(4), 30-35.

Cheenam, B., and Leena, P. (2016). Effects of sunflower seeds on fasting blood glucose in diabetes mellitus type 2 patients. *Journal of Chemical and Pharmaceutical Research*, 8(4), 1211-1217.

Chenafa, H., Mesli, F., Daoud, I., Achiri, R., Ghalem, S., and Neghra, A. (2022). *In silico* design of enzyme α-amylase and α-glucosidase inhibitors using molecular docking, molecular dynamic, conceptual DFT investigation and pharmacophore modelling. *Journal of Biomolecular Structure and Dynamics*, 40(14), 6308-6329.

Choudhary, M. I., Adhikari, A., Rasheed, S., Marasini, B. P., Hussain, N., and Kaleem, W. A. (2011). Cyclopeptide alkaloids of *Ziziphus oxyphylla* Edgw as novel inhibitors of α-glucosidase enzyme and protein glycation. *Phytochemistry Letters*, 4(4), 404-406.

Cornell, S. (2020). A review of GLP-1 receptor agonists in type 2 diabetes: a focus on the mechanism of action of once-weekly agents. *Journal of Clinical Pharmacy and Therapeutics*, 45, 17-27.

de Carvalho, A. P. A., and Conte-Junior, C. A. (2021). Health benefits of phytochemicals from Brazilian native foods and plants: Antioxidant, antimicrobial, anti-cancer, and risk factors of metabolic/endocrine disorders control. *Trends in Food Science and Technology*, 111, 534-548.

de Falco, B., and Lanzotti, V. (2018). NMR spectroscopy and mass spectrometry in metabolomics analysis of *Salvia*. *Phytochemistry Review*s, 17, 951-972.

De, L. C. (2020). Edible seeds and nuts in human diet for immunity development. *International Journal Recent Scientific Research*, 6(11), 38877-38881.

Demir, I. (2019). The effects of sowing date on growth, seed yield and oil content of sunflower (*Helianthus annuus* L.) cultivars under rainfed conditions. *Fresenius environmental Bulletin*, 28 (9), 6849-6857.

Di, S., Han, L., An, X., Kong, R., Gao, Z., Yang, Y., ... and Tong, X. (2021). *In silico* network pharmacology and *in vivo* analysis of berberine-related mechanisms against type 2 diabetes mellitus and its complications. *Journal of ethnopharmacology*, 276, 114180.

Di Magno, L., Di Pastena, F., Bordone, R., Coni, S., and Canettieri, G. (2022). The mechanism of action of biguanides: New answers to a complex question. *Cancers*, 14(13), 3220.

Dwivedi, P. S., Patil, R., Khanal, P., Gurav, N. S., Murade, V. D., Hase, D. P., ... and Gurav, S. S. (2021). Exploring the therapeutic mechanisms of *Cassia glauca* in diabetes mellitus through network pharmacology, molecular docking and molecular dynamics. *RSC Advances*, 11(62), 39362-39375.

Dowarah, J., and Singh, V. P. (2020). Anti-diabetic drugs recent approaches and advancements. *Bioorganic and Medicinal chemistry*, 28(5), 115263.

Egea, M. B., de Oliveira Filho, J. G., Bertolo, M. R. V., de Araújo, J. C., Gautério, G. V., and Lemes, A. C. (2021). Bioactive phytochemicals from sunflower (*Helianthus annuus* L.) oil processing byproducts. *Bioactive Phytochemicals from Vegetable Oil and Oilseed Processing By-products* (pp. 1-16).

Eu, C. H. A., Lim, W. Y. A., Ton, S. H., and Kadir, K. B. A. (2010). Glycyrrhizic acid improved lipoprotein lipase expression, insulin sensitivity, serum lipid and lipid deposition in high-fat diet-induced obese rats. *Lipids in Health and Disease*, 9(1), 1-9.

Florentin, M., Kostapanos, M. S., and Papazafiropoulou, A. K. (2022). Role of dipeptidyl peptidase 4 inhibitors in the new era of antidiabetic treatment. *World Journal of Diabetes*, 13(2), 85.

Gautam, R. K., Kamal, M. A., and Mittal, P. (Eds.). (2023). Computational approaches in drug discovery, development and systems pharmacology. *Elsevier*.

García-González, A., Velasco, J., Velasco, L., and Ruiz-Méndez, M. V. (2021). Characterization of press and solvent extraction oils from new sunflower seeds with modified phytosterol compositions. *Journal of the Science of Food and Agriculture*, 101(1), 101-109.

Gunathilaka, T. L., Samarakoon, K., Ranasinghe, P., and Peiris, L. D. C. (2020). Antidiabetic potential of marine brown algae—a mini review. *Journal of Diabetes Research*, 2020.

Halayal, R. Y., Bagewadi, Z. K., Aldabaan, N. A., Shaikh, I. A., and Khan, A. A. (2024). Exploring the therapeutic mechanism of potential phytocompounds from *Kalanchoe pinnata* in the treatment of diabetes mellitus by integrating network pharmacology, molecular docking and simulation approach. *Saudi Pharmaceutical Journal*, 102026.

Hasanpour, M., Iranshahy, M., and Iranshahi, M. (2020). The application of metabolomics in investigating anti-diabetic activity of medicinal plants. *Biomedicine and Pharmacotherapy*, *128*, 110263.

Harvey, A. L., Edrada-Ebel, R., and Quinn, R. J. (2015). The re-emergence of natural products for drug discovery in the genomics era. *Nature Reviews Drug Discovery*, 14(2), 111-129.

Heber, D. (2010). An integrative view of obesity. *The American Journal Of Clinical Nutrition*, 91(1), 280S-283S.

He, J. H., Chen, L. X., and Li, H. (2019). Progress in the discovery of naturally occurring anti-diabetic drugs and in the identification of their molecular targets. *Fitoterapia*, 134, 270-289.

Ivanova, P., Chalova, V., Koleva, L., and Pishtiyski, I. (2013). Amino acid composition and solubility of proteins isolated from sunflower meal produced in Bulgaria. *International Food Research Journal*, 20(6), 2995.

Jan, B., Zahiruddin, S., Basist, P., Irfan, M., Abass, S., and Ahmad, S. (2022). Metabolomic profiling and identification of antioxidant and antidiabetic compounds from leaves of different varieties of *Morus alba* Linn grown in Kashmir. *ACS Omega*, 7(28), 24317-24328.

Jaakkola, T., Backman, J., Neuvonen, M., Laitila. J., and Neuvonen, P. (2006). Effect of rifampicin on the pharmacokinetics of pioglitazone. *British Journal of Clinical Pharmacology, 61, 70-8.*

Kahksha, Alam, O., Al-Keridis, L. A., Khan, J., Naaz, S., Alam, A., ... and Beg, M. A. (2023). Evaluation of antidiabetic effect of luteolin in stz induced diabetic rats: Molecular docking, molecular dynamics, *in vitro* and *in vivo* studies. *Journal of Functional Biomaterials*, 14(3), 126.

Kalenska, S., Ryzhenko, A., Novytska, N., Garbar, L., Stolyarchuk, T., Kalenskyi, V., and Shytiy, O. (2020). Morphological features of plants and yield of sunflower hybrids cultivated

in the Northern part of the Forest-Steppe of Ukraine. *American Journal of Plant Sciences*, 11(8), 1331-1344.

Karangwa, E., Zhang, X., Murekatete, N., Masamba, K., Raymond, L. V., Shabbar, A., ... and Song, S. (2015). Effect of substrate type on sensory characteristics and antioxidant capacity of sunflower Maillard reaction products. *European Food Research and Technology*, 240(5), 939-960

Kolluri, S., Lin, J., Liu, R., Zhang, Y., and Zhang, W. (2022). Machine learning and artificial intelligence in pharmaceutical research and development: a review. *The AAPS Journal*, 24, 1-10.

Krishnaiah, D., Devi, T., Bono, A., and Sarbatly, R. (2009). Studies on phytochemical constituents of six Malaysian medicinal plants. *Journal of Medicinal Plants Research*, 3(2), 067-072.

Leverrier, A., Daguet, D., Calame, W., Dhoye, P., and Kodimule, S. P. (2019). *Helianthus annuus* seed extract affects weight and body composition of healthy obese adults during 12 weeks of consumption: A randomized, double-blind, placebo-controlled pilot study. *Nutrients*, 11(5), 1080.

Li, S. T., Yu, D. U. A. N., Guo, T. W., Zhang, P. L., Ping, H. E., and Majumdar, K. (2018). Sunflower response to potassium fertilization and nutrient requirement estimation. *Journal of Integrative Agriculture*, 17(12), 2802-2812.

Liu, H., Wang, L., Chen, C., Dong, Z., and Yu, S. (2022). Association between dietary niacin intake and migraine among American adults: National health and nutrition examination survey. *Nutrients*, 14(15), 3052.

Luka, C. D., Tijjani, H., Joel, E. B., Ezejiofor, U. L., and Onwukike, P. (2013). Hypoglycaemic properties of aqueous extracts of *Anacardium occidentale*, *Moringa oleifera*, *Vernonia amygdalina* and *Helianthus annuus*: a comparative study on some biochemical parameters in diabetic rats. *International Journal of Pharmaceutical Science Invention*, 2(7), 16-22.

Lupsa, B. C., and Inzucchi, S. E. (2018). Use of SGLT2 inhibitors in type 2 diabetes: weighing the risks and benefits. *Diabetologia*, *61*(10), 2118-2125.

Luo, W., Deng, J., He, J., Yin, L., You, R., Zhang, L., ... and Guan, Y. (2023). Integration of molecular docking, molecular dynamics and network pharmacology to explore the multi-target

pharmacology of fenugreek against diabetes. *Journal of Cellular and Molecular Medicine*, *27*(14), 1959-1974.

Mahalik, G. (2022). A Review on the Health Benefits of *Helianthus annuus* L. *Indian Journal of Natural Sciences*, 13*(71)*, 0976 – 0997.

Malone, J. I., and Hansen, B. C. (2019). Does obesity cause type 2 diabetes mellitus (T2DM)? Or is it the opposite? *Pediatric Diabetes*, 20(1), 5-9.

Maryia K. (2023). Parts of sunflower plant. Morphology of flowering plant with root system, flower, seeds and titles. *Adobe Stock*.

Menchaca, T. M., Juárez-Portilla, C., and Zepeda, R. C. (2020). Past, present, and future of molecular docking. *In Drug Discovery and Development-New Advances*. *IntechOpen.*

Menendez, S., Falcon, L., Simon, D. R., and Landa, N. (2002). Efficacy of ozonized sunflower oil in the treatment of tinea pedis. *Mycoses*, 45(7-8), 329-332.

Meng, S., Cao, J., Feng, Q., Peng, J., and Hu, Y. (2013). Roles of chlorogenic acid on regulating glucose and lipids metabolism: a review. *Evidence-based Complementary and Alternative Medicine: eCAM*, *2013*.

Mohajan, D., and Mohajan, H. K. (2024). Oral hypoglycaemic agents: Non-insulin medications for type 2 diabetes patients. *Journal of Innovations in Medical Research*, 3(1), 23-31.

Mohajan, D., and Mohajan, H. K. (2024). Sulfonylureas: A widely used oral anti-hyperglycaemic medication for type 2 diabetes management. *Journal of Innovations in Medical Research*, 3(1), 14-19.

Nandha, R., Singh, H., Garg, K., and Rani, S. (2014). Therapeutic potential of sunflower seeds: An overview. *International Journal of Research and Development in Pharmacy and Life Sciences*, 3(3), 967-972.

Nnadi, C. O., Onoja, S. O., Ezeh, G. C., Kipi, C. B., Ezeja, M. L., Udem, S. C., ... and Asuzu, I. U. (2020). Antioxidant and antidiabetic potentials of a dimethoxylated flavone obtained from *Helianthus annuus* L. Leaf extract. *Pak J Pharmacol*, 37(2), 59-69.

Noor, F., Rehman, A., Ashfaq, U. A., Saleem, M. H., Okla, M. K., Al-Hashimi, A., ... and Aslam, S. (2022). Integrating network pharmacology and molecular docking approaches to

decipher the multi-target pharmacological mechanism of *Abrus precatorius* L. acting on diabetes. *Pharmaceuticals*, 15(4), 414

Noor, F., Tahir ul Qamar, M., Ashfaq, U. A., Albutti, A., Alwashmi, A. S., and Aljasir, M. A. (2022). Network pharmacology approach for medicinal plants: review and assessment. *Pharmaceuticals*, 15(5), 572.

NutritionValue.org (2023). Seeds, dried, sunflower seed kernels. [online] *NutritionValue.org.* Available at: www.nutritionvalue.org.

Nuzha Bint Mahdi Bin Ali, A. and Hossain, M. A. (2019). Antimicrobial and cytotoxic potential of seeds and flowers crude extracts of sunflower. *Grain and Oil Science and Technology*, *2*(4), 103-108.

Odabasoglu, F., Halici, Z., Cakir, A., Halici, M., Aygun, H., Suleyman, H., ... and Atalay, F. (2008). Beneficial effects of vegetable oils (corn, olive and sunflower oils) and α-tocopherol on anti-inflammatory and gastrointestinal profiles of indomethacin in rats. *European Journal of Pharmacology*, 591(1-3), 300-306.

Oh, K. K., Adnan, M., and Cho, D. H. (2020). Network pharmacology of bioactives from *Sorghum bicolor* with targets related to diabetes mellitus. *PLoS One*, 15(12), e0240873.

Ojo, O. A., Ojo, A. B., Ajiboye, B., Olayide, I., and Fadaka, A. (2016). *Helianthus annuus* leaf ameliorates postprandial hyperglycaemia by inhibiting carbohydrate hydrolyzing enzymes associated with type-2 diabetes. *Iranian Journal of Toxicology*, 10(5), 17-22.

Ojo, A. B., Adanlawo, I. G., and Ojo, O. A. (2016). Ameliorative potentials of Saponins from *Helianthus annuus* roots on hepatoprotective and some kidney function indices of alloxan-induced diabetic rats. *Pharmaco online*, 3, 73-9

Olokoba, A.B., Obateru, O.A. and Olokoba, L.B. (2012). Type 2 Diabetes Mellitus: A Review of Current Trends. *Oman Medical Journal*, 27(4), pp.269–273.

Onoja, S. O., Udem, S. C., and Anaga, A. O. (2018). Hypoglycemic, antidyslipidemic, hepatoprotective and antilipid peroxidation activities of hydromethanol leaf extract of *Helianthus annuus* in alloxan-induced diabetic rats. *Tropical Journal of Pharmaceutical Research*, 17(9), 1817-1824.

Onoja, S. O., and Anaga, A. O. (2015). Bioassay-guided fractionation, antihyperglycemic and antioxidant properties of the methanol leaf extract of *Helianthus annuus*. *International Journal of Pharmacognosy and Phytochemical Research*, 7(2), 340-346.

Panday, S. K., and Ghosh, I. (2019). *In silico* structure-based prediction of receptor–ligand binding affinity: current progress and challenges. *Structural Bioinformatics: Applications in Preclinical Drug Discovery Process*, 109-175.

Petraru, A., Ursachi, F., and Amariei, S. (2021). Nutritional characteristics assessment of sunflower seeds, oil and cake. Perspective of using sunflower oilcakes as a functional ingredient. *Plants*, 10(11), 2487.

Phillips, K. M., Ruggio, D. M., and Ashraf-Khorassani, M. (2005). Phytosterol composition of nuts and seeds commonly consumed in the United States. *Journal of Agricultural And Food Chemistry*, 53(24), 9436-9445.

Pinotti, L., Manoni, M., Ferrari, L., Tretola, M., Cazzola, R., and Givens, I. (2021). The contribution of dietary magnesium in farm animals and human nutrition. *Nutrients*, *13*(2), 509.

Rampadarath, A., Balogun, F. O., and Sabiu, S. (2023). Insights into the mechanism of action of *helianthus annuus* (sunflower) seed essential oil in the management of type-2 diabetes mellitus using network pharmacology and molecular docking approaches. *Endocrines*, 4(2), 327-349.

Rampadarath, A., Aribisala, J. O., Makunga, N. P., Mazibuko-Mbeje, S., and Sabiu, S. (2023). Molecular bioprospection of *Helianthus annuus* L.(sunflower) cypsela for antidiabetic therapeutics through network pharmacology, density functional theory and molecular dynamics simulation. *South African Journal of Botany*, 162, 72-95.

Ranade, S. D., Alegaon, S. G., Khatib, N. A., Gharge, S., Kavalapure, R. S., and Kumar, B. P. (2024). Design, synthesis, molecular dynamic simulation, DFT analysis, computational pharmacology and decoding the antidiabetic molecular mechanism of sulphonamide-thiazolidin-4-one hybrids. *Journal of Molecular Structure*, 1311, 138359.

Raza, S. A., Chaudhary, A. R., Mumtaz, M. W., Adnan, A., Mukhtar, H., and Akhtar, M. T. (2020). Metabolite profiling and antidiabetic attributes of ultrasonicated leaf extracts of *Conocarpus lancifolius*. *Asian Pacific Journal of Tropical Biomedicine*, 10(8), 353-360.

Rehman, A., Saeed, A., Kanwal, R., Ahmad, S., and Changazi, S. H. (2021). Therapeutic effect of sunflower seeds and flax seeds on diabetes. *Cureus*, 13(8).

Richmond, K., Williams, S., Mann, J., Brown, R., and Chisholm, A. (2013). Markers of cardiovascular risk in postmenopausal women with type 2 diabetes are improved by the daily consumption of almonds or sunflower kernels: a feeding study. *International Scholarly Research Notices*, 2013.

Sabe, V. T., Ntombela, T., Jhamba, L. A., Maguire, G. E., Govender, T., Naicker, T., and Kruger, H. G. (2021). Current trends in computer aided drug design and a highlight of drugs discovered via computational techniques: A review. *European Journal of Medicinal Chemistry*, 224, 113705.

Sabiu, S., Balogun, F. O., and Amoo, S. O. (2021). Phenolics profiling of *Carpobrotus edulis* (L.) NE Br. and insights into molecular dynamics of their significance in type 2 diabetes therapy and its retinopathy complication. *Molecules*, 26(16), 4867.

Sadybekov, A. V., and Katritch, V. (2023). Computational approaches streamlining drug discovery. *Nature*, *616*(7958), 673-685.

Salim, B., Said, G., Kambouche, N., and Kress, S. (2020). Identification of phenolic compounds from nettle as new candidate inhibitors of main enzymes responsible on type-II diabetes. *Current Drug Discovery Technologies*, *17*(2), 197-202.

Saeed, N. A. H., Israa, H. H., and Ghasemian, A. (2022). *Helianthus annuus* seed hydro-alcoholic extract chemical composition and effects on body weight and blood parameters among Iraqi patients suffering from type 2 diabetes mellitus. *Journal of Advanced Biomedical Sciences*, 12(2), 223-228.

Sajal, H., Patil, S. M., Raj, R., Shbeer, A. M., Ageel, M., and Ramu, R. (2022). Computer-aided screening of phytoconstituents from *Ocimum tenuiflorum* against diabetes mellitus targeting DPP-4 inhibition: A combination of molecular docking, molecular dynamics, and pharmacokinetics approaches. *Molecules*, 27(16), 5133.

Saini, S., and Sharma, S. (2013). Antidiabetic effect of *Helianthus annuus* L., seeds ethanolic extract in streptozotocinnicotinamide induced type 2 diabetes mellitus. *International Journal of Pharmacy and Pharmacological Sciences*, 5(2), 382-387.

Saisho, Y. (2020). SGLT2 inhibitors: The star in the treatment of type 2 diabetes? *Diseases*, 8(2), 14.

Salo-Ahen, O. M., Alanko, I., Bhadane, R., Bonvin, A. M., Honorato, R. V., Hossain, S., ... and Vanmeert, M. (2020). Molecular dynamics simulations in drug discovery and pharmaceutical development. *Processes*, 9(1), 71.

Saunders, A. V., Davis, B. C., and Garg, M. L. (2013). Omega-3 polyunsaturated fatty acids and vegetarian diets. *Medical Journal of Australia*, 199, S22-S26.

Sethi, A., Joshi, K., Sasikala, K., and Alvala, M. (2019). Molecular docking in modern drug discovery: Principles and recent applications. *Drug discovery and Development-new Advances*, 2, 1-21.

Sehaki, C., Molinie, R., Mathiron, D., Fontaine, J. X., Jullian, N., Ayati, F., ... and Gontier, E. (2023). Metabolomics-based profiling via a chemometric approach to investigate the antidiabetic property of different parts and origins of *Pistacia lentiscus* l. *Metabolites*, 13(2), 275.

Sinha, S., and Vohora, D. (2018). Drug discovery and development: An overview. *Pharmaceutical Medicine and Translational Clinical Research*, 19-32.

Smith, L. F., Patterson, J., Walker, L. T., and Verghese, M. (2016). Chemopreventive potential of sunflower seeds in a human colon cancer cell line. *International Journal of Cancer Research*, 12(1), 40-50.

Sun, Z., Chen, J., Ma, J., Jiang, Y., Wang, M., Ren, G., and Chen, F. (2012). Cynarin-rich sunflower (*Helianthus annuus*) sprouts possess both antiglycative and antioxidant activities. *Journal of Agricultural and Food Chemistry*, 60(12), 3260-3265.

Sharma, B. (2019). Analyses of flavonoids present in the inflorescence of sunflower. *Brazilian Journal of Botany*, 42(3), 421-429.

Spagnuolo, L., Della Posta, S., Fanali, C., Dugo, L., and De Gara, L. (2021). Antioxidant and antiglycation effects of polyphenol compounds extracted from hazelnut skin on advanced glycation end-products (AGEs) formation. *Antioxidants*, 10(3), 424.

Spring, O. (2019). Spreading and global pathogenic diversity of sunflower downy mildew–Review. *Plant Protection Science*, 55(3), 149-158.

Stanzione, F., Giangreco, I., and Cole, J. C. (2021). Use of molecular docking computational tools in drug discovery. *Progress in Medicinal Chemistry*, 60, 273-343.

Stumpfe, D., Ripphausen, P., and Bajorath, J. (2012). Virtual compound screening in drug discovery. *Future Medicinal Chemistry*, 4(5), 593-602.

Süntar, I. (2020). Importance of ethnopharmacological studies in drug discovery: role of medicinal plants. *Phytochemistry Reviews*, 19(5), 1199-1209.

Tomlinson, B., Patil, N. G., Fok, M., Chan, P., and Lam, C. W. K. (2022). The role of sulfonylureas in the treatment of type 2 diabetes. *Expert Opinion on Pharmacotherapy*, *23*(3), 387-403.

Umar, A. H., Ratnadewi, D., Rafi, M., Sulistyaningsih, Y. C., Hamim, H., and Kusuma, W. A. (2023). Drug candidates and potential targets of *Curculigo spp*. compounds for treating diabetes mellitus based on network pharmacology, molecular docking and molecular dynamics simulation. *Journal of Biomolecular Structure and Dynamics*, 41(17), 8544-8560.

Ungurianu, A., Zanfirescu, A., Nițulescu, G., and Margină, D. (2021). Vitamin E beyond its antioxidant label. *Antioxidants*, 10(5), 634.

Usman, B., Sharma, N., Satija, S., Mehta, M., Vyas, M., Khatik, G. L., ... and Dua, K. (2019). Recent developments in alpha-glucosidase inhibitors for management of type-2 diabetes: An update. *Current Pharmaceutical Design*, 25(23), 2510-2525.

Vemula, D., Jayasurya, P., Sushmitha, V., Kumar, Y. N., and Bhandari, V. (2023). CADD, AI and ML in drug discovery: A comprehensive review. *European Journal of Pharmaceutical Sciences*, 181, 106324.

Woźniak, M., Waśkiewicz, A., and Ratajczak, I. (2022). The content of phenolic compounds and mineral elements in edible nuts. *Molecules*, 27(14), 4326.

WHO (2020). Diabetes. *World Health Organization*.

WHO (2022). Obesity and Overweight. *World Health Organization*.

Wishart, D. S. (2016). Emerging applications of metabolomics in drug discovery and precision medicine. *Nature Reviews Drug discovery*, 15(7), 473-484.

Xin, W. A. N. G., Zi-Yi, W. A. N. G., Zheng, J. H., and Shao, L. I. (2021). TCM network pharmacology: a new trend towards combining computational, experimental and clinical approaches. *Chinese Journal of Natural Medicines*, 19(1), 1-11.

Xu, D. P., Li, Y., Meng, X., Zhou, T., Zhou, Y., Zheng, J., ... and Li, H. B. (2017). Natural antioxidants in foods and medicinal plants: Extraction, assessment, and resources. *International Journal of Molecular Sciences*, 18(1), 96.

Ye, F., Liang, Q., Li, H., and Zhao, G. (2015). Solvent effects on phenolic content, composition, and antioxidant activity of extracts from florets of sunflower (*Helianthus annuus* L.). *Industrial Crops and Products*, 76, 574-581.

Younis, I. Y., Khattab, A. R., Selim, N. M., Sobeh, M., Elhawary, S. S., and Bishbishy, M. H. E. (2022). Metabolomics-based profiling of 4 avocado varieties using HPLC–MS/MS and GC/MS and evaluation of their antidiabetic activity. *Scientific Reports*, 12(1), 4966.

Zare, F., Ataollahi, E., Mardaneh, P., Sakhteman, A., Keshavarz, V., Solhjoo, A., and Emami, L. (2024). A combination of virtual screening, molecular dynamics simulation, MM/PBSA, ADMET, and DFT calculations to identify a potential DPP-4 inhibitor. *Scientific Reports*, 14(1), 7749.

Zhao, L., Zhang, H., Li, N., Chen, J., Xu, H., Wang, Y., and Liang, Q. (2023). Network pharmacology, a promising approach to reveal the pharmacology mechanism of Chinese medicine formula. *Journal of Ethnopharmacology*, *309*, 116306.

Zhang, X., Kupczyk, E., Schmitt-Kopplin, P., and Mueller, C. (2022). Current and future approaches for *in vitro* hit discovery in diabetes mellitus. *Drug Discovery Today*, 27(10), 103331.

Chapter Three

This chapter has been formatted for submission *to Journal of Diabetes & Metabolic Disorders* for publication.

Metabolomics and computational bioprospection of sunflower seeds against the key enzymes implicated in type-2 diabetes mellitus pathogenesis and its complications

Athika Rampadarath[1], Jamiu Olaseni Aribisala[1], Nokwanda Pearl Makunga[2] and Saheed Sabiu[1]*

[1]Department of Biotechnology and Food Science, Faculty of Applied Sciences, Durban University of Technology, Durban 4000, South Africa.

[2]Department of Botany and Zoology, Stellenbosch University, Private Bag X1, Matieland, Stellenbosch 7602, South Africa

***Correspondence: sabius@dut.ac.za**

Abstract

Seeds are rich sources of secondary metabolites which offer significant therapeutic efficacy against many diseases. *Helianthus annuus* (sunflower) seeds are popular and staple ingredients in the food industry and their beneficial effects in the management of type 2 diabetes mellitus (T2DM) have been reported, though without specific mechanism of action. This study profiled the secondary metabolites of six cultivars of sunflower seeds commonly consumed in South Africa using liquid chromatography-mass spectrometry (LC-MS) and gas chromatography-mass spectrometry (GC-MS) techniques and evaluated the mechanism of action of the profiled metabolites against key enzymes [alpha-amylase (AAMY), alpha-glucosidase (AGLU), protein tyrosine phosphatase 1B (PTP1B), dipeptidyl peptidase-4 (DPP-4), aldose reductase and sorbitol dehydrogenase (SDH)] implicated in T2DM and its complications using computational approaches. Molecular docking of 84/94 identified compounds afforded the top five compounds with superior binding fitness towards each of the investigated enzymes. A further probe into the relative stability and compactness of the bound complexes of the top five compounds against each respective enzyme over a 150-ns simulation period, revealed that the integrity and conformation of all the test systems were not compromised. Specifically, SON I-AAMY, GRA C - AAMY, SAC A -AGLU, SON I – AR, SAC A – SDH , PYR – DPP-4, and CGA -PTP1B were identified as potential lead metabolites in sunflower seeds against the respective enzymes. The lead compounds in each case of the enzyme interacted with critical amino acids residues that facilitated their improved stability with the enzymes. These observations are suggestive of the potential modulatory role of these metabolites against the enzyme as leads that could be further developed as drug candidates for the management of T2DM and its retinopathy complications.

Keywords: Metabolomic profiling, molecular dynamic simulations, sunflower seeds, Type-2 diabetes mellitus.

1. Introduction

Diabetes is a highly prevalent chronic endocrine disorder affecting millions of individuals worldwide. This metabolic disorder is primarily characterized by the body's inability to regulate blood sugar levels, leading to hyperglycaemia. This is typically caused by insufficient insulin production or resistance to insulin, which can be attributed to malfunctioning pancreatic β- cells or impaired insulin sensitivity (Galicia-Garcia *et al*., 2020). According to the International Diabetes Federation (IDF), an estimated 537 million people are currently living with diabetes, with a projected increased to 783 million diabetics individuals by 2045 (IDF, 2024). This chronic condition is broadly categorized into two main types: type 1 diabetes (T1DM) and type 2 diabetes (T2DM). T1DM is also known as insulin-dependent diabetes is often diagnosed in children. It occurs due to malfunctioning pancreatic β- cells, resulting in insufficient secretion of insulin. In contrast, T2DM (insulin-independent), accounting for over 90% of all diabetes cases, is marked by either insulin resistance or insufficient insulin secretion (Andreadi *et al*., 2022). When left untreated or not manged efficiently, T2DM can lead to serious complications like nerve damage (neuropathy), kidney disease (nephropathy), and eye problems (retinopathy), significantly impacting quality of life (Zheng *et al.*, 2018). The management of T2DM typically involves a combination of lifestyle modifications and medications, with metformin, a biguanide, often being the first line oral antidiabetic drug of choice (Mathu *et al*., 2021). Other medications commonly used include thiazolidinediones, sulfonylureas, meglitinides, incretin mimetics, DPP-4 inhibitors, and alpha-glucosidase inhibitors (Blahova *et al*., 2021). The optimal treatment strategy varies based on factors such as disease severity, patient preferences, and the presence of comorbidities (Singh and Singh, 2019). While these medications can be effective in managing blood sugar levels, long-term use may be associated with side effects such as liver problems, heart issues, hypoglycaemia, weight gain, and digestive issues (Artasensi *et al*., 2020), and this has prompted the search for alternative antidiabetics with relatively less severe side effects.

The growing interest in plants as potential therapeutic agents is fuelled by their bioactive compounds (secondary metabolites) with established health benefits (Süntar, 2020). Over 400 plants species in literature have demonstrated potential for lowering blood sugar levels,

although further research and analysis are needed to confirm these effects (Rahman *et al*., 2020; Nazarian-Samani *et al*., 2018). Among these plants, *Helianthus annuus* (sunflower) seeds have emerged as a promising candidate. These widely available seeds offer a nutritional profile rich in vitamins, minerals, antioxidants and healthy fats, as well as bioactive compounds like chlorogenic acid, caffeic acid, quinic acid, and rutin, which may contribute to their potential antidiabetic properties (Abdalla *et al*., 2021; Egea *et al*., 2021; Rehman *et al.*, 2021). More relevantly, emerging evidence suggests that sunflower seeds may play a role in managing T2DM. Studies have reported significant reductions in blood sugar levels following sunflower seed consumption (Saeed *et al*., 2022; Nnadi *et al.*, 2020; Cheenam and Leena 2016; Onoja *et al*. 2015; Richmond *et al*. 2013; Shivani and Sunil, 2013). However, the precise mechanism through which sunflower seeds exert their antidiabetic effects remains unclear and requires further investigation.

Management of T2DM primarily focuses on lowering blood sugar levels to ameliorate the symptoms of the disease and prevent further complications. Key drug targets (enzymes) such as alpha-amylase, alpha-glucosidase, aldose reductase, dipeptidyl peptidase IV, protein tyrosine phosphatase 1B and sorbitol dehydrogenase, exist through which this can be attained (Marulkar and Bhatia, 2024). These enzymes present opportunities for therapeutic intervention for T2DM. For instance, drugs like acarbose blocks the enzymes alpha-amylase and alpha-glucosidase, which are responsible for carbohydrate digestion. This reduces the glucose absorbing abilities of both enzymes as a result preventing post-prandial hyperglycaemia. Hence, alpha-amylase and alpha-glucosidase are promising targets for the identification of antidiabetic drug candidates (Altay, 2022).

Another therapeutic approach for T2DM and its complications involves inhibiting key enzymes in the polyol pathway, such as aldose reductase (AR) and sorbitol dehydrogenase (SDH). Under high glucose conditions, AR converts glucose to sorbitol, which is then converted to fructose by SDH (Thakur *et al*., 2021). Elevated sorbitol and fructose levels are linked to diabetic neuropathy (Yang *et al*., 2019). Inhibiting AR and SDH may reduce sorbitol and fructose accumulation, potentially preventing neuropathy. Targeting dipeptidyl peptidase-4 (DPP-4) presents another approach, as this enzyme inactivates incretin hormones like glucagon-like peptide -1 (GLP-1) and glucose-dependent insulinotropic polypeptide (GIP), which stimulate insulin secretion (Deacon, 2020). DPP-4 inhibitors prevent the inactivation of these key hormones, promote glucose-independent insulin secretion and improved blood sugar control

(Yin *et al*., 2022). On the other hand, protein tyrosine phosphatase 1B (PTP1B) acts as a negative regulator of the insulin receptor (IR) pathway, directly affecting insulin sensitivity (Teimouri *et al*., 2022). Inhibition of this enzyme may increase insulin sensitivity in diabetic patients (Rocha *et al*., 2021). Despite being a critical therapeutic target for T2DM, there are currently no clinically approved drugs for PTP1B.

Given the limitations and potential side effects of the existing antidiabetic drugs, there is an urgent need for alternative treatment options. Plants, with their rich source of secondary metabolites, are a promising area for discovering novel antidiabetic agents. Sunflower seeds, in particular, offer a promising avenue due to their abundance of bioactive compounds. Hence, this study aimed to identify compounds from six sunflower seed cultivars that might interact with key enzymes involved in T2DM through application of metabolomic profiling, molecular docking and molecular dynamics (MD) simulations. These techniques allow for identification of lead compounds and assessment of their binding affinities to therapeutic targets such as alpha-amylase (AAMY), alpha-glucosidase (AGLU), AR, DPP-4, PTP1B, and SDH, as explored in this study.

2.0 Materials and Methods

2.1 Metabolomic profiling of six cultivars of sunflower seeds

Fresh seeds of six (AGSUN 5270, AGSUN 8251, AGSUN 5108 CLP, AGSUN 5106 CLP, AGSUN 5103 CLP and AGSUN CLP 5101) cultivars of sunflower seeds commonly consumed in South Africa were obtained from the Agricultural Research Council, Potchefstroom, South Africa. The metabolomic profiling of the six cultivars was performed using Gas chromatography-Mass spectrometry (GC-MS) and liquid chromatography-mass spectrometry (LC-MS) analysis for volatile and non-volatile metabolites identification, respectively (Rampadarath *et al.*, 2023). The baseline variable importance in projection (VIP) score was set to 90%, which was then used to identify the important metabolites.

2.2. Molecular docking analysis

The identified metabolites of the sunflower seed cultivars were screened using Lipinski's rule of five (Ro5). Metabolites that passed the filtering rule were then screened against the enzyme target using molecular docking (Rampadarath *et al*., 2023).. The x-ray crystal structures of targets [AAMY (PDB ID: 4W93), AGLU (PDB ID: 3W37), AR (PDB ID: 3RX3), DPP-4 (PDB ID: 1WCY), PTP1B (PDB ID: 1SUG), and SDH (PDB ID: 1PL7)] were retrieved from the RCSB Protein Data Bank (PDB) (www.rcsb.org) and prepared using UCSF Chimera v1.16

(Pettersen *et al*., 2004). Preparation of the target enzymes involved removing non-standard amino acid residues, water molecules, and co-crystallized ligands. Thereafter the 3D conformers of the sunflower seed metabolites were retrieved from PubChem (https://PubChem.ncbi.nlm.nih.gov/), alongside the reference standards for each enzyme: acarbose (AAMY and AGLU), epalrestat (AR), sitagliptin (DPP-4), ursolic acid (PTP1B), and 4-[2-(1R-hydroxy-ethyl)-pyrimidin-4-yl] piperazine-1-sulfonic acid dimethylamide (SDH). These ligands were then prepared with UCSF Chimera v1.16 by adding Gasteiger charges and non-polar hydrogen atoms (Ammu *et al*., 2019). AutoDock Vina, a docking package plugin on UCSF Chimera was then used to dock each ligand individually into the active site of the respective enzyme. To ensure docking at the active site, the grid box coordinates were adjusted to match the established x-y-z coordinates identified using Discovery Studio version 2021 (BIOVIA, 2021). The docking protocol was validated using a decoy approach (Aribisala and Sabiu, 2022) through superimposition of the best docked ligands and reference standards on the native ligand in the co-crystalized structure of each enzyme as presented in Table 1. The ligands with the lowest docking scores for each enzyme were selected for further analysis using molecular dynamics (MD) simulations.

2.3. Molecular dynamic simulations

The MD simulations were executed as previously described by Aribisala *et al*. (2022). The simulations were run on the Graphical Processing Unit (GPU) using the AMBER 18 software package of the in-house programme (HEAL1361), resident at the Centre for High Performance Computing (CHPC), Cape Town, South Africa. The AMBER force field (FF18SB variant) was used to describe the systems. The partial charges of the sunflower seed ligands (metabolites) were assigned using ANTECHMABER through a standard process involving restrained electrostatic potential (RESP) calculations within the General AMBER Force Field (GAFF). The Leap module in AMBER was used to add hydrogen atoms (H^+), sodium (Na^+) and chloride (Cl^-) ions to neutralize the systems. The sequences for each enzyme namely: Alpha-amylase (495 residues), alpha-glucosidase (826 residues), AR (315 residues), SDH (356 residues), DPP-4 (729 residues) and PTP1B (299 residues) was numbered appropriately.

The system was then deposited into an orthorhombic box of TIP3P water molecules ensuring that all atoms were at least eight angstroms away from any edge of the box. The system minimization was performed in two stages. First, a steep descent minimization with two thousand steps was performed, restraining both the solutes (proteins and ligands) with a force constant of 500 kcal/mol/Å^2, followed by minimization using the conjugate gradient

algorithm. The second minimization stage involved one thousand steps without any restraints, again using the conjugate gradient algorithm.

The heating stage of the MD simulation gradually increased the temperature from 0 Kelvin to three hundred Kelvin over 50 picoseconds, while keeping the volume of both the solutes and water constant. The solutes were then exposed to a weak harmonic restraint (10 kcal/mol) and a collision frequency of 1.0 ps to maintain stability. Following this, the system underwent an equilibration stage of five hundred ps at a constant temperature of 300 Kelvin and pressure of 1 bar, mimicking a realistic physiological environment (isobaric-isothermal ensemble, NPT). The SHAKE algorithm was used to constrain the motion of hydrogen atoms throughout the 150 ns MD simulation.

The binding free energy of the complexes throughout the 150 ns simulation period was calculated using molecular mechanics with the generalized born surface area (MMGBSA) method using the equation $\Delta G_{bind} = G_{complex} - (G_{Receptor} + G_{ligand})$. Parameters including RMSD, root mean square fluctuation (RMSF), solvent accessible surface area (SASA), radius of gyration (RoG), and hydrogen bond dynamics within the proteins, were then computed using Origin data analysis software version 6.0 (OriginLab, Northampton, MA, USA).

3.0 Results

3.1 Metabolomic profiling of cultivars of sunflower seeds

A total of 94 metabolites were identified in sunflower seeds using GC-MS and LC-MS analyses. GC-MS analysis revealed 50 compounds, including organic acids, alkanes, alcohols, terpenes, heterocyclic compounds, and hydrocarbons. Notably, all six cultivars contained these metabolites at similar retention times (Supplementary Figure S1a-f and Supplementary Table S1). LC-MS analysis identified 44 phenolic compounds common in all six cultivars (Supplementary Figure S2a-f and Supplementary Table S2).

Further analysis of LC-MS data revealed that chlorogenic acid, quinic acid, and caffeic acid were present in high abundance in all cultivars, with chlorogenic acid being the most prevalent. Principal component analysis (PCA) of the identified phenolic compounds grouped the six cultivars into distinct clusters (Figure 1), with an overall variance of 39.7%. Finally, PLS-DA analysis revealed VIP which highlighted 14 key metabolites that contribute significantly to the observed variation among cultivars (Figure 2).

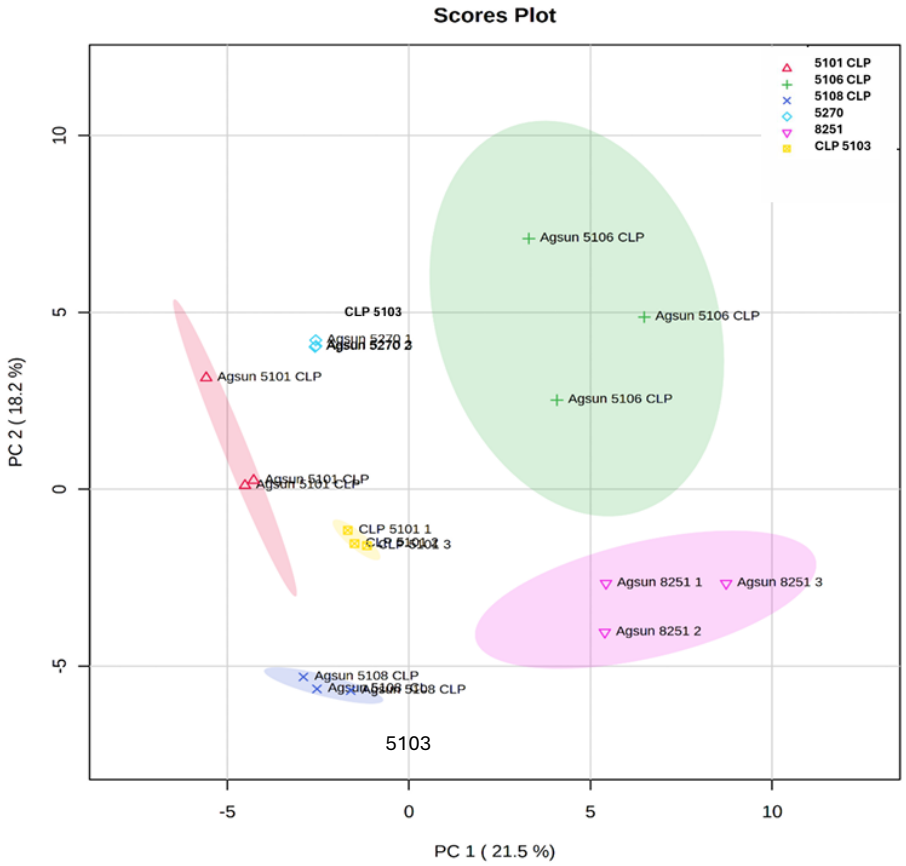

Figure 1. Principle component analysis (PCA) plot of phenolic compounds present in the six investigated sunflower seed cultivars.

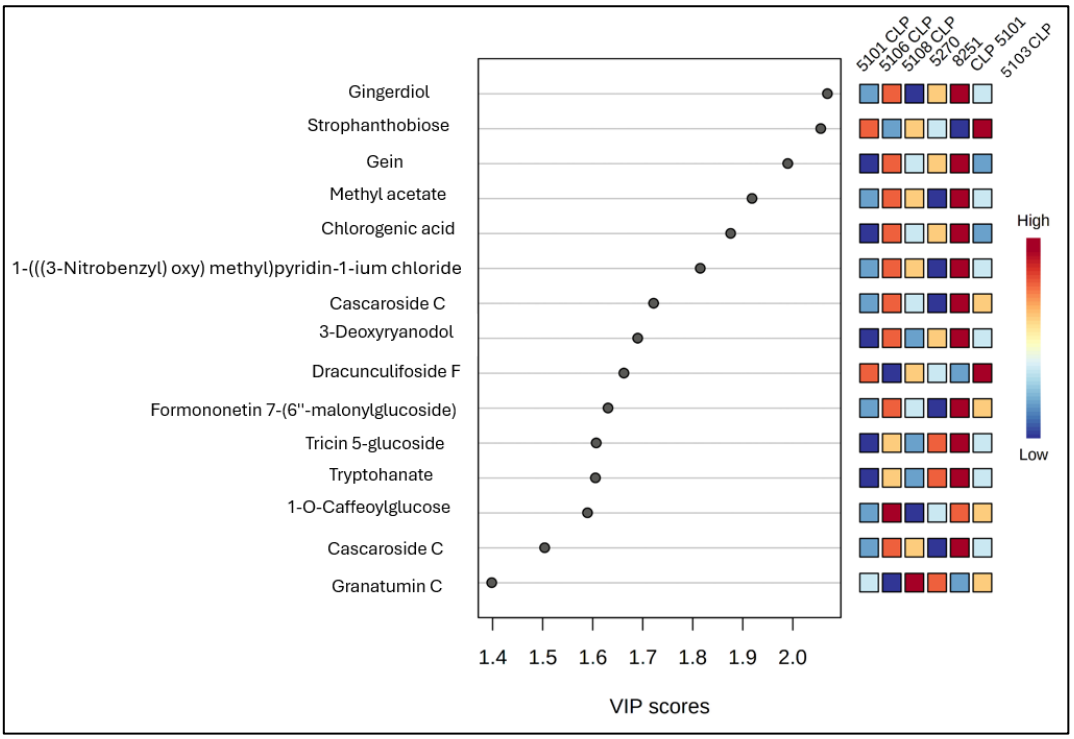

Figure 2. Variable Importance in Projection (VIP) plot displaying important features identified in the six investigated sunflower seeds cultivars of sunflower seeds by PLS-DA.

3.2 Drug-likeness screening of the identified compounds present in sunflower seeds.

After identifying 94 metabolites in sunflower seeds, a drug-likeness assessment using Lipinski's Rule of Five (Ro5) revealed that 84 compounds adhered to the criteria, with one or no violations (Supplementary Table S3).

3.3 Molecular docking

A total of 84 metabolites of sunflower seed that passed the Lipinski's Ro5 were screened against diabetic enzymes, AAMY, AGLU, AR, DPP-4, PTP1B and SDH (Supplementary table S4). Through molecular docking analysis, the top five promising metabolites with superior binding fitness compared to established standards for each of the six diabetic targets was identified (Table 2).

For AAMY and AGLU, FOX B and SAC A displayed the most favourable docking score of -9.6 kcal/mol and -9.1 kcal/mol respectively, exceeding the reference standard **acarbose (AAMY: -7.4 kcal/mol; AGLU: -7.8 kcal/mol)**. ISOM B (-8.5 kcal/mol) emerged as the top candidate against AR, surpassing the reference inhibitor ESPAL (-8.2 kcal/mol). Similarly, several sunflower seed metabolites showed stronger binding affinity to PTP1B and DPP-4 than the standard drugs ursolic acid and sitagliptin, respectively. ISOM B and 7-MET, in particular, exhibited the highest binding fitness with docking scores of -8.0 kcal/mol and -9.6 kcal/mol, respectively against PTP1B and DDP4. Additionally, PYR demonstrated the most negative docking score of -10.2 kcal/mol against SDH, while the standard **[2-1R-hydroxy-ethyl)-pyrimidin-4-yl]piperazine-1-sulfonic acid dimethylamide (4-PSD)** had a docking score of -7.0 kcal/mol.

Table 1: Docking scores of the top five hits from metabolites of sunflower seeds against each key enzyme. For each target the compounds are compared to the standard (italized), with the top performing compound is bolded.

Compound	**Docking score (kcal/mol)**
AAMY	
Acarbose (ACARB)	*-7.4*
Granatumin C (GRA C)	-8.8

(2S)-6-(gamma, gamma-dimethylallyl)-3',4'-dimethoxy-6",6"-dimethylpyran [2",3":7,8] flavanone (FLAV)	-9.5
Formoxanthone B (FOX B)	**-9.6**
Sonchuside I (SON I)	-8.7
4α,6S,7α)-6α-[6-O-(4-Hydroxybenzoyl)-β-D-glucopyranosyloxy]-7β-methyloctahydrocyclopenta[c]pyran-1-one) (PYR)	-8.9
AGLU	
Acarbose (ACARB)	*-7.8*
Granatumin C (GRA C)	-8.7
Formoxanthone B (FOX B)	-8.9
Sacranoside A (SAC A)	**-9.1**
3-O-caffeolyl-4-O-methylquinic acid (CMQ)	-8.4
Ptelatoside A (PLT A)	-8.2
AR	
Epalrestat (ESPAL)	*-8.2*
Formoxanthone B (FOX B)	-7.4
Sonchuside I (SON I)	-7.5
Ptelatoside A (PLT A)	-7.3
7-Methoxyisomorellinol (7-MET)	-7.7
Isomoreollin B (ISOM B)	**-8.5**
PTP1B	
Ursolic acid (URS)	*-6.5*
Granatumin C (GRA C)	-7.4
Formoxanthone B (FOX B)	-7.4
Isomoreollin B (ISOM B)	**-8.0**
Chlorogenic acid (CGA)	-6.9
Icariside (ICAR)	-6.9
DPP-4	
Sitagliptin (SITA)	*-8.4*
Granatumin C (GRA C)	-9.1
(2S)-6-(gamma,gamma-dimethylallyl)-3',4'-dimethoxy-6",6"-dimethylpyran [2",3":7,8] flavanone (FLAV)	-9.1

4α,6S,7α)-6α-[6-O-(4-Hydroxybenzoyl)-β-D-glucopyranosyloxy]-7β-methyloctahydrocyclopenta[c]pyran-1-one) (PYR)	-8.8
7-Methoxyisomorellinol (7-MET)	**-9.6**
Chlorogenic acid (CGA)	-9.0
SDH	
4-[2-1R-hydroxy-ethyl)-pyrimidin-4-yl] piperazine-1-sulfonic acid dimethylamide (4-PSD)	*-7.0*
(2S)-6-(gamma,gamma-dimethylallyl)-3',4'-dimethoxy-6",6"-dimethylpyran [2",3":7,8] flavanone (FLAV)	-9.6
Formoxanthone B (FOX B)	-10.1
Sonchuside I (SON I)	-9.0
4α,6S,7α)-6α-[6-O-(4-Hydroxybenzoyl)-β-D-glucopyranosyloxy]-7β-methyloctahydrocyclopenta[c]pyran-1-one) (PYR)	**-10.2**
Sacranoside A (SAC A)	-9.3

The docking validation revealed the root mean square deviation (RMSD) of the docked ligands from the native inhibitor was 0.5 Å (Table 2).

Table 2: Docking validation illustrating superimposed complexes of key enzymes, with native ligand, top hit compound of sunflower seeds and enzyme standard. The superimposed complexes were simulated using UCSF Chimera version 1.16.

Superimposed complexes	**Description**
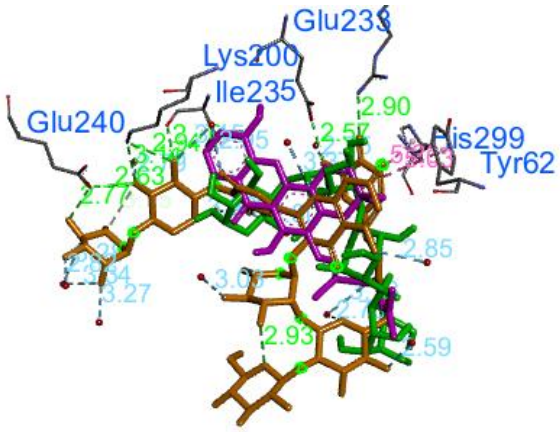	**AAMY:** Native ligand-montbretin A(orange), top hit compound, FOX B (purple), acarbose, (green). RMSD value = 0.5 Å Grid box: Centre (X= -8.37902; Y=5.11163; Z=-17.9775) and

	Size (X=28.4137; Y=21.6333; Z=50.039).
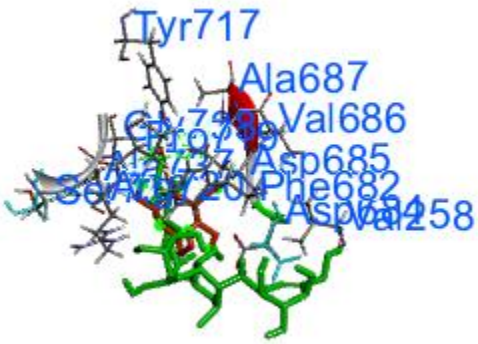	**AGLU:** Native ligand - 2-acetamido-2-deoxy-β--D-glucopyranose (orange), top hit compound, SAC A (purple), acarbose (green). RMSD value = 0.5 Å Grid box: Centre (X= 25.2629; Y= -11.5963; Z= -31.7004) and Size (X= 32.6229; Y= 24.9258; Z= 74.929).
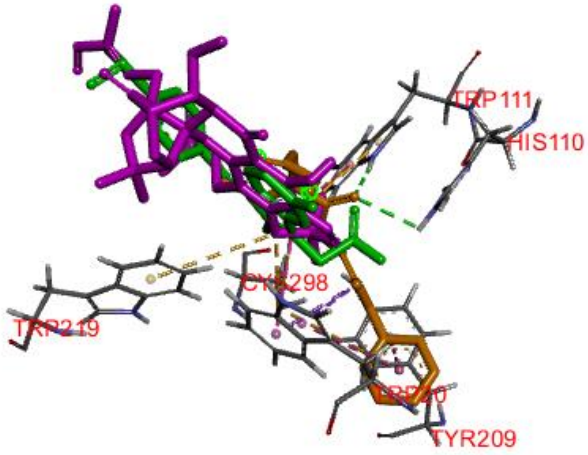	**AR:** Native ligand-Sulindac (orange), top hit compound, ISOM B (purple), espalrestat (green). RMSD value = 0.5 Å Grid box: Centre (X= -4.89047; Y= 6.77641; Z= 16.335) and Size (X= 16.5289; Y= 14.2287; Z= 49.548).

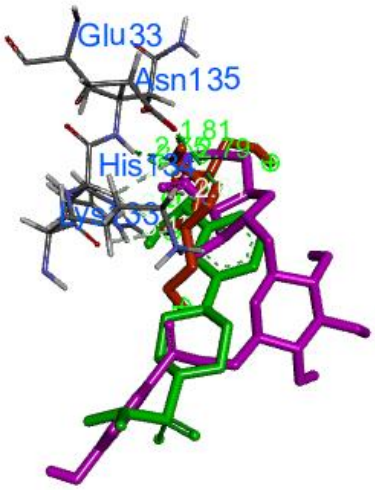	**SDH:** Native ligand - sorbitol(orange), top hit compound, PYR (purple), 4-[2-1R-hydroxy-ethyl)-pyrimidin-4-yl]piperazine-1-sulfonic acid dimethylamide (green). RMSD value = 0.5 Å Grid box: Centre (X= 103.729; Y= 39.5604; Z= 40.3469) and Size (X= 17.4934; Y= 19.6047; Z= 75.9217).
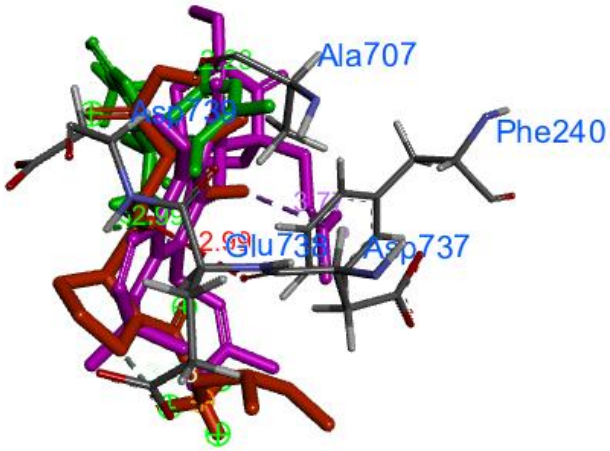	**DPP-4:** Native ligand - Diprotin A (orange), top hit compound, 7-MET (purple), sitagliptin (green). RMSD value = 0.5 Å Grid box: Centre (X= 67.7118; Y= 53.9458; Z= 30.954) and Size (X= 20.9202; Y= 20.1081; Z= 77.56).
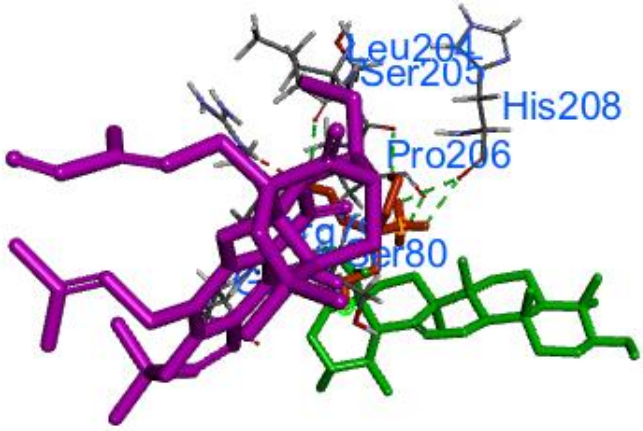	**PTP1B:** Native ligand - 2-Amino-2-hydroxymethyl-propane-1,3-diol (orange), top hit compound, ISOM B (purple), ursolic acid (green). RMSD value = 0.5 Å Grid box:

	Centre (X= 48.3518; Y= 14.7724; Z= 3.5455) and Size (X= 12.2589; Y= 8.73703; Z= 38.171).

3.4 Molecular dynamic simulation analysis

3.4.1 Thermodynamic analysis

Post molecular docking analysis, the top five hits against each enzyme were subjected to 150 ns molecular dynamic simulation. The thermodynamic analysis (Table 3) revealed that SAC-AGLU (-40.10 kcal/mol), PLT-AR (-58.84 kcal/mol), CGA-PTP1B (-24.32 kcal/mol), PYR-DPP-4 (-37.93 kcal/mol) and SAC A-SDH (-49.03 kcal/mol) complexes had the highest negative binding free energy amongst the complexes formed by the top five hits for each enzyme, outperforming the standards **ACARB-AGLU (-16.55 kcal/mol), ESPAL-AR (-13.18 kcal/mol), URS-PTP1B (-18.29 kcal/mol), SITA-DPP-4 (-21.15 kcal/mol)** and **4-PSD-SDH** (-41.24 kcal/mol), respectively. On the other hand, against AAMY, SON-AAMY (-47.26 kcal/mol) performed favourably well with the standard, **ACARB-AMY (-49.08 kcal/mol)**.

Table 3: Thermodynamic analysis of the top-hits from sunflower seed metabolites against key enzymes after 150 ns MD simulation period. For each enzyme, the top metabolites are compared to the standard (italized), with the top performing compound bolded.

Energy components					
AAMY					
Complexes	**ΔE_{vdW}**	**ΔE_{elec}**	**ΔG_{gas}**	**ΔG_{solv}**	**ΔG_{bind}**
ACARB-AAMY	*-51.82 ± 5.30*	*-132.83 ± 15.05*	*184.65 ± 14.87*	*135.57± 10.04*	*-49.08 ±7.99*
FLAV-AAMY	-31.58 ± 4.22	-5.67 ± 4.28	-37.24 ± 6.09	16.92 ± 3.73	-20.32 ± 3.53
FOX-AAMY	-42.00 ± 3.96	-11.87 ± 7.52	-52.87 ± 9.69	21.92 ± 5.55	-31.95 ± 5.00
GRA-AAMY	-49.38 ± 11.80	-9.87 ± 6.40	-59.25 ± 11.35	24.86 ± 4.94	-34.39 ± 10.27
PYR-AAMY	-34.21 ± 3.91	-40.87 ± 5.79	-75.09 ± 6.43	37.72 ±.14	-37.37 ± 4.14
SON-AAMY	-38.20 ± 5.69	-47.35 ± 10.32	-92.95 ± 12.00	45.69 ± 5.62	**-47.26 ± 8.51**
AGLU					
ACARB-AGLU	*-31.65 ± 5.14*	*-161.96 ± 22.73*	*-193.60 ± 23.50*	*177.06 ± 20.09*	*-16.55 ± 6.71*

CMQ-AGLU	-21.73 ± 4.54	-19.14 ± 11.86	-40.87 ± 13.63	26.20 ± 9.81	-14.67 ± 5.73
FOX B-AGLU	-39.11 ± 4.20	-8.95 ± 9.66	-48.06 ± 9.36	19.69 ± 6.04	-28.37 ± 4.85
GRA-AGLU	-17.88 ± 3.56	-17.76 ± 9.26	-37.89 ± 11.63	25.21 ± 7.34	-12.34 ± 3.21
PLT-AGLU	-18.24 ± 3.65	-18.43 ± 8.54	-39.43 ± 12.87	24.54 ± 8.86	-13.23 ± 5.62
SAC-AGLU	-37.07 ± 4.56	-45.22 ± 11.22	-82.28 ± 10.63	42.19 ± 8.54	**-40.10 ± 8.01**
AR					
ESPAL-AR	*-18.59 ± 4.57*	*-5.45 ± 7.21*	*-24.04 ± 7.72*	*10.86 ± 5.71*	*-13.18 ± 3.80*
7-MET-AR	-17.49 ± 7.94	-2.01 ± 3.58	-19.50 ± 9.79	7.80 ± 5.15	-11.69 ± 6.01
FOX B-AR	-41.78 ± 7.24	-8.07 ± 4.61	-49.85 ± 7.99	19.71 ± 3.86	-30.14 ± 7.01
ISOM-AR	-37.48 ± 4.72	-10.24 ± 6.86	-47.72 ± 9.55	21.08 ± 6.12	-26.64 ± 5.03
PLT-AR	-48.29 ± 4.17	-55.22 ± 11.07	-103.51 ± 10.66	44.67 ± 6.83	**-58.84 ± 6.03**
SON-AR	-35.99 ± 4.21	-24.37 ± 10.55	-67.97 ± 10.63	34.37 ± 7.12	-33.70 ± 5.50
PTP1B					
URS-PTP1B	*-30.96 ± 4.37*	*15.50 ± 5.18*	*-39.87 ± 7.53*	*21.57 ± 4.85*	*-18.29 ± 5.27*
CGA-PTP1B	-15.75 ± 3.98	-43.43 ± 9.56	-59.18 ± 8.66	34.86 ± 6.71	**-24.32 ± 4.37**
FLAV-PTP1B	-27.02 ± 6.53	-10.95 ± 5.06	-37.96 ± 10.09	17.00 ± 4.11	-20.96 ± 6.81
GRA-PTP1B	-25.10 ± 5.15	-3.00 ± 7.38	-28.10 ± 8.81	11.59 ± 6.83	-16.51 ± 4.24
ICAR-PTP1B	-24.05 ± 6.37	-31.28 ± 19.58	-55.33 ± 21.85	35.52 ± 15.56	-19.81 ± 7.79
ISOM-PTP1B	-30.80 ± 4.33	-2.25 ± 4.76	33.05 ± 7.06	13.05 ± 4.90	-20.00 ± 4.49
DPP-4					
SITA-DPP-4	*-27.59 ± 4.91*	*-256.08 ± 57.39*	*-283.67 ± 57.05*	*262.52 ± 50.67*	*-21.15 ± 7.99*
7-MET-DPP-4	-40.80 ± 5.12	-8.34 ± 4.51	-49.15 ± 6.87	22.18 ± 4.56	-26.97 ± 4.12
CGA-DPP-4	-27.08 ± 4.54	-49.20 ± 13.03	-72.27 ± 11.90	48.16 ± 7.62	-24.11 ± 6.84
FLAV-DPP-4	-42.96 ± 5.37	-12.87 ± 4.62	-55.84 ± '-5.97	26.52 ± 3.85	-29.32 ± 3.97
GRA-DPP-4	-36.75 ± 4.76	-30.18 ± 9.00	-66.93 ± 9.35	45.17 ± 8.24	-21.76 ± 4.45
PYR-DPP-4	-32.41 ± 4.77	-55.67 ± 15.83	-88.09 ± 16.12	50.16 ± 9.76	**-37.93 ± 8.16**
SDH					
4-PSD-SDH	*-32.62 ± 5.69*	*-12.81 ± 6.22*	*-49.44 ± 9.36*	*8.19 ± 5.02*	*-41.24 ± 9.19*
FLAV-SDH	-47.36 ± 3.86	-8.90 ± 4.01	-56.26 ± 5.64	23.01 ± 3.53	-33.25 ± 3.96
FOX B-SDH	-41.49 ± 2.74	-6.61 ± 5.43	-48.11 ± 6.05	16.63 ± 4.28	-31.48 ± 3.29
PYR-SDH	-46.63 ± 4.92	-55.16 ± 16.00	-101.79 ±13.15	55.14 ± 10.03	-46.65 ± 5.28

SAC A-SDH	-38.91 ± 5.94	-66.06 ± 14.30	-104.97 ± 14.64	56.94 ± 8.43	**-48.03 ± 8.01**
SON-SDH	-37.41 ± 5.98	-31.20 ± 10.62	-76.17 ± 14.35	38.36 ± 7.74	-37.80 ± 8.37

3.4.2 Post-molecular dynamic data analysis

Alpha-amylase (AAMY) complexes achieve convergence after 30 ns, all bound complexes, including the reference standard ACARB-AAMY (1.69 Å), exhibited increased average RMSD values compared to the unbound enzyme (1.33 Å) but still < 3 Å (Figure 3A). Among the metabolites, GRA C-AAMY displayed the most stable conformation, evidenced by the lowest RMSD (1.48 Å) and RMSF (0.89 Å) values. Conversely, PYR-AAMY and FLAV-AAMY showed increased residue fluctuations, particularly within residue ranges 225-250, 300-315, and 340-350 (illustrated in Figure 3B). Ligand-binding also affected RoG and SASA of the AAMY complexes. GRA C-AAMY displayed the lowest RoG value (2.16 Å) compared to APO-AAMY (2.23 Å) seen in Figure 3C and Table 4. Additionally, GRA C-AAMY visibly exhibited the lowest SASA value (14145.75 Å) as seen in Figure 3D, compared to both the unbound enzyme (17308.04 Å) and the acarbose complex (17389.18 Å). Finally, the average number of intramolecular hydrogen bonds formed within the AAMY complexes greatly increased upon ligand binding, apart from GRA C-AAMY and FLAV-AAMY illustrated in Figure 3E.

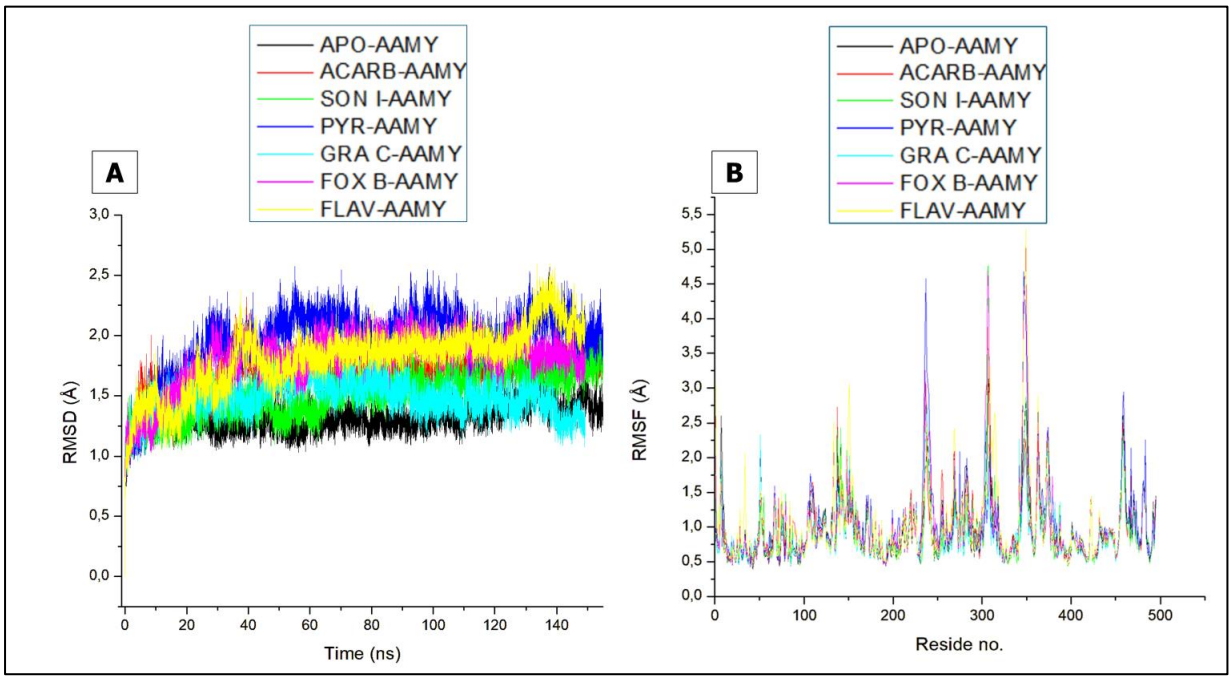

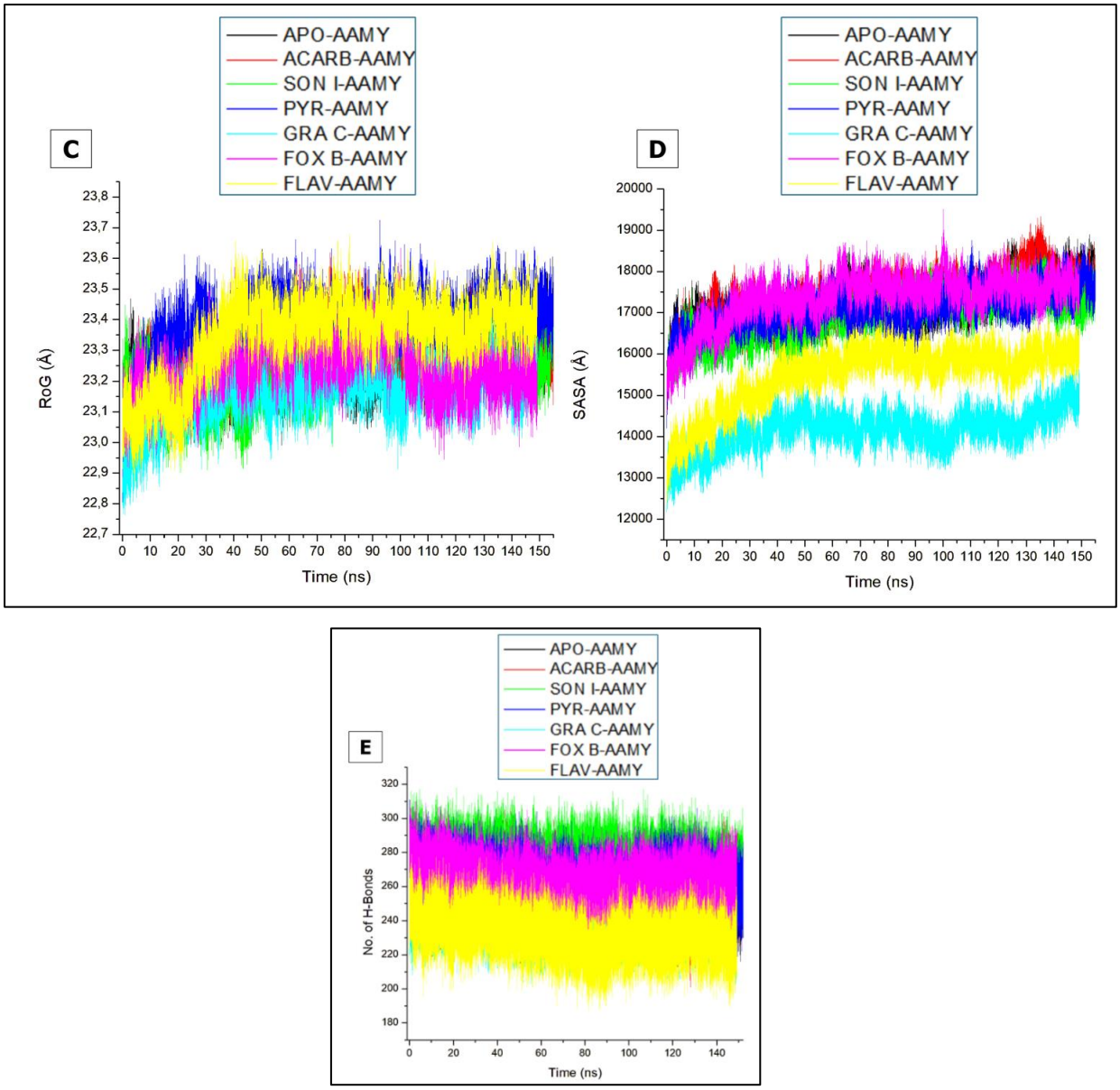

Figure 3. Comparative A) RMSD, B) RMSF, C), RoG, D) SASA, and E) No. of H-bonds of alpha carbon, reference standard and top five hit metabolites of sunflower seeds against AAMY after 150 ns MD simulation

Table 4: Post-molecular dynamic simulation parameters of top-hit metabolites of sunflower seeds against AAMY.

Complexes	No. of H-BONDS	RMSD (Å)	RMSF (Å)	RoG (Å)	SASA (Å)
APO-AAMY	*252.08 ± 10.37*	*1.33 ± 0.12*	*0.97 ± 0.47*	*23.27 ± 0.09*	*17308.04 ± 510.71*
ACARB	*259.22 ± 10.77*	*1.69 ± 0.16*	*0.97 ± 0.45*	*23.29 ± 0.08*	*17389.18 ± 547.05*
SON	273.69 ± 10.65	1.54 ± 0.19	0.94 ± 0.45	23.24 ± 0.09	16953.55 ± 537.45
PYR	261.57 ± 10.72	1.96 ± 0.26	1.03 ± 0.57	23.3 ± 0.10	17141.20 ± 479.40
GRA	243.36 ± 9.87	1.48 ± 0.14	0.89 ± 0.38	23.16 ± 0.08	14145.75 ± 455.10

FOX	262.27 ± 10.85	1.80 ± 0.22	1.00 ± 0.60	23.24 ± 0.09	17335.15 ± 591.62
FLAV	231.49 ± 11.09	1.81 ± 0.26	1.03 ± 0.61	23.35 ± 0.13	15474.02 ± 726.11

All AGLU bound complexes reached convergence in RMSD within 20 ns and maintained system equilibrium as shown in Figure 4A. The average RMSD of all bound complexes was < 3 Å throughout the simulations. Notably, SAC A-AGLU (1.50 Å) exhibited the lowest RMSD values compared to the unbound enzyme (1.73 Å) (Table 5). Moreover, only SAC A-AGLU (0.95 Å) and PLT-AGLU (0.98 Å) showed a decrease in residue fluctuations compared to the unbound enzyme (0.99 Å). Conversely, GRA-AGLU and CMQ-AGLU resulted in a slight increase in average RoG compared to the unbound enzyme. The FOX-AGLU complex, however, maintained a similar RoG value as the unbound enzyme. SASA analysis, revealed that SAC-AGLU (29357.24 Å) saw the most comparable reduction amongst the metabolites relative to the ACARB-AGLU (29310.02 Å). While there was significant increase in the number of intracellular H-Bonds, FOX-AGLU (427.64 H-Bonds) and CMQ-AGLU (427.40 H-Bonds) were the metabolites with the highest number hydrogen bonds relative to acarbose (428.88 H-Bonds) and unbound enzyme (428.88 H-Bonds) (Figure 4E).

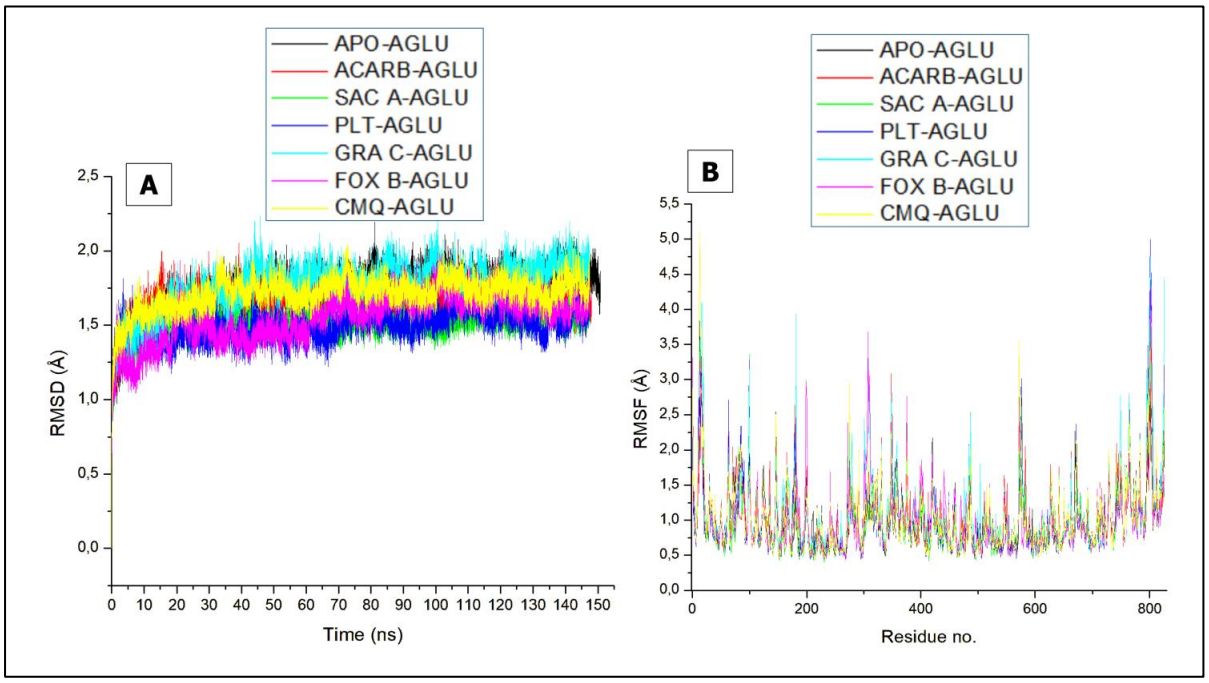

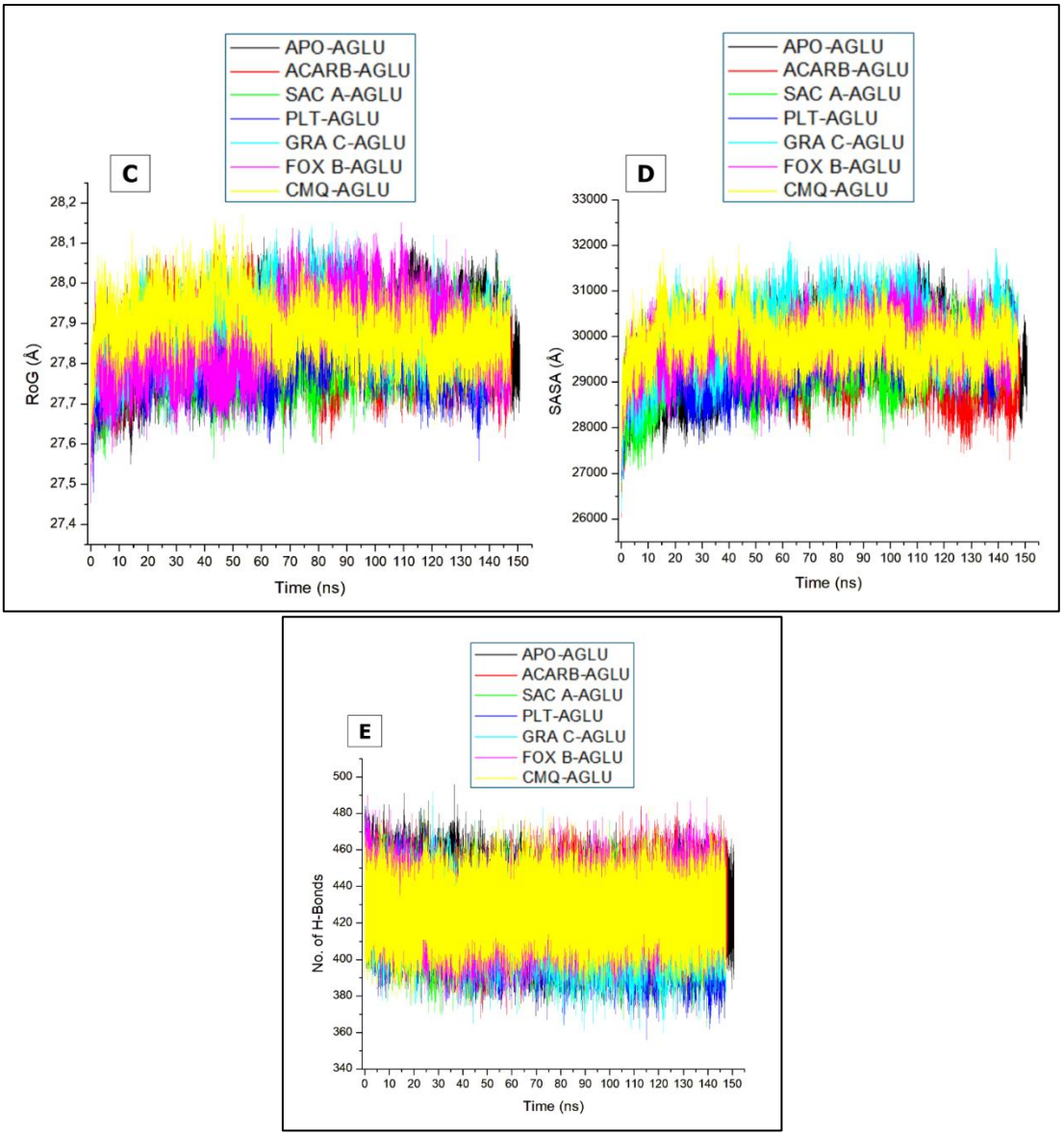

Figure 4. Comparative: A) RMSD, B) RMSF, C), RoG, D) SASA, and E) No. of H-bonds of alpha-carbon, reference standard and top five hit metabolites of sunflower seed cultivars against AGLU after 150 ns MD simulation.

Table 5: : Post-molecular dynamic simulation parameters of top-hit metabolites of sunflower seeds against AGLU.

Complexes	No. of H-BONDS	RMSD (Å)	RMSF (Å)	RoG (Å)	SASA (Å)
APO-AGLU	*428.83 ± 13.92*	*1.73 ± 0.16*	*0.99 ± 0.44*	*27.87 ± 0.08*	*29673.35 ± 680.11*
ACARB	*428.88 ± 13.43*	*1.64 ± 0.10*	*1.02 ± 0.46*	*27.84 ± 0.07*	*29310.02 ± 541.10*
SAC	421.11 ± 12.19	1.51 ± 0.09	0.95 ± 0.47	27.81 ± 0.06	29357.24 ± 549.82
PLT	418.90 ± 13.73	1.50 ± 0.10	0.98 ± 0.51	27.82 ± 0.06	29486.08 ± 515.49

GRA	420.11 ± 13.72	1.77 ± 0.17	1.10 ± 0.59	27.88 ± 0.07	30066.03 ± 668.55
FOX	427.64 ± 13.53	1.55 ± 0.16	1.01 ± 0.51	27.87 ± 0.09	29798.17 ± 498.38
CMQ	427.40 ± 12.81	1.71 ± 0.11	1.02 ± 0.52	27.89 ± 0.06	29897.90 ± 458.12

Aldose reductase (AR) system achieved equilibrium within 20 ns and remained stable throughout the simulation until 110 ns where PLT-AR and ISOM-AR appears to diverge (Figure 5A). Regardless, the average RMSD for all bound complexes was <3.5 Å, with SON I-AR and ISOM-AR exhibiting the lowest value both at 1.46 Å, compared to the unbound enzyme (1.72 Å). SON I-AR and ISOM-AR also displayed the lowest RMSF value (0.95 and 0., and the system experienced minor fluctuations except at residues 225-235 (Figure 5B). Notably, RoG analysis revealed significant instability throughout the simulation for 7-MET-AR (Figure 5C). Remarkably, SON I-AR maintained the lowest RoG (19.19 Å) and SASA (12739.48 Å) values among all bound complexes, even compared to the standard drug, espalrestat (RoG- 19.38 Å; SASA- 13113.15 Å**)** and the unbound enzyme (RoG - 19.27 Å; SASA- 13172.31 Å), Table 6**.** While all complexes displayed a similar hydrogen bond pattern (Figure 5E), 7-MET-AR showed an increase in intracellular hydrogen bonds.

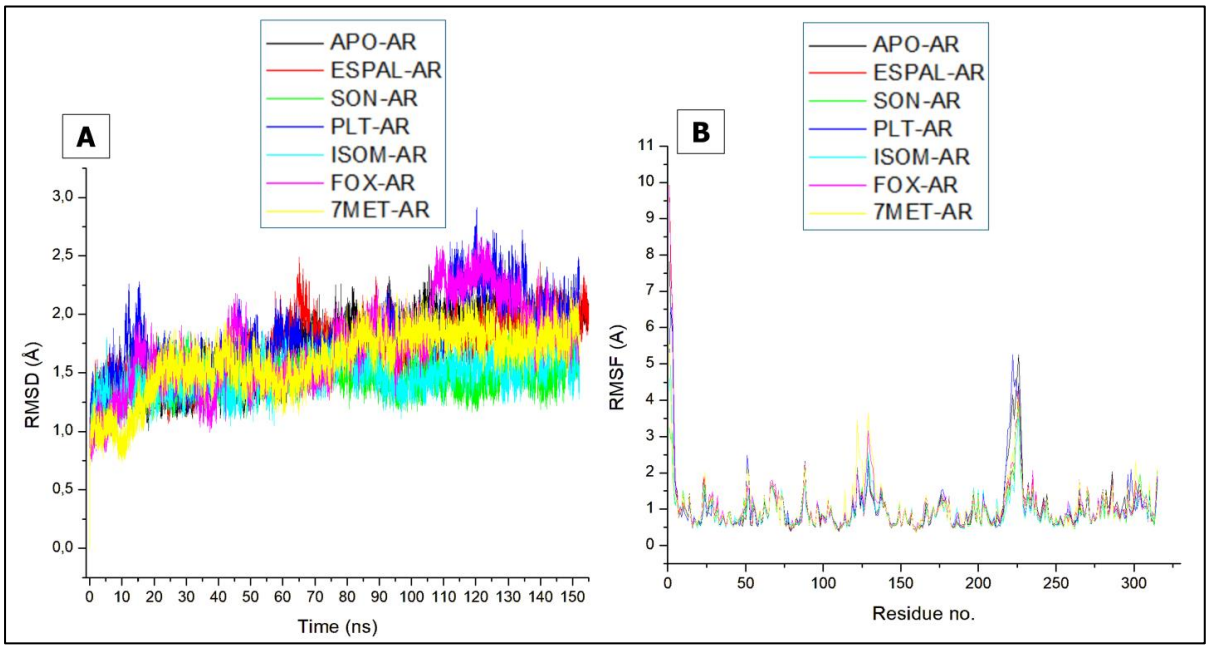

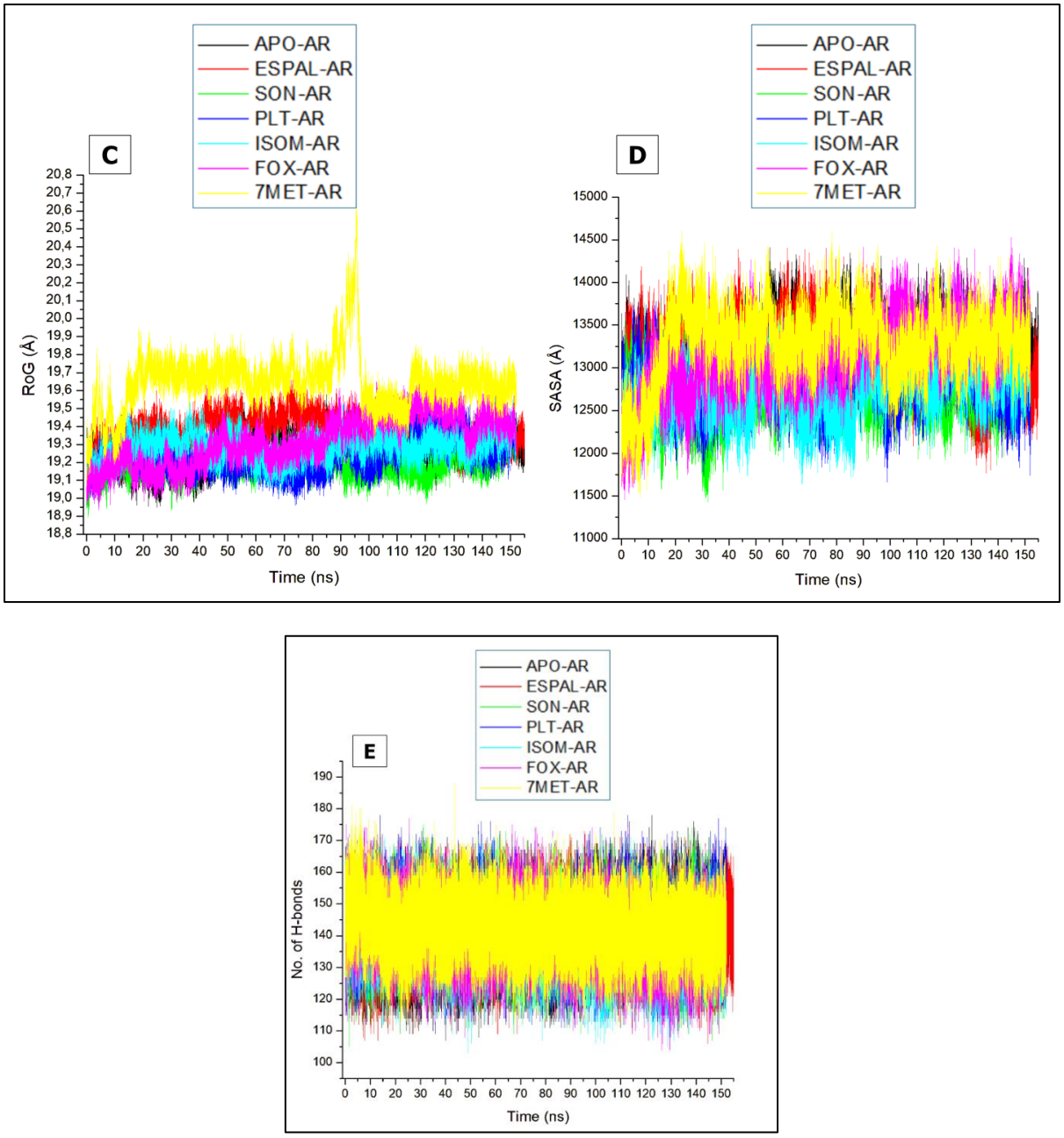

Figure 5. Comparative A) RMSD, B) RMSF, C), RoG, D) SASA, and E) No. of H-bonds of alpha carbon, reference standard and top five hit metabolites of sunflower seeds against AR after 150 ns

Table 6: : Post-molecular dynamic simulation parameters of top-hit metabolites of sunflower seeds against AGLU.

Complexes	No. of H-BONDS	RMSD (Å)	RMSF (Å)	RoG (Å)	SASA (Å)
APO-AR	*140.55 ± 8.1*	*1.72 ± 0.29*	*1.07 ± 0.84*	*19.27 ± 0.09*	*13172.31 ± 315.70*
ESPAL - AR	*140.26 ± 7.95*	*1.72 ± 0.25*	*1.04 ± 0.86*	*19.38 ± 0.08*	*13113.15 ± 341.32*

SON I- AR	141.71 ± 7.95	1.46 ± 0.14	0.95 ± 0.5	19.19 ± 0.06	12739.48 ± 290.92
PLT - AR	142.62 ± 8.13	1.80 ± 0.30	1.06 ± 0.81	19.24 ± 0.09	12853.91 ± 297.49
ISOM - AR	138.83 ± 8.13	1.46 ± 0.15	0.97 0.51	19.28 ± 0.07	12769.42 ± 318.76
FOX -B AR	140.87 ± 8.37	1.72 ± 0.36	1.11 ± 0.86	19.32 ± 0.14	13135.51 ± 407.00
7-MET - AR	142.99 ± 8.1	1.6 ± 0.27	1.1 ± 0.65	19.65 ± 0.15	13288.28 ± 406.21

While all bound PTP1B complexes remained stable throughout the simulation with an average RMSD < 2 Å, ISOM-PTP1B exhibited the lowest structural fluctuations (RMSD = 1.12 Å, RMSF = 0.95 Å) compared to the apo form (RMSD = 1.44 Å, RMSF = 1.20 Å), Figure 6A and Table 7. Furthermore, ISOM-PTP1B displayed the largest solvent accessible surface area (SASA = 131411.94 Å²) compared to the reference (URS, 12860.75 Å²). In contrast, GRA C-PTP1B showed a unique divergence after 50 ns in all analyses (RMSD, RoG and SASA), Figure(s) 6A, C and E. Additionally, ISOM-PTP1B formed more hydrogen bonds (163.71) compared to the unbound enzyme (160.43). Uniquely, FLAV-PTP1B displayed the greatest reduction in RoG value of 19.24 Å.

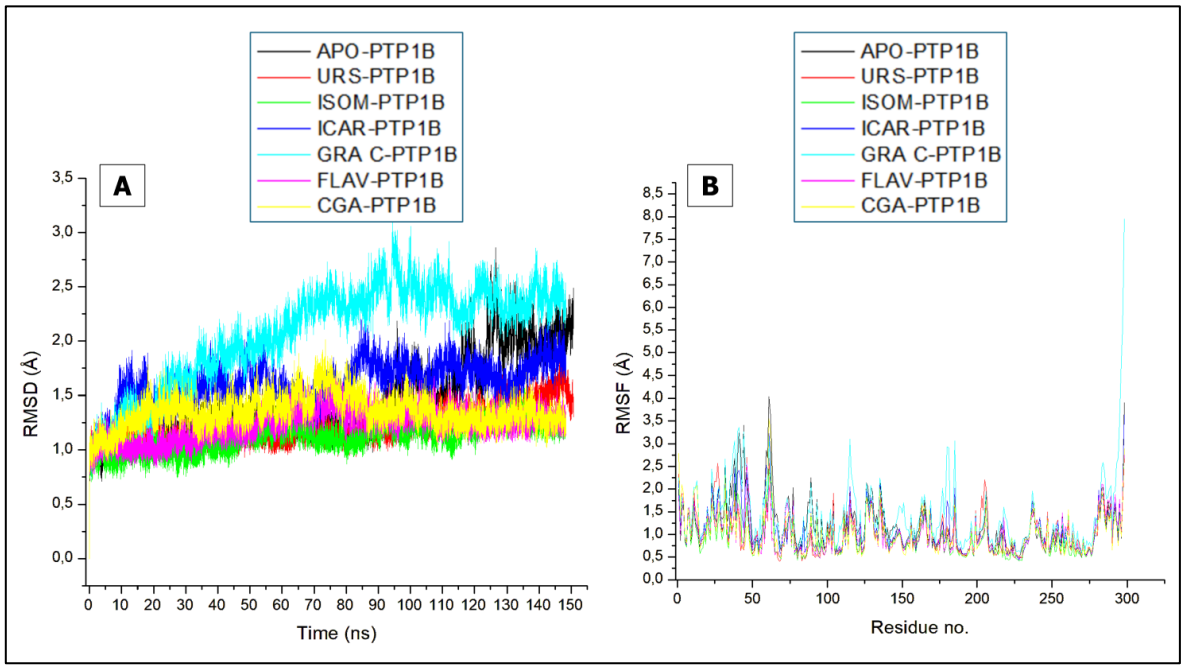

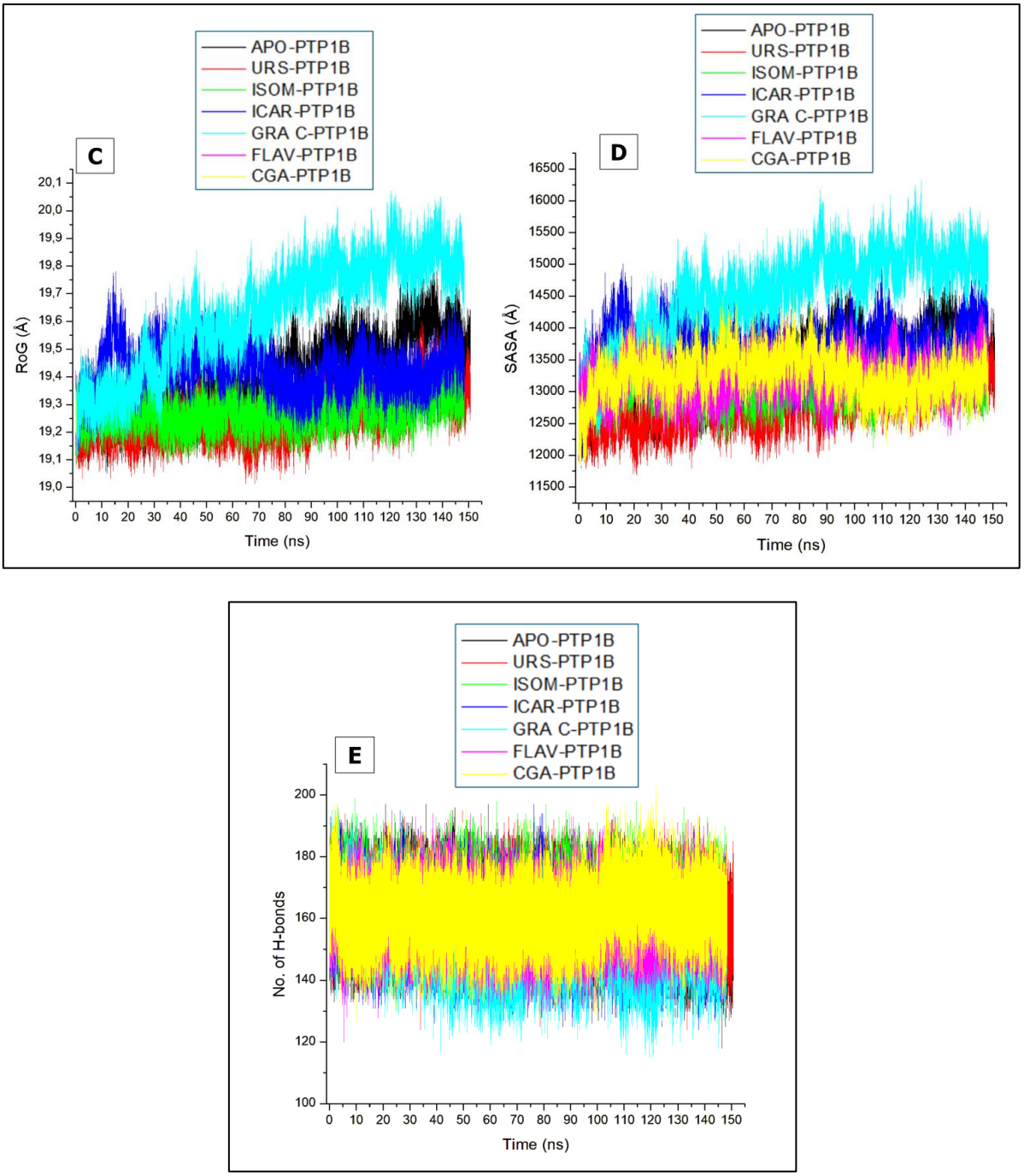

Figure 6. Comparative A) RMSD, B) RMSF, C), RoG, D) SASA, and E) No. of H-bonds of alpha carbon, reference standard and top five hit metabolites of sunflower seeds against PTP1B after 150 ns MD simulation.

Table 7: : Post-molecular dynamic simulation parameters of top-hit metabolites of sunflower seeds against PTP1B.

Complexes	No. of H-BONDS	RMSD (Å)	RMSF (Å)	RoG (Å)	SASA (Å)
APO-PTP1B	*160.43433 ± 8.56*	*1.44 ± 0.36*	*1.20 ± 0.59*	*19.40 ± 0.13*	*13329.16 ± 471.35*

URS	*161.28 ± 8.12*	*1.22 ± 0.15*	*1.04 ± 0.47*	*19.26 ± 0.08*	*12860.75 ± 363.50*
ISOM	163.71 ± 8.30	1.122 ± 0.13	0.95 ± 0.42	19.28 ± 0.05	13141.94 ± 252.79
ICAR	158.84 ± 8.29	1.61 ± 0.2	1.10 ± 0.49	19.43 ± 0.08	13703.37 ± 355.94
GRA	152.53 ± 9.28	2.07 ± 0.45	1.42 ± 0.77	19.63 ± 0.19	14526.80 ± 666.37
FLAV	160.68 ± 7.98	1.23 ± 0.14	1.01 ± 0.42	19.24 ± 0.05	13194.84 ± 284.81
CGA	162.12 ± 8.52	1.35 ± 0.14	1.00 ± 0.48	19.26 ± 0.04	13248.84 ± 312.98

The DPP-4 enzyme system reached equilibrium within 15 ns and remained stable throughout the simulation (Figure 7A). All bound complexes displayed an average RMSD below 3.5 Å, with 7-MET-DPP-4 exhibiting the lowest (1.98 Å) compared to the unbound enzyme (2.21 Å) (Table 8). Both CGA-DPP-4 and 7MET-DPP-4 had the lowest RMSF (1.17 Å), surpassing the standard (SITA-DPP-4, 1.43 Å) and unbound enzyme (1.23 Å). Notably, residues 200-230 showed some fluctuation, while negligible fluctuation is observed at the rest of the residual amino acids (Figure 7B)**.** RoG analysis saw increased in compactness measure by identified PYR-DPP-4 (26.72 Å), followed by 7-MET-DPP-4 (27.05 Å) and GRA-DPP-4 (27.05 Å). SASA analysis revealed a decrease in surface area for all complexes except CGA-DPP-4 (30017.08 Å) compared to SITA-DPP-4 and the unbound enzyme (30094.84 Å). H-Bond analysis showed an increase for CGA-DPP-4 (384.41 H-Bond) compared to SITA-DPP-4 (381.54 H-Bonds).

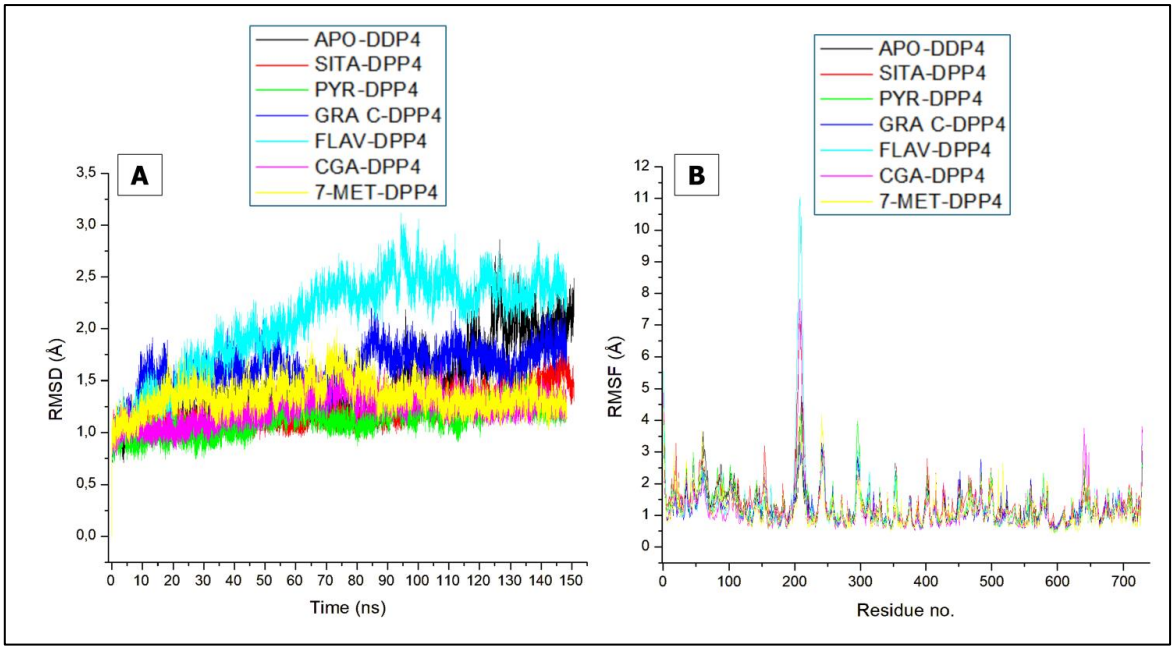
A
APO-DDP4
SITA-DPP4
PYR-DPP4
GRA C-DPP4
FLAV-DPP4
CGA-DPP4
7-MET-DPP4
RMSD (Å)
Time (ns)
B
RMSF (Å)
Residue no.

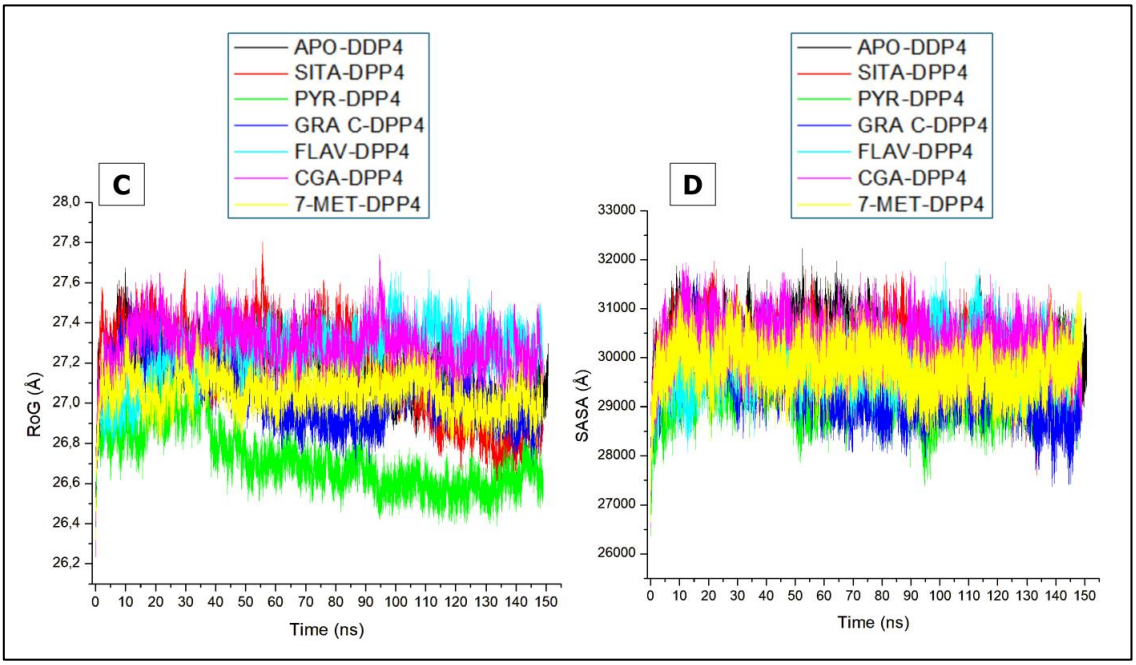
C
APO-DDP4
SITA-DPP4
PYR-DPP4
GRA C-DPP4
FLAV-DPP4
CGA-DPP4
7-MET-DPP4
RoG (Å)
Time (ns)
D
SASA (Å)
Time (ns)

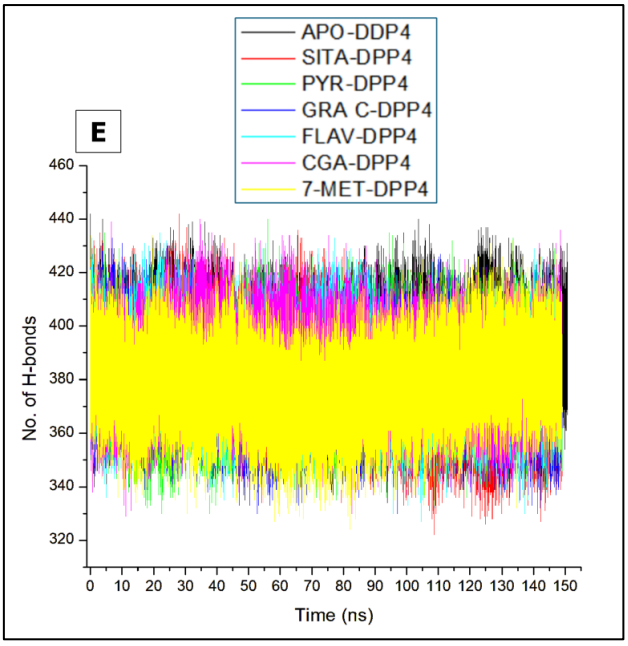

Figure 7. Comparative A) RMSD, B) RMSF, C), RoG, D) SASA, and E) No. of H-bonds of alpha carbon, reference standard and top five hit metabolites of sunflower seeds against DPP-4 after 150 ns

Table 8: : Post-molecular dynamic simulation parameters of top-hit metabolites of sunflower seeds against DPP-4.

Complexes	No. of H-BONDS	RMSD (Å)	RMSF (Å)	RoG (Å)	SASA (Å)
APO-DPP-4	*388.63 ± 12.68*	*2.21 ± 0.211*	*1.23 ± 0.57*	*27.16 ± 0.14*	*30094.84 ± 517.67*
SITA-DPP-4	*381.54 ± 13.93*	*2.48 ± 0.32*	*1.42 ± 0.75*	*27.17 ± 0.22*	*30017.08 ± 484.25*
PYR-DPP-4	381.87 ± 12.39	2.26 ± 0.26	1.27 ± 0.61	26.72 ± 0.15	29379.95 ± 479.71
GRA-DPP-4	380.27 ± 12.51	2.49 ± 0.17	1.21 ± 0.50	27.05 ± 0.15	29444.51 ± 534.02
FLAV-DPP-4	382.85 ± 12.79	2.63 ± 0.42	1.28 ± 1.04	27.25 ± 0.14	29917.47 ± 466.55
CGA-DPP-4	384.41 ± 12.49	2.44 ± 0.29	1.17 ± 0.76	27.28 ± 0.12	30275.69 ± 441.70
MET-DPP-4	378.44 ± 12.71	1.98 ± 0.11	1.17 ± 0.56	27.05 ±0.09	29811.76 ± 428.84

Sorbitol dehydrogenase (SDH) system attains converges by 8 ns and maintains equilibrium throughout the simulation, with an average < 3.5 Å, Figure 8A. Among the metabolites, FLAV-SDH had the lowest RMSD value of 2.42 Å compared to the unbound enzyme (2.56 Å). In contrast, SON I-SDH appeared to be the best compound amongst the top-ranked metabolites

for RMSF (Figure 8B), RoG (Figure 8C), SASA (Figure 8D), and H-bonds analysis (Figure 8E), retaining the lowest values compared to other bound complexes the reference standard and the unbound enzyme (Table 9). H-bonds also saw a noticeable increase in H-bonds post binding of SON I-SDH (170.13 H-bonds) compared to the unbound enzyme (167.06 H-bonds).

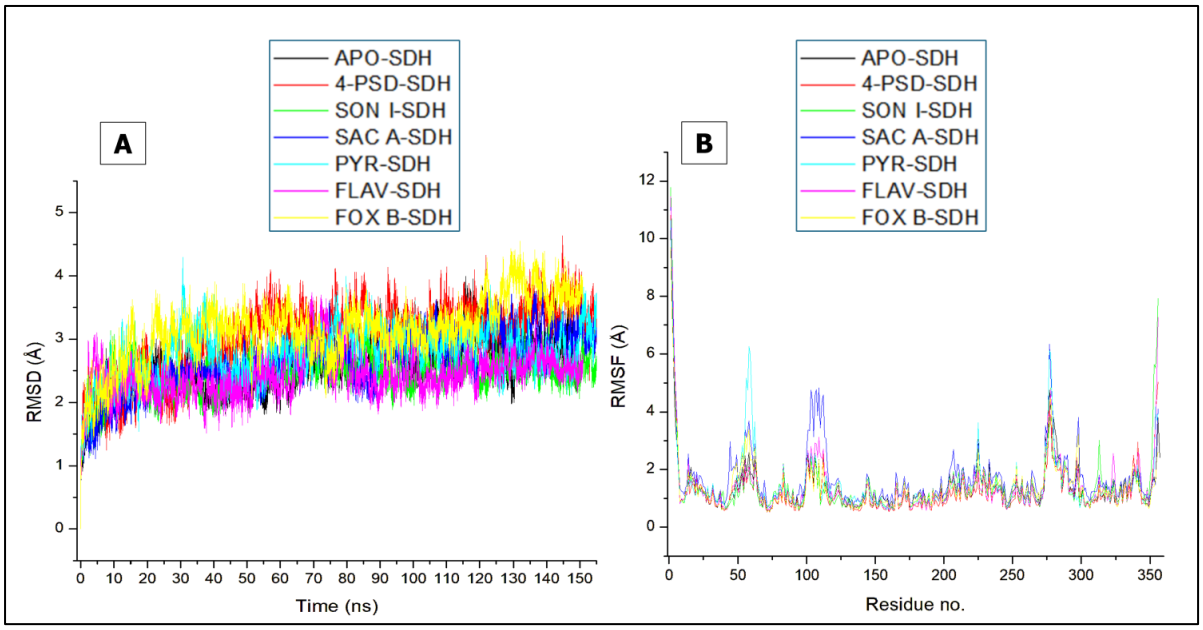

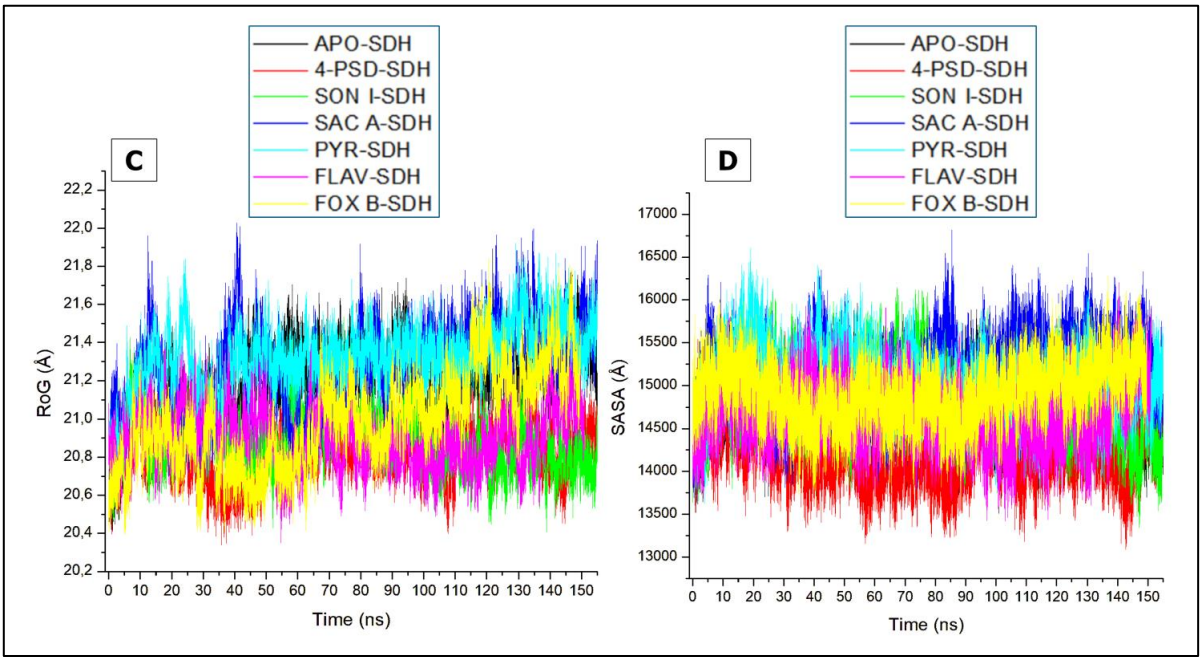

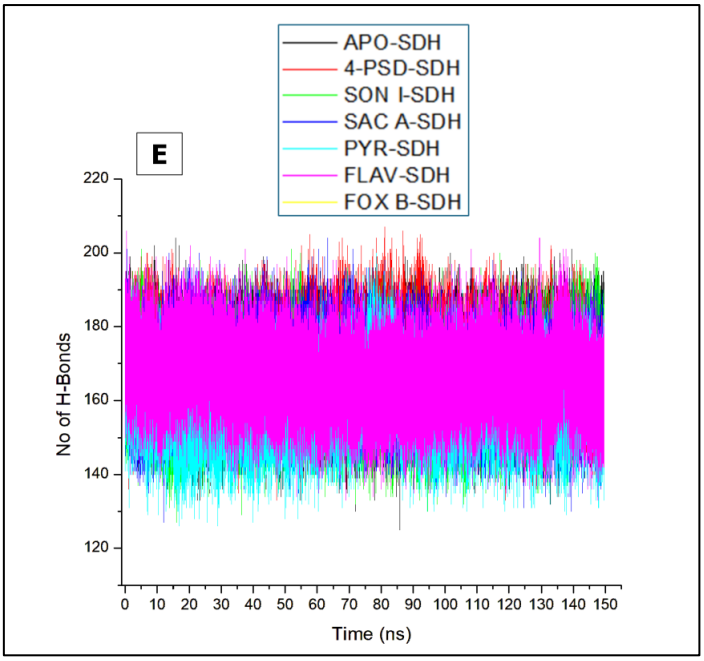

Figure 8. Comparative A) RMSD, B) RMSF, C), RoG, D) SASA, and E) No. of H-bonds of alpha carbon, reference standard and top five hit metabolites of sunflower seeds against SDH after 150 ns MD simulation.

Table 9: Post-molecular dynamic simulation parameters of top-hit metabolites of sunflower seeds against SDH.

Complexes	No. of H-BONDS	RMSD (Å)	RMSF (Å)	RoG (Å)	SASA (Å)
APO-SDH	*167.06 ± 8.52*	*2.56 ± 0.41*	*1.39 ± 0.88*	*20.99 ± 0.24*	*14909.03 ± 319.54*
STA-SDH	*166.81 ± 8.40*	*3.05 ± 0.54*	*1.37 ± 0.91*	*21.20 ± 0.19*	*14740.20 ± 289.45*
SON-SDH	170.13 ± 8.47	2.48 ± 0.29	1.27 ± 0.97	20.84 ± 0.13	14271.70 ± 328.77
SAC-SDH	164.51 ± 8.59	2.67 ± 0.45	1.42 ± 1.12	20.89 ± 0.14	14837.67 ± 365.52
PYR-SDH	165.91 ± 8.41	2.79 ± 0.39	1.72 ± 1.13	21.28 ± 0.22	15174.58 ± 362.54
FOX-SDH	160.43 ± 8.57	3.14 ± 0.50	1.46 ± 1.11	21.33 ± 0.17	15043.95 ± 342.4
FLAV-SDH	166.8 ± 8.59	2.42 ± 0.32	1.41 ± 1.08	20.90 ± 0.15	14671.55 ± 343.65

3.4.3 Intermolecular interactions between top hit metabolites of sunflower seed cultivars and target enzymes during MD-simulation

The intermolecular analysis focused on bound complexes with the highest negative binding free energy at four time points: 0 ns, 50 ns, 100 ns, and 150 ns is in Figure 9A-L. SAC A-AGLU complex averaged 16-18 interactions, with 2-3 hydrogen bonds observed throughout the simulation (Figure 9A), with a vast majority of the interactions being van der Waal forces, comparable with the standard ACARB-AGLU (Figure 9B). Figure 9C shows that the PLT-AR complex formed 20-24 interactions, including 4-6 hydrogen bonds and numerous van der Waals forces (compared to its standard in Figure 9D). PYR-DPP-4 (Figure 9E) exhibited stronger interactions than its standard, SITA-DPP-4 (Figure 9F), averaging around fourteen interactions throughout the simulation, with 3-6 hydrogen bonds and mostly van der Waals forces. CGA-PTP1B complex (Figure 9G) on the other hand maintained an average of twelve interactions and 2-3 hydrogen bonds throughout the simulation, similar to its reference, URS-PTP1B (Figure 9H). While the SAC A-SDH complex (Figure 9I), formed 3-6 hydrogen bonds, 6-7 van der Waals forces, and several pi-alkyl interactions. Similar interactions were observed for its reference standard, 4-PSD-SDH (Figure 9J) except for the formation of 1-4 hydrogen bonds during the simulation.

Lastly, SON I-AAMY (Figure 9K) and ACARB-AAMY (Figure 9L) formed roughly 15-17 and 18-20 interactions, respectively throughout the simulation. Specific to the SON-I -AAMY system the number of hydrogen bonds decreased with progression of the simulation, from 4 (0 ns) to 2 (150 ns).

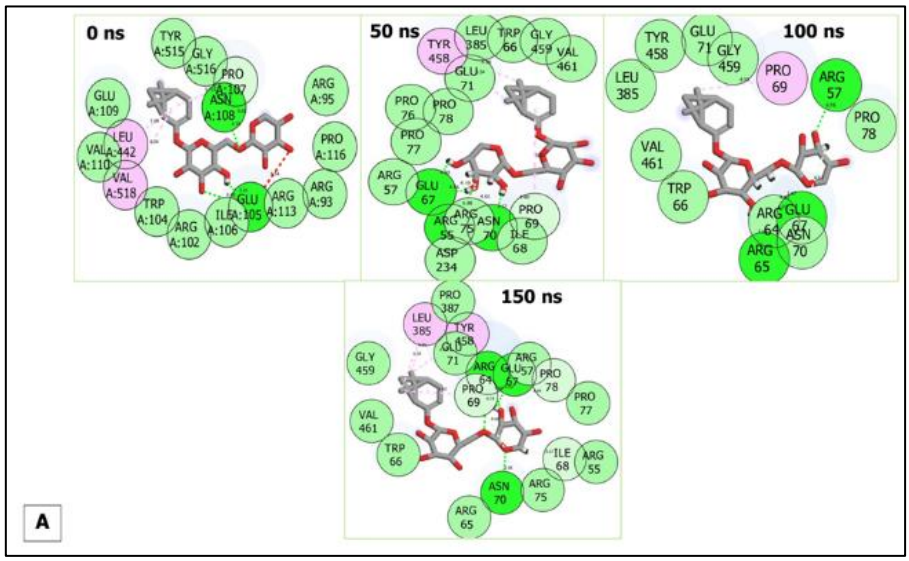

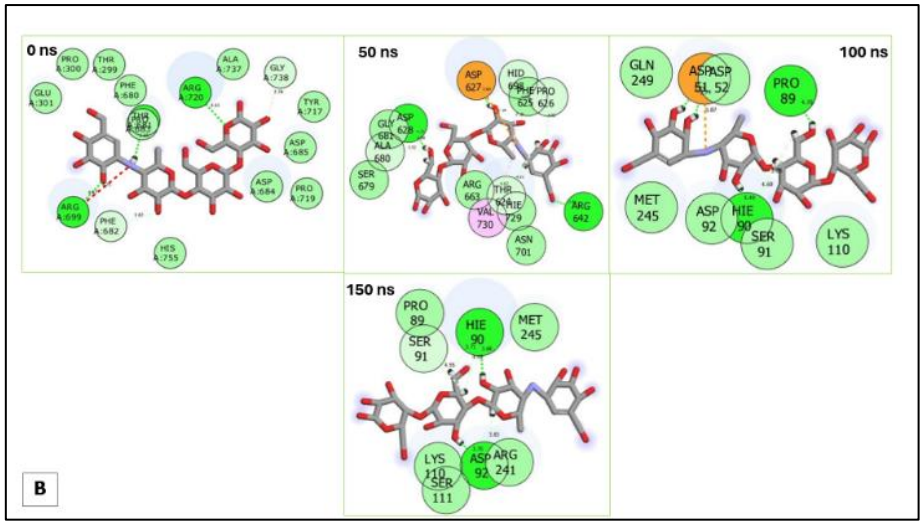
0 ns
50 ns
100 ns
150 ns
B

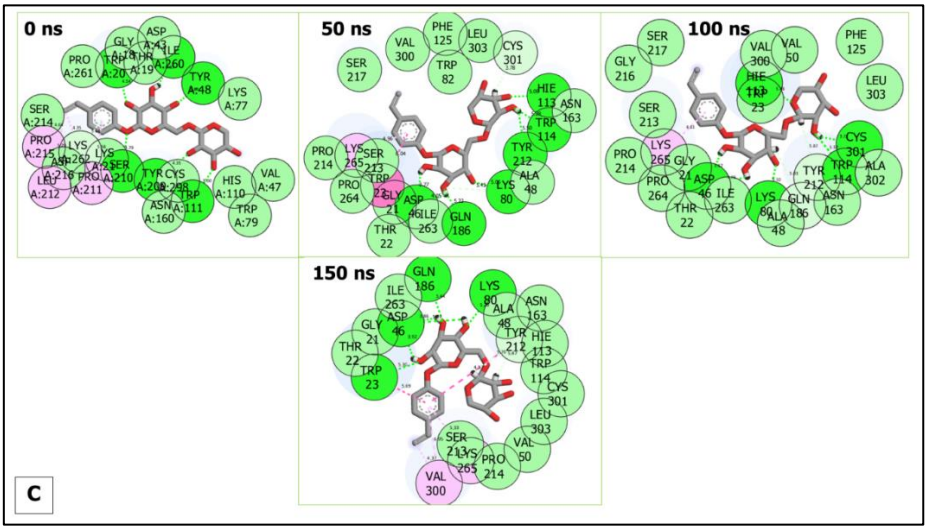
0 ns
50 ns
100 ns
150 ns
C

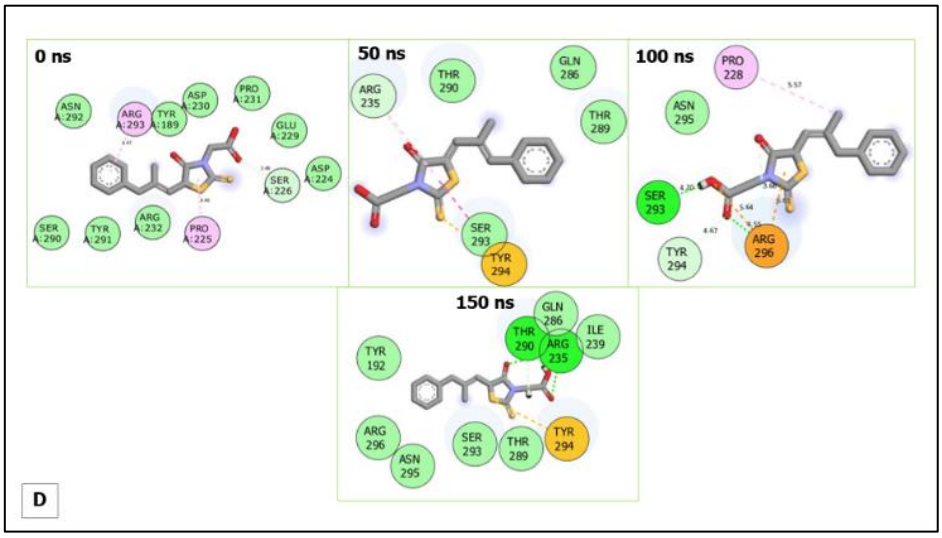
0 ns
50 ns
100 ns
150 ns
D

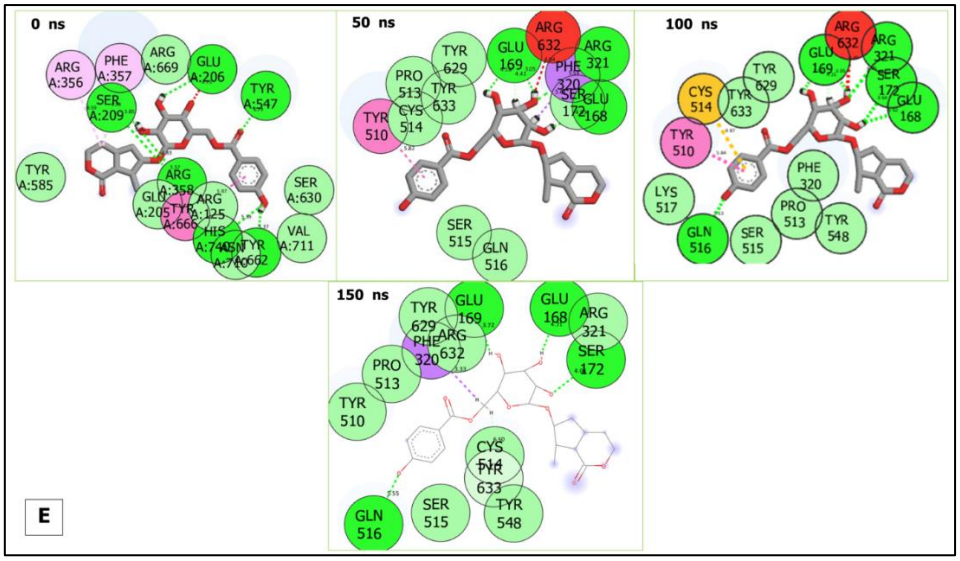
0 ns
ARG A:356
PHE A:357
ARG A:669
GLU A:206
TYR A:547
SER A:209
TYR A:585
ARG A:358
GLU A:205
ARG A:125
TYR A:666
HIS A:74
ASN A:74
TYR A:662
SER A:630
VAL A:711
50 ns
ARG 632
GLU 169
ARG 321
TYR 629
PRO 513
TYR 633
PHE 320
SER 172
GLU 168
TYR 510
CYS 514
SER 515
GLN 516
100 ns
ARG 632
ARG 321
GLU 169
TYR 629
SER 172
GLU 168
CYS 514
TYR 633
TYR 510
PHE 320
LYS 517
PRO 513
GLN 516
SER 515
TYR 548
150 ns
TYR 629
GLU 169
GLU 168
ARG 321
PHE 320
ARG 632
SER 172
PRO 513
TYR 510
CYS 514
TYR 633
GLN 516
SER 515
TYR 548
E

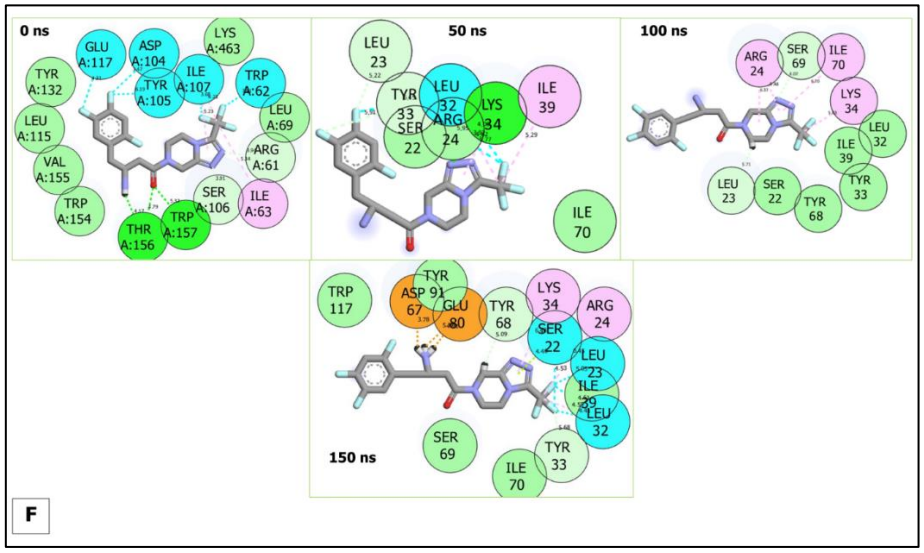
0 ns
GLU A:117
ASP A:104
LYS A:463
TYR A:132
TYR A:105
ILE A:107
TRP A:62
LEU A:69
LEU A:115
ARG A:61
VAL A:155
SER A:106
ILE A:63
TRP A:154
THR A:156
TRP A:157
50 ns
LEU 23
TYR 33
LEU 32
ARG 24
LYS 34
ILE 39
SER 22
ILE 70
100 ns
ARG 24
SER 69
ILE 70
LYS 34
LEU 32
ILE 39
LEU 23
SER 22
TYR 68
TYR 33
150 ns
TRP 117
TYR ASP 91 67
GLU 80
TYR 68
LYS 34
ARG 24
SER 22
LEU 23
ILE 39
LEU 32
SER 69
TYR 33
ILE 70
F

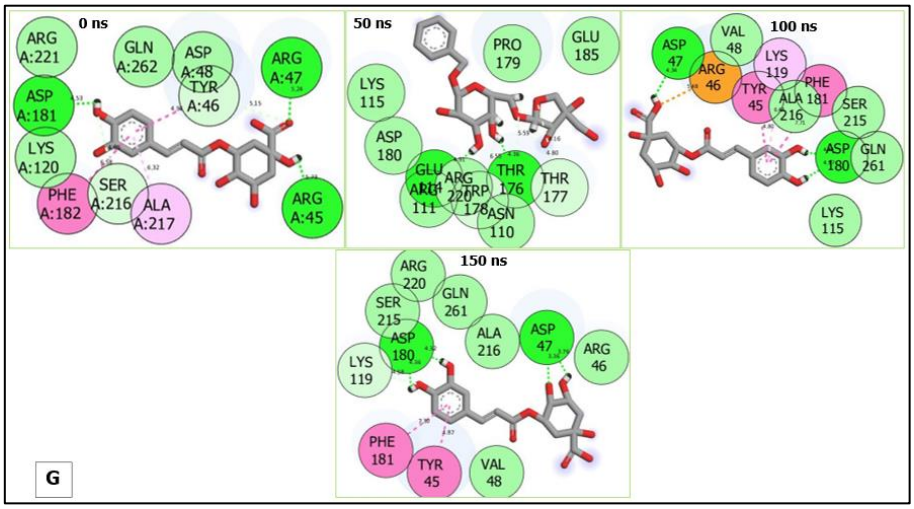
0 ns
ARG A:221
GLN A:262
ASP A:48
ARG A:47
TYR A:46
ASP A:181
LYS A:120
PHE A:182
SER A:216
ALA A:217
ARG A:45
50 ns
PRO 179
GLU 185
LYS 115
ASP 180
GLU 111
ARG 220
TRP 178
THR 176
THR 177
ASN 110
100 ns
VAL 48
ASP 47
LYS 119
ARG 46
PHE 181
TYR 45
ALA 216
SER 215
ASP 180
GLN 261
LYS 115
150 ns
ARG 220
GLN 261
SER 215
ALA 216
ASP 47
ASP 180
ARG 46
LYS 119
PHE 181
TYR 45
VAL 48
G

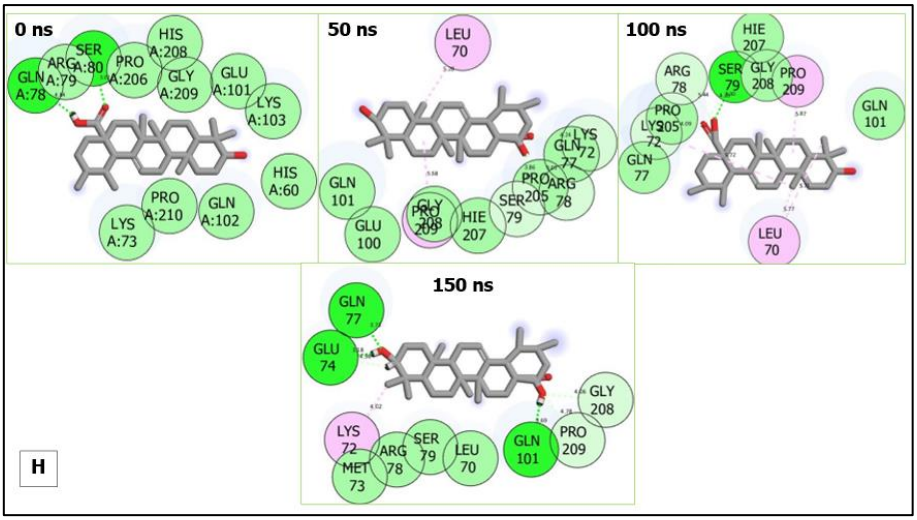
0 ns
50 ns
100 ns
150 ns
H

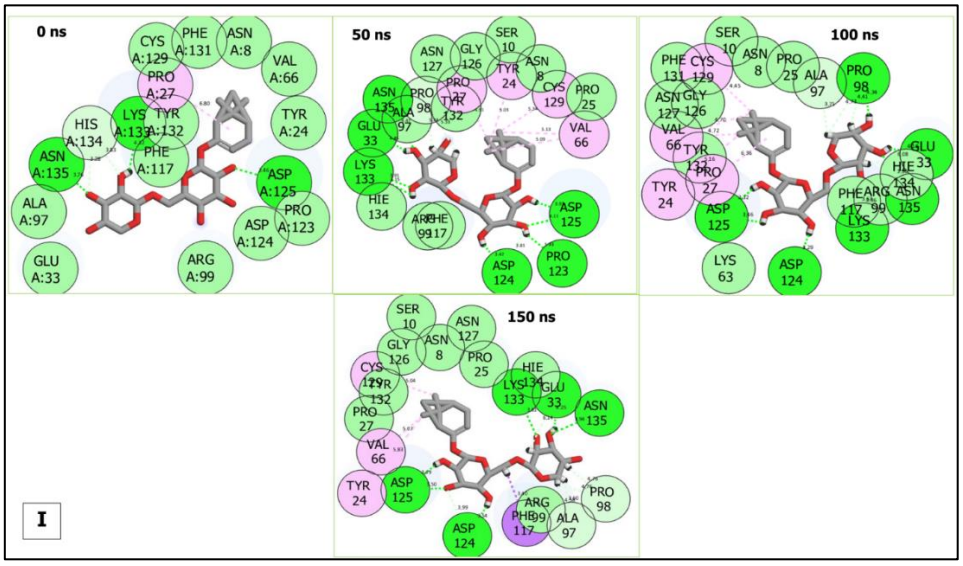
0 ns
50 ns
100 ns
150 ns
I

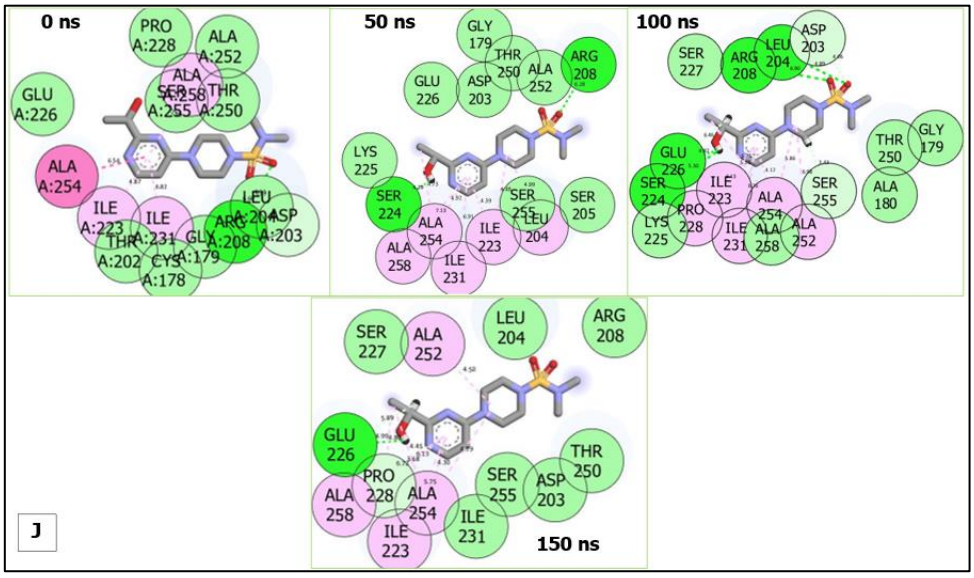
0 ns
50 ns
100 ns
150 ns
J

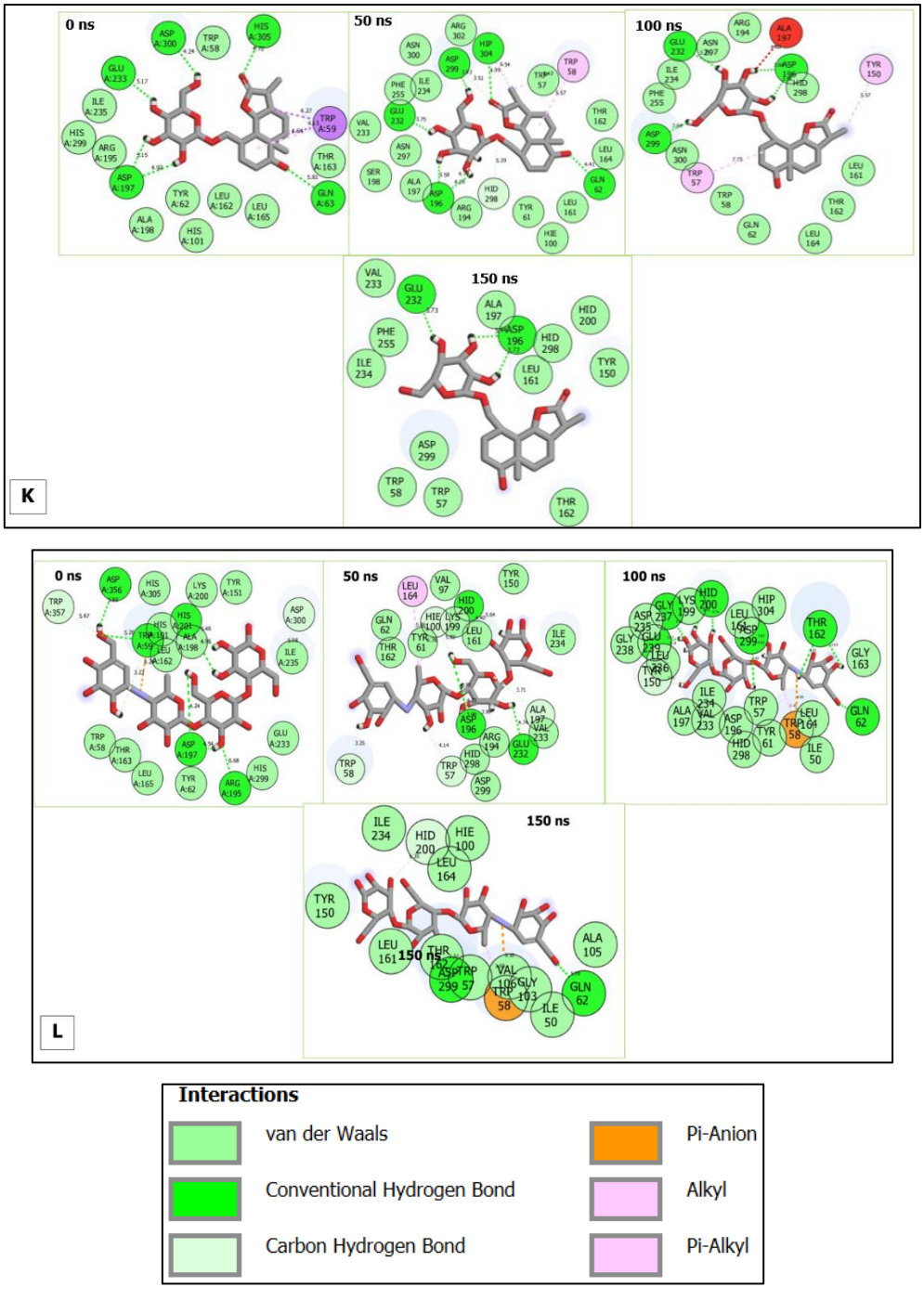

Figure 9: 2D interactions plots of enzyme complexes with the highest binding free energy. The bound complex of top-hit metabolite against each target is illustrated at time points of 0 ns, 50 ns, 100 ns and 150 ns: A) SAC A-AGLU, B) ACARB-AGLU, C)PLT-AR, D) ESPAL-AR, E) PYR-DPP-4, F) SITA-DPP-4, G) CGA-PTP1B, H) URS-PTP1B, I) SAC A-SDH, J) 4-PSD-SDH, K) SON I-AAMY and L) ACARB-AAMY.

4. Discussion

The alarming rise of T2DM and its devastating complications presents a compelling need to explore novel therapeutic options that are safe, accessible and effective. While current

medications like metformin offer some benefits, long-term use can lead to unwanted side effects (Engler *et al.*, 2020). Plants, brimming with a vast array of bioactive compounds known as secondary metabolites, present a promising avenue to synthetic drugs due to their well-documented health benefits (Süntar, 2020). *H. annuus*, the common sunflower and its seeds presents an exciting prospect due to its readily available source of essential nutrients, and abundance of phytoconstituents that may hold untapped potential as a natural therapeutic against diabetes. This study evaluated six cultivars of sunflower seeds popular in South African namely, AGSUN 8251, 5720, 5108 CLP, 5206 CLP, 5103 CLP and 5101 CLP. Through metabolomic profiling, 94 metabolites were tentatively identified mainly phenolic acids and volatile compounds. Though all six cultivars shared fairly the same metabolites, PCA analysis showed a minor variance indicating a slight variation in metabolite profile. The PLS-DA analysis and VIP directly points to the discrepancy in the abundance of the metabolites as the major reason for the slight variation amongst the cultivars as revealed by the PCA analysis. Those metabolites identified from VIP analysis and their varying abundance across the cultivars could potentially be the driving factor behind the cultivar-specific properties of the six cultivars, and the observed minor variation amongst them.

Molecular docking is a structure-based analysis, which evaluates a ligand's fitness for a receptor (protein), by predicting the best binding mode adopted by the ligand-receptor (Fan *et al*., 2019). Furthermore, the binding pose of the bound complex can be assessed on the basis of a docking score and the interactions that form by the ligand and receptor. A more negative docking score indicates a strong binding fitness for the receptor at the active site (Ece, 2020). In this study, molecular docking analysis served as a preliminary screening for the identification of the top five hit metabolites against alpha-amylase, alpha- glucosidase, aldose reductase, protein tyrosine phosphatase 1B, dipeptidyl-protein IV, and sorbitol dehydrogenase, relative to their respective standards. The highest negative docking scores of FOX B(AAMY), SAC A (AGLU), ISOM B (AR), ISOM B (PTP1B), 7-MET(DPP-4), and PYR (SDH) among the top-ranked compounds relative to their respective standard implies that these metabolites structurally have a better fitness for the actives site of the enzyme(s), suggesting the possibility for their role as potential inhibitor of the target enzymes. Despite the valuable findings from the molecular docking analysis, there is limitation in accounting for receptor flexibility that may hinder its accuracy in identifying active molecules. By assuming a rigid receptor conformation, molecular docking fails to capture the dynamic nature of protein-ligand interactions, limiting the reliability of its predictions and as a result these findings might not be

sufficient to draw any conclusive evidence. Thus, the top five hit metabolites against each diabetic target, at their most favourable binding pose were subjected to MD simulation. Evaluating the ligand-receptors dynamic conformational changes were subject to a time period of 150 ns. This analysis examined the affinity of each metabolite against the enzyme and thus its inhibitory potential. Molecular dynamics (MD) simulations provided a more comprehensive analysis of the stability and compactness of the bound complexes which further complement the docking study.

Acarbose, an AAMY and alpha-glucosidase inhibitor slows down the breakdown of carbohydrates, reducing postprandial hyperglycaemia (Kaur *et al*., 2021). However, due to the side effects associated with this drug, safer and long-term antidiabetics are of interest. Among the sunflower seed metabolites investigated, SON I and GRA C emerged as promising candidates for alpha-amylase inhibition. The superior binding affinities of their respective metabolite-enzyme complexes, coupled with their increased stability and structural compactness throughout molecular dynamics simulations as revealed by the binding free energy and post-dynamic data, suggest their potential as effective and long-term inhibitors. These findings align with previous research by Zhang *et al*. (2022), on eriodictyol, another natural compound with alpha-amylase inhibitory properties. These findings collectively highlight the importance of alpha-amylase as a therapeutic target for T2DM, while the findings of this present study emphasise the importance of plant-based compounds such as sunflower seed metabolites as promising antidiabetics.

For the AGLU systems, SAC A emerged as the lead candidate against the target enzyme. This was confirmed by strongest affinity exemplified by the highest binding free energy and increased stability of the complex, as confirmed by the post-dynamic data, surpassing even acarbose (standard). These findings strongly suggest the potential of SAC A as a novel antidiabetic agent targeting alpha-glucosidase. This is further supported by a recent study by Sharma *et al*. (2024) who also identified plant-derived compounds namely: (Carpaine - *Trigonella foenum-graecum*; Pseudocarpaine - *Carica papaya*; Pollinastanol -*Zea mays*; and Annosquamosin C - *Annona squamosa*) with potent alpha-glucosidase inhibitory activity through molecular dynamics simulations, also outperforming acarbose. Together, both studies provide evidence of plant-derived compounds as therapeutics, even out-performing established inhibitors such as acarbose *in silico*. This affirms the probable antidiabetic action of sunflower seed metabolites as alpha-glucosidase inhibitors.

Aldose reductase (AR) is an enzyme linked to diabetic complications like neuropathy, nephropathy, and retinopathy. Inhibiting AR in hyperglycaemic conditions can prevent sorbitol accumulation, potentially mitigating nerve damage and diabetic complications (Yang *et al*., 2019). Among the sunflower seed metabolites investigated, PLT emerged as the most promising candidate for AR inhibition, exhibiting the strongest binding affinity and increased stability in the enzyme-inhibitor complex. These findings align with previous research by Gautam *et al*. (2023), identifying the lead compound (65) to have the have strongest binding affinity and inclination for binding pocket of aldose reductase using molecular docking and MD-simulation. Collectively, these studies suggest that sunflower seed metabolites, particularly PLT, may have therapeutic potential for managing diabetic complications by targeting aldose reductase.

Sorbitol dehydrogenase (SDH) is another key enzyme in the polyol pathway, which becomes activated in hyperglycaemic conditions, leading to increased fructose production. Inhibiting SDH may help alleviate diabetic complications like neuropathy, nephropathy, and retinopathy. Among the top-hit sunflower seed metabolites, ISOM B initially emerged as the leading candidate for SDH inhibition. However, further analysis revealed that SAC A exhibited a high negative binding free energy, superior structural characteristics and a better fitness for SDH, suggesting it may be a more effective inhibitor. Overall, SAC A demonstrate potential as SDH inhibitor further highlighting the role sunflower seed metabolites may play in contributing to the management of T2DM and its complications.

Dipeptidyl peptidase 4 (DPP-4) is enzyme responsible for inactivation of incretion hormones leading to reduced insulin secretion. Elevated DPP-4 levels are a hallmark symptom of T2DM patients (Yin et al., 2022). Inhibition of DPP-4 can promote glucose-independent insulin secretion by increasing GLP-1 and GIP levels, while uniquely avoiding the risk of hypoglycaemia. Amongst, the top-ranked metabolites of sunflower seeds, PYR-DPP-4 complex displayed most promising characteristics as a potential DPP-4 inhibitor. The strong binding affinity of the complex, suggest that PYR exhibits favourable inhibitory potential, relative to sitagliptin. A study by (Nath *et* ., 2021) also deduced similar findings, the lead compound "(2-(3-((4-(1-methyl-1H-benzo[d]imidazol-2-yl) piperidin-1-yl)methyl)phenyl) ethanamine)" had formed a stable complex through hydrophobic interactions at the binding pocket with increase stability. Hence, this analysis also suggest that sunflower seed metabolites may promise potent antidiabetic action through modulation of insulin secretion.

Lastly, amongst the enzymes PTPB 1B, a negative regulator of the IR signalling pathway is an emerging drug target for T2DM (Rocha *et al*., 2021). In the case of T2DM , PTP1B inhibition may reduce the downregulating of insulin receptor substrate (IRS), increasing insulin sensitivity contributing to the maintenance of glucose homeostasis. Despite the lack of clinically approved PTP1B inhibitors, ongoing research seeks safer and more effective alternatives. This study identified CGA as a promising PTP1B inhibitor, exhibiting strong binding affinity and favourable structural characteristics. Unlike GRA C, which displayed unfavourable interactions, CGA demonstrated superior binding affinity and stability, even outperforming ursolic acid. The strong binding affinity and presence of stabilizing intermolecular forces such as hydrophobic interactions between CGA and PTP1B, reinstates the inhibitory potential of CGA amongst the top-hit metabolites of sunflower seeds. These findings align with recent research by Kabra and Kohona (2024), identified other natural compounds (naringin 6'-malonate, naringin 4'-O-glucoside (216), and theaflavin 3,3'-O-digallate) display favourable dynamic changes (stability, flexibility and binding energy) during MD simulations indicating its potency as PTP1B inhibitors. Together, these studies highlight the potential of sunflower seed metabolites, such as CGA, as promising candidates for the development of novel PTP1B inhibitors and, consequently, for the treatment of T2DM.

5. Conclusion

Metabolomic profiling of sunflower seed revealed the same core metabolites across six cultivars with slight variations as suggested by PCA analysis. Molecular docking analysis identify the top-ranked metabolites against enzymes implicated in T2DM progression and its complications: AAMY, AGLU, AR, SDH, DPP-4 and PTP1B. The top hit metabolites identified against each enzyme through molecular docking were further analysed through detailed molecular dynamics (MD) simulations. On the basis of increased structural stability and compactness, reduced fluctuations and solvent accessibly as well as strong binding affinity and intermolecular interactions, SON I-AAMY, GRA C-AAMY, SAC A-AGLU, PLT-AR, SAC A-SDH, PYR-DPP-4, and CGA-PTP1B emerged as promising candidates for further investigation as inhibitors against their respective enzymes for T2DM management. However, further *in vitro* and *in vivo* studies are crucial to validate the actual inhibitory and antidiabetic effects of these metabolites, as computational analysis only provides preliminary predictions.

References

Abdalla, A. A., Yagi, S., Abdallah, A. H., Abdalla, M., Sinan, K. I., and Zengin, G. (2021). Phenolic profile, antioxidant and enzyme inhibition properties of seed methanolic extract of seven new Sunflower lines: From fields to industrial applications. *Process Biochemistry*, 111, 53-61.

Ammu, L., Jasmine, J.B., Arunima, C. (2019). *In silico* analysis and molecular docking studies of C-glycosyl flavonoids of *Mimosa pudica* for neuropathic pain. *Journal of Global Trends Pharmaceutical sciences*. 10 (3), 6439–6449

Altay, M. (2022). Acarbose is again on the stage. *World Journal of Diabetes*, 13(1), 1.

Andreadi, A., Bellia, A., Di Daniele, N., Meloni, M., Lauro, R., Della-Morte, D., and Lauro, D. (2022). The molecular link between oxidative stress, insulin resistance, and type 2 diabetes: A target for new therapies against cardiovascular diseases. *Current opinion in pharmacology*, 62, 85-96.

Aribisala, J. O., Abdulsalam, R. A., Dweba, Y., Madonsela, K., and Sabiu, S., 2022. Identification of secondary metabolites from *Crescentia cujete* as promising antibacterial therapeutics targeting type 2A topoisomerases through molecular dynamics simulation. *Computers in Biology and Medicine*, 145, 105432.

Aribisala, J. O., and Sabiu, S., 2022. Cheminformatics identification of phenolics as modulators of penicillin-binding protein 2a of *Staphylococcus aureus*: A Structure–Activity-Relationship-Based Study. *Pharmaceutics*, 14(9), 1818.

Artasensi, A., Pedretti, A., Vistoli, G., and Fumagalli, L. (2020). Type 2 diabetes mellitus: a review of multi-target drugs. *Molecules*, *25*(8), 1987.

Bashary, R., Vyas, M., Nayak, S. K., Suttee, A., Verma, S., Narang, R., and Khatik, G. L. (2020). An insight of alpha-amylase inhibitors as a valuable tool in the management of type 2 diabetes mellitus. *Current diabetes reviews*, *16*(2), 117-136.

Bitew, M., Desalegn, T., Demissie, T. B., Belayneh, A., Endale, M., and Eswaramoorthy, R. Pharmacokinetics and drug-likeness of antidiabetic flavonoids: Molecular docking and DFT study. *Plos one*, *16*(12), e0260853.

Blahova, J., Martiniakova, M., Babikova, M., Kovacova, V., Mondockova, V., and Omelka, R. (2021). Pharmaceutical drugs and natural therapeutic products for the treatment of type 2 diabetes mellitus. *Pharmaceuticals*, 14(8), 806.

Daina, A., Michielin, O. and Zoete, V., 2017. SwissADME: a free web tool to evaluate pharmacokinetics, drug-likeness and medicinal chemistry friendliness of small molecules. *Scientific Reports* **7**, 42717.

De, L. C. (2020). Edible seeds and nuts in human diet for immunity development. *International Journal of Recent Scientific Research, 6*(11), 38877-38881.

Deacon, C. F. (2020). Dipeptidyl peptidase 4 inhibitors in the treatment of type 2 diabetes mellitus. *Nature Reviews Endocrinology*, 16(11), 642-653.

Dirir, A. M., Daou, M., Yousef, A. F., and Yousef, L. F. (2022). A review of alpha-glucosidase inhibitors from plants as potential candidates for the treatment of type-2 diabetes. *Phytochemistry Reviews*, 21(4), 1049-1079.

Ece, A., (2020). Towards more effective acetylcholinesterase inhibitors: A comprehensive modelling study based on human acetylcholinesterase protein drug complex. *Journal of Biomolecular Structure and Dynamics*. 38 (2), 565–572

Egea, M. B., de Oliveira Filho, J. G., Bertolo, M. R. V., de Araújo, J. C., Gautério, G. V., and Lemes, A. C. (2021). Bioactive phytochemicals from sunflower (*Helianthus annuus* L.) oil processing byproducts. *Bioactive Phytochemicals from Vegetable Oil and Oilseed Processing By-products* (pp. 1-16).

Engler, C., Leo, M., Pfeifer, B., Juchum, M., Chen-Koenig, D., Poelzl, K., ... and Ebenbichler, C. (2020). Long-term trends in the prescription of antidiabetic drugs: real-world evidence from the Diabetes Registry Tyrol 2012–2018. *BMJ Open Diabetes Research and Care*, *8*(1), e001279.

Fan, J., Fu, A., and Zhang, L. (2019). Progress in molecular docking. *Quantitative Biology*, 7, 83-89.

Galicia-Garcia, U., Benito-Vicente, A., Jebari, S., Larrea-Sebal, A., Siddiqi, H., Uribe, K. B., ... and Martín, C. (2020). Pathophysiology of type 2 diabetes mellitus. *International Journal of Molecular Sciences*, *21*(17), 6275

Gautam, P., Bisht, P., Gautam, A., Gupta, G. D., Singh, R., and Verma, S. K. (2023). A comprehension on structure guided alignment dependent 3D-QSAR modelling, and molecular dynamics simulation on 2, 4-thiazolidinediones as aldose reductase inhibitors for the

management of diabetic complications. *Journal of Biomolecular Structure and Dynamics*, 1-20.

International Diabetes Federation. (2024). International Diabetes Federation - Facts and Figures. Idf.org

Kaur, N., Kumar, V., Nayak, S. K., Wadhwa, P., Kaur, P., and Sahu, S. K. (2021). Alpha-amylase as molecular target for treatment of diabetes mellitus: A comprehensive review. *Chemical Biology and Drug Design*, *98*(4), 539-560.

Kabra, U., & Khona, P. (2024). Molecular docking and dynamic simulation analysis of natural polyphenols for identifying potential PTP1B inhibitors for type 2 diabetes. *Indian Journal of Chemistry (IJC)*, 63(5), 506-517.

Mathu, R., Abarnadevika, A., and Ariharasivakumar, G. (2021). A study of biguanides in the care of type II diabetes mellitus. *Journal of Pharmaceutical Sciences and Drug Discovery*, 1(1), 1-9.

Marulkar, V. S., and Bhatia, N. M. (2024). Chalcone and derived natural products: versatile scaffolds for multiple targets in treatment of type 2 diabetes. *Phytochemistry Reviews*, 1-38.

Moemen, L. A., Abdel Hamid, M. A., Wahab, S. A., Kenawy, M. K. M., Abuelela, M. H., Hassanin, O. A., ... and Osman, Z. M. (2020). Role of advanced glycation end products and sorbitol dehydrogenase in the pathogenesis of diabetic retinopathy. *Bulletin of the National Research Centre*, *44*, 1-11.

Nath, V., Ramchandani, M., Kumar, N., Agrawal, R., and Kumar, V. (2021). Computational identification of potential dipeptidyl peptidase (DPP)-IV inhibitors: structure based virtual screening, molecular dynamics simulation and knowledge-based SAR studies. *Journal of Molecular Structure*, *1224*, 129006.

Nazarian-Samani, Z., Sewell, R. D., Lorigooini, Z., and Rafieian-Kopaei, M. (2018). Medicinal plants with multiple effects on diabetes mellitus and its complications: a systematic review. *Current diabetes reports*, *18*, 1-13.

Pettersen, E.F., Goddard, T.D., Huang, C.C., Couch, G.S., Greenblatt, D.M., Meng, E.C., Ferrin, T.E. (2004). UCSF Chimera - a visualization system for exploratory research and analysis. *Journal of Computational Chemistry*. 25 (13), 1605–1612.

Rampadarath, A., Balogun, F. O., Pillay, C., and Sabiu, S. (2022). Identification of flavonoid C-glycosides as promising antidiabetics targeting protein tyrosine phosphatase 1B. *Journal of Diabetes Research*, *2022*.

Redondo, M. J., Steck, A. K., and Pugliese, A. (2018). Genetics of type 1 diabetes. *Pediatric diabetes*, *19*(3), 346-353.

Rahman, M. M., Dhar, P. S., Anika, F., Ahmed, L., Islam, M. R., Sultana, N. A., ... and Rauf, A. (2022). Exploring the plant-derived bioactive substances as antidiabetic agent: an extensive review. *Biomedicine and Pharmacotherapy*, 152, 113217.

Rehman, A., Saeed, A., Kanwal, R., Ahmad, S., and Changazi, S. H. (2021). Therapeutic effect of sunflower seeds and flax seeds on diabetes. *Cureus*, 13(8).

Rocha, S., Corvo, M. L., Fernandes, E., and Freitas, M. (2021). The emerging target protein tyrosine phosphatase 1B (PTP1B) for type 2 diabetes mellitus management. *Journal of Diabetes and Clinical Research*, *3*(4), 99-105.

Singh, P., Singh, V. K., and Singh, A. K. (2019). Molecular docking analysis of candidate compounds derived from medicinal plants with type 2 diabetes mellitus targets. *Bioinformation*, *15*, 179.

Sharma, P., Sharma, V., Mathpal, S., Tewari, D., Chandra, S., and Tamta, S. (2024). Identification of alpha-glucosidase enzyme inhibitors from phytochemicals via integrated deep learning, molecular docking, molecular dynamics simulation, and MMPBSA analysis. *South African Journal of Botany*, *167*, 48-61.

Süntar, I. (2020). Importance of ethnopharmacological studies in drug discovery: role of medicinal plants. *Phytochemistry Reviews*, *19*(5), 1199-1209.

Teimouri, M., Hosseini, H., ArabSadeghabadi, Z., Babaei-Khorzoughi, R., Gorgani-Firuzjaee, S., and Meshkani, R. (2022). The role of protein tyrosine phosphatase 1B (PTP1B) in the pathogenesis of type 2 diabetes mellitus and its complications. *Journal of Physiology and Biochemistry*, 1-16.

Thakur, S., Gupta, S. K., Ali, V., Singh, P., and Verma, M. (2021). Aldose Reductase: a cause and a potential target for the treatment of diabetic complications. *Archives of Pharmacal Research*, *44*, 655-667.

Yang, B. B., Hong, Z. W., Zhang, Z., Yu, W., Song, T., Zhu, L. L., ... and Dai, Y. T. (2019). Epalrestat, an aldose reductase inhibitor, restores erectile function in streptozocin-induced diabetic rats. *International Journal of Impotence Research*, *31*(2), 97-104.

Yin, R., Xu, Y., Wang, X., Yang, L., and Zhao, D. (2022). Role of dipeptidyl peptidase 4 inhibitors in antidiabetic treatment. *Molecules*, *27*(10), 3055.

Zhang, J., Ding, W., Tang, Z., Kong, Y., Liu, J., and Cao, X. (2022). Identification of the effective α-amylase inhibitors from *Dalbergia odorifera*: Virtual screening, spectroscopy, molecular docking, and molecular dynamic simulation. *Spectrochimica Acta Part A: Molecular and Biomolecular Spectroscopy*, 280, 121448.

Zheng, Y., Ley, S. H., and Hu, F. B. (2018). Global aetiology and epidemiology of type 2 diabetes mellitus and its complications. *Nature Reviews Endocrinology*, *14*(2), 88-98.

Supplementary Files

Table S1: Tentative identification of metabolites present in selected six cultivars of sunflower seeds through GC-MS and LC-MS analysis

No.	Compound	Chromatographic technique
1	Trimethylsilanol	GC-MS
2	Octamethylcyclotetrasiloxane	GC-MS
3	Hexanal	GC-MS
4	β--Pinene	GC-MS
5	Undecane	GC-MS
6	Sabinene	GC-MS
7	(-)-Limonene	GC-MS
8	Tridecane	GC-MS
9	Decamethylcyclopentasiloxane	GC-MS
10	2,2,4,4,6,8,8-Heptamethylnonane	GC-MS
11	1-Hexanol	GC-MS
12	Dodecamethylcyclohexasiloxane	GC-MS
13	Acetoin	GC-MS
14	2-Butoxyethanol	GC-MS
15	Acetic Acid	GC-MS
16	Ethyl decanoate	GC-MS
17	2-Ethyl-3-hydroxyhexyl 2-methylpropanoate	GC-MS
18	Benzyl alcohol	GC-MS
19	Nonan-1-ol	GC-MS

20	Calarene	GC-MS
21	Methenamine	GC-MS
22	3-methylbutan-1-OL	GC-MS
23	Benzaldehyde	GC-MS
24	Dodecane	GC-MS
25	2-Methyl-1-butanol	GC-MS
26	Benzene, ethenyl-, polymer with 2-methyl-1,3-butadiene, hydrogenated	GC-MS
27	β--Bisabolene	GC-MS
28	Myrtenol	GC-MS
29	Hexamethylcyclotrisiloxane	GC-MS
30	Propanoic acid, 2-methyl-, 3-hydroxy-2,4,4-trimethylpentyl ester	GC-MS
31	Ethanol	GC-MS
32	verbenene	GC-MS
33	gamma-Terpinene	GC-MS
34	Bicyclo[4.2.0]octa-1,3,5-triene	GC-MS
35	Terpinolene	GC-MS
36	Pinocarveol	GC-MS
37	Mentha-1,4,8-triene	GC-MS
38	TRANS-(+)-CARVEOL	GC-MS
39	Camphene Bicyclo[2.2.1]heptane, 2,2-dimethyl-3-methylene-	GC-MS
40	Propane, 1-methoxy-2-methyl-	GC-MS
41	Benzeneacetaldehyde	GC-MS
42	2,6,10-Trimethyldodecane	GC-MS
43	1-Pentanol	GC-MS
44	Tetradecane	GC-MS
45	Propylene glycol	GC-MS
46	gamma-Butyrolactone	GC-MS
47	4-Methyldecane	GC-MS
48	2,6-Dimethylpyrazine	GC-MS
49	1-Heptanol	GC-MS
50	1-Octanol	GC-MS
51	Xanthine	LC-MS
52	Dihydroxyacetone gluconate	LC-MS
53	Cinnzeylanol	LC-MS
54	Tryptophanate	LC-MS
55	Chlorogenic acid	LC-MS
56	isomoreollin B	LC-MS
57	7-Methoxyisomorellinol	LC-MS
58	2-Isopropylmalic acid	LC-MS
59	Dihydrophaseic acid 4'-O-β-D-glucopyranoside	LC-MS
60	1-O-Caffeoylglucose	LC-MS
61	Strophanthobiose	LC-MS

62	Quinic acid	LC-MS
63	Safflor Yellow B	LC-MS
64	Kaempferide 3-rhamnoside-7-(6"-succinylglucoside)	LC-MS
65	Methyl asterrate	LC-MS
66	Caffeic acid	LC-MS
67	Phenylacetic acid	LC-MS
68	Piceol;4'-Hydroxyacetophenone;p-Hydroxyacetophenone	LC-MS
69	Icariside F2	LC-MS
70	Gein	LC-MS
71	3'-O-β--Glucopyranosyl plumbagic acid methyl ester	LC-MS
72	3-O-Caffeoyl-4-O-methylquinic acid	LC-MS
73	Tricin 5-O-β-D-glucopyranoside;Tricin 5-glucoside	LC-MS
74	Ptelatoside A	LC-MS
75	Sonchuside I	LC-MS
76	Granatumin C	LC-MS
77	Hymenoside R	LC-MS
78	(2S)-6-(γ,γ-dimethylallyl)-3',4'-dimethoxy-6",6"-dimethylpyran[2",3":7,8]flavanone	LC-MS
79	4α,6S,7αa)-α-[6-O-(4-Hydroxybenzoyl)-β-D-glucopyranosyloxy]-7β-methyloctahydrocyclopenta[c]pyran-1-one	LC-MS
80	1-(((3-Nitrobenzyl)oxy)methyl)pyridin-1-ium chloride	LC-MS
81	Chrysanthemorimic acid A	LC-MS
82	[4]-Gingerdiol	LC-MS
83	Dracunculifoside Q	LC-MS
84	Dracunculifoside F	LC-MS
85	Formononetin 7-(6"-malonylglucoside)	LC-MS
86	Fluorescein-digalactoside	LC-MS
87	Azelaic acid	LC-MS
88	Ferulic acid	LC-MS
89	Seguinoside J	LC-MS
90	Cascaroside C	LC-MS
91	Methyl 2-[(3-acetyloxy-4,5-dimethoxyoxan-2-yl)methoxy]acetate	LC-MS
92	Sacranoside A	LC-MS
93	Formoxanthone B	LC-MS
94	Methyl asterate	LC-MS

Table S2: Tentative identification of metabolites of sunflower seeds through GC-MS analysis

Compound Identity	**Molecular Formula**	**AGSUN8251**	**AGSUN5270**	**AGSUN5108**	**AGSUN5106**	**AGSUN5103**	**AGSUN5101**	Retention time (min)

				CLP	CLP	CLP	CLP	
Propane, 1-methoxy-2-methyl-	$C_5H_{12}O$	4,21	4,25	4,21	4,23	4,31	4,21	
Trimethylsilanol	$C_3H_{10}OSi$	5,35	5,55	5,57	5,38	5,49	5,34	
gamma-Terpinene	$C_{10}H_{16}$	5,68	5,63	5,58	5,89	5,67	5,72	
Camphene Bicyclo [2,2,1] heptane, 2,2-dimethyl-3-methylene-	$C_{10}H_{16}$	6,08	6,16	6,09	6,24	6,08	6,25	
verbenene	$C_{10}H_{14}$	6,40	6,43	6,48	6,42	6,41	6,03	
Hexanal	$C_6H_{12}O$	7,09	6,97	7,25	7,11	7,17	6,84	
Trans- (+)-carveol	$C_{10}H_{16}O$	7,23	7,33	7,13	7,42	7,30	7,35	
beta-Pinene	$C_{10}H_{16}$	7,44	7,34	7,47	7,43	7,49	7,50	
Undecane	$C_{11}H_{24}$	7,60	7,28	7,61	7,60	7,67	7,33	
Pinocarveol	$C_{10}H_{16}O$	7,86	7,90	7,88	7,77	7,89	7,84	
Sabinene	$C_{10}H_{16}$	8,14	8,33	8,10	8,14	8,20	8,22	
4-Methyldecane	$C_{11}H_{24}$	8,30	8,32	8,35	8,33	8,33	8,34	
Limonene	$C_{10}H_{16}$	10,87	11,42	10,98	10,65	10,86	10,96	
Dodecane	$C_{12}H_{26}$	11,18	11,14	11,17	11,18	11,08	11,19	
Tridecane	$C_{13}H_{28}$	11,26	11,45	11,38	11,23	11,25	11,32	
Bicyclo [4,2,0] octa-1,3,5-triene	C_8H_6O	11,53	11,54	11,55	11,57	11,57	11,57	
Decamethylcyclopentasiloxane	$C_{10}H_{30}O_5Si_5$	12,26	12,35	12,35	12,10	12,07	12,27	
3-methylbutan-1-ol	$C_5H_{12}O$	12,66	12,64	12,42	12,91	12,95	12,54	
2-Methyl-1-butanol	$C_5H_{12}O$	12,86	12,87	12,86	12,86	12,89	12,84	
Terpinolene	$C_{10}H_{16}$	13,38	13,42	13,40	13,39	13,39	13,40	

1-Pentanol	$C_5H_{12}O$	13,54	13,64	13,48	13,73	13,56	13,76	
2,2,4,4,6,8,8-Heptamethylnonane	$C_{16}H_{34}$	14,16	14,15	13,90	14,16	13,95	14,31	
Acetoin	$C_4H_8O_2$	15,25	15,55	15,80	14,99	15,02	15,76	
2,6-Dimethylpyrazine	$C_6H_8N_2$	15,47	15,35	15,52	15,57	15,65	15,56	
1-Hexanol	$C_6H_{14}O$	16,20	16,14	16,16	16,25	16,25	16,19	
Dodecamethylcyclohexasiloxane	$C_{12}H_{36}O_6Si_6$	16,58	16,59	16,59	16,57	16,57	16,58	
Tetradecane	$C_{14}H_{30}$	16,79	17,17	16,83	16,29	16,57	16,67	
2,6,10-Trimethyldodecane	$C_{15}H_{32}$	17,44	17,53	17,32	17,46	17,65	17,59	
2-Butoxyethanol	$C_6H_{14}O_2$	17,25	17,18	17,18	17,31	17,78	17,21	
1-Heptanol	$C_7H_{16}O$	18,32	18,23	18,54	17,31	18,36	18,33	
Acetic Acid	$C_2H_4O_2$	18,56	18,57	18,50	18,42	18,36	18,47	
Benzaldehyde	C_7H_6O	19,64	19,67	19,62	19,61	19,61	19,65	
1-Octanol	$C_8H_{18}O$	20,34	20,21	20,24	20,26	20,22	20,26	
Octamethylcyclotetrasiloxane	$C_8H_{24}O_4Si_4$	20,13	20,25	20,31	20,29	20,28	20,30	
Calarene	$C_{15}H_{24}$	20,68	20,78	20,77	20,76	20,63	20,69	
Propylene glycol	$C_3H_8O_2$	20,91	20,94	20,87	20,94	20,98	20,95	
Mentha-1,4,8-triene	$C_{10}H_{14}$	21,09	21,52	21,50	21,50	21,50	21,47	

gamma-Butyrolactone	$C_4H_6O_2$	21,54	21,54	21,53	21,61	21,54	21,51	
Ethyl decanoate	$C_{12}H_{24}O_2$	21,67	21,72	21,73	21,61	21,60	21,68	
Benzeneacetaldehyde	C_8H_8O	21,83	21,77	21,74	21,81	21,82	21,74	
Nonan-1-ol	C_9H20O	22,05	22,07	22,02	22,08	22,03	22,05	
beta-Bisabolene	$C_{15}H_{24}$	23,22	23,42	23,77	23,05	23,04	23,12	
Benzene, ethenyl-, polymer with 2-methyl-1,3-butadiene, hydrogenated	$C_{13}H_{16}$	23,78	23,21	23,22	23,81	23,63	22,36	
Myrtenol	$C_{10}H_{16}O$	24,23	24,22	24,24	24,20	24,20	24,23	
Hexamethylcyclotrisiloxane	$C_6H_{18}O_3Si_3$	24,53	24,47	24,94	24,49	24,49	24,49	
Propanoic acid, 2-methyl-, 3-hydroxy-2,4,4-trimethylpentyl ester	$C_{12}H_{24}O_3$	25,40	25,41	25,43	25,39	25,39	25,41	
Benzyl alcohol	C_7H_8O	25,57	25,57	25,49	25,57	25,57	24,55	
Ethanol	C_2H_6O	25,57	25,57	25,59	25,57	25,58	25,55	
Methenamine	$C_6H_{12}N_4$	26,04	26,09	26,04	26,07	26,07	26,04	

Figure S1: GC-MS-TIC

a. **TIC of AGSUN 8251**

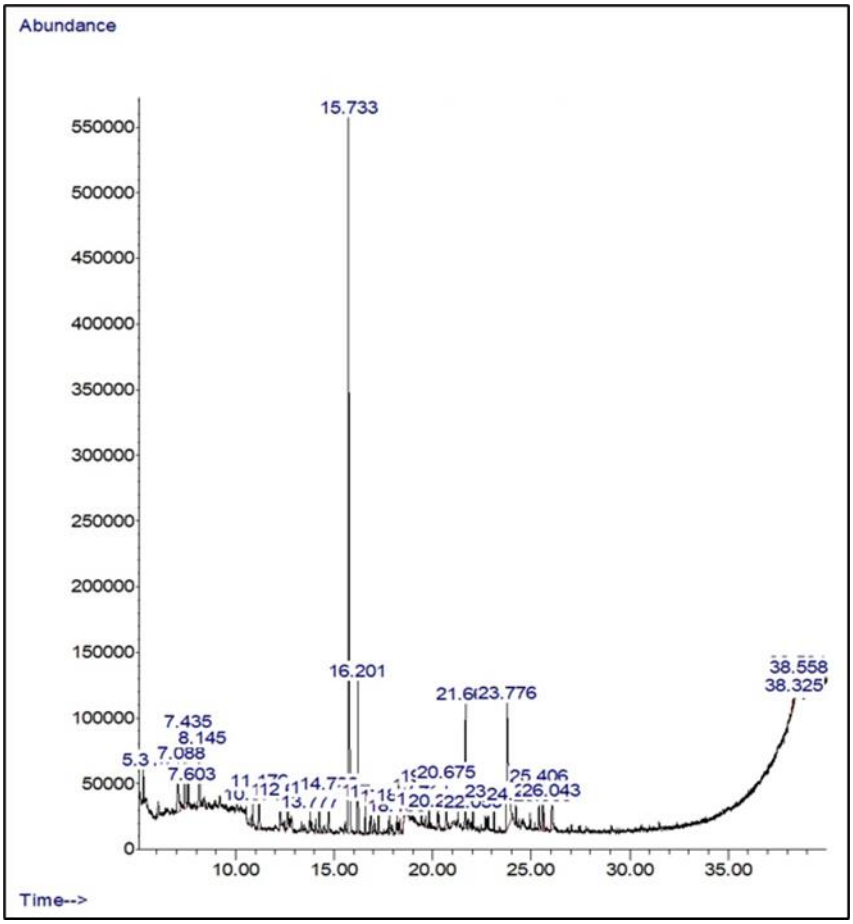
Abundance
15.733
16.201
7.435
8.145
7.088
7.603
5.3
21.6
23.776
20.675
38.558
38.325
550000
500000
450000
400000
350000
300000
250000
200000
150000
100000
50000
0
10.00
15.00
20.00
25.00
30.00
35.00
Time-->

b. TIC of AGSUN 5270

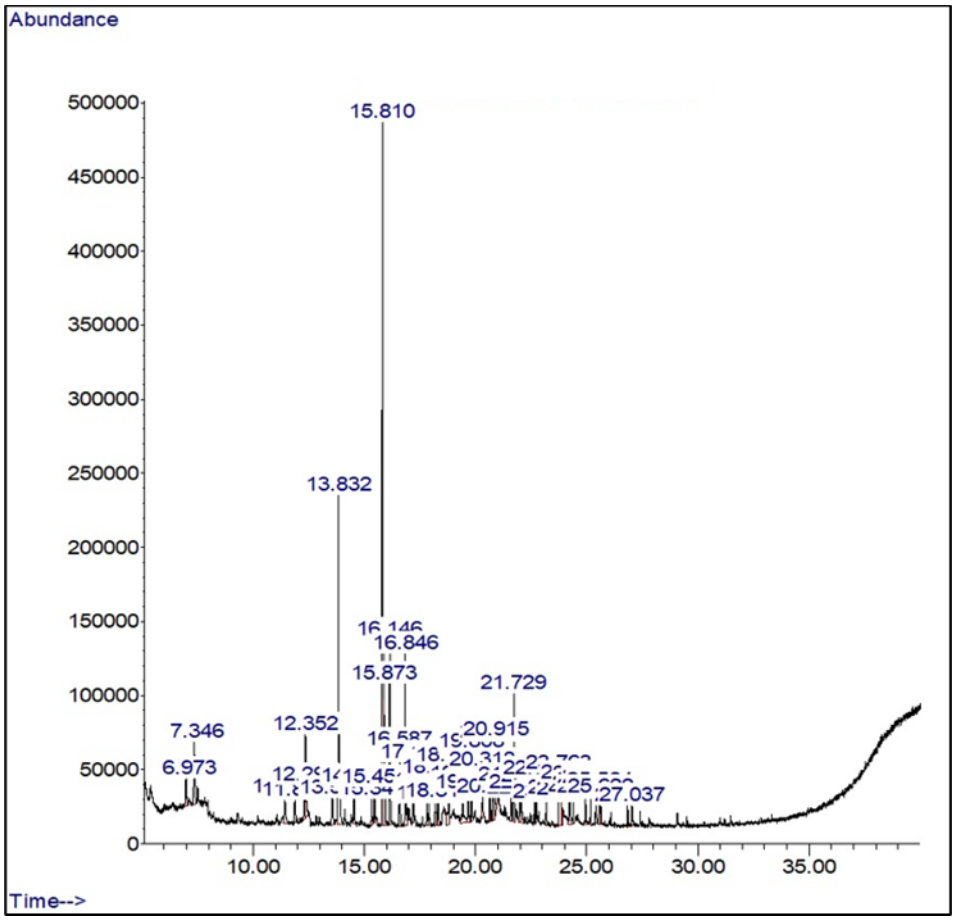

c. TIC of AGSUN 5108 CLP

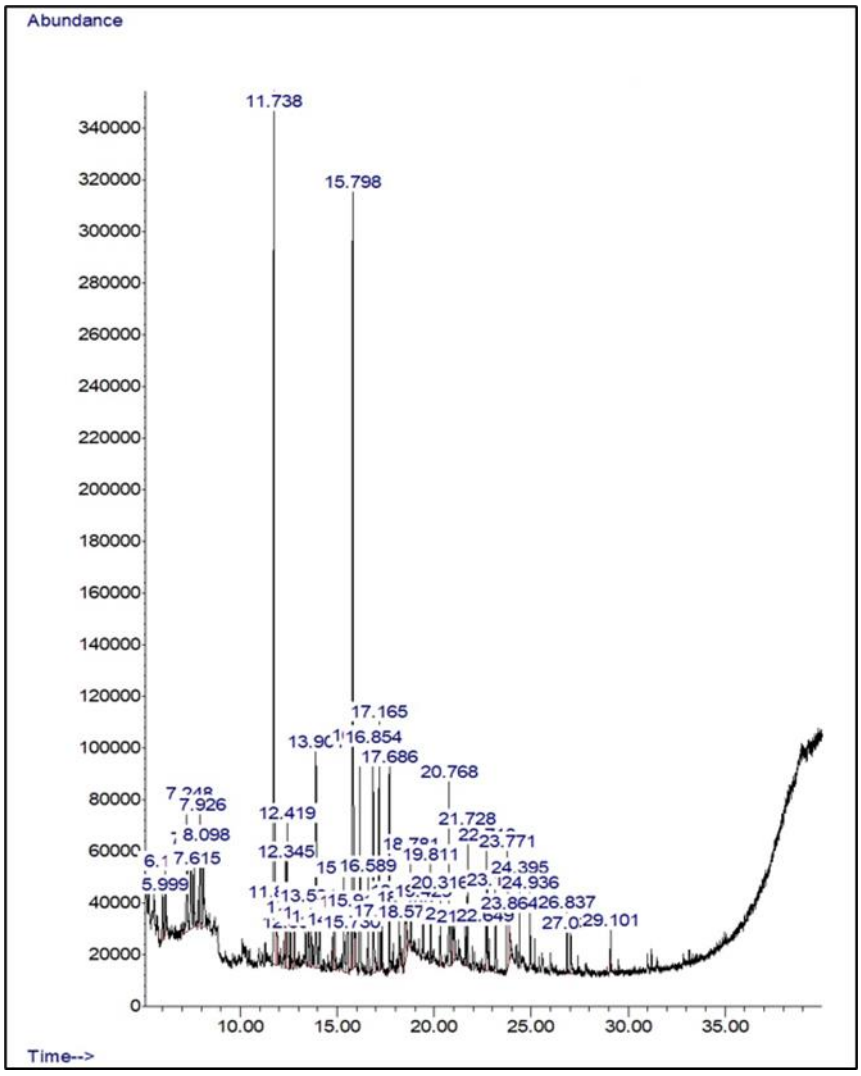

d. TIC of AGSUN 5106 CLP

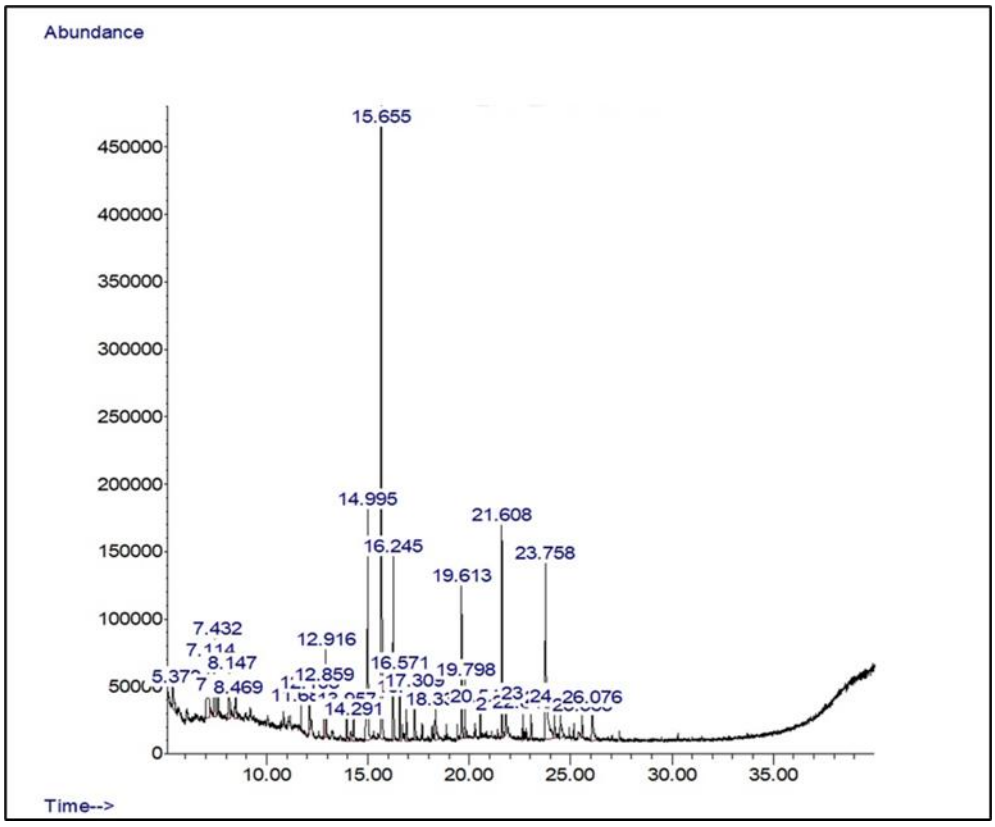

e. TIC of AGSUN 5103 CLP

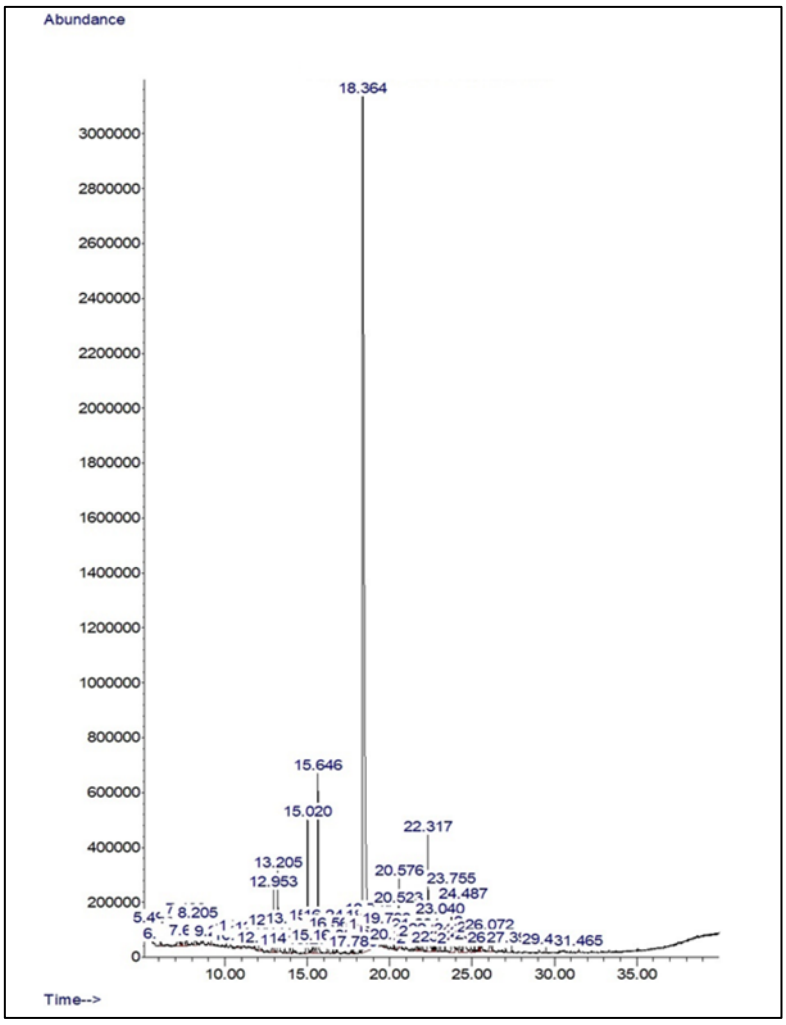

f. TIC of AGSUN 5101 CLP

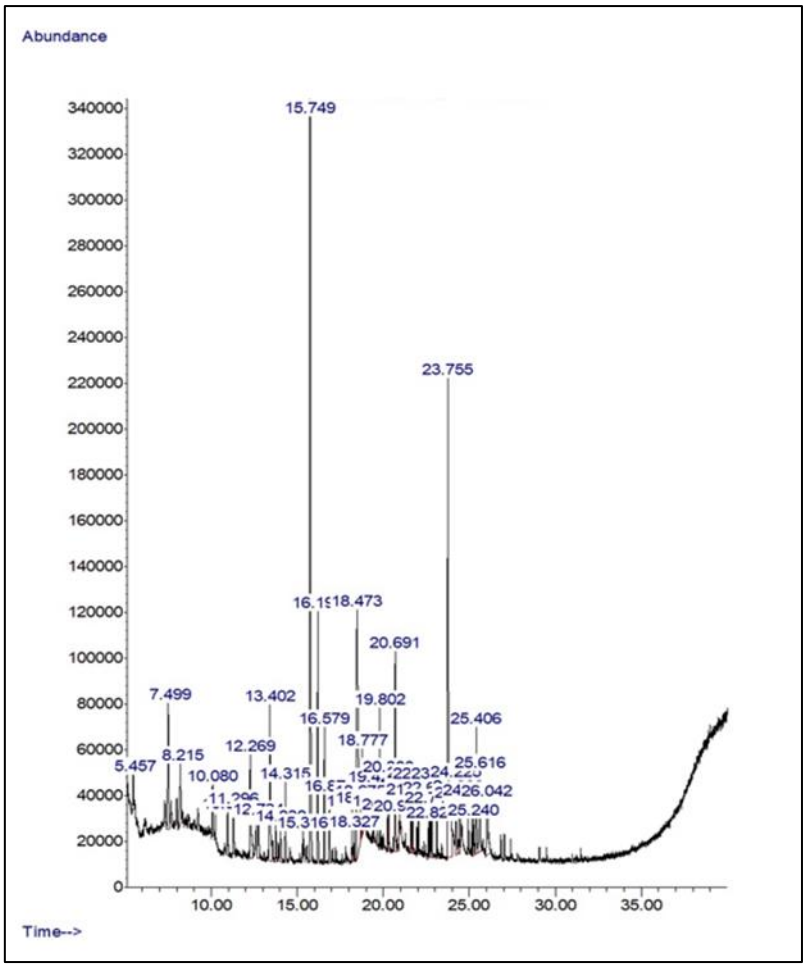

Table S3: Tentative identification of metabolites and its relative (%) abundance in sunflower seed cultivars through LC-MS analysis

Compounds	RT	M/Z	Molecular Formula	AGSUN 8251	AGSUN 5720	AGSUN 5108 CLP	AGSUN 5106 CLP	AGSUN 5103 CLP	AGSUN 5101 CLP	
Xanthine	6.711	151.0268	$C_5H_4N_4O_2$	0,51	0,48	0,46	0,51	0,47	0,47	
Dihydroxyacetone gluconate	6.709	283.2	$C_9 H_{16} O_{10}$	3,22	2,62	3,08	2,68	2,81	2,65	
3-Deoxyryanodol	8.65	383.21	$C_{20} H_{32} O_7$	0,32	0,11	0,08	0,22	0,09	0,07	
Tryptophanate	9.273	203.08	$C_{11} H_{11} N2 O_2$	2,39	1,10	0,70	1,20	0,75	0,50	
Chlorogenic acid	9.53	353.08	$C_{16} H_{18} O_9$	45,60	49,70	48,03	45,85	48,35	43,23	
isomoreollin B	9.88	575.26	$C_{34} H_{40} O_8$	1,61	1,65	1,79	0,47	1,28	1,94	
7-Methoxyisomorellinol	10.054	576.7	$C_{34} H_{40} O_8$	0,17	0,52	0,20	0,57	0,08	1,08	
2-Isopropylmalic acid	10.596	175.25	$C_7 H_{12} O_5$	0,48	0,57	0,37	0,37	0,44	0,49	
Dihydrophaseic acid 4'-O-beta-D-glucopyranoside	11.25	443.19	$C_{21} H_{32} O_{10}$	1,99	2,85	2,21	1,48	2,03	2,07	
1-O-Caffeoylglucose	11.49	341.08	$C_{15} H_{18} O_9$	0,64	0,36	0,09	0,67	0,85	0,28	
Strophanthobiose	11.68	324.3	$C_{13} H_{24} O_9$	0,96	2,09	1,79	1,29	2,17	2,35	
Quinic acid	11.96	191.05	$C_7 H_{12} O_6$	11,58	13,57	12,42	12,47	12,23	18,02	
Safflor Yellow B	11.96	1061.27	$C_{48} H_{54} O_{27}$	1,63	1,88	1,90	1,71	1,16	1,69	
Kaempferide 3-rhamnoside-7-(6"-succinylglucoside)	12.08	707.18	$C_{32} H_{36} O_{18}$	1,17	1,86	2,10	1,53	0,12	2,24	
Methyl asterrate	12.48	361.09	$C_{18} H_{18} O_8$	0,63	0,14	0,60	0,66	0,71	0,65	
Caffeic acid	12.63	179.03	$C_9 H_8 O_4$	4,63	2,88	3,45	6,97	2,90	2,38	
Phenylacetic acid	12.63	135.04	$C_8 H_8 O_2$	1,82	1,03	1,42	2,65	1,04	0,96	
Piceol;4'-Hydroxyacetophenone;p-Hydroxyacetophenone	12.79	135.04	$C_8 H_8 O_2$	0,07	0,06	0,07	0,12	0,04	0,07	Relative abundance (%)
Icariside F2;Benzyl beta-D-Apiofuranosyl-(1->6)-O-beta-D-glucopyranoside	13.07	401.14	$C_{18} H_{26} O_{10}$	0,82	0,94	0,77	0,89	0,61	0,37	

Gein	13.10	457.17	$C_{21}H_{30}O_{11}$	0,13	0,00	0,00	0,09	0,05	0,70
3'-O-beta-Glucopyranosyl plumbagic acid methyl ester	13.81	399.12	$C_{18}H_{24}O_{10}$	0,13	0,05	0,07	0,05	0,42	0,06
3-O-Caffeoyl-4-O-methylquinic acid	15.29	367.10	$C_{17}H_{20}O_{9}$	0,32	0,13	0,34	0,28	0,29	0,22
Tricin 5-glucoside	15.34	491.12	$C_{23}H_{24}O_{12}$	0,57	0,23	0,08	0,16	0,11	0,11
Ptelatoside A	15.36	413.14	$C_{19}H_{26}O_{10}$	0,14	0,06	0,46	0,24	0,50	0,41
Sonchuside I	15.46	429.21	$C_{21}H_{34}O_{9}$	0,21	0,14	0,33	0,04	0,12	0,11
Granatumin C	15.63	565.24	$C_{32}H_{38}O_{9}$	0,16	0,36	0,07	0,08	0,22	0,23
Hymenoside R	15.89	413.14	$C_{19}H_{26}O_{10}$	0,15	0,19	0,33	0,12	0,39	0,27
(2S)-6-(gamma,gamma-dimethylallyl)-3',4'-dimethoxy-6",6"-dimethylpyran[2",3":7,8]flavanone	15.97	433.20	$C_{27}H_{30}O_{5}$	0,25	0,29	0,08	0,12	0,26	0,22
4aalpha,6S,7aalpha)-6alpha-[6-O-(4-Hydroxybenzoyl)-beta-D-glucopyranosyloxy]-7beta-methyloctahydrocyclopenta[c]pyran-1-one	16.67	452.2	$C_{22}H_{28}O_{11}$	0,34	0,22	0,36	0,12	0,35	0,29
1-(((3-Nitrobenzyl)oxy)methyl)pyridin-1-ium chloride	16.87	245.09	$C_{13}H_{13}N_{2}O_{3}$	0,44	0,00	0,10	0,16	0,10	0,09
Chrysanthemorimic acid A	17.14	642.6	$C_{31}H_{30}O_{15}$	1,71	1,69	1,79	1,62	1,32	1,02
Dracunculifoside J	17.56	412.4	$C_{20}H_{28}O_{9}$	0,34	0,15	0,48	0,16	0,73	0,71
Gingerdiol	18.41	267.15	$C_{15}H_{24}O_{4}$	0,85	0,04	0,02	0,24	0,03	0,03
Dracunculifoside F	18.52	529.19	$C_{19}H_{24}O_{10}$	0,14	0,24	0,38	0,13	0,50	0,53
Formononetin 7-(6"-malonylglucoside)	19.27	515.11	$C_{25}H_{24}O_{12}$	3,44	2,60	3,65	3,00	3,09	2,53
Fluorescein-digalactoside	19.31	656.6	$C_{32}H_{32}O1_{5}$	1,62	2,12	1,39	0,76	1,21	0,94
Azelaic acid	19.84	187.09	$C_{9}H_{16\ O4}$	0,68	0,75	0,63	0,86	0,61	0,67
trans-Ferulic acid	20.40	193.04	$C_{10}H_{10}O_{4}$	2,02	2,29	0,87	3,38	2,43	2,02
Seguinoside J	20.42	500.5	$C_{23}H_{32}O_{12}$	0,15	0,14	0,15	0,14	0,26	0,15
Cascaroside C	20.52	563.17	$C_{27}H_{32}O_{13}$	0,31	1,46	2,13	2,89	2,24	1,99
Methyl 2-[(3-acetyloxy-4,5-dimethoxyoxan-2-yl)methoxy]acetate	20.77	306.31	$C_{13}H_{22}O_{8}$	0,38	0,03	0,08	0,23	0,05	0,05
Sacranoside A	23.42	445.20	$C_{21}H_{34}O_{10}$	1,38	1,08	1,41	1,08	1,92	1,73
Formoxanthone B	23.42	491.20	$C_{28}H_{30}O_{5}$	0,61	0,50	0,61	0,60	0,91	0,77

Figure S2: LC-MS chromatograms of sunflower seed cultivars

a) Chromatogram of AGSUN 8251

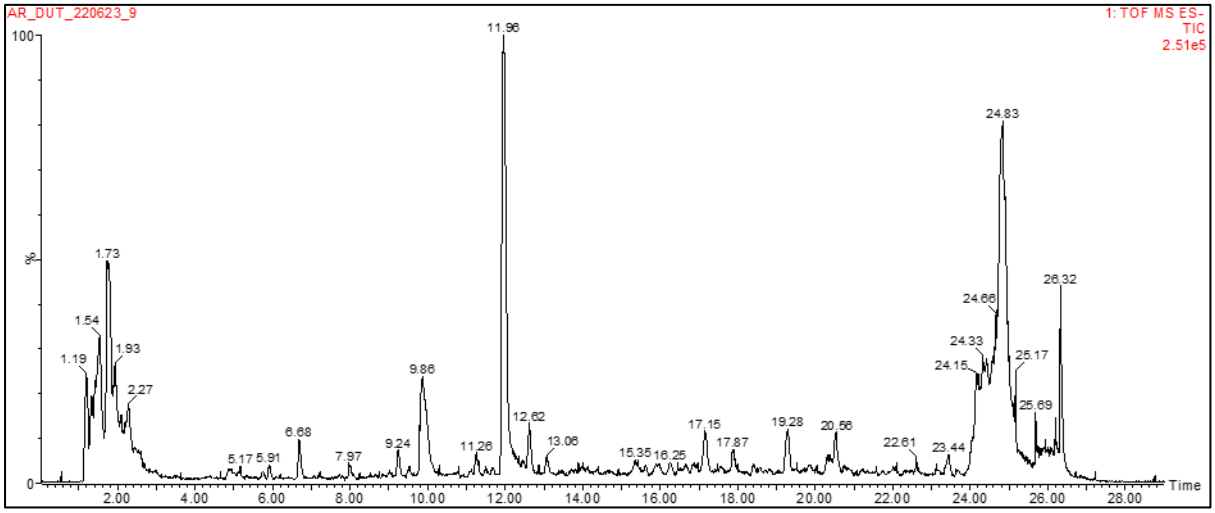

b) Chromatogram of AGSUN 5270

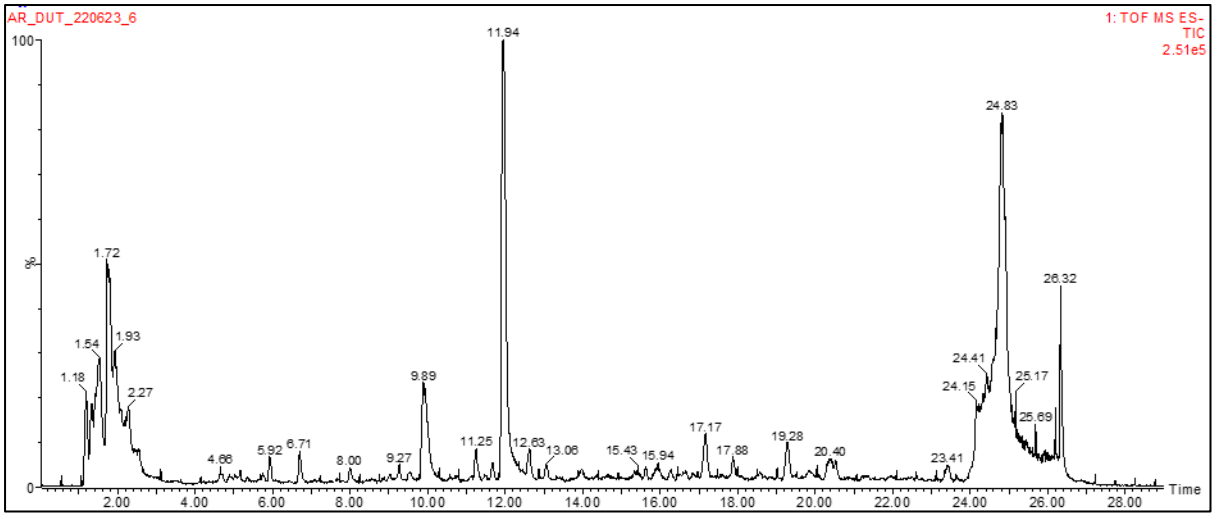

c) Chromatogram of AGSUN 5108 CLP

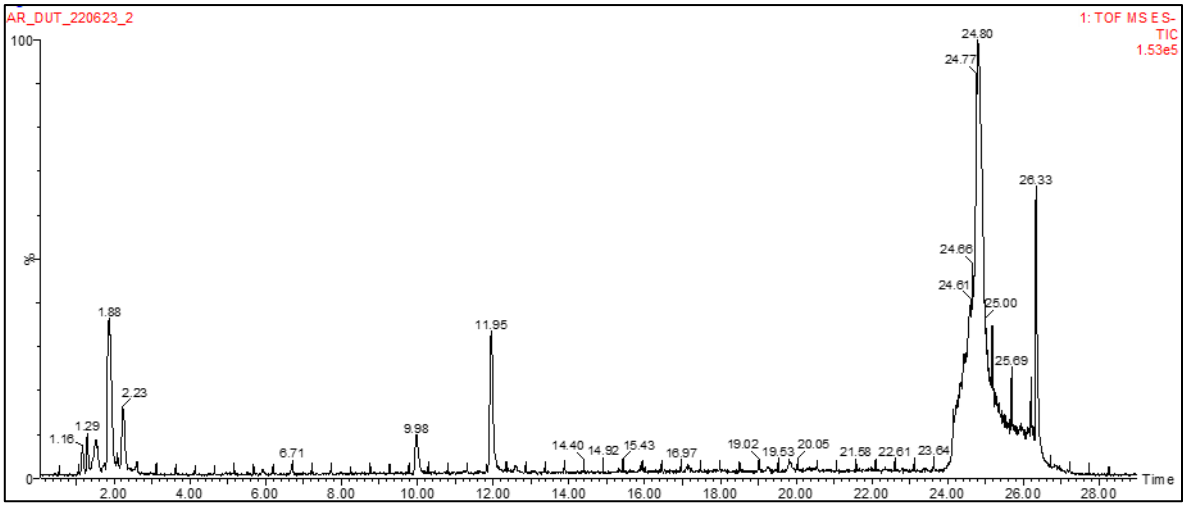

d) Chromatogram of AGSUN 5106 CLP

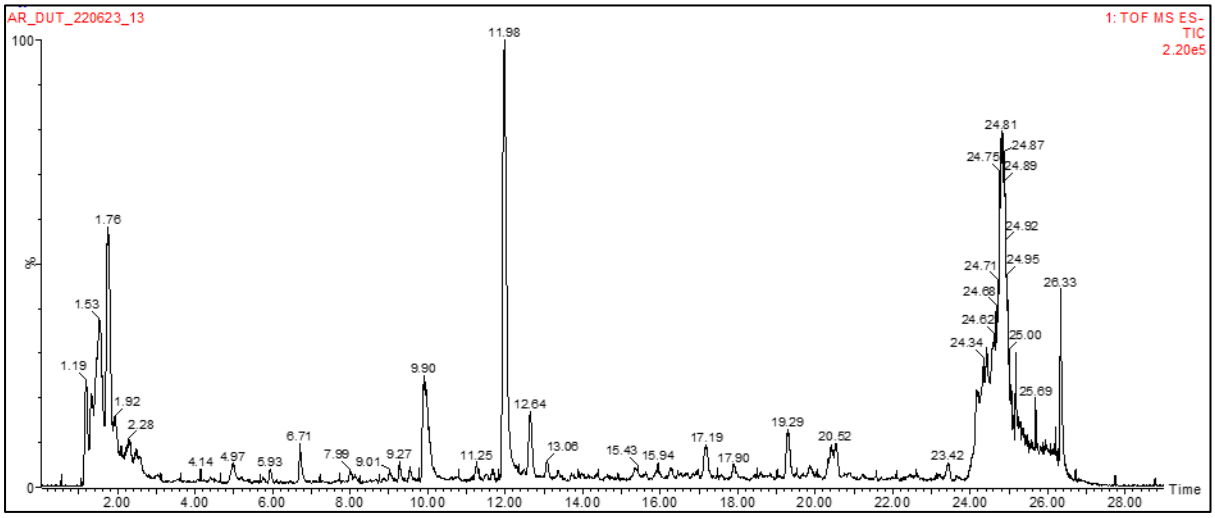

e) Chromatogram of AGSUN 5103 CLP

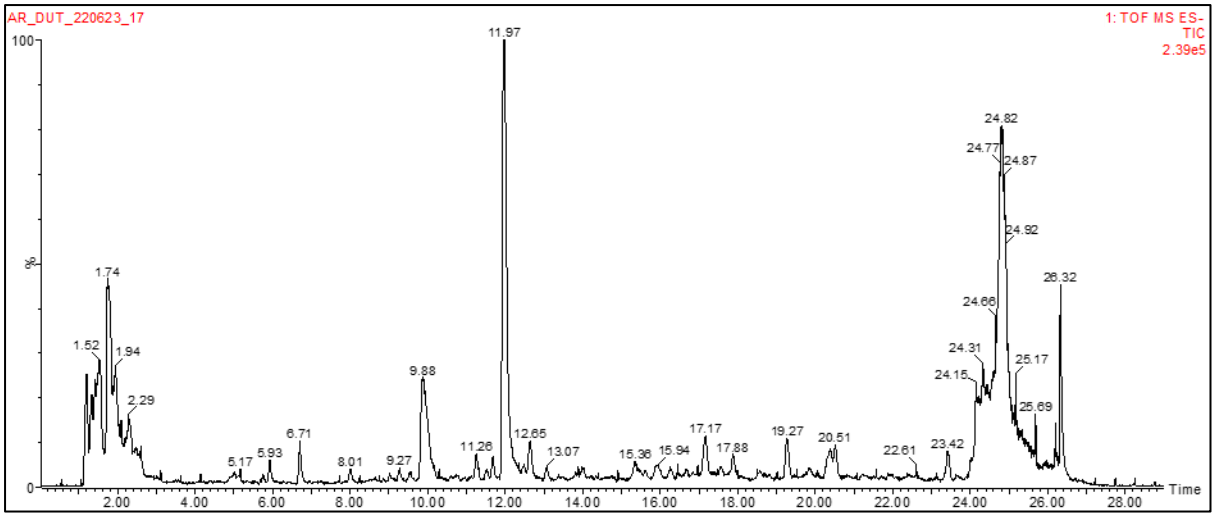

f) Chromatogram of AGSUN 5101 CLP

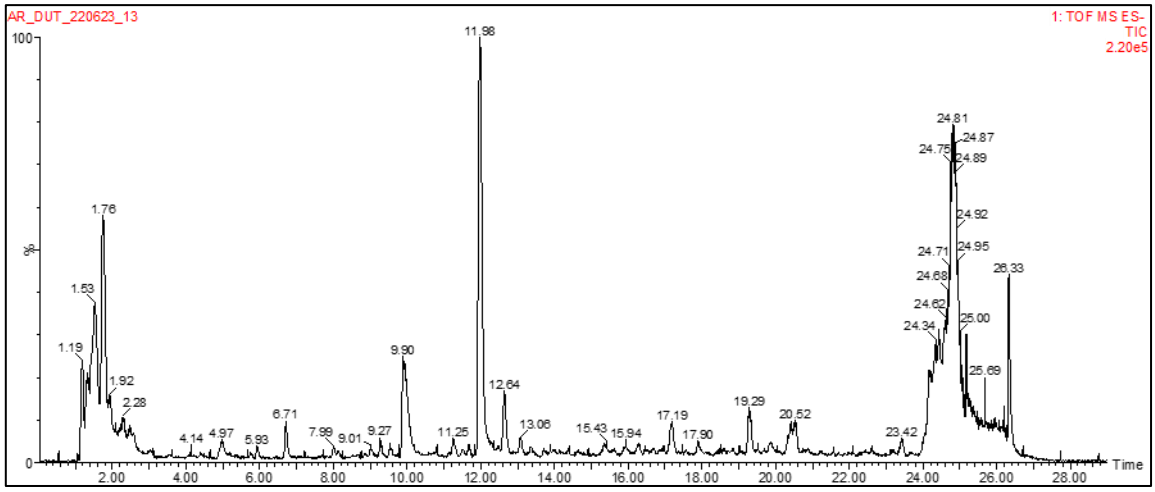

Table S4: Compounds filtered against Lipinski's rule of 5

No.	Compound	Lipinski's Rule of 5	Violations
1	Trimethylsilanol	Pass	-
2	Octamethylcyclotetrasiloxane	Pass	-
3	Hexanal	Pass	-
4	β--Pinene	Pass	-
5	Undecane	Pass	-
6	Sabinene	Pass	-
7	(-)-Limonene	Pass	-
8	Tridecane	Pass	-
9	Decamethylcyclopentasiloxane	Pass	-

10	2,2,4,4,6,8,8-Heptamethylnonane	Pass	-
11	1-Hexanol	Pass	-
12	Dodecamethylcyclohexasiloxane	Pass	-
13	Acetoin	Pass	-
14	2-Butoxyethanol	Pass	-
15	Acetic Acid	Pass	-
16	Ethyl decanoate	Pass	-
17	2-Ethyl-3-hydroxyhexyl 2-methylpropanoate	Pass	-
18	Benzyl alcohol	Pass	-
19	Nonan-1-ol	Pass	-
20	Calarene	Pass	-
21	Methenamine	Pass	-
22	3-METHYLBUTAN-1-OL	Pass	-
23	Benzaldehyde	Pass	-
24	Dodecane	Pass	-
25	2-Methyl-1-butanol	Pass	-
26	Benzene, ethenyl-, polymer with 2-methyl-1,3-butadiene, hydrogenated	Pass	-
27	β--Bisabolene	Pass	-
28	MYRTENOL	Pass	-
29	Hexamethylcyclotrisiloxane	Pass	-
30	Propanoic acid, 2-methyl-, 3-hydroxy-2,4,4-trimethylpentyl ester	Pass	-
31	Ethanol	Pass	-
32	verbenene	Pass	-
33	gamma-Terpinene	Pass	-
34	Bicyclo[4.2.0]octa-1,3,5-triene	Pass	-
35	Terpinolene	Pass	-
36	Pinocarveol	Pass	-
37	Mentha-1,4,8-triene	Pass	-
38	TRANS-(+)-CARVEOL	Pass	-
39	Camphene Bicyclo[2.2.1]heptane, 2,2-dimethyl-3-methylene-	Pass	-
40	Propane, 1-methoxy-2-methyl-	Pass	-
41	Benzeneacetaldehyde	Pass	-
42	2,6,10-Trimethyldodecane	Pass	-
43	1-Pentanol	Pass	-
44	Tetradecane	Pass	-
45	Propylene glycol	Pass	-
46	gamma-Butyrolactone	Pass	-
47	4-Methyldecane	Pass	-
48	2,6-Dimethylpyrazine	Pass	-
49	1-Heptanol	Pass	-
50	1-Octanol	Pass	-
51	Xanthine	Pass	-

52	Dihydroxyacetone gluconate	Pass	-
53	Cinnzeylanol	Pass	-
54	Tryptophanate	Pass	-
55	Chlorogenic acid	Pass	-
56	isomoreollin B	Pass	-
57	7-Methoxyisomorellinol	Pass	-
58	2-Isopropylmalic acid	Pass	-
59	Dihydrophaseic acid 4'-O-β--D-glucopyranoside	Pass	-
60	1-O-Caffeoylglucose	Pass	-
61	Strophanthobiose	Pass	-
62	Quinic acid	Pass	-
63	Safflor Yellow B	Fail	3 Violations (MW>500, NorO>10, NHorOH>5)
64	Kaempferide 3-rhamnoside-7-(6"-succinylglucoside)	Fail	3 Violations (MW>500, NorO>10, NHorOH>5)
65	Methyl asterrate	Pass	-
66	Caffeic acid	Pass	-
67	Phenylacetic acid	Pass	-
68	Piceol;4'-Hydroxyacetophenone;p-Hydroxyacetophenone	Pass	-
69	Icariside F2	Pass	-
70	Gein	Fail	2 Violations (NorO>10, NHorOH>5)
71	3'-O-β--Glucopyranosyl plumbagic acid methyl ester	Pass	-
72	3-O-Caffeoyl-4-O-methylquinic acid	Pass	-
73	Tricin 5-O-β--D-glucopyranoside;Tricin 5-glucoside	Fail	2 Violations (NorO>10, NHorOH>5)
74	Ptelatoside A	Pass	-
75	Sonchuside I	Pass	-
76	Granatumin C	Pass	-
77	Hymenoside R	Pass	-
78	(2S)-6-(gamma,gamma-dimethylallyl)-3',4'-dimethoxy-6",6"-dimethylpyran[2",3":7,8]flavanone	Pass	-
79	4α,6S,7α)-6α-[6-O-(4-Hydroxybenzoyl)-β-D-glucopyranosyloxy]-7β-methyloctahydrocyclopenta[c]pyran-1-one)	Pass	-
80	1-(((3-Nitrobenzyl)oxy)methyl)pyridin-1-ium chloride	Pass	-
81	Chrysanthemorimic acid A	Fail	3 violations (MW>500, NorO>10, NHorOH>5)
82	[4]-Gingerdiol	Pass	-
83	Dracunculifoside Q	Pass	-
84	Dracunculifoside F	Fail	3 Violations (MW>500, NorO>10, NHorOH>5)

85	Formononetin 7-(6"-malonylglucoside)	Fail	2 Violations (MW>500, NorO>10)
86	Fluorescein-digalactoside	Fail	3 Violations (MW>500, NorO>10, NHorOH>5)
87	Azelaic acid	Pass	-
88	Ferulic acid	Pass	-
89	Seguinoside J	Fail	3 Violations (MW>500, NorO>10, NHorOH>5)
90	Cascaroside C	Fail	3 Violations (MW>500, NorO>10, NHorOH>5)
91	Methyl 2-[(3-acetyloxy-4,5-dimethoxyoxan-2-yl)methoxy]acetate	Pass	-
92	Sacranoside A	Pass	-
93	Formoxanthone B	Pass	-
94	Methyl asterate	Pass	-

Table S5: Docking scores of sunflower seed metabolites against six key enzymes implicated in T2DM and its pathogenesis. Enzyme standards are bolded, while top-5-hit compounds against each enzyme is highlighted.

COMPOUND	**Alpha-amylase**	**Alpha-glucosidase**	**DPP-IV**	**PTP1B**	**Sorbitol dehydrogenase**	**Aldose reductase**
Acarbose	**-7.4**	**-7.8**	**-**	**-**	**-**	**-**
Epalrestat	**-**	**-**	**-**	**-**	**-**	**-8.2**
Sitagliptin	**-**	**-**	**-8.4**	**-**	**-**	**-**
Ursolic acid	**-**	**-**	**-**	**-6.5**	**-**	**-**
4-[2-1R-hydroxy-ethyl)-pyrimidin-4-yl]piperazine-1-sulfonic acid dimethylamide	**-**	**-**	**-**	**-**	**-7.0**	**-**
Trimethylsilanol	-5.2	-6.4	-4.7	-2.2	-5.0	-5.7
Octamethylcyclotetrasiloxane	-	-	-	-	-	-
Hexanal	-3.7	-4.1	-3.5	-2.0	-3.7	-4.1
β--Pinene	-5.4	-5.8	-4.8	-4.0	-5.4	-5.9
Undecane	-4.4	-5.3	-4.8	-1.9	-4.9	-5.0
Sabinene	-5.9	-5.1	-4.6	-4.0	-5.9	-5.8
(-)-Limonene	-5.7	-5.7	-6.8	-5.2	-5.7	-5.9
Tridecane	-4.5	-5.1	-5.1	-1.7	-4.2	-5.2
Decamethylcyclopentasiloxane	-	-	-	-	-	-
2,2,4,4,6,8,8-Heptamethylnonane	-2.0	-3.6	-3.0	-2.5	-4.0	-3.5
1-Hexanol	-4.0	-4.2	-4.3	-3.8	-4.7	-3.9

Dodecamethylcyclohexasiloxane	-	-	-	-	-	-
Acetoin	-3.7	-4.4	-3.7	-3.5	-4.3	-3.2
2-Butoxyethanol	-3.8	-3.9	-3.1	-3.0	-4.1	-3.9
Acetic Acid	-3.1	-3.5	-3.6	-4.0	-3.3	-2.5
Ethyl decanoate	-3.7	-4.5	-4.0	-4.5	-5.2	-5.5
2-Ethyl-3-hydroxyhexyl 2-methylpropanoate	-5.6	-5.0	-3.7	-5.2	-5.5	-4.0
Benzyl alcohol	-4.9	-5.2		-5.3	-5.1	-5.5
Nonan-1-ol	-4.3	-5.1	-3.5	-3.5	-4.6	-4.9
Calarene	-7.2	-6.6	-3.5	-6.3	-6.6	-7.7
Methenamine	-4.5	-4.2	-2.9	-5.0	-4.3	-4.4
3-METHYLBUTAN-1-OL	-3.8	-4.6	-3.2	-4.2	-3.9	-4.0
Benzaldehyde	-4.7	-5.2	-3.6	-3.3	4.7	-5.0
Dodecane	-4.6	-5.4	-5.7	-2.0	-4.5	-5.0
2-Methyl-1-butanol	-3.6	-3.8	-3.3	-2.8	-4.0	-3.9
Benzene, ethenyl-, polymer with 2-methyl-1,3-butadiene, hydrogenated	-3.3	-4.4	-3.0	-3.0	-3.7	-3.5
β--Bisabolene	-6.1	-7.4	-4.7	-5.5	-6.3	-7.2
MYRTENOL	-5.7	-6.2	-3.7	-4.2	-5.7	-5.9
Hexamethylcyclotrisiloxane	-	-	-	-	-	-
Propanoic acid, 2-methyl-, 3-hydroxy-2,4,4-trimethylpentyl ester	-5.1	-6.0	-3.4	-4.5	-5.7	-6.0
Ethanol	-3.1	-2.8	-2.7	-3.0	-2.6	-2.9
verbenene	-5.4	-5.5	-4.0	-4.0	-5.5	-5.9
gamma-Terpinene	-5.9	-6.8	-3.6	-4.5	-5.7	-6.1

Bicyclo[4.2.0]octa-1,3,5-triene	-4.5	-5.0	-5.5	-4.0	-4.2	-3.5
Terpinolene	-5.6	-6.2	-5.0	-5.5	-5.4	-6.4
Pinocarveol	-5.9	-5.7	-5.6	-5.6	-5.5	-6.2
Mentha-1,4,8-triene	-5.9	-6.3	-4.8	-5.4	-5.9	-6.0
TRANS-(+)-CARVEOL	-5.7	-6.4	-5.0	-4.9	-5.9	-6.7
Camphene Bicyclo[2.2.1]heptane, 2,2-dimethyl-3-methylene-	-5.5	-5.6	-4.9	-4.5	-5.2	-5.9
Propane, 1-methoxy-2-methyl-	-3.4	-3.9	-3.2	-3.6	-3.5	-3.2
Benzeneacetaldehyde	-5.0	-5.4	-4.5	-4.9	-5.3	-5.5
2,6,10-Trimethyldodecane	-3.0	-2.8	-3.0	-4.2	-4.3	-3.2
1-Pentanol	-3.7	-4.4	-3.8	-3.5	-4.0	-3.8
Tetradecane	-3.5	-4.3	-4.5	-4.9	-4.8	-4.2
Propylene glycol	-3.8	-4.0	-3.5	-4.0	-3.9	-3.4
gamma-Butyrolactone	-3.5	-4.2	-4.8	-3.9	-4.2	-3.9
4-Methyldecane	-3.5	-4.3	-4.4	-4.2	-3.0	-3.3
2,6-Dimethylpyrazine	-4.5	-4.8	-4.0	-4.4	-4.9	-5.0
1-Heptanol	-4.2	-4.6	-3.9	-4.2	-4.4	-4.3
1-Octanol	-4.5	-4.9	-4.3	-4.0	-4.4	-4.6
7-Methoxyisomorellinol	-9.4	-7.6	-9.6	-6.8	-9.0	-7.7
1-O-Caffeoylglucose	-7.3	-8.1	-7.9	-6.4	-8.3	-6.2
Cinnzeylanol	-7.6	-6.2	-8.0	-6.5	-8.1	-6.8
Dihydroxyacetone gluconate	-5.3	-5.4	-6.8	-6.5	-6.1	-5.2

3'-O-β--Glucopyranosyl plumbagic acid methyl ester	-7.4	-7.0	7.3	-5.9	-8.1	-5.6
2-Isopropylmalic acid	-6.8	-6.3	-5.7	-5.5	-5.5	-4.5
1-(((3-Nitrobenzyl)oxy)methyl)pyridin-1-ium chloride	-6.4	-6.4	-6.7	-6.3	-6.8	-5.0
Tryptophanate	-5.5	-5.7	-6.3	-5.6	-6.7	-5.2
Xanthine	-5.6	-6.2	-6.4	-5.7	-5.7	-5.3
Chlorogenic acid	-8.0	-8.0	-9.0	-6.9	-8.1	-6.5
Caffeic acid	-6.6	-6.3	-6.9	-6.2	-8.5	-6.0
Icariside	-8.0	-7.5	-7.7	-6.9	-6.1	-6.2
Granatumin C	-8.8	-8.7	-9.1	-7.4	-9.1	-6.5
Hymenoside R	-6.9	-7.4	-8.1	-6.3	-8.3	-5.9
Gingerdiol	-6.0	-6.9	-6.6	-5.2	-6.6	-5.7
Dracunculifoside Q	-7.3	-7.5	-7.4	-6.5	-7.8	-6.2
(2S)-6-(gamma,gamma-dimethylallyl)-3',4'-dimethoxy-6",6"-dimethylpyran[2",3":7,8]flavanone	-9.5	-8.1	-9.1	-7.4	-9.6	-6.8
Azelaic acid	-5.4	-5.1	-5.3	-5.1	-5.5	-4.5
Ferulic acid	-6.5	-7.0	-6.4	-6.4	-6.3	-5.1
Formoxanthone B	-9.6	-8.9	-8.2	-8.0	-10.1	-7.5
Dihydrophaseic acid 4'-O-β--D-glucopyranoside	-7.7	-7.6	-7.3	-6.5	-8.6	-6.2
Sacranoside A	-8.3	-8.2	-8.7	-7.1	-9.3	-7.3
Sonchuside I	-8.7	-7.2	-8.8	-7.1	-9.0	-7.5
Strophanthobiose	-5.7	-5.3	-6.1	-5.0	-6.3	-4.6

Methyl asterrate	-6.5	-5.9	-5.9	-5.5	-7.3	-5.2
Methyl 2-[(3-acetyloxy-4,5-dimethoxyoxan-2-yl)methoxy]acetate	-5.3	-4.6	-5.7	-5.2	-6.1	-4.2
Phenylacetic acid	-5.6	-5.7	-5.8	-5.2	-5.8	-5.0
Piceol;4'-Hydroxyacetophenone;p-Hydroxyacetophenone	-5.4	-5.4	-5.7	-5.7	-6.3	-4.9
4α,6S,7α)-6α-[6-O-(4-Hydroxybenzoyl)-β-D-glucopyranosyloxy]-7β-methyloctahydrocyclopenta[c]pyran-1-one)	-8.9	-8.0	-8.8	-6.8	-10.2	-7.0
Quinic acid	-5.7	-6.7	-5.9	-5.7	-6.2	-5.5
Isomoreollin B	-8.7	-6.7	-8.0	-8.0	-7.2	-8.5
3-O-caffeolyl-4-O-methylquinic acid	-7.4	-8.4	-8.4	-6.0	-6.8	-6.2
Ptelatoside A	8.1	-9.1	-8.0	-7.0	-8.2	-7.3

Chapter Four

Molecular bioprospection of *Helianthus annuus* L. (sunflower) cypselae for antidiabetic therapeutics through network pharmacology, density functional theory and molecular dynamics simulation

The chapter was published in *South African Journal of Botany*. https://doi.org/10.1016/j.sajb.2023.08.045

South African Journal of Botany 162 (2023) 72–95

Contents lists available at ScienceDirect

South African Journal of Botany

journal homepage: www.elsevier.com/locate/sajb

Molecular bioprospection of *Helianthus annuus* L. (sunflower) cypselae for antidiabetic therapeutics through network pharmacology, density functional theory and molecular dynamics simulation

Athika Rampadarath[a], Jamiu Olaseni Aribisala[a], Nokwanda Pearl Makunga[b], Sithandiwe Mazibuko-Mbeje[c], Saheed Sabiu[a,*]

[a] Department of Biotechnology and Food Science, Faculty of Applied Sciences, Durban University of Technology, Durban 4000, South Africa
[b] Department of Botany and Zoology, Stellenbosch University, Private Bag X1, Matieland, Stellenbosch 7602, South Africa
[c] Department of Biochemistry, North-West University, Mafikeng Campus, Mmabatho, South Africa

ARTICLE INFO

Article History:
Received 19 July 2023
Revised 19 August 2023
Accepted 21 August 2023
Available online 8 September 2023

Edited by Dr I. Famuyide

Keywords:
Sunflower
Type-2 diabetes mellitus
PPAR pathway
MMP1 and PPARA

ABSTRACT

Helianthus annuus cypsela (sunflower) is a staple oilseed crop with significant therapeutic applications against diverse diseases including type 2 diabetes mellitus (T2DM). Despite its reported antidiabetic potential, the implicated molecular mechanism of action is yet to be unravelled to date. This study evaluated the molecular mechanism of the antidiabetic activity of sunflower cypsela using network pharmacology (NP), density functional theory, and molecular dynamics (MD) simulation approaches. The six cultivars of sunflower cypsela used were profiled for their secondary metabolites using LC-MS and GC–MS techniques. Subsequently, the genes associated with the identified metabolites were screened against T2DM-associated genes using NP. Based on the KEGG enrichment analysis of the identified common genes, signaling pathways were subsequently identified. The results obtained revealed 87 intersecting genes between the metabolites of sunflower cypsela and T2DM, while the KEGG analysis identified 35 signaling pathways with the PPAR route and its associated genes as the most implicated in T2DM progression with respect to sunflower cypsela. Both MMP1 and PPARA in the PPAR pathways interacted most with the identified metabolites, with CGA (−43.74 kcal/mol), GPA (−41.62 kcal/mol), and CFG (−45.36 kcal/mol) having higher binding free energy than both ROS and MET (reference standards) against MMP1 after 100,000 ps MD simulation. In contrast, ROS (−46.98 kcal/mol) had better affinity against PPARA compared to the top hits of sunflower cypsela. However, against both gene targets, the top hits had significant thermodynamic stability, flexibility, and compactness, which are attributable to their bond interactions and molecular orbital properties. These findings are suggestive of the essential role of the top-hits in the antidiabetic potential of sunflower cypsela through activation of the PPAR signalling pathway and most especially MMP1. In this regard, the modulation of MMP1 and PPARA genes by the identified metabolites of sunflower cypsela may enhance insulin sensitivity and glucose homoeostasis in the management of T2DM.

1. Introduction

Alongside heart diseases and cancer, type-2 diabetes mellitus (T2DM) remains one of the most chronic disorders responsible for the decline in human longevity (Centers for Disease Control and Prevention, 2021). Just recently, over 537 million people were reported to be diabetic, with a projected increase to 643 million in 2030 if no suitable solution is provided (International Diabetes Federation, 2021). Insufficient insulin secretion by the β-cells and/or failure of insulin-sensitive cells to respond to the secreted insulin have been identified as major contributory factors to the pathogenesis of T2DM (Galicia-Garcia et al., 2020; Roden et al., 2017). The impaired cells fail to maintain glucose homeostasis, thereby elevating blood glucose levels, which could progress to the onset of hyperglycemia (Artasensi et al., 2020; Schinner et al., 2005). To manage T2DM and prevent the onset of its secondary complications such as cardiovascular disease, nephropathy, neuropathy, and retinopathy (Zheng et al., 2018), oral antidiabetic drugs such as sulfonylureas, biguanides, and thiazolidinediones are often prescribed to patients (Singh et al., 2019). However, the accompanying adverse effects of these drugs, such as hypoglycemia, liver damage, and chronic heart failure, have limited their application in clinical practice to date (Artasensi et al., 2020). Hence, the need to bioprospect for safer, more effective, and affordable antidiabetic therapeutics.

* Corresponding author.
E-mail address: sabius@dut.ac.za (S. Sabiu).

https://doi.org/10.1016/j.sajb.2023.08.045
0254-6299/

Plants have been used as therapeutic agents since prehistoric times (Saggar et al., 2022) due to the presence of various secondary metabolites such as polyphenols, alkaloids, and terpenes (Awuchi, 2019). By the early nineteenth century, the isolation of these metabolites from plants had begun, creating the new era of "natural compounds" as therapeutics (Süntar, 2020). One of such plants with remarkable nutritional and therapeutic potential is *Helianthus annuus* L., commonly referred to as sunflower, an oilseed plant in the family Asteraceae (Nguyen et al., 2021) with native range distribution across South Africa, Canada, Mexico and US (Hernández et al., 2019). Sunflower is rich in phenolic compounds that have been reported to have antioxidant and antidiabetic activity, with 70% of the phenolics present in sunflower being chlorogenic acid, caffeic acid, and ferulic acid (Anjum et al., 2012; Adeleke and Babalola, 2020). Sunflower cypsela, being an edible plant component, present great potential as an antidiabetic agent, as dietary intervention and overall lifestyle changes have proven to have a significant influence in the prevention of T2DM in high-risk individuals (Rehman et al., 2021; Zheng et al., 2018).

Although, previous studies have reported on the antidiabetic activity of sunflower cypsela using *in vitro* (Sun et al., 2012) and *in vivo* (Richmond et al., 2013; Shivani and Sunil, 2013) methods, unfortunately, none of the studies reported on the underlying molecular mechanism of action of the cypsela. More recently, the significance of computer-aided drug design using advanced methods such as network pharmacology (NP) and molecular dynamic (MD) simulation has been demonstrated in T2DM studies, and the results have been significant. For instance, the application of NP approach to investigate the antidiabetic potential of mulberry leaf, revealed gallic acid and chlorogenic acid as the key metabolites from the plants in the management of T2DM through regulation of insulin, inflammatory pathways, and glucose metabolism (Ge et al., 2018). Similarly, Dwivedi et al. (2021), combined NP, molecular docking, and MD simulation and identified the PI3K-Akt signalling pathway and, most especially, the aldose reductase gene as the most regulated by the metabolites of *Cassia glauca*. in the management of T2DM. Beside that no studies exit on the molecular mechanism of antidiabetic action of sunflower cypsela, there is also a dearth of information on its antidiabetic effect using advanced computational methods to date, albeit its oil (Rampadarath et al., 2023). It is on this background that the present study was conceptualized to provide novel insights into the molecular mechanism of antidiabetic action of sunflower cypsela through NP, density functional theory (DFT), and MD simulation strategies with a view to exploring gene targets and their role in signalling pathways implicated in T2DM pathogenesis.

2. Materials and method

2.1. Sunflower cypsela collection and processing

Fresh cypsela of six of the most consumed cultivars of sunflower cypsela (AGSUN 5270, AGSUN 8251, AGSUN 5101 CLP, AGSUN 5106 CLP and AGSUN CLP 5103) in South Africa were used in this study. The cypsela were collected from the Agricultural Research Council, Potchefstroom, South Africa. Each cultivar was de-husked, washed, and oven-dried at 60 °C before grinding using mortar and pestle. The powdered cypsela were then subjected to liquid chromatographic–mass spectrometry (LC–MS) and gas chromatography–mass spectrometry (GC–MS) analyses for non-volatile and volatile metabolite identification, respectively.

2.2. Identification of metabolites present in cultivars of sunflower cypsela

2.2.1. Liquid chromatography–mass spectrometry (LC–MS) for non-volatile constituents' identification

The powdered cypsela (2 g each) were extracted using a solvent system containing 15 ml of 50% methanol and 0.1% formic acid for 24 h (Kaigongi et al., 2020). Following ultrasonication (Bransonic 220, USA) for 1 h, the resulting supernatant in each case was analysed using Waters Synapt G2 Quadrupole time-of-flight (QTOF) mass spectrometer (MS) connected to a Waters Acquity ultra-performance liquid chromatograph (UPLC) (Waters, Milford, MA, USA) for high-resolution UPLC-MS analysis. Column eluate first passed through a Photodiode Array (PDA) detector before going to the mass spectrometer, allowing simultaneous collection of UV and MS spectra. Electrospray ionization was used in negative mode with a cone voltage of 15 V, desolvation temperature of 275 °C, desolvation gas at 650 L/h, and the rest of the MS settings optimized for best resolution and sensitivity. Data were acquired by scanning from *m/z* 150 to 1500 *m/z* in resolution mode as well as in MSE mode. In MSE mode two channels of MS data were acquired, one at a low collision energy (4 V) and the second using a collision energy ramp (40–100 V) to obtain fragmentation data as well. Leucine enkaphalin was used as lock mass (reference mass) for accurate mass determination and the instrument was calibrated with sodium formate. Separation was achieved on a Waters HSS T3, 2.1 × 100 mm, 1.7 μm column. An injection volume of 2 μL was used and the mobile phase consisted of 0.1% formic acid (solvent A) and acetonitrile containing 0.1% formic acid as solvent B. The gradient started at 100% solvent A for 1 min and changed to 28% B over 22 min in a linear way. It then went to 40% B over 50 s and a wash step of 1.5 min at 100% B, followed by re-equilibration to initial conditions for 4 min. The flow rate was 0.3 mL/min, and the column temperature was maintained at 55 °C. Compounds were quantified in a relative manner against a calibration curve established and further processed using MSDIAL and MSFINDER (RIKEN Centre for Sustainable Resource Science: Metabolome Informatics Research Team, Kanagawa, Japan).

2.2.2. Gas chromatography–mass spectrometry (GC–MS) for volatile constituents' identification

For this analysis, the powdered seed samples (2 g per cultivar) were subjected to GC–MS on a on an Agilent 5973 mass selective detector (Palo Alto, CA) connected to an Agilent 6890 gas chromatograph, equipped with a 60 m × 0.25 mm × 0.25 (FFAP) μm capillary column (Magangana et al., 2021). The oven temperature was adjusted from 70 °C for 1 min, increased to 142 °C at 3 min, and then increased at 5 °C per minute up to 225 °C (which was then held for 3 min). The transfer line was heated at 250 °C. Helium was used as a carrier gas at a linear velocity of 1.9 ml min ^{1}. The operating conditions of the mass detector were set at 230 °C for the source temperature; and electronic impact (EI) mode of 70 eV, with a speed of 4.38 scan s^{-1} over the mass range *m/z* 30–350 amu in a one-second cycle, was employed in a full scan mode. The identification of volatile compounds was performed by comparing the mass spectra against the National Institute of Standards and Technology (NIST) library and a library match above 75% was a hit (Wallace and Moorthy, 2023).

2.3. Network pharmacology

2.3.1. Druglike-ness screening of bioactive compounds

A library of both the non-volatile and volatile compounds identified in the six cultivars of sunflower cypsela was constructed (Supplementary Table S1) and the compounds were subsequently subjected to Lipinski's rule of five (Ro5) to identify orally bioavailable compounds (Lipinski et al., 1997). This was performed by retrieving the canonical SMILES of each compound from PubChem (https://pubchem.ncbi.nlm.nih.gov/) and input onto SWISS ADME (http://www.swissadme.ch/) for assessment (Daina et al., 2017). Compounds with two or more violations (<5 hydrogen bond donors; ≤10 hydrogen bond acceptors; molecular weight ≤ 500 g/mol and partition co-efficient <5) were identified as Lipinski's Ro5 violators and were discarded from subsequent analysis (Bitew et al., 2021).

2.3.2. Target data mining

Metabolites that passed the Ro5 were taken for target data mining using two independent databases [Similarity Ensemble Approach (SEA) (http://www.sea.bkslab.org) and Swiss Target Predication (STP) (http://www.swisstargetprediction.ch/)] for gene targets associated with the compounds, with the search parameters being in *Homo sapiens* mode. Retrieval of genes associated with sunflower cypsela' metabolites from SEA and STP was accomplished using the canonical smile of the metabolites.

For the T2DM targets, DisGeNet (https://www.disgenet.org/) and Gene Cards (https://www.genecards.org/) were used to retrieve T2DM associated genes, while Venn diagrams were constructed using Venny v2.1. (https://bioinfogp.cnb.csic.es/tools/venny/) to seamlessly identify intersecting targets between the databases for the sunflower cypsela' metabolites and T2DM, respectively.

2.3.3. Protein-protein interactions (PPI)

The PPI was analysed using STRING [STRING: functional protein association networks (string-db.org)] software v11.5. The parameters for the analysis were set to *Homo sapiens* with a confidence level $> .4$, followed by the input of the common target genes between bioactive compounds and T2DM. Thereafter, Cytoscape v3.8.2 was employed to construct a network classification of the PPI. The degree algorithm was utilized to identify key genes (Zeng et al., 2021).

$$\text{Degree}(v) = \left|N(v)\right|$$

Node neighbours are represented by "N(v)" and each node's neighbor "v".

2.3.4. Kyoto encyclopaedia of genes and genomes (KEGG) pathway enrichment and gene ontology (GO) analysis

The functional enrichment of the target genes in the PPI network was done using the STRING software v 11.5 (Oh et al., 2020). One of the analyses performed was KEGG pathway enrichment of the target genes. The resulting pathways were studied for direct association with T2DM. The pathway with the lowest false discovery rate (FDR < 0.05) was taken as the most enriched and significantly associated with the intersecting targets. Subsequently, GO of the targets was performed using Database for Annotation, Visualization and Integrated Discovery (DAVID) database (https://david.ncifcrf.gov/tools.jsp) (Di et al., 2021). Search parameters were set to *Homo sapiens* and the selected gene identifier was "OFFICIAL GENE SYMBOL". Gene target list was generated in a consistent format and thereafter analysed using the "Functional annotation" tool (Sherman et al., 2021).

The output of the analysis was categorized into three descripted terms: Biological processes (BP), cellular components (CC) and molecular function (MF). Based on the *p*-value (<0.05), the most significant functions were identified for each category. The KEGG enrichment and GO analysis data was plotted using SRplot (http://www.bioinformatics.com.cn/en).

2.3.5. Pathway compound target

Graphical representations of pathway-compound-target network were constructed using Cytomerger plugin in Cytoscape software v3.9.1. (Dwivedi et al., 2021). Cytoscape network analyzer plugin was used to carry out network topology parameter analysis, where the nodes in the network represented sunflower cypsela' metabolites and targets in the pathway identified from KEGG pathway enrichment analysis. The edges highlighted the interactions between the nodes, identifying the metabolites interaction with each target. Where more edges are directed between nodes, a higher degree of interactions was noted (Adnan et al., 2022).

2.4. Molecular docking and dynamic simulation

Following the identification of the most enriched pathway through KEGG analysis, the targets with the most interactions with the metabolites of sunflower cypsela were selected as the key targets for molecular docking. The X-ray crystal structures of the two key and most enriched targets (MMP1 (PDB ID: 966C) and PPARA (PDB ID: 3ET1)) were downloaded from RSCB Protein data bank (https://www.rcsb.org/) subsequent to preparation on USCF Chimera v1.16 (Pettersen et al., 2004) through the deletion of non-standard amino acid residues, water molecules and co-crystallized ligand. On the other hand, the 3D conformers of the metabolites (Table S1) interacting with the respective key target, in addition to rosiglitazone (an agonist of the hub signalling pathway, PPARA) and the \standard antidiabetic drug (metformin), were retrieved from PubChem. These metabolites (ligands) were prepared by the addition of Gastierger charges and non-polar hydrogen atom using USCF Chimera v1.16. Subsequently, the ligands were individually docked at the active site of their respective target genes (MMP1 and PPARA) using AutoDock Vina plugin on USCF Chimera (Ammu et al., 2019). Docking at the active site of the target MMP1 and PPARA was assured by adjusting the grid box coordinates to match the established x-y-z coordinates identified on Discovery studio version 2021 (BIOVIA, 2021). The ligands with highest binding free energy against each target was selected as the best compounds and taken to MD simulation analyses.

In preparation for MD simulation, the validation of the docking protocol was performed using decoy method (Aribisala and Sabiu, 2022). This was carried out by superimposing the best docked ligands and standards on the native ligand in the co-crystal structure of each target as presented in Fig. 1. The Root Mean Square Deviation (RMSD) of the docked ligands from the native inhibitor was 0.5 Å for both MMP1 (Fig. 1A) and PPARA (Fig. 1B).

The MD simulation was performed as previously described by Aribisala et al. (2022). The simulation was carried out on the Graphical Processing Unit (GPU) of the AMBER 18 package of the Centre for High Performance Computing (CHPC), Cape Town, South Africa. The systems were described using the AMBER force field (FF18SB variant). The sunflower cypsela' ligands partial charges were assigned by ANTECHMABER through restrained electrostatic potential (RESP) general AMBER force field (GAFF) steps. The Leap module aid the addition of hydrogen atom (H^+), $Na^{+\cdot}$ and Cl^-counter ions for system neutralization and the sequences for MMP1 (264) and PPARA (486) were numbered accordingly. The system was then deposited into orthorhombic box of TIP3P water molecules ensuring all atoms are within 8 at 1 bar Å of any box edge. The system was then minimized following the steepest descent procedure with 2000 minimization steps and restricting 500 kcal/mol for both solutes followed by conjugate gradients. The full minimization steps began with 1000 steps, without restraint through the conjugate gradient algorithm. The heating stage of the MD simulation proceeded at 50 ps, from 0 K to 300 K, warranting constant volume of both, atoms and water. Following the exposure of the solutes to potential harmonic restraint of 10 kcal/mol and collision frequency of 1.0 ps. Thereafter, the equilibrium stage begins with the system equilibrating at 500 ps and simultaneously maintain the constant heating temperature at 300 k and pressure at 1 bar to imitate an isobaric-isothermal ensemble (NPT). The SHAKE algorithm was then adopted to restrain hydrogen atoms during the MD simulation, which was conducted for a period of 100 ns. The binding free energy of the complexes throughout the simulation period was calculated using molecular mechanics with the generalized born surface area (MMGBSA) method. Post-dynamic parameters including root mean square deviation (RMSD), root mean square fluctuation (RMSF), solvent accessible surface area (SASA), radius of gyration (RoG) and intracellular hydrogen bond (H-Bond) dynamics were subsequently generated using the Origin data analysis software v6.0 (OriginLab, Northampton, MA, USA).

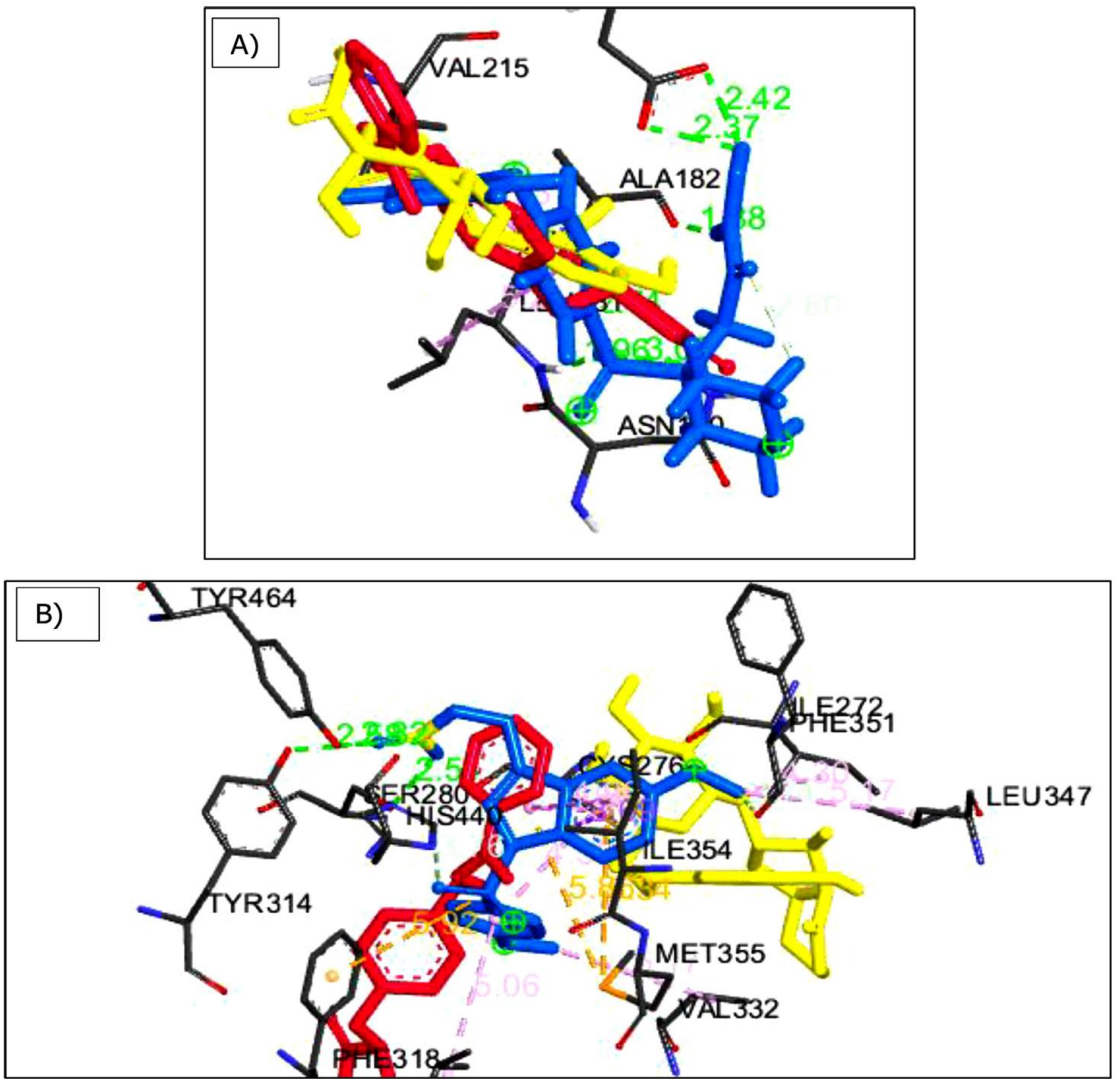

Fig. 1. Superimposition on co-crystalzed structure of A) MMP1: Native ligand 'n-hydroxy-2-[4-(4-*phenoxy-benzenesulfonyl*)-*tetrahydro-pyran*-4-*yl*]-acetamide' (Blue), standard 'rosiglitazone' (pink) and compound with highest docking score 'chlorogenic acid' (yellow). RMSD value of 0.5 Å. Grid box co-ordinates: Centre (X = 8.79488; Y = −10.1808; Z = 36.3525) and size (X = 10.5691; Y = 7.7166; Z = 34.627) and B) PPARA: : Native ligand '3-{5-methoxy-1-[(4-*methoxyphenyl*)*sulfonyl*]−1H-indol-3-yl}propanoic acid' (Blue), standard 'rosiglitazone' (pink) and compound with highest docking score '4aalpha,6S,7aalpha)-6alpha-[6-O-(4-H*ydroxybenzoyl*)-*beta-D-glucopyranosyloxy*]-7beta-methyloctahydrocyclopenta[*c*]pyran-1-one' (yellow). RMSD value of 0.5 Å. Grid box co-ordinates: Centre (X = 11.6401; Y = 27.5908; Z = 24.0673) and size (X = 11.4991; Y = 11.392; Z = 24.1566).(For interpretation of the references to color in this figure legend, the reader is referred to the web version of this article.)

2.5. Quantum chemical calculations

This analysis was done to predict the molecular properties of the top-hit compounds of sunflower cypsela as identified from their significant interactions with MMP1 and PPARA. The most commonly used DFT/B3LYP/631 G/+ (d,p) basic set (Kruse et al., 2012) was employed to optimise the top-hits using the Gaussian 16 program package of the CHPC, Cape Town, South Africa, and the result was viewed using GaussView 6 software V. 6.0.16. For every investigated ligand, the conceptual DFT descriptors such as hardness, softness, ionization energy, energy gap, chemical potential and electrophilicity index were subsequently calculated from the energies of frontier highest occupied molecular orbital (HOMO) and lowest unoccupied molecular orbital (LUMO) taking into consideration the Parr and Pearson interpretation (Calais, 1993) of DFT and Koopmans theorem (Luo, 2006) on the correlation of ionization potential (I) and electron affinities (E) with HOMO and LUMO energy. The following equations were used for the calculations:

$$\text{Energy gap}(\Delta E)[\text{E\_LUMO} - \text{E\_HOMO}](\text{eV}) \quad (1)$$

$$\text{Ionization energy}(I)[I = - - E\text{\_HOMO}](\text{eV}) \quad (2)$$

$$\text{Electron affinity}(A)[A = - - \text{E\_LUMO}) \quad (3)$$

$$\text{Hardness}(\eta)[\eta = (I - A)/2](\text{eV}) \quad (4)$$

$$\text{Softness}(S)[S = 1/\eta](\text{eV}) \quad (5)$$

$$\text{Electronegativity}(\chi)[\chi = (I + A)/2](\text{eV}) \quad (6)$$

$$\text{Chemical potential}(\mu)[\mu = -\chi = -(I+A)/2](\text{eV}) \quad (7)$$

$$\text{Electrophilicity index}(\omega)\left[\omega = \mu^2/2\eta\right](\text{eV}) \quad (8)$$

3. Results

3.1. Metabolite profiles of sunflower cypsela

The data obtained with respect to the metabolite profiles of the investigated sunflower cypsela as revealed by GC–MS and LC–MS analyses is presented in Supplementary Table S1. A total of 94 compounds were identified. While GC–MS analysis identified 50 compounds including organic acids, alkanes, alcohols, terpenes, heterocyclic compounds, 44 phenolics compounds were identified from the LC–MS analysis (Supplementary Table S1). The principal component analysis of the LC–MS obtained data revealed a variance of 39.7% among the six cultivars (Fig. S1).

3.2. Drug-likeness screening of the identified compounds present in sunflower cypsela

Of the 94 compounds identified, 84 fulfilled the Lipinski's Ro5 (Table S1) and were subjected to NP analysis.

3.3. Network pharmacology analysis of sunflower cypsela and T2DM

3.3.1. Sunflower cypsela and T2DM gene acquisition

The canonical SMILES of the 84 Lipinski-filtered compounds present in sunflower cypsela after being subjected to STP and SEA mapped closely with 984 and 654 genes, respectively, while 163 (11.1%) of these genes were found to be common between both databases (Fig. 2A). For the genes related to T2DM, 13 335 and 3134 genes were retrieved from GeneCards and DisGeNet databases, respectively, with identifiable 2603 (18.7%) overlapping genes (Fig. 2B). A probe into the degree of association of the genes related to the identified metabolites and those implicated in T2DM revealed 87 (3.2%) common genes as depicted in Fig. 2C.

3.3.2. PPI analysis

The result of subjecting the 87 genes common to both T2DM and those of the metabolites of the cypsela to PPI on STRING showed a network construction of 87 nodes, 437 edges and PPI enrichment p-value $< 1.0 \times 10^{-16}$ (Fig. 3). While the nodes represented the genes, the edges reflected the interactions taking place among the genes. The PPI network had an average node degree of 10 with GSTK1, CCKAR and MMP26 in exclusive isolation from other networks (Fig. 3).

3.3.3. GO and Kegg enrichment analysis

The GO functional analysis of the 87 genes reflects biological functions that the intersected genes are implicated in with reference to the biological processes (BP), cellular components (CC) and molecular function (MF). The most enriched in each category was identified, and the top ten functions for BP, CC and MF based on lowest p value (<0.05) are shown in Fig. 4. Positive regulation of transcription from RNA polymerase II promoter (p value = 9.7×10^{-14}) was the most important of the BP, plasma membrane (P value = 2.4×10^{-9}) for CC

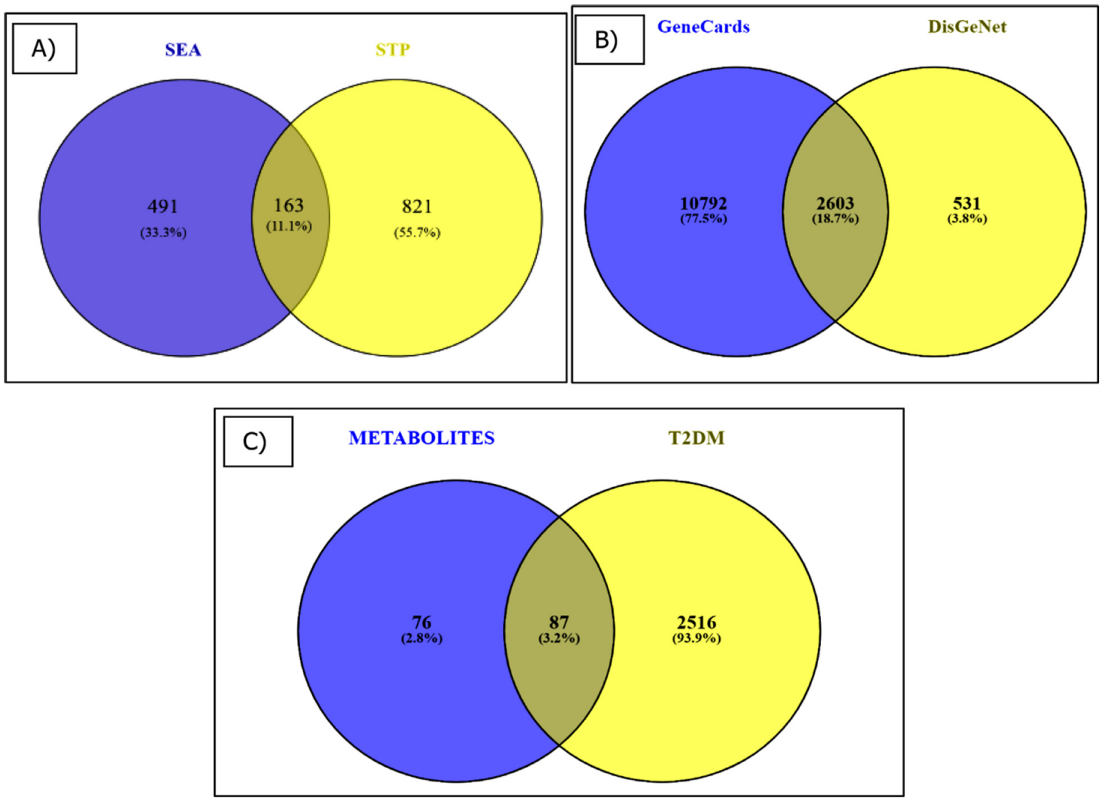

Fig. 2. Venn diagram illustrating the overlapping genes common to (A) SEA and STP relating to sunflower cypsela, (B) GeneCards and DisGeNet relating to T2DM, (C) both sunflower cypsela metabolites and T2DM.

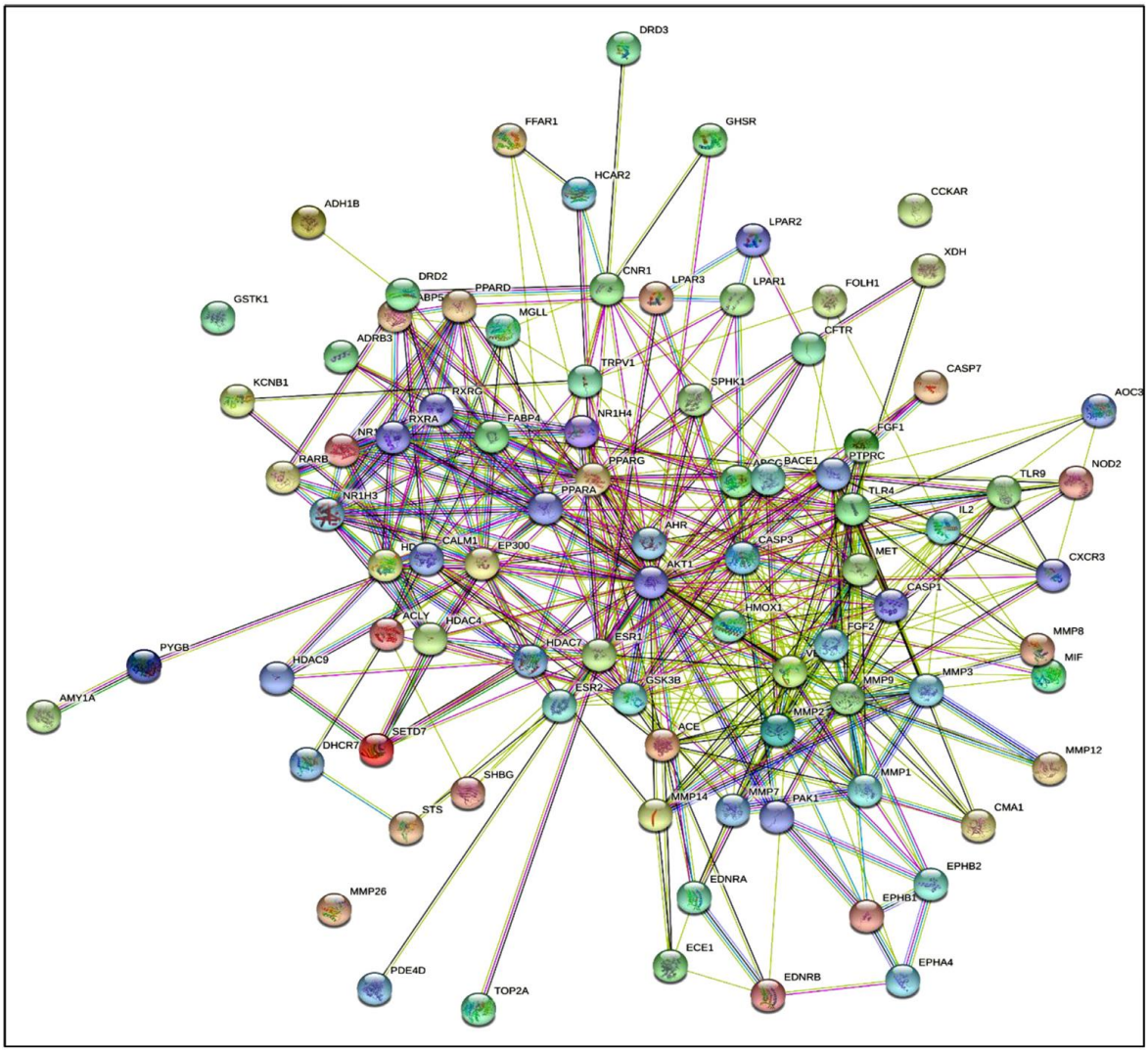

Fig. 3. Gene-gene interaction amongst the 87 genes common to both sunflower cypsela bioactive compounds and T2DM.

and RNA polymerase II transcription factor activity, ligand-activated sequence-specific DNA binding (p value = 7.3×10^{-16}) for MF (Fig. 4).

The KEGG enrichment analysis predicted 35 signalling pathways, 34 of which are implicated alongside the associated genes in T2DM progression (Fig. 5, Table 1). Judging by the FDR, the 14 signalling pathways with the lowest FDR rate values are illustrated on the bubble chart, with PPAR signalling pathway being the most significant with FDR rate of 2.02×10^{-8} and thus identified as the hub signalling pathway of sunflower cypsela against T2DM (Table 1). The interaction between the nine genes involved in the PPAR signalling pathway is shown in Fig. 6. Eight of the nine genes interacted with each other, except for MMP1 that existed in isolation.

3.3.4. Pathway compound target network

Among the metabolites present in sunflower cypsela, 38 interacted directly with the nine genes involved in the PPAR signalling pathway (Fig. 7). Regarding interactions with each individual gene, MMP1 and PPARA interacted with 19 and 14 compounds, respectively (Figs. 8 and 9), followed by PPARD and FABP5 that interacted with 10 compounds each (Supplementary Figs. S2 and S3). The remaining five genes (NR1H3, PPARG FABP4, RXRA and RXRG) were associated with 9, 6, 6, 4 and 3 compounds, respectively (Figs. S4–S8).

3.4. Molecular docking and MD simulation analysis of the interacting compounds against MMP1 and PPARA in PPAR signalling pathway

MMP1 and PPARA were identified as the key targets in the PPAR pathway due to the high degree of interactions with sunflower cypsela' metabolites and were selected as therapeutic target for molecular docking analysis in this study. The docking scores of the 19 and 14 metabolites that interacted with MMP1 and PPARA are shown in Tables 2 and 3, respectively. Five compounds, CGA (−9.7 kcal/mol), GPA (−9.6 kcal/mol), FOX (−9.2 kcal/mol), CFG (−8.9 kcal/mol) and HGM (−8.9 kcal/mol) had higher negative docking scores for MMP1 than the antidiabetic standard, metformin (−5.8 kcal/mol), while two compounds, CGA and GPA had a higher negative docking score than the agonist ROS (−9.4 kcal/mol) (Table 2). On the other hand, 3

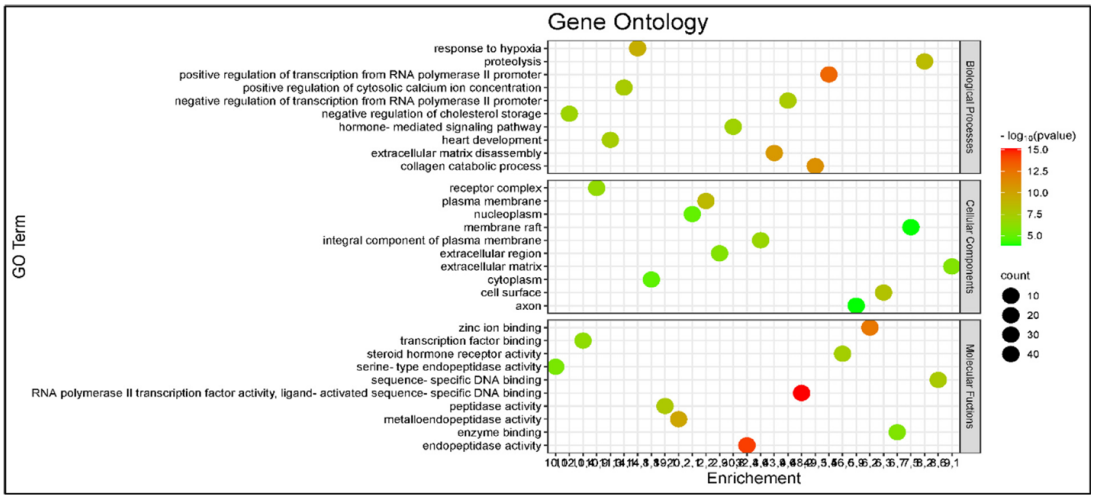

Fig. 4. Bubble plot of GO analysis of 87 gene common to T2DM and bioactive compounds of sunflower cypsela.

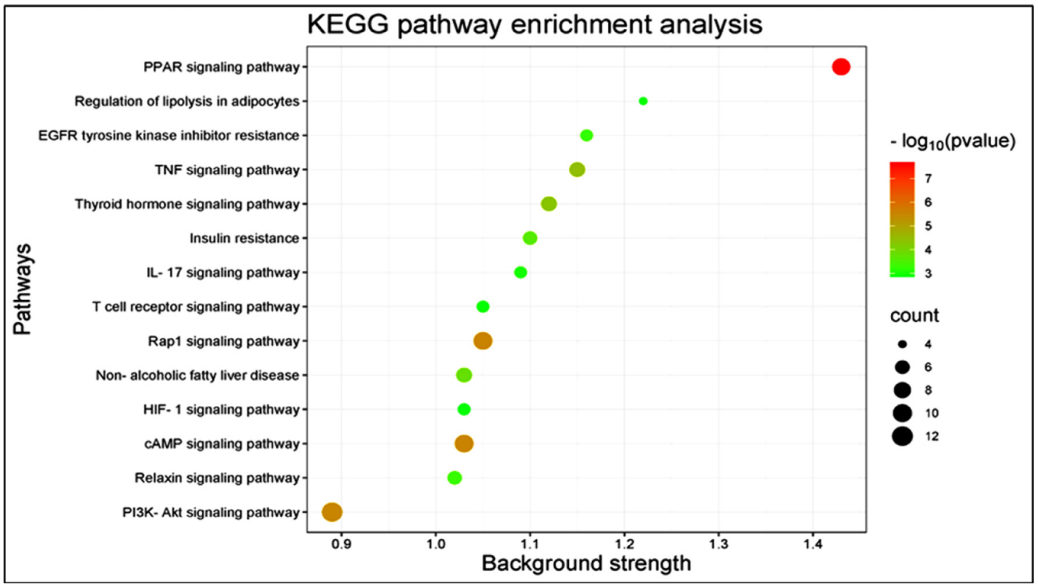

Fig. 5. Bubble chart illustrating the top 14 signalling pathways associated with T2DM.

compounds, HGM (−8.3 kcal/mol), PPA (−7.4 kcal/mol) and AA (−6.4 kcal/mol) had higher negative docking scores than metformin (−5.2 kcal/mol) against PPARA while only HGM (−8.3 kcal/mol) had docking score that compared to the agonist ROS (−8.6 kcal/mol) with other compounds having relatively lower docking score to ROS (Table 3).

Following identification of top-hit compounds of sunflower cypsela against PPARA and MMP1 based on higher negative docking score, MD simulation was performed over 100 000 ps. Relative to the reference standard (ROS), GPA (−41.62 kcal/mol), CGA (−43.74 kcal/mol) and CFG (−45.36 kcal/mol) against MMPI had higher binding free energy, while against PPRAR, ROS had higher binding free energy than the top hits of sunflower cypsela. On the other hand, except for FOX-MMPI (−16.51 kcal/mol), all the top hits against MMPI and PPARA had higher binding free energy than MET after 100,000 ps energy refinement (Table 4).

The RMSD plots for MMP1 and PPARA show convergence after 60,000 ps and 30,000 ps, respectively (Fig. 10A and B). Post-convergence, both MMP1 and PPARA systems appear to be equilibrated and were relatively stable for the rest of the simulation. All protein-ligand complexes for both systems retained an average RMSD value < 3.5 Å. Except for GPA-MMP1 complex (1.99 Å), the remaining bound complexes had increased average RMSD values compared to the unbound MMP1 (2.06 Å). Regarding the PPARA bound systems, AZA-PPARA had the lowest average RMSD value at 2.05 Å which was lower than the unbound PPARA (2.25 Å). The results obtained for RMSF analysis of the MMP1 system (Fig. 10C) showed fluctuations around amino acid resides 165−175, this behavior is primarily and largely exhibited by the binding of GPA to MMP1 which had a RMSF value of 1.41 Å (Table 5). Overall, among the investigated compounds, HGM (1.32 Å) < CGA (1.31 Å) < CFG (1.21 Å) exhibited favorably lesser swaying than the agonist ROS-MMP1 (1.67 Å) by the decrease in fluctuations

Table 1
Pathway enrichment of targets genes related to T2DM.

KEGG ID	Signalling pathways	False discovery rate	Target gene
hsa03320	PPAR	2.02×10^{-8}	PPARG; FABP5; PPARD; MMP1; RXRG; PPARA; RXRA; NR1H3
hsa04015	Rap1	2.86×10^{-6}	FGF2; FGF3; FGF4; FGF5; FGF6; FGF8; FGF7; FGF9; FGF10; FGF11
hsa04024	cAMP	2.86×10^{-6}	CFTR; GHSR; EP300; PAK1; EDNRA; PDE4D; DRD2; HCAR2; PPARA; AKT1
hsa04151	PI3K-Akt	3.13×10^{-6}	IL2; FGF2; MET; GSK3B; TLR4; LPAR1; LPAR3; RXRA; LPAR2; AKT1; VEGFA; FGF1
hsa04668	TNF	3.65×10^{-5}	MMP3; NOD2; MMP14; CASP3; CASP7; MMP9; AKT1
hsa04919	Thyroid hormone	4.83×10^{-5}	HDAC3; GSK3B; RXRG; ESR1; RXRA; AKT1
hsa04932	Non-alcoholic fatty liver disease	1.6×10^{-4}	GSK3B; CASP7; PPARA; RXRA; AKT1; NR1H3
hsa04931	Insulin resistance	2×10^{-4}	NR1H2; GSK3B; PPARA; AKT1; NRIH3
hsa04926	Relaxin	5.1×10^{-4}	MMP1; MMP9; EDNRB; AKT1; VEGA
hsa01521	EGFR tyrosine kinase inhibitor resistance	5.6×10^{-4}	MET; GSK3B; AKT1; VEGFA
hsa04657	IL-17	9.9×10^{-4}	CASP3; MMP1; GSK3B; MMP9
hsa04660	T cell receptor	1.2×10^{-3}	PAK1; GSK3B; PTPRC; AKT1
hsa04066	HIF-1	1.4×10^{-3}	HMOX1:EP300; TLR4; AKT1; VEGFA
hsa04923	Regulation of lipolysis in adipocytes	1.4×10^{-3}	FABP4; MGLL; ADRB3; AKT1
hsa04010	MAPK	2.7×10^{-3}	FGF2; PAK1; CASP3; MET; AKT1; VEGFA; FGF1
hsa04917	Prolactin	2.7×10^{-3}	GSK3B; ESR2; ESR1; AKT1
hsa04920	Adipocytokine	2.7×10^{-3}	RXRG; PPARA; RXRA; AKT1
hsa04915	Estrogen	2.8×10^{-3}	MMP2; ESR2; MMP9; ESR1; AKT1
hsa05418	Fluid shear stress and atherosclerosis	2.7×10^{-3}	HMOX1; MMP2; MMP9; AKT1; VEGFA
hsa04014	Ras	4.1×10^{-3}	FGF2; PAK1; MET; AKT1; VEGFA; FGF1
hsa04072	Phospholipase D	4.1×10^{-3}	SPHK1; LPAR1; LPAR3; LPAR2; AKT1
hsa00350	Tyrosine metabolism	4.3×10^{-3}	MIF; ADH1B; AOC3
hsa04933	AGE-RAGE in diabetic complications	6.6×10^{-3}	MMP2; CASP3; AKT1; VEGFA
hsa04659	Th17 cell differentiation	7.2×10^{-3}	IL2; AHR; RXRG; RXRA
hsa04922	Glucagon	7.2×10^{-3}	PYGB; EP300; PPARA; AKT1
hsa04935	Growth hormone synthesis	8.8×10^{-3}	GHSR; EP300; GSK3B; AKT1
hsa04728	Dopaminergic synapse	1.39×10^{-2}	GSK3B; DRD2; DRD3; AKT1
hsa04924	Renin secretion	1.71×10^{-2}	ACE; EDNRA; ADRB3
hsa04310	Wnt	2.46×10^{-2}	MMP7; EP300; PPARD; GSK3B
hsa04614	Renin-angiotensin system	2.47×10^{-2}	CMA1; ACE
hsa04022	cGMP-PKG	2.81×10^{-2}	EDNRA; ADRB3; EDNRB; AKT1
hsa04012	ErbB	2.84×10^{-2}	PAK1; GSK3B; AKT1
hsa04215	Apoptosis - Multiple species	3.7×10^{-2}	CASP3; CASP7
hsa04062	Chemokine	4.14×10^{-2}	PAK1; GSK3B; CXCR3; AKT1
hsa01100	Metabolic pathways	4.70×10^{-2}	HMOX1; PYGB; ACLY; FOLH1; MGLL; SETD7; ADH1B; AOC3; SPHK1; PDE4D; DHCR7; XDH

after binding to MMP1. PPARA bound systems expressed a high degree of fluctuations throughout simulation especially between residues 30 and 55 (Fig. 10D). Among the compounds, AZA with an average RMSF value of 1.23 Å (Table 6) had the least RMSF value, which is lesser than the agonist, ROS (1.21 Å) after binding to PPARA. The RoG analysis (Fig. 10E and F) revealed CGA-MMP1 (15.05 Å) and AZA-PPARA (18.95 Å) to be the most compact complexes among the bioactive compounds, competing favorably with the reference standards, MET-MMP1 (15.15 Å), ROS-MMP1 (15.37 Å), MET-PPARA (18.86 Å) and ROS-PPARA (18.80 Å). In comparison to the apo-protein, both

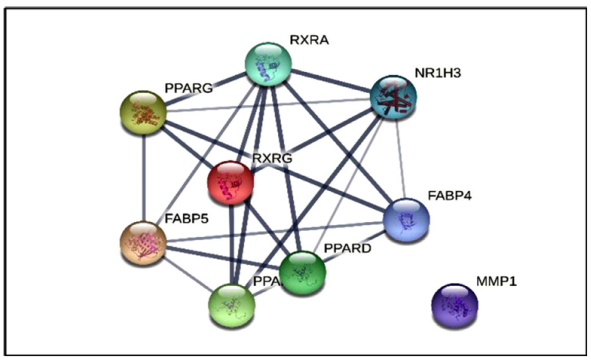

Fig. 6. Gene-gene interaction of the nine genes involved in the PPAR signalling pathway.

CGA-MMP1 and AZA-PPARA also emerged competitively among the compounds (Apo-MMP1 = 5.15 Å; Apo-PPARA = 18.08 Å) (Tables 5 and 6). The SASA plot (Fig. 10G) revealed GPA-MMP1 (8581.74 Å) < CFG-MMP1 (8348.91 Å) < CGA-MMP1 (8211.48) least fluctuations upon binding to the protein compared to the unbound system which had an average SASA value of 8661.24 Å. Fig. 10H shows the SASA plot obtained for the PPARA system. PAA-PPARA (13,819.62 Å) and AZA-PPARA (13,944.68 Å) complexes had the least fluctuations during the simulation period as compared to the unbound system which had an average SASA value of 14,174.17 Å. The intramolecular hydrogen bonds formed between the complexes was also evaluated and are presented in Fig. 10I and J. An increased in hydrogen bond formation was observed with the MMP1 bound systems relative to the unbound protein which had an average hydrogen bond of 59.82 (Fig. 10I and Table 5). The bond systems had average hydrogen bonds that follows the pattern FOX-MMP1 (63.67) < HGM-MMP1 (63.86) < GPA-MMP1 (64.70) < CFG- MMP1 (68.14) < CGA-MMP1(71.88) (Table 4). The bioactive compounds binding to PPARA also displayed an increased in intramolecular hydrogen bonds relative to the unbound protein (123.37) (Fig. 10J). The increase in H-Bonds can be seen in the following order, HGM-PPARA (125.45) < PAA-PPARA (127.78) < AZA -PPARA (130.40), shown Table 6.

The 2D plot shown in Figs. 11 and 12 illustrated the intermolecular interactions over 100 000 ps between the bound complexes systems. The MMP1 systems formed hydrogen bonds, Van der Waal, pi-akyl, pi amide, pi-sigma, carbon-hydrogen bonds and unfavorable interactions (Fig. 11. CFG formed four hydrogen bonds at 0 ps which increased to eight at the end of the simulation (Fig. 11A). At

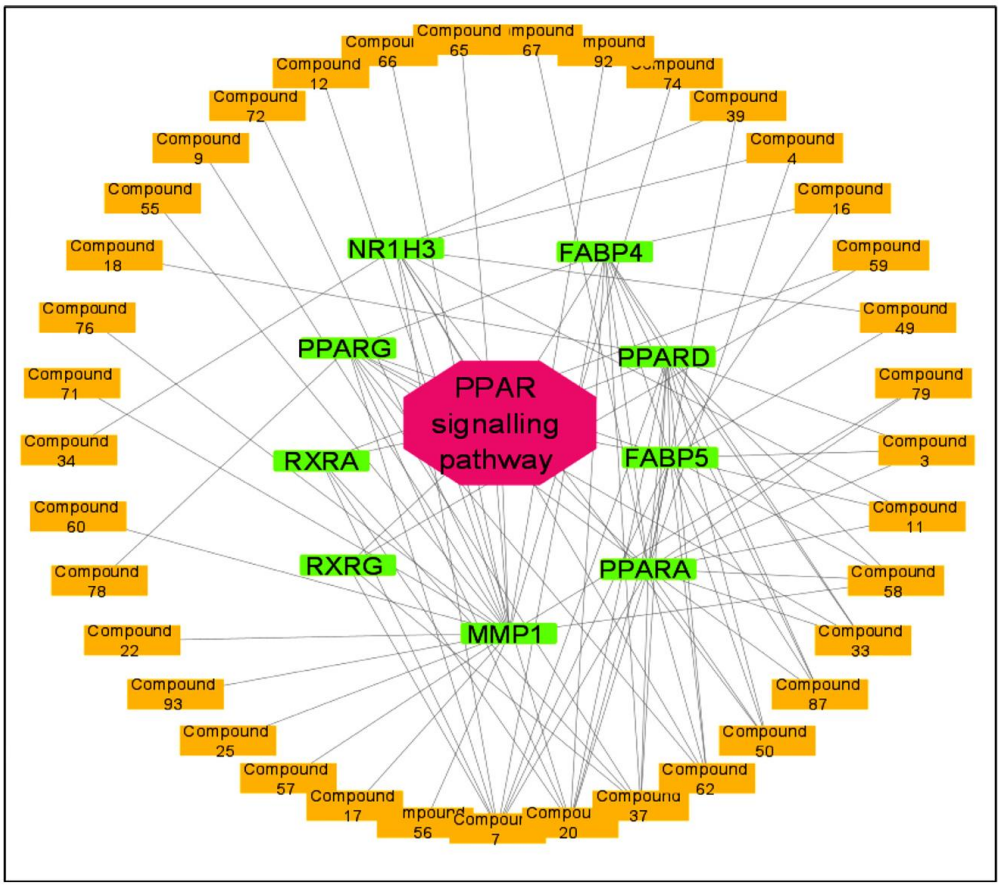

Fig. 7. Pathway-compound network illustrating bioactive compounds in sunflower cypsela interacting with genes implicated in the PPAR signalling pathway.

50 000 ps and 100,000 ps, CFG-MMP1 retained interactions at amino acids GLU112, SER132, THR 134 and GLN140 accounting for more than 50% of hydrogen bonds at each time shot. While at 50 000 ps (Fig. 11B), CGA had four hydrogen bonds interactions which increased to five hydrogen bonds at 100,000 ps. The amino acids involved are ARG107, GLU112, SER132, THR134 and GLU140. Fig. 10C showed that FOX-MMP1 had a decrease in the number of interactions from 14 (0 ps) to 5 (50,000 ps) and at 100 000 ps an increase to 9 interactions can be observed. Regarding FOX-MMPI complex (Fig. 11C), one hydrogen bond was recorded at 0 ps with THR24, 0 hydrogen bonds at 50,000 ps, and 1 at 100,000 ps with ASP147. GPA-MMP1 (Fig. 11D), formed 3 hydrogen bonds at 0 ps, 4 at 50,000 ps and 5 at 100,000 ps. However, at 50,000 and 100,000 ps, hydrogen bond interactions with GLY120, SER132 and THR134 was conserved. Number of hydrogen bonds formed in HGM-MMP1 (Fig. 11E) were 1, 3 and 1 respectively at 0, 50,000 and 100 000 ps. MET interacted with MMP1 through the formation of multiple carbon hydrogen bonds (Fig. 11F). At 0 ps, 3 hydrogen bonds can be noted, which increased to 5 and 6 hydrogens bonds at 50,000 and 100 000 ps respectively. While, the pathway agonist, ROS bound to MMP1 with multiple hydrogen bonds at each of the timeframe taken with 3, 5, and 6 hydrogen bonds at 0, 50,000 and 100 000 ps respectively (Fig. 11G). Interestingly, 4 interactions were conserved at both 50,000 and 100 000 ps (GLY120, SER132, SER134 and GLY140). Lastly, most of the interactions in ROS-MMP1 complex were van der Waal interactions in all the timeframes, except for the two hydrogen bonds observed at 0 ps (Fig. 11G).

AZA-PPARA complex (Fig. 12A) formed strong intermolecular interactions that included conventional hydrogen bond, van der Waals forces, carbon hydrogen and pi-alkyl at each timeframe of the simulation. Although, AZA-PPARA had no hydrogen bond interactions at 0 ps, but the number of hydrogen bond interactions increase as the simulation progresses with 3 hydrogen bonds contact at both 50,000 and 100,000 ps. Two of the hydrogen bond interactions with PHE146 and HIS235 were retained after 50,000 ps. AZA-PPARA complex also retained the pi-alkyl bond with CYS71 and MET150 at both 50,000 and 100,000 ps, while forming additional pi-alkyl bonds at PHE68 and ILE149 at 100,000 ps which was previously van der Waals interactions at 50,000 ps. PAA-PPARA (Fig. 11B) formed 1 hydrogen bond at both 50,000 and 100,000 ps at TYR109 and HIS315 respectively. A clear observation can be made that 98% of the intermolecular interactions that occurs at 50,000 ps was retained at 100,000 ps. Regarding HGM-PPARA complex (Fig. 11C), majority of the interactions that occur at 50,000 ps were retained at 100,000 ps. At 50,000 ps, four hydrogen bonds were observed and two of those interactions at GLU53 and THR55 were consistent at 100,000 ps with the other two interactions with VAL57 and CYS70 transforming to van der Waals interactions. MET-PPARA (Fig. 11D) formed only a single hydrogen bond at 0 and two at 50,000 ps. However, this increase

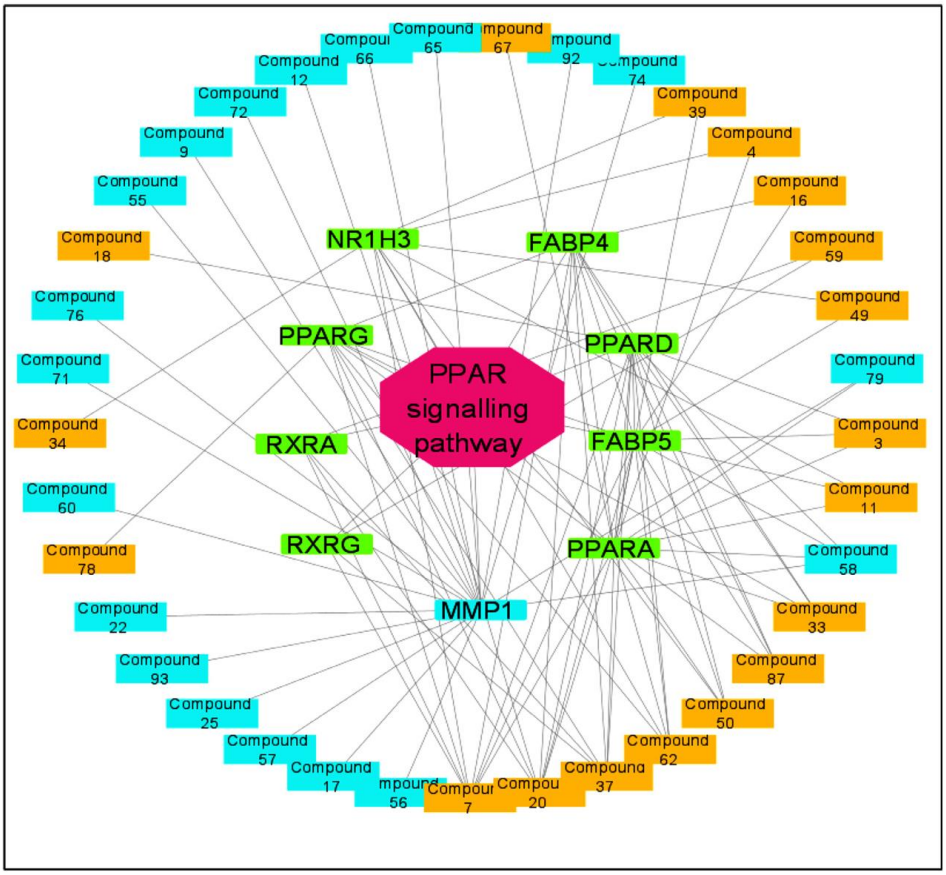

Fig. 8. Pathway-compound target interaction network of MMP1 and 19 bioactive compounds (blue nodes) present in sunflower cypsela.(For interpretation of the references to color in this figure legend, the reader is referred to the web version of this article.)

in trend was not retained at 100,000 ps, as a single hydrogen bond as well as an unfavorable interaction was observed. Consequently, Van der Waals interactions dominated throughout the simulation period of MET-PPARA. On the other hand, ROS-PPARA (Fig. 11E) had a greater quality of interactions evident by the presence of hydrogen bonds throughout the simulation.

3.5. Molecular orbital properties of top-hits sunflower seed metabolites

The top-hit compounds of sunflower cypsela had LUMO energies ranging between −2.2769 and −0.2133 eV with ROS (−1.4313 eV) having value within the range of the top hits, while MET (−0.2001 eV) had value slightly higher than the range of the top hits. In contrast, both reference standards had HOMO energies (MET: −5.8475 eV and ROS: −5.7279 eV) that were higher to the transition HOMO energies of the top-hit compounds (between −7.9393 and −5.8849 eV) (Table 7 and Fig. 13). Among the investigated compounds, FOX at 4.007 eV, followed by CGA and CFG at 4.0723 eV and 4.0734 eV, respectively, had the lowest energy gap (Table 7 and Fig. 13). Consequentially, these compounds had the highest softness (FOX: 0.4991 eV, CGA: 0.4911, CFG: 0.4909 eV) and the lowest hardness (FOX: 2.0035 eV, CGA: 2.03611 eV, CFG: 2.0367 eV). Other top-hits compounds of sunflower cypsela, while having energy gaps, softness and hardness values that compared well with MET, had slightly higher energy gaps, lesser softness and greater hardness than ROS (Table 7). Lastly, GPA, CGA and CFG, had the highest electronegativity, electron affinity, electrophilicity index and the lowest chemical potential (Table 7).

4. Discussion

Plants serve a promising role in medicine due to the abundance of phytochemicals present in them and thus paves the way for the use of plants as therapeutic agents. In this study, the most prominent pathways implicated with T2DM was identified in association with the bioactive compounds of sunflower cypsela using Network pharmacology. Afterward, molecular docking and MD simulation techniques were applied as a well-structured mechanistic approach to predict hit compounds in sunflower cypsela responsible for the therapeutic action of sunflower in the management of T2DM (Pan et al., 2020). Through DFT, the molecular properties of the top-hit compounds of sunflower cypsela were predicted to gain relevant information as to the practical applications of the top-hits as therapeutic molecules.

The identification of 94 bioactive compounds in all six sunflower seed cultivars using LC–MS and GC–MS techniques demonstrated the richness of volatile and non-volatile secondary metabolites in sunflower cypsela with little variance between cultivars in terms of chemical profiles and abundance of metabolites. The small variance observed between cultivars suggests that each of the cultivars

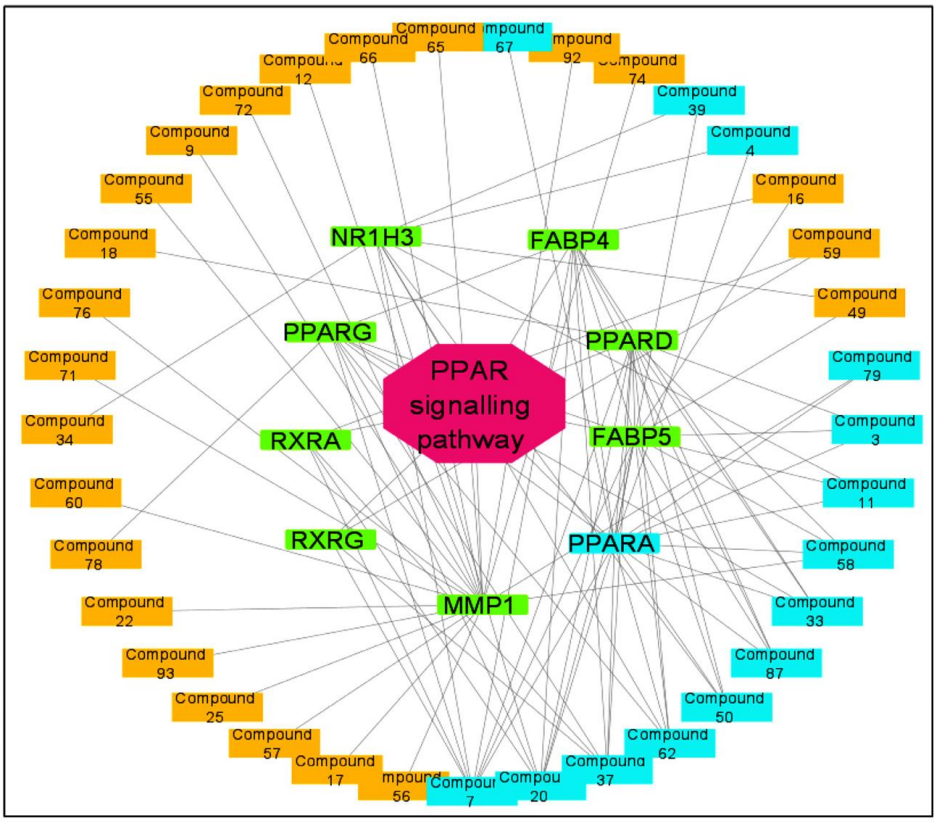

Fig. 9. Pathway-compound target interaction network of PPARA and 14 bioactive compounds (blue nodes) present in sunflower cypsela.(For interpretation of the references to color in this figure legend, the reader is referred to the web version of this article.)

Table 2
Docking scores of 19 metabolites from sunflower cypsela against MMP1.

Compound	Identity	Binding energy (kcal/mol)
79	4aalpha,6S,7aalpha)-6alpha-[6-O-(4-Hydroxybenzoyl)-beta-D-glucopyranosyloxy]−7beta-methyloctahydrocyclopenta[c]pyran-1-one (HGM)	−8.9
58	2-Isopropylmalic acid	−6.3
56	Isomollerin B	−5.7
17	2-Ethyl-3-hydroxyhexyl 2-methylpropanoate	−6.5
57	7-Methoxyisomorellinol	−5.8
25	2-Methyl-1-butanol	−4.2
93	Formoxanthone B (FOX)	−9.2
22	3-Methylbutan-1-ol	−4.1
60	1-O-Caffeoylglucose (CFG)	−8.9
71	3′-O-beta-Glucopyranosyl plumbagic acid methyl ester (GPA)	−9.6
55	Chlorogenic acid (CGA)	−9.7
76	Granatumin C	−7.4
9	Decamethylcyclopentasiloxane	−5.2
72	3-O-Caffeoyl-4-O-methylquinic acid	−8.7
12	Dodecamethylcyclohexasiloxane	−4.2
66	Caffeic acid	−7.1
94	Methyl asterate	−5.5
92	Sacranoside A	−8.4
74	Ptelatoside A	−8.0
–	Metformin (MET)	−5.8
–	Rosiglitazone (ROS)	−9.4

Table 3
Docking scores of 14 metabolites from sunflower cypsela against PPARA.

Compound	Identity	Binding energy (kcal/mol)
79	4aalpha,6S,7aalpha)-6alpha-[6-O-(4-Hydroxybenzoyl)-beta-D-glucopyranosyloxy]−7beta-methyloctahydrocyclopenta[c]pyran-1-one (HGM)	−8.3
3	hexanal	−4.4
11	1-Hexanol	−4.3
58	2-Isopropylmalic acid	−5.2
87	Azelaic acid (AZA)	−6.4
33	gamma-Terpinene	−5.9
50	1-Octanol	−4.6
62	Quinic acid	−6.0
37	Mentha-1,4,8-triene	−6.0
20	Calarene	−5.5
7	Limonene	−6.3
67	Phenylacetic acid (PAA)	−7.4
39	Camphene Bicyclo[2.2.1] heptane, 2,2-dimethyl-3-methylene-	−5.6
4	beta-Pinene	−5.8
–	Metformin (MET)	−5.2
–	Rosiglitazone (ROS)	−8.6

Table 4
Thermodynamic analysis of the top hits from sunflower cypsela against MMP1 and PPARA systems over a-100 ns MD simulation.

	Energy components (kcal/mol)				
	MMP1				
Complexes	ΔE_{vdW}	ΔE_{elec}	ΔG_{gas}	ΔG_{solv}	ΔG_{bind}
ROS - MMP1	−48.91 ± 3.90	−20.38 ± 6.39	−69.29 ± 8.29	33.09 ± 5.21	−36.20 ± 5.01
MET- MMP1	−20.21 ± 2.62	−283.93 ± 14.36	−304.15 ± 13.58	286.17 ± 12.45	−17.98 ± 2.90
HGM- MMP1	−36.70 ± 8.02	−34.86 ± 12.95	−71.56 ± 18.43	39.08 ± 10.25	−32.48 ± 9.60
GPA- MMP1	−47.95 ± 3.53	34.33 ± 12.97	−82.28 ± 12.63	40.66 ± 8.08	−41.62 ± 5.97
FOX- MMP1	−22.23 ± 9.27	−8.42 ± 11.23	−30.65 ± 15.35	14.12 ± 10.07	−16.51 ± 7.59
CGA- MMP1	−46.28 ± 3.77	−57.97 ± 9.40	−104.26 ± 9.50	60.51 ± 6.08	−43.74 ± 5.38
CFG- MMP1	−41.40 ± 4.12	−79.51 ± 8.96	−120.91 ± 7.63	75.55 ± 5.87	−45.36 ± 4.12
PPARA					
ROS – PPARA	−52.33 ± 3.10	−17.10 ± 4.87	−69.43 ± 5.01	22.45 ± 3.30	−46.98 ± 3.85
MET- PPARA	−20.34 ± 2.50	−153.31 ± 12.93	−173.66 ± 13.35	155.42 ± 11.41	−18.24 ± 3.69
HGM- PPARA	−39.11 ± 5.90	−28.06 ± 10.62	−67.17 ± 12.12	33.34 ± 8.38	−33.83 ± 5.83
PAA- PPARA	−21.83 ± 1.92	−15.35 ± 2.86	−37.18 ± 2.92	16.48 ± 1.81	−20.70 ± 2.03
AZA – PPARA	−31.49 ± 2.50	−16.35 ± 3.94	−47.84 ± 3.91	16.24 ± 1.24	−31.60 ± 3.18

ΔE_{vdW}: van der Waals energy; ΔE_{elec}: electrostatic energy; ΔE_{gas}: gas-phase free energy; ΔG_{solv} solvation free energy and ΔG_{bind}: total binding free energy.

contained key compounds that may have antidiabetic properties. Thus, all the investigated varieties in this study are important sources of potential antidiabetic drug candidates. Afterward, data mining identifying 87 common genes between the bioactive of sunflower cypsela and T2DM suggests the several genes that may be involved in the progression of T2DM. Similar studies have also identified several key genes between T2DM and the bioactive compounds of plants such as Sorghum bicolor and *Caesalpinia sappan* L (Adnan et al., 2022; Oh et al., 2020). GO annotation of the therapeutic targets further suggests that the molecular function of sunflower cypsela as an antidiabetic agent is enriched in RNA polymerase II transcription factor activity, and ligand-activated sequence-specific DNA binding. The positive regulation of the transcription from RNA polymerase II promoter was the most enriched biological process and plasma membrane for cellular components. The KEGG pathway enrichment analysis of the 87 genes identified 34 pathways directly implicated in the progression of T2DM. Based on the FDR value, the most significant pathway related to T2DM progression was identified to be Peroxisome proliferator-activated receptors (PPAR) signalling pathway (Yousef et al., 2021). The PPAR pathway is majorly implicated in management of T2DM through the alleviation of hyperglycaemia via regulation of blood glucose levels, insulin secretion and fatty acid oxidation (Frkic et al., 2021). The metabolites identified within the cultivars of the sunflower cypsela are most strongly associated with the PPAR signalling pathway, thus potentially exhibiting their antidiabetic activity through this route. Interestingly, Adnan et al. (2022) and Oh et al. (2020) have also validated PPAR signalling pathway as a key pathway of importance in developing T2DM therapeutics. Thus, while there might be growing evidence of the PPAR signalling pathway's potential role in T2DM therapy, the findings of this study focus on the relationship between sunflower cypsela and the pathway for its antidiabetic activity. Other important pathways identified include: the Rap1 signalling pathway, which is linked to the pathways reported by Kaneko et al. (2021) implicated in the antidiabetic effects observed in diet-induced hyperglycemic rats; the cAMP signalling pathway, a pathway implicated in the suppression of hepatic gluconeogenesis in response to fasting hyperglycaemia when downregulated (Cao et al., 2022) and lastly; the PI3K/AKT pathway whose genes when upregulated have been shown to ameliorate the onset of insulin resistance and hyperglycaemia (Li et al., 2019).

Peroxisome proliferator-activated receptors signalling pathway as the hub pathway sees the participation of nine genes, PPARA, MMP1, PPARD, PPARG, FABP4, FABP5, RXRG, RXRA and NR1H3. The role of PPAR signalling has been demonstrated in the pathogenesis of obesity and insulin resistance which overtime may give rise to the onset of T2DM (Jay and Ren, 2007). PPAR fatty acid receptors are modulated by the PPAR signalling pathway to play a key role in glucose and lipid uptake by promoting glucose oxidation, reducing free fatty acid levels and improving insulin resistance (Jay and Ren, 2007). A study by Wang et al. (2016) also suggested that PPARγ and PPARα agonist specifically promote insulin sensitization in T2DM. The identification of nine genes in the PPAR pathway in this study is consistent with our previous study on the antidiabetic mechanism of action of sunflower seed essential oil constituents (Rampadarath et al., 2023). While the identification of the PPARA signalling pathway as the hub pathway in this study is in agreement with our earlier report (Rampadarath et al., 2023), at least four (PPARA, PPARD, PPARG and FABP4) of the nine genes in the pathway were remarkable in both studies. Upon the recognition of the role of PPAR signalling pathway in the probable antidiabetic efficacy of sunflower seed, the key target genes in the pathway, MMP1 and PPARA, based on their significant interactions with the key bioactive compounds of the cypsela is suggestive of their role in the antidiabetic management /treatment of T2DM and thus were explored further through molecular docking and MD simulation.

The molecular docking study served as a preliminary screening analysis for the identification of the best bioactive compounds against each gene based on the compounds binding affinity at the active site of the target. The higher the negative docking score of the bound complexes, the better the fitness of the bioactive compound for the target (Ece, 2020). The higher negative docking score of CGA, GPA, FOX, HGM, CFG against MMP1 as well as HGM, PAA and AZA against PPARA from sunflower cypsela relative to the reference standards, suggest that these compounds had better binding fitness for the active site of the respective targets than the standards. This observation agrees with earlier reports (Adnan et al., 2022; Di et al., 2021; Oh et al., 2020) and the network pharmacology findings of this study where the higher interactions of the sunflower bioactive compounds with MMPI and PPARA denote their suitable molecular attraction to the targets. Of the sunflower seed bioactive compounds, CGA and HGM having the best docking score against MMP1 and PPARA, respectively, could possibly suggest them as the lead antidiabetic compounds in the seed. However, since molecular docking is merely an assessment of rigid protein–ligand binding at the active site of a receptor, MD simulation was performed to provide more in-depth analysis of the receptor–ligand stability, affinity and overall conformational behavior.

The thermodynamic binding free energy over 100 000 ps of the top-hit compounds against the target genes, provides a more in-depth analysis of the compound's affinity for the target genes. This in turn unravels the effect the bioactive compounds may have on the biological activity of the targets. CFG-MMP1, CGA-MMP1, HGM-PPARA, and AZA-PPARA complexes retaining the highest binding affinity relative to MET (reference standard) is presumptive of the positive conformational behavior of MMP1 and PPARA in response to binding of these ligands. A high thermodynamic binding free energy value means an increase in thermodynamic stability, which could enhance the biological activity of the target genes (Ece, 2020). Against PPARA, ROS seems to have the best thermodynamic binding free energy, which pinpoints its advantage over the top hits as a potential antidiabetic drug. The findings of this analysis correlate with the study performed by Lee et al. (2020), where a higher binding free energy was taken as confirmation of a more stable complex,

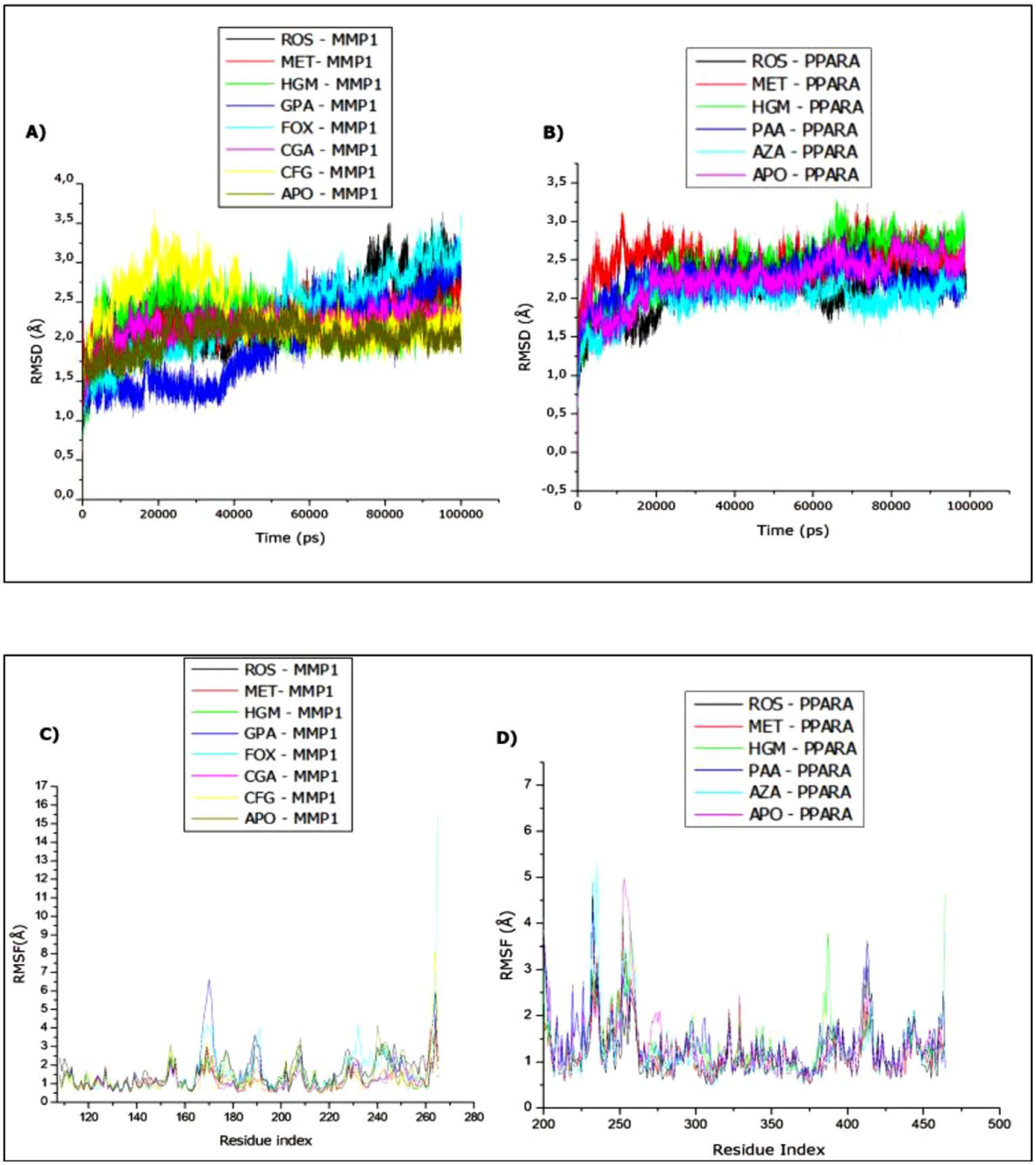

Fig. 10. Comparative post-dynamic data presented as RMSD (A and B), RMSF (C and D), RoG (E and F), SASA (G and H) and Hydrogen bonds (I and J) of bound and unbound MMP1 and PPARA complexes, respectively over 100 000 ps.

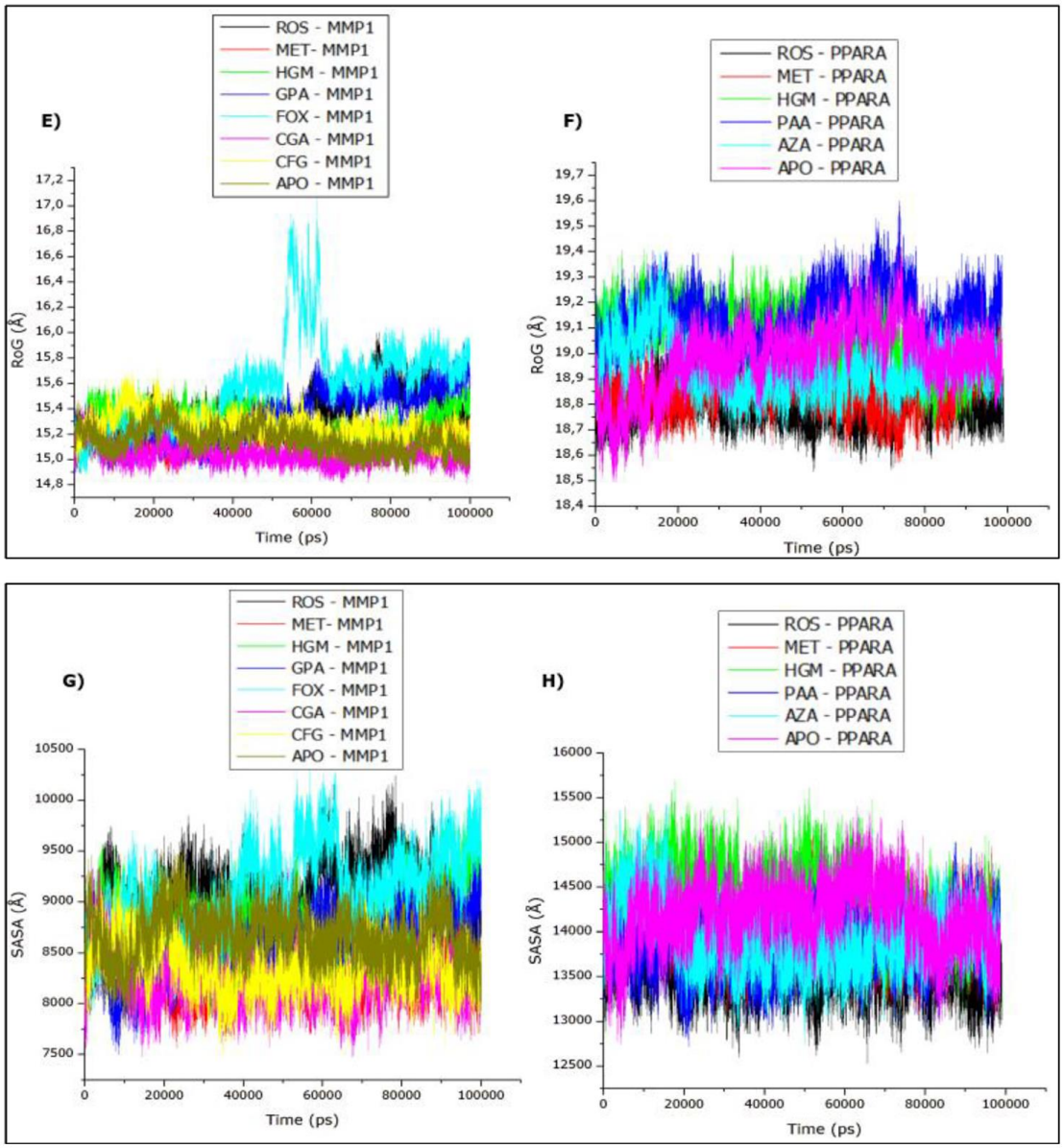

Fig. 10. Continued.

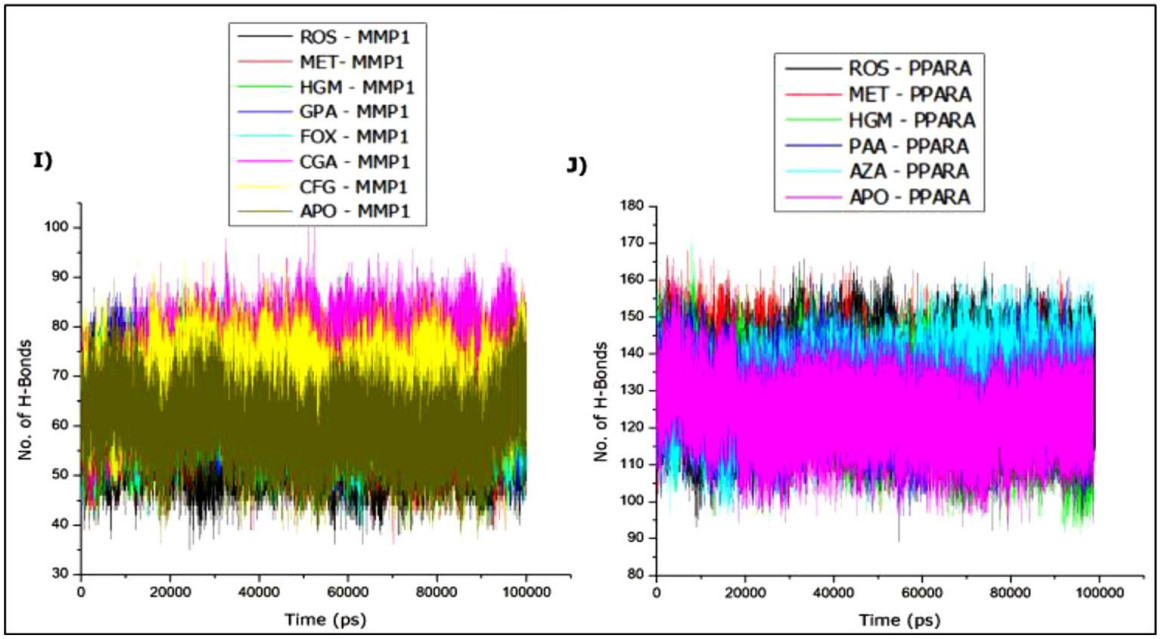

Fig. 10. Continued.

augmenting the biological activity of the target and thus predicting the lead compounds.

The MD simulation allowed the study of the thermodynamic stability, flexibility and compactness of the bound complexes through analysis of the RMSD, RMSF, SASA and intramolecular hydrogen bond analysis over 100 000 ps. RMSD analysis is an index of structural stability with lower RMSD value signifying better thermodynamic stability (Aribisala and Sabiu, 2022). Both MMP1 and PPARA bound systems retained an average RMSD value < 3 Å (Ramirex and Caballero, 2016). GPA-MMP1, CGA-MMP1, HGM-PPARA and AZA-PPARA bound systems emerged as the most stable complex relative to the complexes formed with the reference standards. This observation while in correlation with the binding free energy of this study, is indicative of the enhanced thermodynamic stability of MMP1 and PPARA following binding of these compounds, which in turn may improve the biological activity of the target. The RMSF of protein–ligand system investigates the displacement of the residual atoms upon ligand binding to the receptor relative to the reference structure (Mandal et al., 2022). Within the MMP1 system, significant fluctuations at residues 165–175 can be attributed to conformation changes that took place during ligand binding. However, the stability of the complexes did not appear to be adversely compromised as the active site residues (His112, His118, His218 and catalytic zinc) and catalytic site residues (Gly79, Leu81, Ala81, Glu119, Pro138 and Tyr140) that are key for substrate binding experienced negligible fluctuation. Although, this observation is not entirely true for FOX-MMP1, exhibiting unfavorable atomic displacements (high fluctuations) in most of the residues and thus suggest instability of the complex. Therefore, FOX may not be the most suitable ligand for MMP1 as upon binding the structural integrity of MMP1 become compromised which may potentially adversely affect the biological activity of MMP1 instead of enhancement. Similar to the MMP1 system, the high fluctuations within the PPARA system at residues 30–55, excluded the active site residues Tyr314, Ser280, Ile354, Val332, Ile241, Ala250, Leu254, Val255, suggesting the lesser influence of residues fluctuation on the stability of bounded systems of PPARA. This observation while in agreement with earlier publication (Akoonjee et al., 2022) was further highlighted as residues vibrations reduces significantly at the active sites region (between 250 and 350) of PPARA. Except for FOX-MMP1, the reduced fluctuation of MMP1 residues following binding of the top hit compounds of sunflower cypsela relative to ROS suggests their advantage over ROS as modulators of MPP1. This observation is false against PPARA, as ROS significantly reduces residue fluctuation relative to the top hits. This observation could have impacted the binding free energy observed in this study, where the top hits had better affinity against MMP1 than ROS and *vice versa* against PPARA. The RoG measured the overall structure compactness and stability of the formed complex with reference to the protein backbone (Joshi et al., 2021). Within the MMP1 system the binding of FOX-MMP1, may have affected the structural integrity of the protein at 50,000–60,000 ps. The plausible explanation of this observation could be protein unfolding. This further confirms FOX as an unfavorable ligand for MMP1, while the remaining bound complexes appear to remain compact and structurally stable. On the other hand, PPARA bound complexes appeared to adopt a similar behavior to each other with negligible differences in the RoG values, indicating insignificant effects or changes on the overall compactness and stability of the complexes (Rampadarath et al., 2022).

The SASA analysis evaluated the surface area of the bound ligand–protein system's accessibility to the solvent molecules (Akoonjee et al., 2022). An increase in SASA values is reflective of an increased surface area (Rampadarath et al., 2022). The decrease in SASA values of CGA-MMP1, CFG-MMP1, and GPA-MMP1 relative to ROS-MMP1 and apo-MMPI suggests the complexes have reduced surface area and residues available for solvent interaction, which might contribute to stability. Among the MMP1 systems, the lowest SASA value of CGA-MMP1 suggests a better augmentation of the MMP1's biological activity by CGA relative to other investigated compounds due to better folding or compactness of CGA-MMP1. The opposite can be said for the FOX-MMP1 complex, particularly between 40,000 and 70,000 ps. The binding of FOX resulted in increased surface area and

Table 5
Post-molecular dynamic simulation parameters of top hits compounds in sunflower cypsela that interacted with MMP1 in the PPAR signalling pathway.

	MMP1				
Complexes	RMSD (Å)	RMSF (Å)	RoG (Å)	SASA (Å)	No. of H-Bonds
ROS - MMP1	2.38 ± 0.43	1.67 ± 0.82	15.37 ± 1.56	9047.42 ± 320.52	57.86 ± 5.49
MET - MMP1	2.28 ± 0.25	1.16 ± 0.56	15.15 ± 0.08	8329.29 ± 221.40	62.2 ± 5.77
HGM - MMP1	2.25 ± 0.26	1.32 ± 0.65	15.30 ± 0.11	8791.47 ± 271.77	63.86 ± 5.86
GPA - MMP1	1.99 ± 0.55	1.41 ± 0.92	15.34 ± 0.20	8581. 74 ± 303.60	64.7 ± 5.78
FOX - MMP1	2.32 ± 0.50	1.69 ± 1.43	15.58 ± 0.34	9097.66 ± 399.65	63.67 ± 5.92
CGA - MMP1	2.21 ± 1.89	1.31 ± 0.55	15.04 ± 0.08	8211.48 ± 223.46	71.88 ± 6.60
CFG - MMP1	2.37 ± 0.36	1.21 ± 0.85	15.27 ± 0.10	8348.91 ± 233.34	68.14 ± 5.98
APO - MMP1	2.06 ± 0.19	1.36 ± 0.73	15.15 ± 0.10	8661.24 ± 240.63	59.82 ± 6.14

Table 6
Post-molecular dynamic parameters of essential bioactive compounds in sunflower cypsela that interacted with PPARA in the PPAR signalling pathway.

	PPARA				
Complexes	RMSD (Å)	RMSF (Å)	RoG (Å)	SASA (Å)	No. of H-Bonds
ROS - PPARA	2.10 ± 0.29	1.21 ± 0.67	18.80 ± 0.07	13,572.90 ± 263.15	132.17 ± 8.61
MET - PPARA	2. 47 ± 0.22	1.22 ± 0.56	18.86 ± 0.08	13,981.97 ± 271.95	132.89 ± 8.25
HGM - PPARA	2.43 ± 0.34	1.39 ± 0.65	19.06 ± 0.10	14,366.57 ± 348.75	125.45 ± 8.91
PAA - PPARA	2.23 ± 0.22	1.43 ± 0.63	19.14 ± 0.10	13,819.62 ± 279.55	127. 78 ± 8.01
AZA - PPARA	2.00 ± 0.23	1.23 ± 0.73	18.95 ± 0.10	13,944.68 ± 342.54	130.40 ± 8.42
APO - PPARA	2.25 ± 0.29	1.32 ± 0.71	18.98 ± 0.13	14,174.17 ± 338.04	123.37 ± 8.16

residues available for solvent interaction, which may introduce instability through compromised structural integrity of MMP1. This observation may in turn have unfavorable effects on the inherent biological activity of MMP1. The opposite can be said for the FOX-MMP1 complex, particularly between 40,000 and 70,000 ps. On the other hand, within the PPARA system, the reduced SASA value of ROS-PPARA relative to top hits is suggestive of the benefit of ROS over the metabolites of sunflower in the modulation of PPARA. Among the top hits, AZA-PPARA and PAA-PPARA have the lowest SASA value, which means better modulating effects compared to other top hits when bonded to PPARA. The highest SASA value was noted with HGM-PPARA, which could suggest compromised stability of the bound complex, which isn't favorable. This could mean that among the PPARA systems, HGM ranked lower than AZA and PAA as potential leads against PPARA. The intra-molecular hydrogen bond analysis was able to reflect the intra-structural stability of the complexes. An increase in intra-molecular H-bonds suggests an increase in stability as a result of ligand binding, which may contribute to the enhancement of biological activity (Jairajpuri et al., 2021). The increase in intramolecular H-bonds of MMP1 following binding of the top hit compounds of sunflower cypsela relative to the apo-MMP1 and ROS-MMP1 suggests enhanced thermodynamic stability of MMP1, which could in turn encourage the biological effect of the targets. Against PPARA, while an increase in H-bonds relative to apo-PPARA was observed with the complexes formed with the top-hit compounds, suggesting enhanced modulatory effects of the top hits, ROS seems to have the best effects amongst the investigated compounds. This observation corresponds with the findings of other thermodynamic metrics in this study and is also consistent with previous studies where ligand binding enhanced the thermodynamic stability of drug targets (Akoonjee et al., 2022; Aribisala et al., 2022; Mandal et al., 2022; Rampadarath et al., 2022; Dwivedi et al., 2021; Sabiu et al., 2021).

The 2D interaction plots revealed the intermolecular interactions formed between the ligand and protein at intervals of 50,000 ps throughout the 100 000 ps simulation. The interaction plots of the bioactive compounds with MMP1 and PPARA had hydrogen bonds (conventional and carbon), van der Waals forces as well as pi-pi stacked, pi-alkyl, amide-pi stacked, pi-sulphur and pi-sigma. All of these interactions contributed towards the binding affinity and increased stability of the bound complexes observed in this study. Conventional hydrogen bonds are particularly known to contributed significantly to a greater stability of complexes and thus is considered one of the most important and favorable intermolecular interactions formed by the bioactive compound with MMPI and PPARA (Rampadarath et al., 2022). This observation was corroborated as bioactive compounds with the highest binding free energy (CFG against MMP1 and HGM against PPARA) against MMPI and PPARA had the highest number of hydrogen bonds and other important interactions that was consistent throughout the 100 ns simulation. Hence, it can be suggested that the intermolecular interactions are associated with the binding free energy and the post-dynamic findings of this study which affirms the results of the network pharmacology analysis. Overall, the observations of this study imply that CFG, and HGM are key components of sunflower cypsela that may act through the PPAR signalling pathway as potential agonist against MMPI and PPARA, respectively, in ensuring modulation of glucose homeostasis and insulin sensitivity.

The top-hit compounds of sunflower cypsela were characterized using quantitative chemical parameters to probe into their potential molecular properties of therapeutic importance. The HOMO and LUMO parameters are key to identifying the chemical reaction of a system (Aihara, 1999). Thus, studying the HOMO and LUMO parameters of drug compounds could provide important information for investigating the mechanism of action and identifying active sites for structural modification (Ayers et al., 2006). The energy gap (LUMO—HOMO) of a compound offers insight into stability, with a higher energy gap suggesting high stability, which could deter ligand binding to a protein, and *vice versa* for a smaller energy gap (Aihara, 1999). In this study, compared to other investigated compounds, the lowest energy gap observed with CGA and CFG could have positively influenced their higher binding free energy with MMP1. This observation is not true for FOX, which has a lesser affinity for MMP1 compared to CGA and CFG; however, the high fluctuations of the residues of MMP1 following binding of FOX could have had a major impact on the lesser affinity. Also, compared to other compounds, the binding

of FOX to MMP1 causes a significant increase in its surface area. These observations point to the lesser thermodynamic compatibility of FOX with MMPI as the major reason for the lesser binding free energy rather than the instability of FOX. Similarly, GPA with a higher affinity for MMP1 also had a smaller energy gap relative to other top-hit compounds in sunflower cypsela. This observation is true with the top-hit compounds towards PPARA, where the reference standard, ROS, with the highest binding free energy had the smallest energy gap among the investigated compounds with PPARA. Also, HGM among the top hits against PPARA with the highest binding free energy also had the lowest energy gap among the top hits. The correlation of lower energy gaps with higher binding free energy observed in this study is consistent with the observation of Ma et al. (2022), where amentoflavone and hinokiflavone with smaller energy gaps had higher binding free energy against the main protease of SARS-CoV-2.

Other CDFT descriptors were evaluated, including ionization potential, electron affinity, electronegativity, chemical potential,

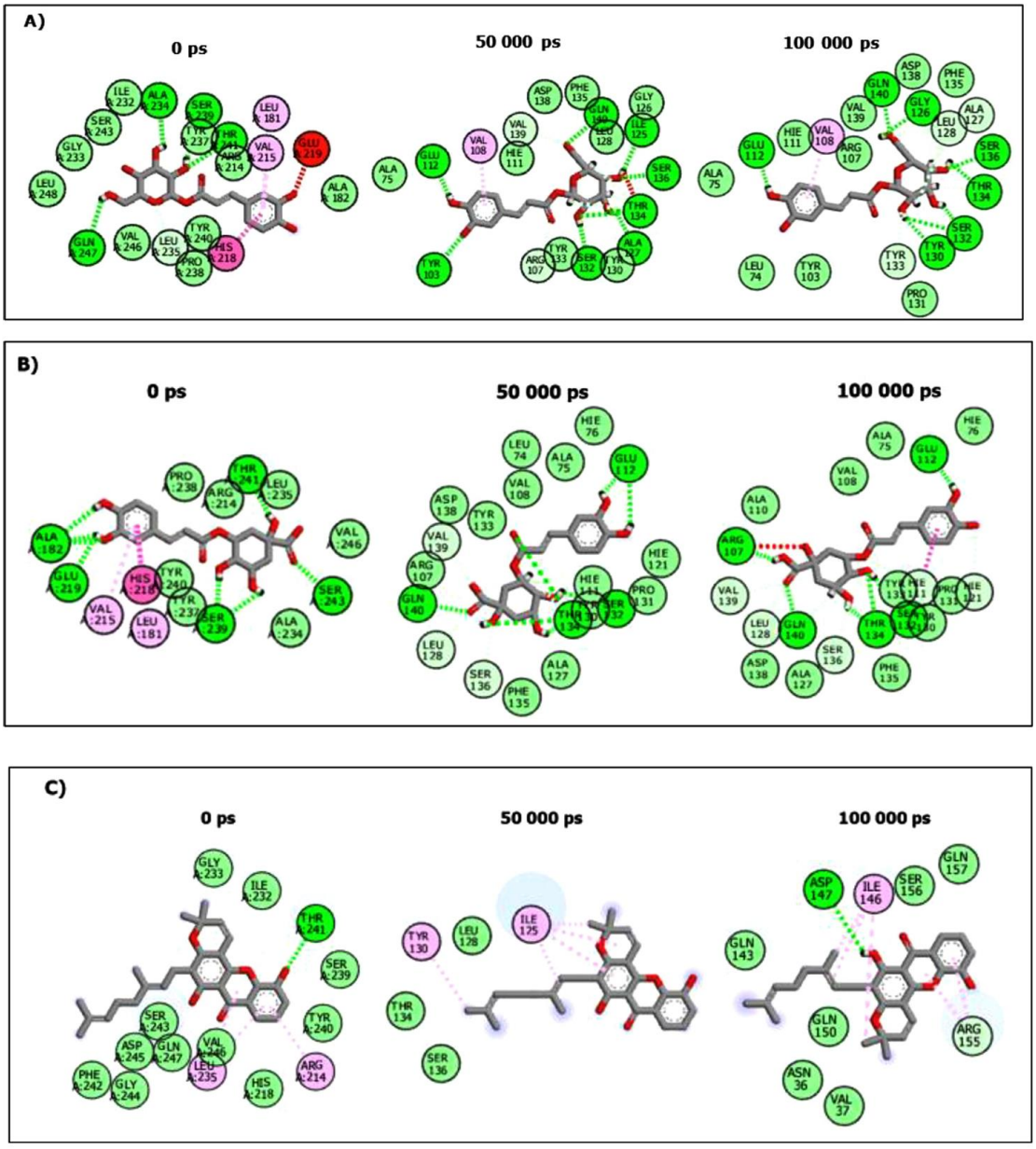

Fig. 11. 2D interaction plot of (A) CFG-MMP1, (B) CGA-MMP1, (C) FOX-MMP1, (D) GPA-MMP1, (E) HGM-MMP1, (F) MET-MMP11 and (G) ROS-MMP1 at 0, 50,000 and 100,000 ps.

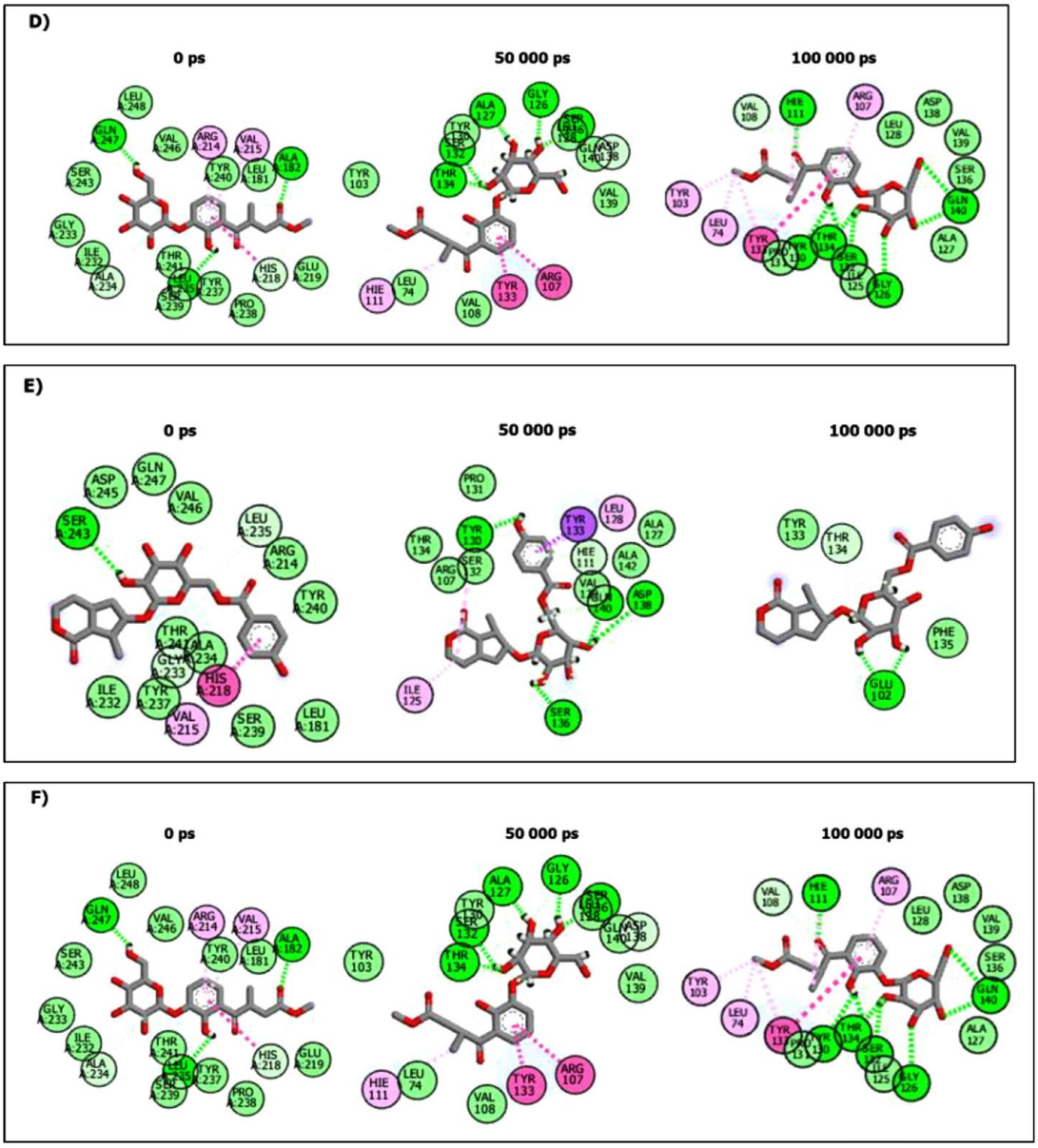

Fig. 11. Continued.

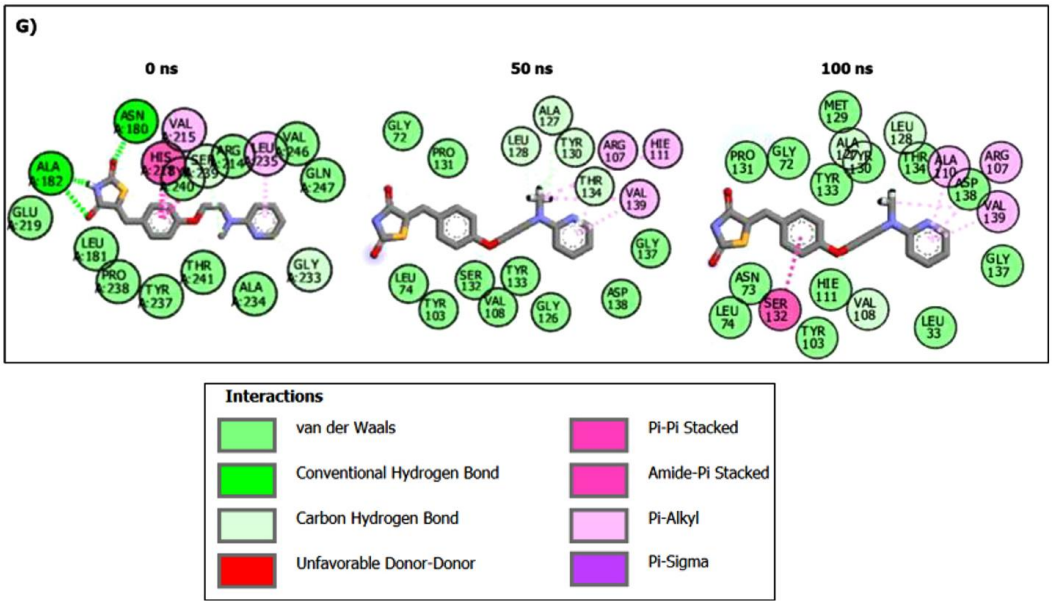

Fig. 11. Continued.

chemical hardness, chemical softness, and electrophilicity, which could provide essential molecular information relevant to the compounds practical applications as therapeutic molecules. Chemical hardness and softness offer relevant information on the reactivity of a molecule, and based on Pearson's HSAB principle (Pearson, 1995), higher chemical softness and lower chemical hardness signify higher compound reactivity (Pearson, 1986). In this regard, the higher chemical softness and the lower chemical hardness of CGA and CFG mean that the compounds are highly reactive and thus could have impacted their higher binding free energy against MMP1 relative to other studied compounds. As stated in the energy gap analysis, the higher residue fluctuation and the increase in surface area of MMP1 following FOX binding might have lessened the impact of the high reactivity of FOX on binding free energy. Similar observations were also noted with ROS and HGM against PPARA, with their higher affinity for the target correlating with their higher reactivity. Electronegativity and chemical potential measure the ability of an atom or a functional group to attract electrons (Pearson, 1986), which signifies that the highest electron attracting abilities of GPA, CGA, and CFG make them promising ligand molecules and might have potentiated their higher binding free energy with MMP1 in this study. FOX, while having a smaller energy gap, higher chemical softness, and lower chemical hardness, which all denote good ligand reactivity, had a lesser ability to attract electrons relative to GPA, CGA, and CFG. This observation could have negatively impacted FOX's lower binding free energy against MMP1. The electrophilicity index defines the tendency of an electrophile to acquire a given amount of electron density and the resistance of a molecule to exchange electron density (Luo et al., 2006). Like the electronegativity and chemical potential, FOX's lesser electrophilicity index relative to GPA, CGA, and CFG suggests that the compound has a lesser tendency to acquire non-donating electrons, which could also impair the likelihood of FOX binding to MMP1. Against PPARA, the electronegativity, chemical potential, and electrophilicity index all suggest that ROS is an active molecule, which could have enhanced its higher binding free energy against the target relative to the top-hit compounds of sunflower cypsela in this study. Overall, GPA, CGA, CFG, and ROS are highly active molecules relative to other investigated compounds. This observation is a further attestation that supports their ability to bind and significantly interact with MMP1 and PPARA. On the other hand, while FOX is an unstable molecule, it lacks the necessary electron-donating and acquiring capability, resulting in its lesser affinity against MMP1in this study.

5. Conclusion

Metabolite characterization of the six cultivars used in this study showed little variance between cultivars in terms of profile and abundance. The top-hit metabolites from the six cultivars, appear to be majorly involved in the modulation of the PPAR signalling pathway to induce an antidiabetic effect. Furthermore, several of the bioactive compounds were active in the PPAR signalling pathway mostly against MMP1 and PPARA, and thus were exploited as key therapeutic target genes in this study. Based on structural stability and affinity, CGA, CFG, and GPA were identified as the lead compounds against MMP1, while HGM and AZA were the best compounds against PPARA. This observation pinpoints these compounds as the "key components" of sunflower cypsela that may act as agonists of the PPAR pathway. However, the reference standard, ROS, had the best affinity against PPARA relative to the top hits, suggesting that the metabolites of sunflower cypsela had better potential for modulating MMP1 of the PPAR signalling pathway. Interestingly, the molecular properties of the top-hit compounds evaluated against MMP1 suggested that CGA, CFG, and GPA are highly active molecules relative to ROS. While against PPARA, ROS had better molecular properties that suggested its better reactivity compared to the top-hit compounds of sunflower cypsela investigated against PPARA. Hence, it may be deduced that sunflower cypsela act by modulating the PPAR signalling pathway and, most especially, through the MMP1 gene in the management of T2DM. The findings from this study further enrich the body of knowledge regarding the molecular mechanism of action of sunflower cypsela as a promising antidiabetic agent. Although, the study identified and focused on the

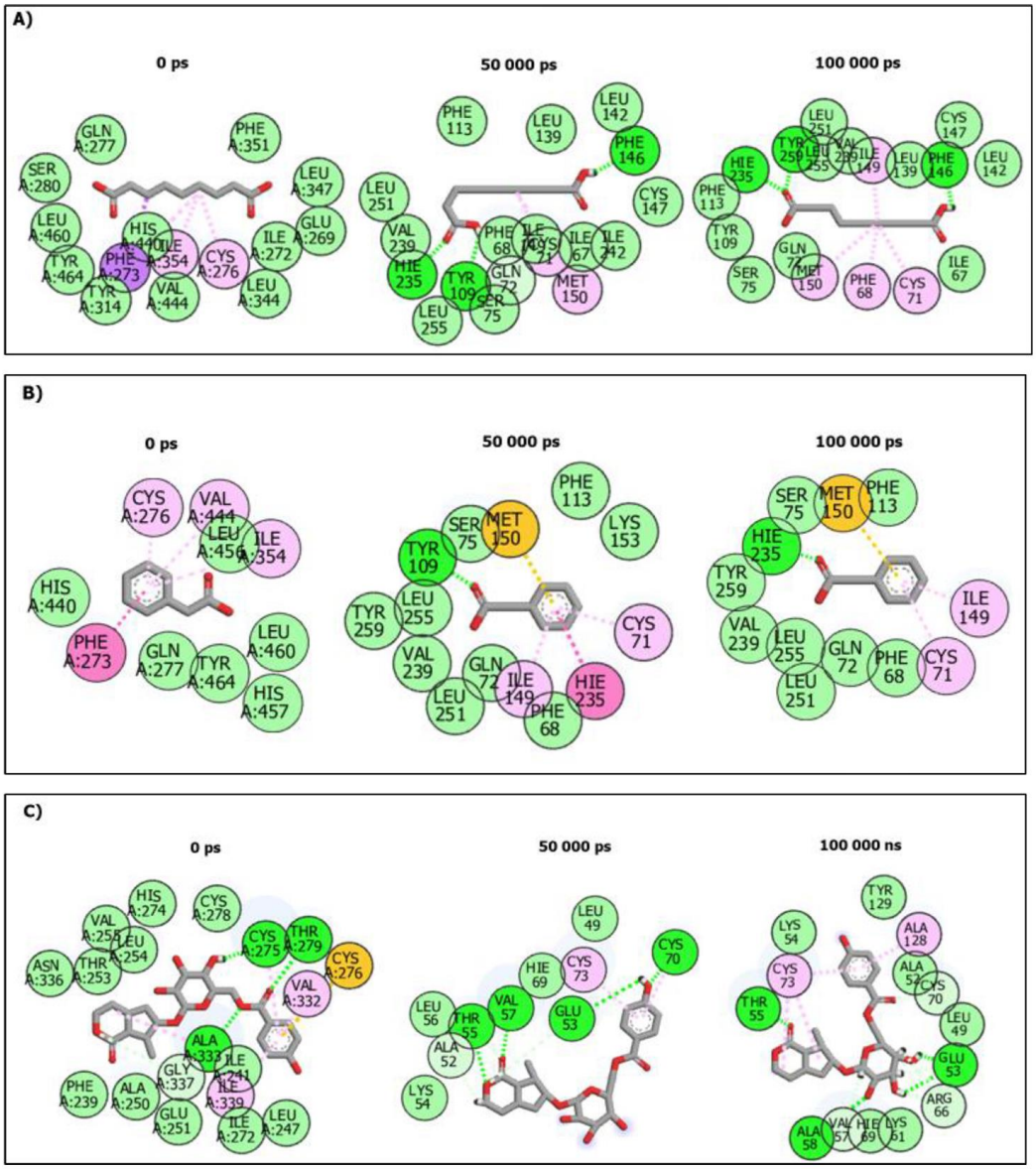

Fig. 12. 2D interaction plot snapshots of (A) AZA-PPARA, (B) PAA-PPARA, (C) HGM-PPARA, (D) MET-PPARA and (E) ROS-PPARA at 0, 50,000 and 100,000 ps.

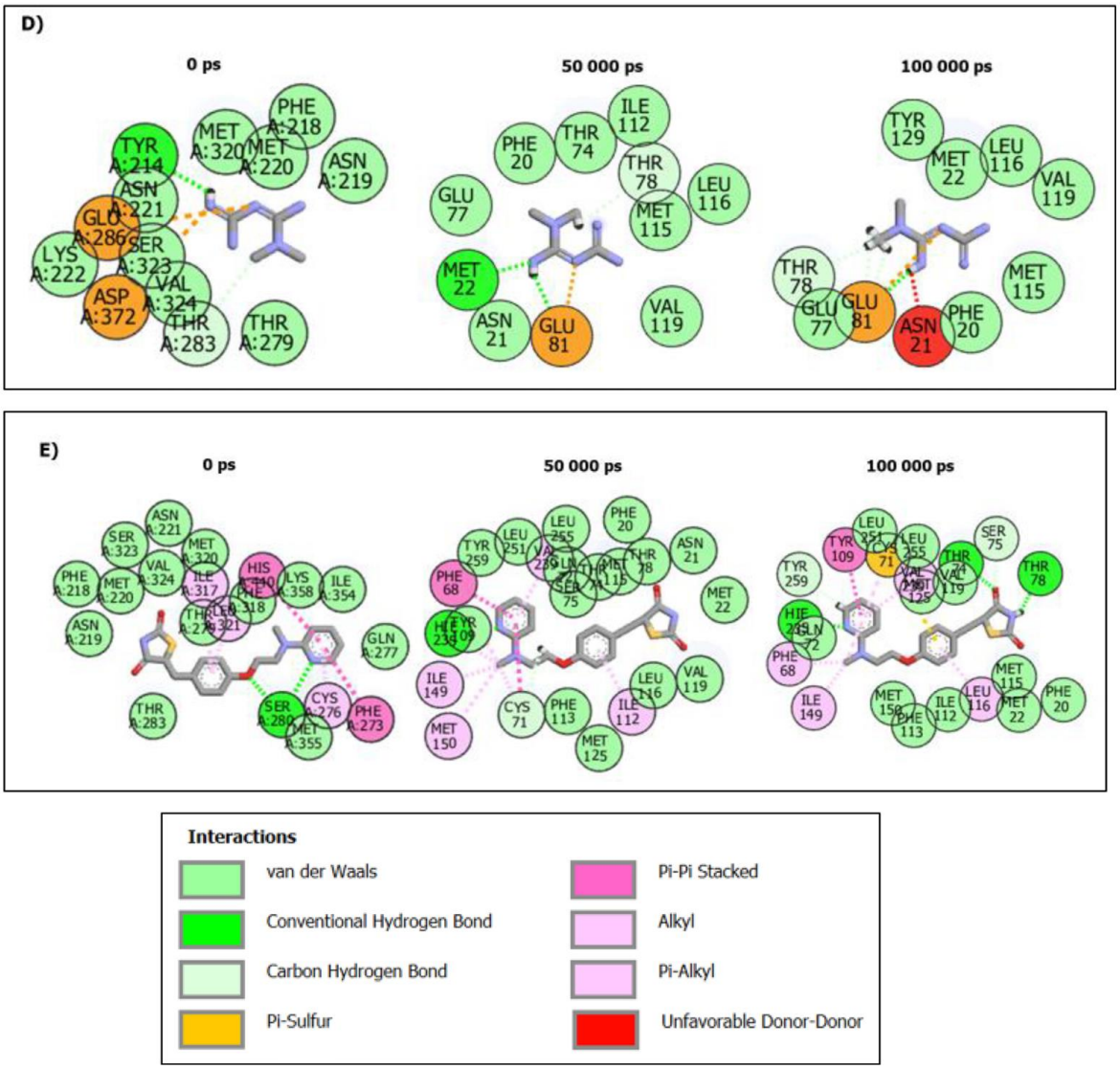

Fig. 12. Continued.

Table 7
The Conceptual density functional theory (CDFT) of top-hits of sunflower cypsela metabolites using DFT calculated at B3LYP/6-31 G+(dp).

CDFT descriptors (eV)	AZA	CFG	CGA	FOX	GPA	HGM	PAA	MET	ROS
E_LUMO	−0.2133	−2.2769	−2.1786	−1.8779	−2.1248	−0.3214	−0.6011	−0.2001	−1.4313
E_HOMO	−7.9393	−6.3503	−6.2509	−5.8849	−6.8982	−6.1518	−6.9659	−5.8475	−5.7279
Energy gap (ΔE)	7.7260	4.0734	4.0723	4.007	4.7734	5.8303	6.3648	5.6473	4.2965
Ionization energy (I)	7.9393	6.3503	6.2509	5.8849	6.8982	6.1518	6.9659	5.8475	5.7279
Electron affinity (A)	0.2132	2.2769	2.1785	1.8779	2.1247	0.3214	0.6011	0.2001	1.4313
Hardness (η)	3.8630	2.0367	2.03611	2.0035	2.3867	2.9151	3.1824	2.8236	2.1482
Softness (S)	0.2588	0.4909	0.4911	0.4991	0.4189	0.3430	0.3142	0.3541	0.4654
Electronegativity (χ)	4.0763	4.3136	4.214	3.8814	4.5115	3.2366	3.7835	3.0238	3.5796
Chemical potential (μ)	−4.0763	−4.3136	−4.2147	−3.8814	−4.5115	−3.2366	−3.7835	−3.0238	−3.5795
Electrophilicity index	2.1506	4.5680	4.3621	3.7597	4.2639	1.7967	2.2490	1.6191	2.9823

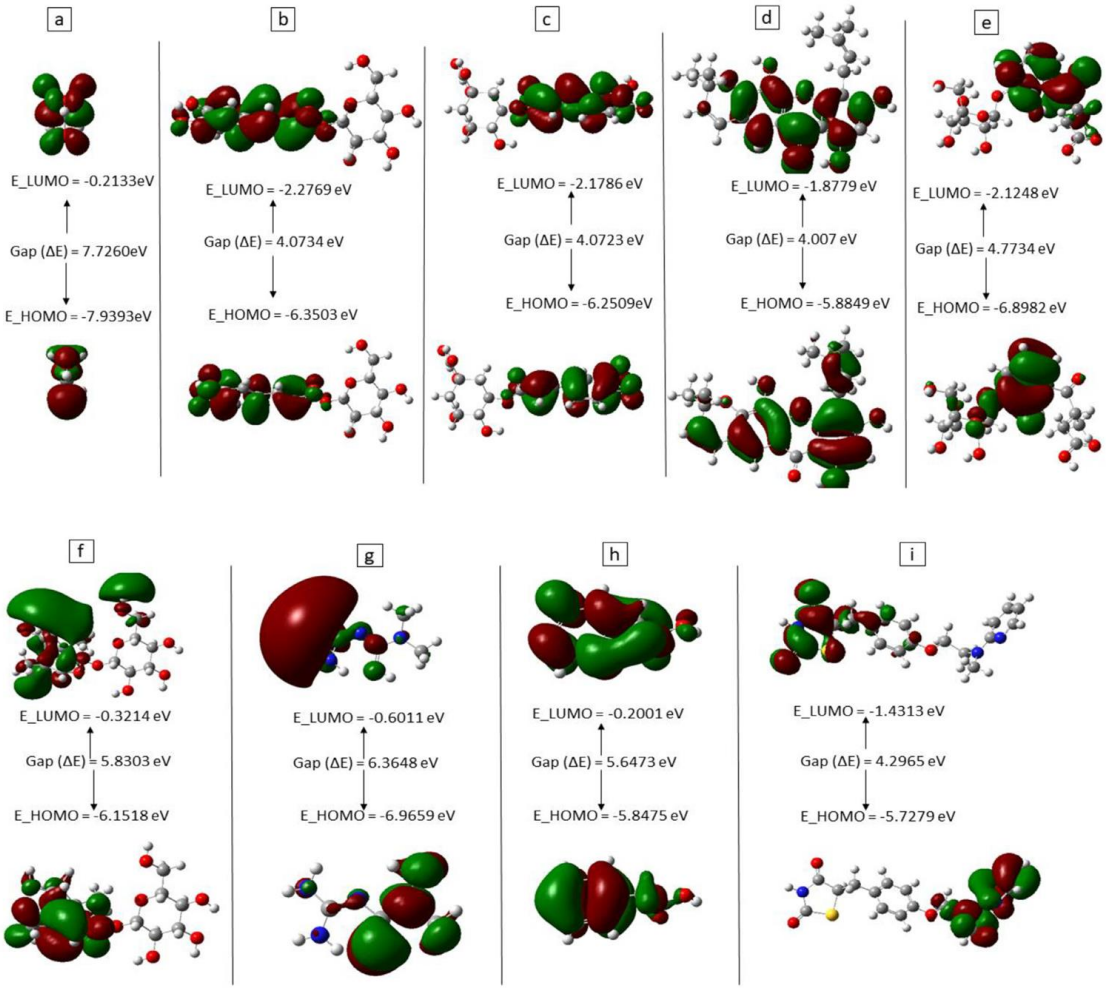

Fig. 13. Frontier molecular orbitals and associated transition energies for (a) AZA, (b) CFG, (c) CGA, (d) FOX, (e) GPA, (f) HGM (g) MET, (h) PAA, and (i) ROS.

hub PPAR signalling pathway, the other 34 pathways identified are also promising and may be further explored with the bioactive compounds of sunflower cypsela for T2DM care. Overall, the findings of this study motivate further *in vitro*, and *in vivo* validation studies and evaluation of potential toxicity effects and effort are underway in this regard.

Declaration of Competing Interest

The authors declare that they have no known competing financial interests or personal relationships that could have appeared to influence the work reported in this paper.

CRediT authorship contribution statement

Athika Rampadarath: Data curation, Formal analysis, Writing – original draft, Writing – review & editing. **Jamiu Olaseni Aribisala:** Writing – original draft, Writing – review & editing. **Nokwanda Pearl Makunga:** Supervision, Writing – review & editing. **Sithandiwe Mazibuko-Mbeje:** Writing – review & editing. **Saheed Sabiu:** Conceptualization, Resources, Supervision, Writing – review & editing.

Acknowledgments

The assistance of the National Research Foundation (NRF Master Scholarship, grant number: 141557), South Africa, to Ms Athika Rampadarath is duly and thankfully acknowledged. The Centre for High Performance Computing (CHPC), Cape Town, South Africa is equally acknowledged for granting access to the computing software and modules used in this study.

Funding

The authors specially acknowledge the financial assistance of the Directorate of Research and Postgraduate Support, Durban University of Technology, the South African Medical Research Council (SAMRC) under a Self-Initiated Research Grant, the Technology Innovative Agency as well as the National Research Foundation (NRF) Research Development Grant for Rated Researchers (Grant number 120433) and the Competitive Programme for Rated Researchers Support

(SRUG2204193723) to S. Sabiu. The views and opinions expressed in this paper are those of the authors and do not necessarily represent the official views of the funders.

Supplementary materials

Supplementary material associated with this article can be found, in the online version, at doi:10.1016/j.sajb.2023.08.045.

References

Adeleke, B.S., Babalola, O.O., 2020. Oilseed crop sunflower (*Helianthus annuus*) as a source of food: nutritional and health benefits. Food Sci. Nutr. 8 (9), 4666–4684.

Adnan, M., Jeon, B.B., Chowdhury, M.H.U., Oh, K.K., Das, T., Chy, M.N.U., Cho, D.H., 2022. Network pharmacology study to reveal the potentiality of a methanol extract of *Caesalpinia sappan* L. Wood against type-2 diabetes mellitus. Life 12 (2), 277.

Aihara, J., 1999. Reduced HOMO−LUMO Gap as an index of kinetic stability for polycyclic aromatic hydrocarbons. J. Phys. Chem. A 103, 7487–7495.

Akoonjee, A., Rampadarath, A., Aruwa, C.E., Ajiboye, T.A., Ajao, A.A.N., Sabiu, S., 2022. Network pharmacology-and molecular dynamics simulation-based bioprospection of *Aspalathus linearis* for type-2 diabetes care. Metabolites 12 (11), 1013.

Ammu, L., Jasmine, J.B., Arunima, C., 2019. *In silico* analysis and molecular docking studies of C-glycosyl flavonoids of *Mimosa pudica* for neuropathic pain. J. Glob. Trends Pharm. Sci. 10 (3), 6439–6449.

Anjum, F.M., Nadeem, M., Khan, M.I., Hussain, S., 2012. Nutritional and therapeutic potential of sunflower cypsela: a review. Br. Food J. 114 (4), 544–552.

Aribisala, J.O., Abdulsalam, R.A., Dweba, Y., Madonsela, K., Sabiu, S., 2022. Identification of secondary metabolites from *Crescentia cujete* as promising antibacterial therapeutics targeting type 2A topoisomerases through molecular dynamics simulation. Comput. Biol. Med. 145, 105432.

Aribisala, J.O., Sabiu, S., 2022. Cheminformatics identification of phenolics as modulators of penicillin-binding protein 2a of *staphylococcus aureus*: a structure−activity-relationship-based study. Pharmaceutics 14 (9), 1818.

Artasensi, A., Pedretti, A., Vistoli, G., Fumagalli, L., 2020. Type 2 diabetes mellitus: a review of multi-target drugs. Molecules 25 (8), 1987.

Awuchi, C.G., 2019. Medicinal plants: the medical, food, and nutritional biochemistry and uses. Int. J. Adv. Acad. Res. 5, 220–241.

Ayers, P.W., Parr, R.G., Pearson, R.G., 2006. Elucidating the hard/soft acid/base principle: a perspective based on half-reactions. J. Chem. Phys. 124,, 194107 1-8.

BIOVIA; Dassault Systèmes. *Discovery Studio*, version 21.1.0; Dassault Systèmes: San Diego, CA, USA, 2021.

Bitew, M., Desalegn, T., Demissie, T.B., Belayneh, A., Endale, M., Eswaramoorthy, R., 2021. Pharmacokinetics and drug-likeness of antidiabetic flavonoids: molecular docking and DFT study. PLoS One 16 (12), e0260853.

Calais, J.L., 1993. Density-functional theory of atoms and molecules. RG Parr and W Yang, Oxford University Press, New York, Oxford, 1989. IX + 333 pp. *International Journal of Quantum Chemistry* 47, 101.

Cao, J., Zheng, R., Chang, X., Zhao, Y., Zhang, D., Gao, M., Yin, Z., Jiang, C., Zhang, J., 2022. Cyclocarya paliurus triterpenoids suppress hepatic gluconeogenesis via AMPK-mediated cAMP/PKA/CREB pathway. Phytomedicine 102, 154175.

Centers for Disease Control and Prevention., 2021. *About chronic diseases*. Centers for Disease Control and Prevention. https://www.cdc.gov/chronicdisease/about/index.htm.

Daina, A., Michielin, O., Zoete, V., 2017. SwissADME: a free web tool to evaluate pharmacokinetics, drug-likeness and medicinal chemistry friendliness of small molecules. Sci. Rep. 7, 42717.

Dwivedi, P.S., Patil, R., Khanal, P., Gurav, N.S., Murade, V.D., Hase, D.P., Gurav, S.S., 2021. Exploring the therapeutic mechanisms of *Cassia glauca* in diabetes mellitus through network pharmacology, molecular docking and molecular dynamics. RSC Adv. 11 (62), 39362–39375.

Di, S., Han, L., An, X., Kong, R., Gao, Z., Yang, Y., Tong, X., 2021. *In silico* network pharmacology and *in vivo* analysis of berberine-related mechanisms against type 2 diabetes mellitus and its complications. J. Ethnopharmacol. 276, 114180.

Ece, A., 2020. Towards more effective acetylcholinesterase inhibitors: a comprehensive modelling study based on human acetylcholinesterase protein−drug complex. J. Biomol. Struct. Dyn. 38 (2), 565–572.

Frkic, R.L., Richter, K., Bruning, J.B., 2021. The therapeutic potential of inhibiting PPARγ phosphorylation to treat type 2 diabetes. J. Biol. Chem. 297 (3).

Galicia-Garcia, U., Benito-Vicente, A., Jebari, S., Larrea-Sebal, A., Siddiqi, H., Uribe, K.B., Martín, C., 2020. Pathophysiology of type 2 diabetes mellitus. Int. J. Mol. Sci. 21 (17), 6275.

Ge, Q., Chen, L., Tang, M., Zhang, S., Liu, L., Gao, L., Chen, K., 2018. Analysis of mulberry leaf components in the treatment of diabetes using network pharmacology. Eur. J. Pharmacol. 833, 50–62.

Hernández, F., Presotto, A., Poverene, M., Mandel, J.R., 2019. Genetic diversity and population structure of wild sunflower (*Helianthus annuus* L.) in Argentina: reconstructing its invasion history. J. Hered. 110 (6), 746–759.

International Diabetes Federation., 2021. *International Diabetes Federation - Facts & Figures*. Idf.org.

Jairajpuri, D.S., Hussain, A., Nasreen, K., Mohammad, T., Anjum, F., Rehman, M.T., Hassan, M.I., 2021. Identification of natural compounds as potent inhibitors of SARS-CoV-2 main protease using combined docking and molecular dynamics simulations. Saudi J. Biol. Sci. 28 (4), 2423–2431.

Jay, M.A., Ren, J., 2007. Peroxisome proliferator-activated receptor (PPAR) in metabolic syndrome and type 2 diabetes mellitus. Curr. Diabetes Rev. 3 (1), 33–39.

Joshi, T., Sharma, P., Joshi, T., Pundir, H., Mathpal, S., Chandra, S., 2021. Structure-based screening of novel lichen compounds against SARS coronavirus main protease (Mpro) as potentials inhibitors of COVID-19. Mol. Divers. 25, 1665–1677.

Kaigongi, M.M., Lukhoba, C.W., Ochieng, P.J., Taylor, M., Yenesew, A., Makunga, N.P., 2020. LC-MS-Based metabolomics for the chemosystematics of Kenyan dodonaea viscosa jacq (sapindaceae) populations. Molecules 25 (18), 4130.

Kaneko, K., Lin, H.Y., Fu, Y., Saha, P.K., Ana, B., Xu, Y., Fukuda, M., 2021. Rap1 in the VMH regulates glucose homeostasis. JCI Insight 6 (11), e142545.

Kruse, H., Goerigk, L., Grimme, S., 2012. Why the standard b3lyp/6-31 g* model chemistry should not be used in dft calculations of molecular thermochemistry: understanding and correcting the problem. J. Org. Chem. 77, 10824–10834.

Lee, K.E., Bharadwaj, S., Yadava, U., Kang, S.G., 2020. Computational and *in vitro* investigation of (-)-epicatechin and proanthocyanidin B2 as inhibitors of human matrix metalloproteinase 1. Biomolecules 10 (10), 1379.

Li, Y., Liu, Y., Liang, J., Wang, T., Sun, M., Zhang, Z., 2019. Gymnemic acid ameliorates hyperglycemia through PI3K/AKT-and AMPK-mediated signaling pathways in type 2 diabetes mellitus rats. J. Agric. Food Chem. 67 (47), 13051–13060.

Lipinski, C.A., Lombardo, F., Dominy, B.W., Feeney, P.J., 1997. Experimental and computational approaches to estimate solubility and permeability in drug discovery and development settings. Adv. Drug Deliv. Rev. 23 (1−3), 3–25.

Luo, J., Xue, Z.Q., Liu, W.M., Wu, J.L., Yang, Z.Q., 2006. Koopmans' theorem for large molecular systems within density functional theory. J. Phys. Chem. 110 (43), 12005–12009.

Ma, Y., Tao, Y., Qu, H., Wang, C., Yan, F., Gao, X., Zhang, M., 2022. Exploration of plant-derived natural polyphenols toward COVID-19 main protease inhibitors: DFT, molecular docking approach, and molecular dynamics simulations. RSC Adv. 12 (9), 5357–5368.

Magangana, T.P., Stander, M.A., Masondo, N.A., Makunga, N.P., 2021. Steviol glycoside content and essential oil profiles of Stevia rebaudiana Bertoni in response to NaCl and polyethylene glycol as inducers of salinity and drought stress *in vitro*. Plant Cell, Tissue Organ Cult. 145 (1), 1–18.

Mandal, S.K., Kumar, B.K., Sharma, P.K., Murugesan, S., Deepa, P.R., 2022. *In silico* and *in vitro* analysis of PPAR−α/γ dual agonists: comparative evaluation of potential phytochemicals with anti-obesity drug orlistat. Comput. Biol. Med. 147, 105796.

Nguyen, D.T.C., Nguyen, T.T., Le, H.T., Nguyen, T.T.T., Bach, L.G., Nguyen, T.D., Van Tran, T., 2021. The sunflower plant family for bioenergy, environmental remediation, nanotechnology, medicine, food and agriculture: a review. Environ. Chem. Lett. 19, 3701–3726.

Pan, L., Li, Z., Wang, Y., Zhang, B., Liu, G., Liu, J., 2020. Network pharmacology and metabolomics study on the intervention of traditional Chinese medicine Huanglian Decoction in rats with type 2 diabetes mellitus. J. Ethnopharmacol. 258, 112842.

Pearson, R.G., 1995. The HSAB Principle-more quantitative aspects. Inorg. Chim. Acta 240, 93–98.

Pearson, R.G., 1986. Absolute electronegativity and hardness correlated with molecular orbital theory. Proc. Natl. Acad. Sci. 83, 8440–8441.

Pettersen, E.F., Goddard, T.D., Huang, C.C., Couch, G.S., Greenblatt, D.M., Meng, E.C., Ferrin, T.E., 2004. UCSF Chimera−a visualization system for exploratory research and analysis. J. Comput. Chem. 25 (13), 1605–1612.

Oh, K.K., Adnan, M., Cho, D.H., 2020. Network pharmacology of bioactives from *Sorghum bicolor* with targets related to diabetes mellitus. PLoS One 15 (12), e0240873.

Rampadarath, A., Balogun, F.O., Sabiu, S., 2023. Insights into the mechanism of action *of Helianthus annuus* (sunflower) seed essential oil in the management of type-2 diabetes mellitus using network pharmacology and molecular docking approaches. Endocrines 4, 327–349.

Rampadarath, A., Balogun, F.O., Pillay, C., Sabiu, S., 2022. Identification of flavonoid C-glycosides as promising antidiabetics targeting protein tyrosine phosphatase 1B. J. Diabetes Res. 2022, 6233217.

Ramirex, D., Caballero, J., 2016. Is it reliable to use common molecular docking methods for comparing the binding affinities of Enantiomer pairs for their protein target. Int. J. Mol. Sci. 17, 525–545.

Rehman, A., Saeed, A., Kanwal, R., Ahmad, S., Changazi, S.H., 2021. Therapeutic effect of sunflower cypsela and flax cypsela on diabetes. Cureus 13, e17256.

Richmond, K., Williams, S., Mann, J., Brown, R., Chisholm, A., 2013. Markers of cardiovascular risk in postmenopausal women with type 2 diabetes are improved by the daily consumption of almonds or sunflower kernels: a feeding study. Int. Sch. Res. Not. 2013, 1–9.

Roden, M., Petersen, K., Shulman, G., 2017. Insulin resistance in type 2 diabetes. Textbook of Diabetes. Wiley, pp. 174−186.

Sabiu, S., Balogun, F.O., Amoo, S.O., 2021. Phenolics profiling of *Carpobrotus edulis* (L.) NE Br. and insights into molecular dynamics of their significance in type 2 diabetes therapy and its retinopathy complication. Molecules 26 (16), 4867.

Saggar, S., Mir, P.A., Kumar, N., Chawla, A., Uppal, J., Kaur, A., 2022. Traditional and herbal medicines: opportunities and challenges. Pharm. Res. 14 (2), 107–114.

Schinner, S., Scherbaum, W.A., Bornstein, S.R., Barthel, A., 2005. Molecular mechanisms of insulin resistance. Diabet. Med. 22 (6), 674–682.

Sherman, B.T., Hao, M., Qiu, J., Jiao, X., Baseler, M.W., Lane, H.C., Imamichi, T., Chang, W., 2021. DAVID: a web server for functional enrichment analysis and functional annotation of gene lists. Nucleic Acids Res. 50 (W1), W216–W221.

Shivani, S., Sunil, S., 2013. Antidiabetic effect of *Helianthus annuus* L., cypsela ethanolic extract in streptozotocinnicotinamide induced Type 2 diabetes mellitus. Int. J. Pharm. Sci. 5, 382–387.

Singh, P., Singh, V.K., Singh, A.K., 2019. Molecular docking analysis of candidate compounds derived from medicinal plants with type 2 diabetes mellitus targets. Bioinformation 15, 179.

Sun, Z., Chen, J., Ma, J., Jiang, Y., Wang, M., Ren, G., Chen, F., 2012. Cynarin-rich sunflower (*Helianthus annuus*) sprouts possess both antiglycative and antioxidant activities. J. Agric. Food Chem. 60, 3260–3265.

Süntar, I., 2020. Importance of ethnopharmacological studies in drug discovery: role of medicinal plants. Phytochem. Rev. 19 (5), 1199–1209.

Wallace, W.E., Moorthy, A.S., 2023. NIST mass spectrometry data center standard reference libraries and software tools: application to seized drug analysis. J. Forensic Sci.. https://doi.org/10.1111/1556-4029.15284.

Wang, S., Dougherty, E.J., Danner, R.L., 2016. PPARγ signaling and emerging opportunities for improved therapeutics. Pharmacol. Res. 111, 76–85.

Yousef, M., Ülgen, E., Sezerman, O.U., 2021. CogNet: classification of gene expression data based on ranked active-subnetwork-oriented KEGG pathway enrichment analysis. PeerJ Comput. Sci. 7, e336.

Zeng, Z., Hu, J., Jiang, J., Xiao, G., Yang, R., Li, S., Bi, X., 2021. Network pharmacology and molecular docking-based prediction of the mechanism of Qianghuo Shengshi decoction against rheumatoid arthritis. Biomed. Res. Int. 2021.

Zheng, Y., Ley, S.H., Hu, F.B., 2018. Global aetiology and epidemiology of type 2 diabetes mellitus and its complications. Nat. Rev. Endocrinol. 14 (2), 88–98.

Chapter Five

This chapter has been formatted for submission in this format to *Journal of Molecular Biology* for publication.

Unveiling the mechanism of antidiabetic action of sunflower seeds through modulation of *MMP1* and *PPARA* in HepG2 cells

Athika Rampadarath[1], Terisha Ghazi[2], Anil Chuturgoon[2], and Saheed Sabiu[1]*

[1]Department of Biotechnology and Food Science, Faculty of Applied Sciences, Durban University of Technology, P.O. Box 1334, Durban 4000, KwaZulu-Natal, South Africa.

[2]Department of Medical Biochemistry, University of KwaZulu-Natal, Durban, South Africa.

*Correspondence: sabius@dut.ac.za

Abstract

Helianthus annuus L. (sunflower) seed is a popular oilseed crop with documented antidiabetic potential. This study elucidated the possible mechanism of antidiabetic action of its cultivars on the *in vitro* modulation of Peroxisome Proliferator Activated Receptor (PPAR) Signalling pathway, focusing on Matrix Metalloproteinase 1 (*MMP1*) and Peroxisome Proliferator Activated Receptor Alpha (*PPARA*), as derived from the network pharmacology study. Prior to confirming the antidiabetic activity, the cytotoxicity assessment of the six cultivars revealed the optimal concentrations for AGSUN 5108 CLP and AGSUN 5270 at 100 µg/ml; AGSUN 5103 CLP and AGSUN 5101 CLP at 75 µg/ml; and last AGSUN 5206 CLP and AGSUN 8251 at 50 and 25 µg/ml, respectively, to promote cell viability of HepG2 cells. Thereafter, the glucose consumption assay demonstrated that treatment with three of the investigated cultivars [AGSUN 5103 CLP, AGSUN 8251, and AGSUN 5101 CLP] significantly reduced (13.25 – 14.85 mmol/L) the glucose levels compared to those of reference standards [metformin (14.85 mmol/L), insulin (13 mmol/L)] and the untreated insulin-resistant HepG2 cells (17 mmol/L). Additionally, these cultivars upregulated the expression of *MMP1* and *PPARA*, the key genes involved in the PPAR signalling pathway. Amongst the cultivars, AGSUN 5101 CLP exhibited the most potent antidiabetic effects, with the highest fold increases in *MMP1* (1.88) and *PPARA* (4.59) expression., relative to metformin (*MMP1*= 8.25; *PPARA* = 12.38) and insulin (*MMP1*= 3.71; *PPARA* = 10.37). These findings highlight the potential of sunflower seeds, particularly cultivar 5101 CLP, as natural therapeutic agents for T2DM through the augmentation of the PPAR signalling pathway. Particularly through the modulation of *MMP1* and *PPARA* within the pathway, these seeds may improve insulin sensitivity, and promote glucose uptake as well as fatty acid oxidation, which may aid in reducing the risk of T2DM.

Keywords: HepG2, *MMP1*, PPAR signalling pathway, *PPARA*, Type-2 diabetes, sunflower seed.

1.0 Introduction

Helianthus annuus L., the popular sunflower, is widely known for its, applications in the food industry. Its seeds are rich in healthy fats, protein, fibres, and several bioactive compounds (De, 2020). Their consumption has been associated with potential health benefits, including reducing the risk of cardiovascular disease and cancer, and displaying anti-inflammatory, anti-asthmatic, and antidiabetic potential (Adeleke and Babalola, 2020). Recently, there has been growing interest in exploring the potential antidiabetic properties of sunflower seeds as a potential complementary/alternative to currently available antidiabetic drugs (Saeed *et al*., 2022; Nnadi *et al.*, 2020; Richmond *et al.*, 2013). Type 2 diabetes mellitus (T2DM) is a chronic metabolic disorder characterized by hyperglycaemia (high blood sugar) resulting from either insulin resistance or impaired insulin secretion (Artasensi *et al*., 2020). Therapeutic approaches typically focus on lowering blood sugar levels, often initiated with the first line of treatment, metformin. Other strategies include enhancing insulin sensitivity with drugs like thiazolidinediones. Similarly, targeting of the peroxisome proliferator-activated receptor (PPAR) signalling pathway has been increasingly implicated for its insulin sensitization potential due to its key role in regulating glucose and lipid metabolism (Montaigne *et al*., 2021). Interestingly, a recent *in silico* study that employed integrated network pharmacology and molecular dynamics (MD) simulation strategy established significant modulation of *PPARA* and matrix metalloproteinase 1 (*MMP1*) of the PPAR signalling pathway as two therapeutic genes of interest implicated in antidiabetic potential of sunflower seeds (Rampadarath *et al*., 2023). While the study established a putative mechanism of action of sunflower seeds against T2DM, an appropriate experimental validation was lacking. Experimental validation is essential to complement the results of *in silico* analysis to ascertain the possible mechanism of action of a drug candidate (Agamah *et al*., 2020). Mammalian cells such as HepG2 cells have been adopted to establish the antidiabetic potential of therapeutics *in vitro* (Yang *et al*., 2019) and the findings from such studies have been significant (Hu *et al*., 2023; Kheirollahzadeh *et al*., 2022; Liu *et al*., 2019 and Odeyemi and Dewar, 2019). Considering the foregoing and building on the established modulatory role of sunflower metabolites on *PPARA* and *MMP1*,

this study validated how sunflower seed extracts might regulate glucose uptake and subsequent expression of *PPARA* and *MMP1* in insulin-resistant HepG2 cells.

2.0 Materials and methods

2.1 Cell Culture and sunflower seed treatment

HepG2 cells (HB-8065) were purchased from American Type Culture Collection (ATCC), Johannesburg, South Africa. The cells were cultured in Dulbecco's Modified Eagle's Medium (DMEM) supplemented with 10% fetal bovine serum FBS and 1% penicillin and streptomycin at 37°C with 5% CO2. All cell culture reagents were purchased from Sigma-Aldrich, Inc. (St. Louis, MO, USA). Sunflower seed extracts and metformin treatments were prepared in growth media as per working concentrations.

2.2 Viability of HepG2 cells treated with sunflower seed extracts

This study evaluated the viability of HepG2 cells using 3-(4, 5-dimethyl 2 thiazolyl)-2,5-diphenyl 2 tetrazolium bromide (MTT) assay in accordance with the protocol described by Kheirollahzadeh *et al.* (2022) with slight modifications. HepG2 cells (1.5×10^4) were seeded per well of a 96-well plate and incubated at 37°C for 48 H until confluency. Confluent HepG2 cells were exposed to various concentrations (5, 25, 50, 75 and 100 μg/ml) of sunflower seed cultivars or insulin (1 μM) (Hao *et al*., 2018) or metformin (10 μg/ml) (Alaaeldin *et al*., 2021) for 24 h under standard culture growth conditions. The untreated cells (growth media only) served as the experimental control. Post 24-h treatment, growth media containing treatments were discarded and replaced with MTT reagent (2 mg/mL) and incubated at 37°C for three hours. Post incubation, MTT salt solution was discarded from the treatment wells and 100 μL DMSO was added and incubated for 1 h to solubilize MTT formazan crystals. The optical density (OD) of each well was determined at 570 nm on a BioTek uQuant microplate spectrophotometer. Viability of cells was then determined using the absorbance readings of the treated cells relative to the untreated ones and expressed as a relative percentage. Within each cultivar, the concentrations with ideal cell viability were selected as the optimum concentration for further analysis of each cultivar. All treatments were performed in three independent experiments.

2.3 Establishment of insulin resistance in HepG2 cell line

Induction of insulin resistance in HepG2 cells was achieved as described by Alaaeldin *et al*. (2021). HepG2 cells were starved in FBS-free media for 6 h before treatment with 0.005 μM of insulin for 24 h. The difference in glucose concentration of cells treated with insulin was compared to those of the untreated (not treated with insulin) cells to confirm the establishment of insulin resistance.

2.4 Cell viability with optimum concentration of sunflower seed cultivars in IR-HepG2 cells

Approximately 1.5 x 10^4 cells were seeded in each well and incubated at 37°C in a humidified atmosphere at 5% CO_2. IR was established post-confluency, thereafter, subjecting the IR-HepG2 cells to treatment with optimal concentrations of sunflower seeds extracts or metformin or insulin for 24 h. MTT assay of IR-HepG2 cells treated with sunflower seeds was conducted and cell viability was calculated as described in 2.2.

2.5 Glucose consumption assay of sunflower seed treated IR-HepG2 cells

No less than 1.5 x 10^4 cells were seeded in each well in optimum culture conditions and grown until confluency, before inducing insulin resistance. After induction of IR, cells were treated with optimal concentrations of each cultivar for 24 h. Thereafter, aliquots of the growth media from treated and untreated cells were measured using the Accu-Check glucose monitoring system (Roche Diabetes Care, Inc.) The concentration of glucose present in the media after 24 h was compared to the control (untreated) cells (Varshney *et al*., 2019).

2.6 RNA isolation, cDNA synthesis and qPCR analysis of target genes in IR-HepG2 cells after treatment with sunflower seeds extracts

Insulin resistant-HepG2 cells were treated with the six sunflower seed cultivars at their respective optimum concentrations. Post-treatment, the cells were lysed, and total ribonucleic acid (RNA) extraction was performed using QIAzol lysis reagent (79306), Qiagen, Germany, according to the manufacturers protocol. The RNA in each case was quantified using the Nanodrop2000 spectrophotometer, Thermo-Fisher Scientific, United States, standardized to 1,000 ng/μL, and reverse transcribed into complementary deoxyribonucleic acid (cDNA) using the Maxima H Minus First Strand cDNA Synthesis Kit (K1652),Thermo-Fisher Scientific,

United States. The cDNA was then subjected to qPCR using gene-specific primers as presented in Table 1. Primers were designed using PrimerBank (https://pga.mgh.harvard.edu/primerbank/) and subsequently purchased from Inqaba Biotechnical Industries (Pty) Ltd, Pretoria, South Africa. Glyceraldehyde 3-phosphate dehydrogenase (*GAPDH*) was used as in-house gene for expression normalization. The qPCR was performed using the PowerUp™ SYBR™ Green Master Mix (A25742 - Thermo-Fisher Scientific, United States) and QuantStudio 3 qPCR system at the following PCR conditions: denaturation at 95 °C for 15 s, annealing at 52 °C for 1 minute followed by extension at 60 °C for 1 min, for 40 cycles. The PCR amplicons were then resolved on 1.5% agarose gel and visualized under UV light. qPCR data was analyzed using QuantStudio design and analysis software version 1.5.1. The comparative threshold cycle (Ct) method was used to determine the relative changes in expression (Mazibuko *et al*., 2024).

Table 1: Primer sequences of target genes

Target gene	Primer sequence	PCR product length (bp)
MMP1	Sense: CTCTGGAGTAATGTCACACCTCT Anti-sense: TGTTGGTCCACCTTTCATCTTC	199 bp
PPARA	Sense: CGGTGACTTATCCTGTGGTCC Anti-sense: CCGCAGATTCTACATTCGATGTT	79 bp
GADPH	Sense: TCCACCACCCTGTTGCTGTA Anti-sense: ACCACAGTCCATGCCATCAC	452 bp

2.7 Statistical analysis

Where applicable, three independent experiments (n=3) were performed. Data was analysed by one-way analysis of variance complemented with post hoc Tukey test using IBM SPSS software 29.0.2.0. Results were presented as mean ± standard deviation (SD). The level of statistical significance was set at $p < 0.05$.

3.0 Results

3.1 Cell viability assessment

Figure 1 presents the effects of various concentrations of sunflower seed cultivars on the viability of HepG2 cells. The percentage cell viability was compared to the control (untreated) HepG2 cells. Statistically significant increases in cell viability ($p<0.05$) were observed across all concentrations and cultivars compared to the control. Interestingly, the optimal concentrations promoting cell viability differed among the sunflower seed cultivars. AGSUN 5108 CLP and 5270 promoted the highest viability at 100 µg/ml, while AGSUN 5103 CLP and 5101 CLP demonstrated the most viable effects at 75 µg/ml. In contrast, AGSUN 5106 CLP and AGSUN 8251 displayed peak viability at lower concentrations of 50 and 25 µg/ml, respectively.

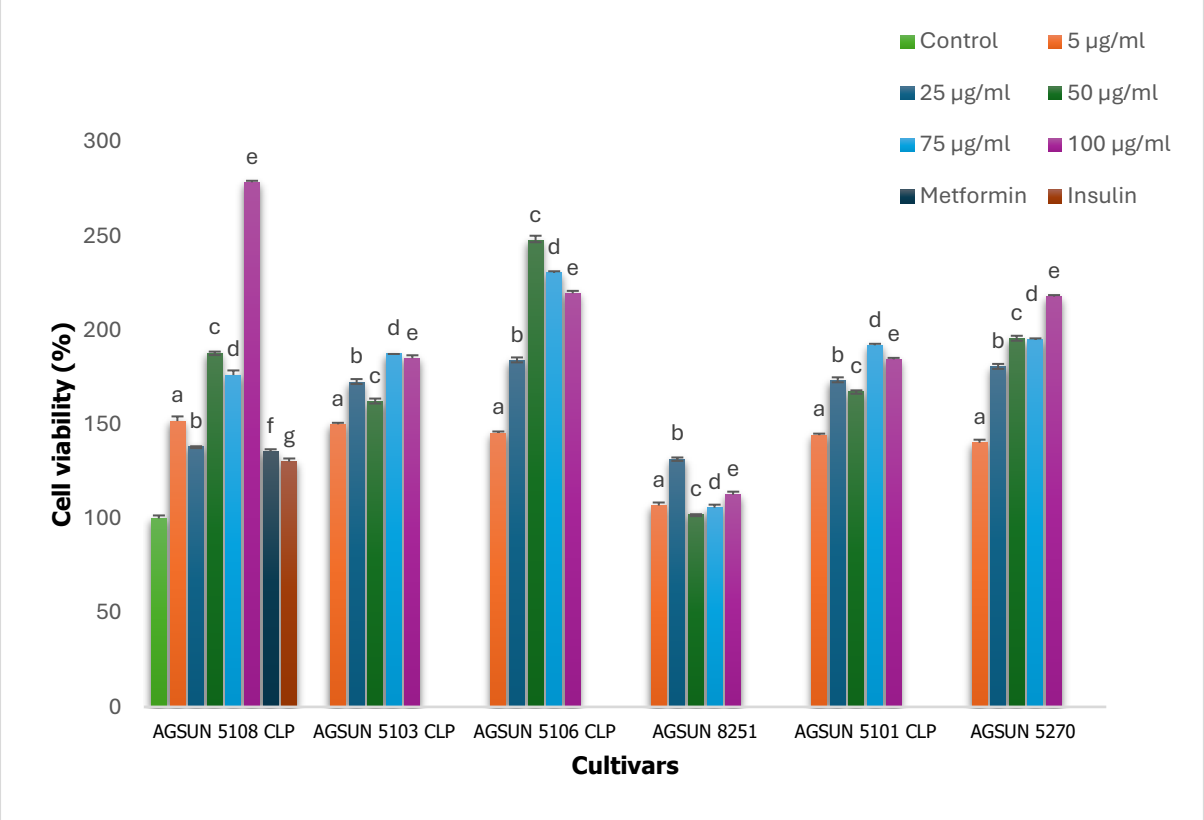

Figure 1. Cell viability after treatment with different concentrations (25, 50, 75, and 100 µg/ml) of sunflower seed cultivars, metformin (1 µM) or insulin (10 µg/ml) for 24 h. Bars represent mean ± SD. Statistical significance ($p < 0.05$) amongst concentrations within each cultivar is represented by differing alphabets, compared to untreated (control) HepG2 cells.

Table 1 presents the data obtained regarding establishment of insulin-resistant (IR) HepG2 cell model. Compared to non-IR cells, IR-HepG2 cells displayed significantly ($p < 0.05$) lower glucose consumption after 24 h. Figure 2, illustrates the effects of treatment with optimal concentrations of sunflower seed extracts from each cultivar on the viability of IR-HepG2 cells. All cultivars significantly ($p < 0.05$) increased cell viability compared to the untreated control cells.

Table 1: Glucose consumption after 24 h in control and insulin-resistant (IR) HepG2 cells

Cells	Glucose consumption (mmol/L)
non-IR-HepG2 cells (control)	3.8
IR-HepG2 cells (model)	1.2[a]

Note: [a] = $p < 0.05$

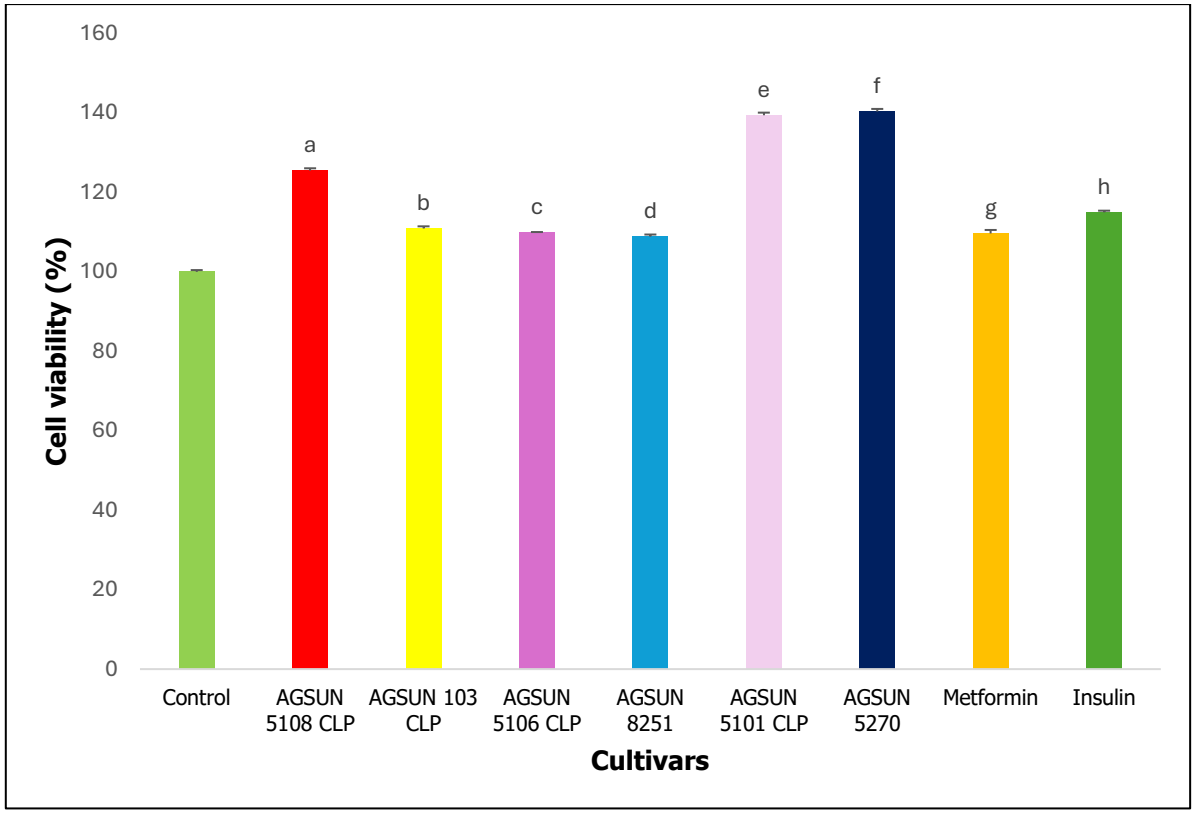

Figure 2. Cell viability after treatment of IR-HepG2 cells with optimum concentrations of each respective sunflower seed cultivars or metformin (1 μM) or insulin (10 μg/ml) for 24 h. Bars represent mean ± SD., Statistical significance ($p < 0.05$) amongst concentrations within each cultivar is represented by differing alphabets, compared to untreated (control) IR-HepG2 cells.

3.2 Effect of sunflower seed extracts on glucose consumption in HepG2 cells

Figure 3 illustrates the 24-h treatments with sunflower seed extracts from different cultivars, where they significantly ($p < 0.05$) reduced glucose concentration of cells compared to the untreated control cells. IR-HepG2 cells that were treated with sunflower seed extracts exhibited an increase in glucose consumption. Amongst the cultivars, AGSUN 5101 CLP, 5103 CLP and 8251 saw the greatest reduction in glucose concentration exceeding, relative to the positive controls, metformin and insulin.

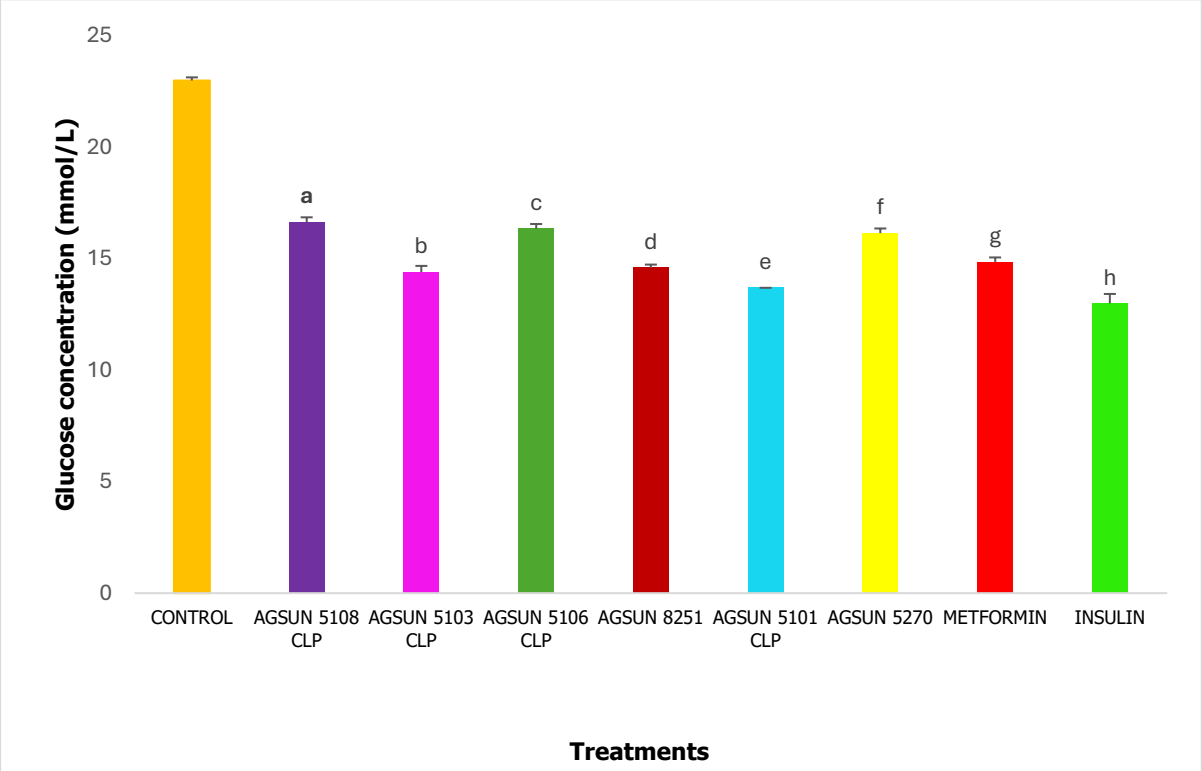

Figure 3. Glucose concentration of media after 24-hour treatment with cultivars of sunflower seed, metformin, insulin and untreated (control) IR-HepG2 cells. Bars represent mean ± SD. Statistical significance is represented by differing alphabets ($p < 0.001$), compared to untreated (control) IR-HepG2 cells.

3.3 Effect of sunflower seed extracts of cultivars AGSUN 5103 CLP, 8251 and 5101 CLP on *MMP1* and *PPARA* of the PPAR signalling pathway

Quantitative analysis of gene expression (Figure 4A-C) revealed that all three cultivars (AGSUN 5101 CLP, AGSUN 5103 CLP, and AGSUN 8251 that displayed superior glucose-lowering properties) upregulated *MMP1* expression compared to the control (untreated) cells. AGSUN 5101 CLP displayed the highest fold-change increase (1.88), followed by AGSUN 5103 CLP (1.66) and AGSUN 8251 (1.39). While these fold-changes were lower compared to the positive controls, metformin (8.75) and insulin (3.71), AGSUN 5101 CLP demonstrated the most promising upregulation amongst the cultivars. These observations were further supported by the gel electrophoresis results of the qPCR amplicons for *MMP1* and GAPDH (housekeeping gene) following treatment with sunflower seed extracts (Figures 4 B and C). The gel electrophoresis was able to confirm the upregulation of MMP1 post-treatment with cultivars of sunflower seed, emphasised by the increased florescence of the bands compared to the untreated control particularly AGSUN 5101 CLP.

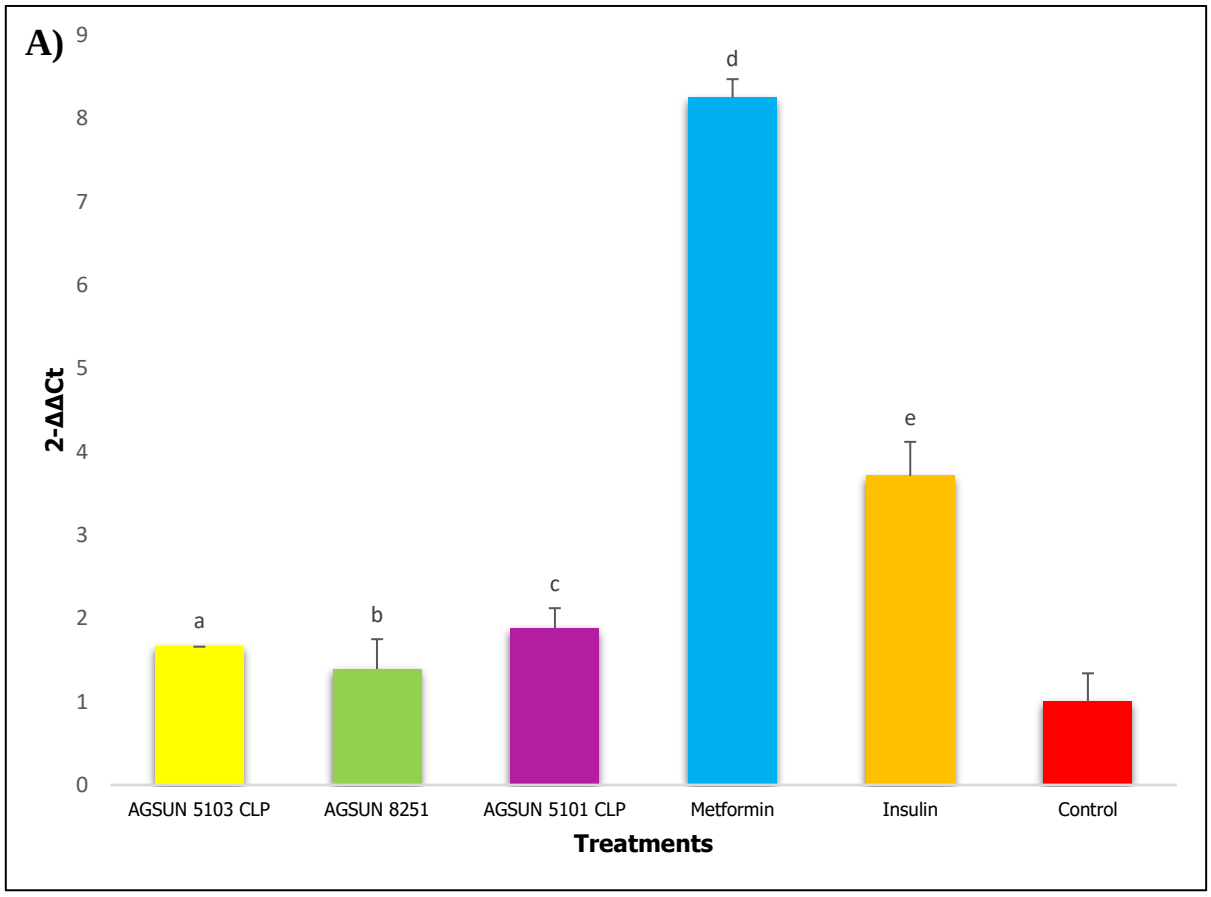

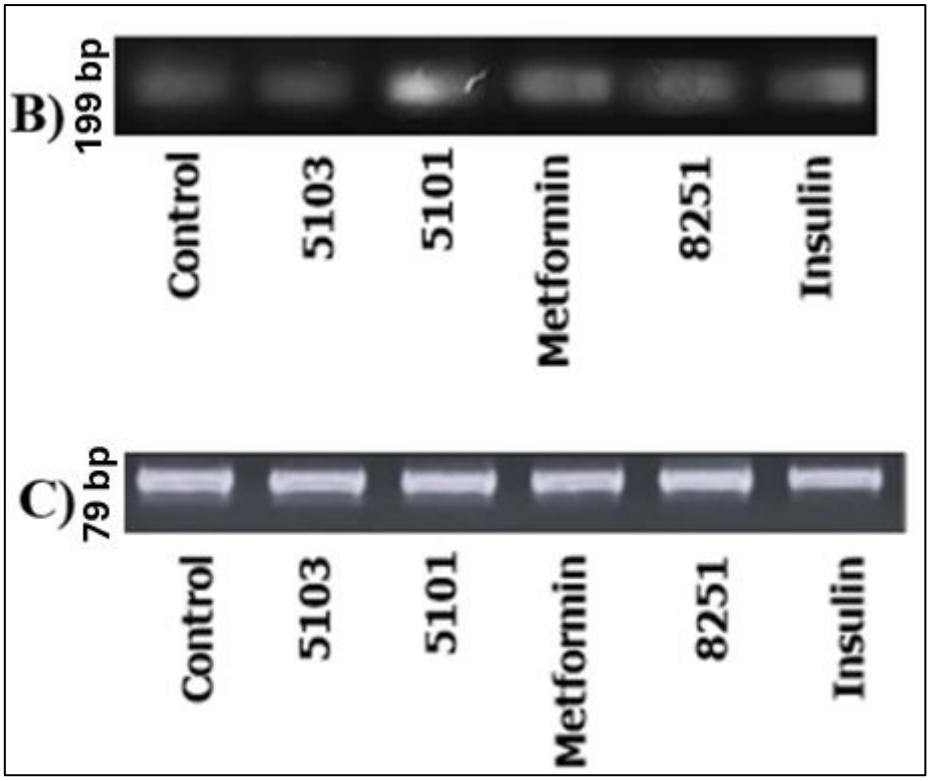

Figure 4. Effect of lead cultivars of sunflower seeds on expression of *MMP1* in IR-HepG2 cells. A) Bar graph presenting effect of fold change through relative fold-change. Bars represent mean ± SD. Statistical significance is represented by differing alphabetically symbols = $p < 0.05$, compared to untreated (control) IR-HepG2 cells. Gel electrophoresis of PCR products of B) *MMP1* (199 bp) , C) *GADPH* (79 bp), house-keeping gene).

Similarly, all three sunflower seed extracts increased *PPARA* gene expression compared to the control (Figure 5A-C). While metformin and insulin again induced significantly higher fold-change increases (12.28 and 10.37, respectively), AGSUN 5101 CLP showed the greatest upregulation once again amongst the cultivars (4.59), followed by AGSUN 8251 (3.12) and AGSUN 5103 CLP (1.96). ???

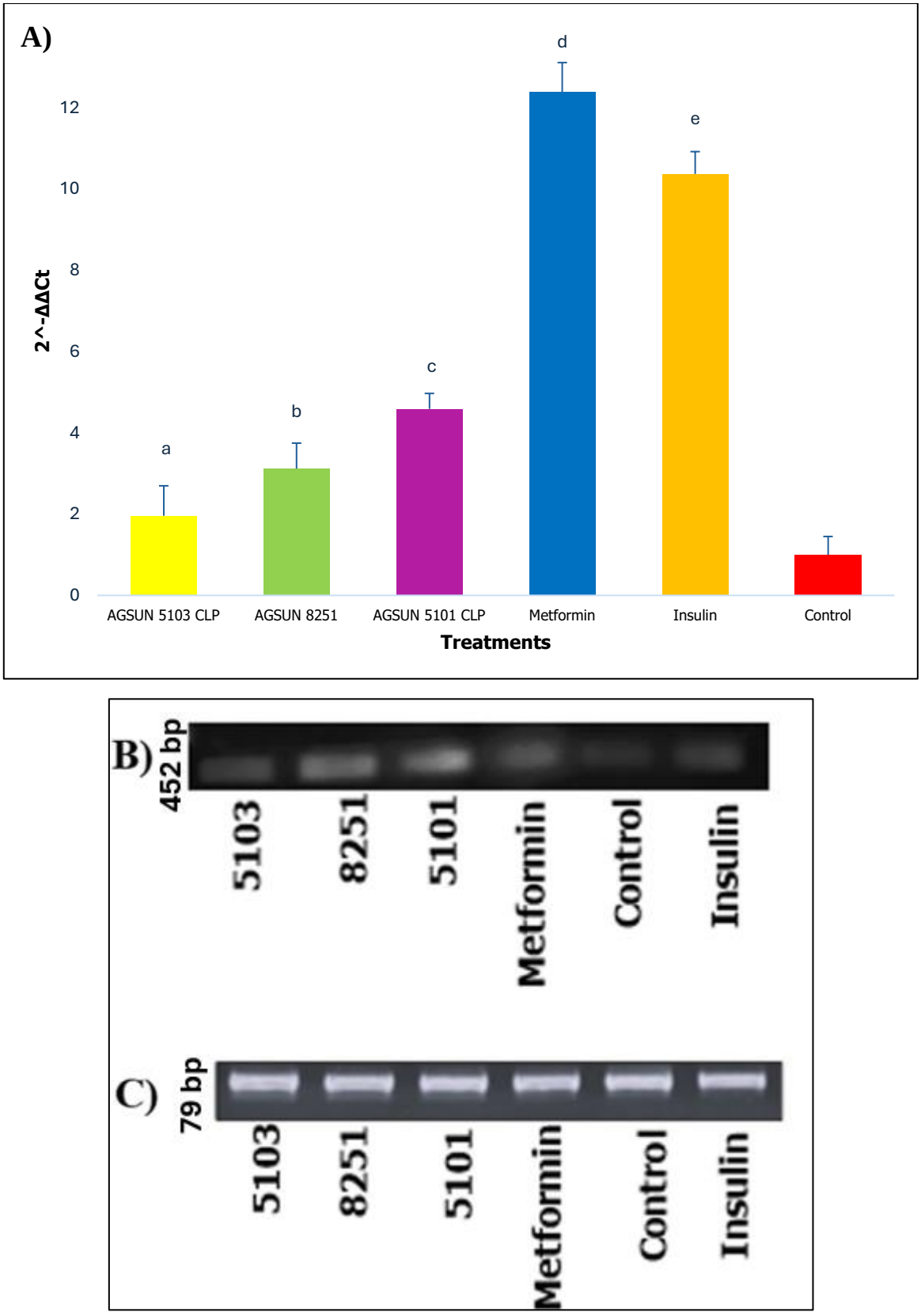

Figure 5 . Effect of lead cultivars of sunflower seeds on expression of *PPARA* in IR-HepG2 cells. A) Bar graph presenting effect of fold change through relative fold-change. Bars

represent mean ± SD. Significant difference was analysed by one-way ANOVA test followed by post hoc Tukey test, statistical significance is represented by differing alphabetically symbols = $p < 0.05$, compared to untreated (control) IR-HepG2 cells. Gel electrophoresis of PCR products of B) *PPARA* (452 bp) and C) *GADPH* (79 bp).

4.0 Discussion

The PPAR signalling pathway, a key regulator of glucose and lipid metabolism, presents a promising therapeutic target for type 2 diabetes mellitus (T2DM) (Palomer *et al*., 2018). PPARs, a family of nuclear receptors, are activated by various ligands, including fatty acids and thiazolidinediones (TZDs) (Montaigne *et al*., 2021). Upon activation, PPARs promote fatty acid storage, enhance insulin sensitivity, and exert anti-inflammatory effects. Although previous TZD drugs targeting *PPARγ* faced limitations, current research is focused on developing more selective PPAR modulators. A previous study revealed that *PPARA* and *MMP1*, show potential for the management of T2DM, but their precise roles remain unclear. Hence, this study investigated their therapeutic potential against T2DM using sunflower seed cultivars.

The antidiabetic behaviour of six cultivars of sunflower seeds, by assessing their glucose-lowering potential and their influence on *MMP1* and PPARA expression in HepG2 cells was investigated. Before confirming the antidiabetic properties of sunflower seeds**,** the cytotoxicity across various concentrations for all six cultivars was assessed. Fortunately, all cultivars exhibited no toxicity at the chosen concentrations, as evidenced by consistently higher cell viability compared to untreated cells. The concentration that resulted in highest cell viability within each cultivar group was selected as the optimal concentration for studying the antidiabetic activity**.** This ensured that the chosen concentration would not inhibit the viability of the HepG2 cell line. Interestingly though, the initial cytotoxicity analysis displayed maximum cell viability at different concentrations across the cultivars. These findings suggest cultivar-specific effects of sunflower seed extracts on HepG2 cell viability.

To specifically assess the antidiabetic potential of sunflower seeds in the context of T2DM**,** insulin resistance (IR) was induced in HepG2 cells to mimic a key symptom of the disease. The success of this model was confirmed by observing a significant difference in glucose consumption compared to non-IR HepG2 cells. Finally, the optimal concentrations of each

sunflower seed cultivar, as determined previously, were not toxic to the IR-HepG2 cells, ensuring cell viability throughout the antidiabetic activity analysis. Treatment with the six sunflower seed cultivars on IR-HepG2 cells confirmed their antidiabetic activity, as evidenced by a reduction in glucose concentration compared to untreated controls. However, a direct comparison with metformin and insulin, which caused the greatest reductions in glucose, revealed three particularly promising cultivars: AGSUN 5101 CLP, 5103 CLP, and 8251. These top three cultivars displayed the most significant glucose reduction among the sunflower seeds, suggesting their superior potential in managing hyperglycaemia. This characteristic could be attributed to their individual cultivar-specific metabolite composition, as all six cultivars had saw the presence of similar metabolites profiles but with varying degrees of abundance. These observations were similar to that of Azimian *et a*l (2023) that saw ceylon cinnamon water extract increased glucose uptake in IR-HepG2 cells (compared to the untreated) to the same degree as metformin. Therefore, to further explore the underlying antidiabetic mechanism, we investigated the effect of these three cultivars on *MMP1* and *PPARA*, the key target genes identified within the PPAR signalling pathway for sunflower seed antidiabetic activity.

All three sunflower seed cultivars upregulated the expression of both *MMP1* and *PPARA*, supporting their potential as activators/agonists of the PPAR signalling pathway and their antidiabetic efficacy. The observed upregulation of both *MMP1* and *PPARA* by all three sunflower seed cultivars validates the findings of Rampadarath *et al* (2023), suggesting activation of the PPAR signalling pathway. While the present study focuses on T2DM, it's noteworthy that Hu *et al.* (2021) demonstrated the activation of the PPAR pathway for managing hyperlipidaemia. Their study showed that Atorvastatin ester upregulated genes within the pathway, including *PPARA*, in agreement with the observations of this analysis. These findings support the notion that PPAR signalling plays a crucial role in metabolic regulation, providing a rationale for investigating its potential in regulating glucose metabolism for T2DM management, as explored in the present study. Hence, despite the limited research directly exploring the upregulation of PPAR signalling genes for T2DM treatment, this broader context highlights the versatility of PPAR signalling in regulating various metabolic processes, including those relevant to both hyperlipidaemia and diabetes. Interestingly with this present study, AGSUN 5101 CLP treatment resulted in the greatest upregulation of both genes, and this cultivar also exhibited the highest glucose consumption in the previous assay. This finding

strengthens the link between AGSUN 5101 CLP's ability to lower glucose levels and its observed upregulation of the target genes, which are known to play a role in regulating glucose and lipid metabolism through the PPAR pathway. The distinct metabolite composition of AGSUN 5101 CLP may be the underlying factor responsible for its enhanced gene upregulation and glucose-lowering activity compared to the other cultivars. While all six cultivars share the same metabolites, subtle variations in their abundance could significantly impact their biological effects, as demonstrated by this analysis.

At the time of this study, no research has reported on the upregulation of *MMP1* and *PPARA* by sunflower seed metabolites to modulate the PPAR signalling pathway. Undisputedly, the PPAR signalling pathway offers a promising target for T2DM management by promoting healthy fat metabolism, enhancing insulin sensitivity, and potentially reducing inflammation. PPAR research is ongoing, with scientists investigating the potential of targeting different PPAR subtypes or combinations for a more comprehensive therapeutic approach.

5.0 Conclusion

This cell-based validation using HepG2 cells supports the findings of prior *in silico* study suggesting the potential antidiabetic properties of sunflower seed extracts. All cultivars, at their optimal concentrations, not only increased cell viability but demonstrated glucose-lowering capabilities, confirming their antidiabetic effect. Notably, AGSUN 5103 CLP, AGSUN 8251, and AGSUN 5101 CLP displayed superior glucose-lowering potential in the glucose consumption assay, making them strong candidates for further investigation. The qPCR analysis confirmed the upregulation of both *MMP1* and *PPARA*, the key genes within the PPAR signalling pathway for T2DM management. AGSUN 5101 CLP displayed the most promising upregulation of *MMP1* and *PPARA* while exhibiting superior glucose-lowering effects. Based on these findings, this study identifies AGSUN 5101 CLP as a potential lead cultivar for further investigation as an activator of the PPAR signalling pathway for T2DM treatment. While this study provides valuable insights, further research is necessary to solidify these findings. Future studies could explore the effects of these cultivars on other genes implicated in the PPAR signalling pathway. This would provide an interesting and holistic insight towards sunflowers seeds antidiabetic mechanism. Additionally, *in vivo* studies using animal models with T2DM would be crucial to assess the efficacy and safety of these sunflower seed extracts in a whole-

organism setting. Elucidating the specific mechanisms by which AGSUN 5101 CLP activates the PPAR pathway would offer valuable information for future therapeutic development.

References

Adeleke, B. S., and Babalola, O. O. (2020). Oilseed crop sunflower (*Helianthus annuus*) as a source of food: Nutritional and health benefits. *Food Science and Nutrition*, 8(9), 4666-4684.

Agamah, F. E., Mazandu, G. K., Hassan, R., Bope, C. D., Thomford, N. E., Ghansah, A., & Chimusa, E. R. (2020). Computational/in silico methods in drug target and lead prediction. *Briefings in Bioinformatics*, 21(5), 1663-1675.

Alaaeldin, R., Abdel-Rahman, I. A., Hassan, H. A., Youssef, N., Allam, A. E., Abdelwahab, S. F., ... and Fathy, M. (2021). Carpachromene ameliorates insulin resistance in HepG2 cells via modulating IR/IRS1/PI3k/Akt/GSK3/FoxO1 pathway. *Molecules*, 26(24), 7629.

Artasensi, A., Pedretti, A., Vistoli, G., and Fumagalli, L. (2020). Type 2 diabetes mellitus: a review of multi-target drugs. *Molecules*, 25(8), 1987.

Azimian, L., Weerasuriya, N. M., Munasinghe, R., Song, S., Lin, C. Y., & You, L. (2023). Investigating the effects of Ceylon cinnamon water extract on HepG2 cells for Type 2 diabetes therapy. *Cell Biochemistry and Function*, 41(2), 254-267.

Bougarne, N., Weyers, B., Desmet, S. J., Deckers, J., Ray, D. W., Staels, B., and De Bosscher, K. (2018). Molecular actions of PPAR α in lipid metabolism and inflammation. *Endocrine reviews*, 39(5), 760-802.

Corrales, P., Vidal-Puig, A., and Medina-Gómez, G. (2018). PPARs and metabolic disorders associated with challenged adipose tissue plasticity. *International Journal of Molecular Sciences*, 19(7), 2124.

De, L. C. (2020). Edible seeds and nuts in human diet for immunity development. *International Journal of Recent Scientific Research*, 6(11), 38877-38881.

Ghazi, T., Nagiah, S., Dhani, S., and Chuturgoon, A. A. (2020). Fusaric acid-induced epigenetic modulation of hepatic H3K9me3 triggers apoptosis *in vitro* and *in vivo*. *Epigenomics*, 12(11), 955-972.

Hao, J., Huang, K., Chen, C., Liang, Y., Wang, Y., Zhang, X., & Huang, H. (2018). Polydatin improves glucose and lipid metabolisms in insulin-resistant HepG2 cells through the AMPK pathway. *Biological and Pharmaceutical Bulletin*, 41(6), 891-898.

He, J. H., Chen, L. X., and Li, H. (2019). Progress in the discovery of naturally occurring anti-diabetic drugs and in the identification of their molecular targets. *Fitoterapia*, 134, 270-289.

Hu, N., Chen, C., Wang, J., Huang, J., Yao, D., and Li, C. (2021). Atorvastatin ester regulates lipid metabolism in hyperlipidemia rats via the PPAR-signaling pathway and HMGCR expression in the liver. *International Journal of Molecular Sciences*, 22(20), 11107.

Hu, K., Sun, Y., Wang, J., Wu, S., Ren, J., Su, D., ... & Yang, H. (2023). Integrating network analysis and experimental validation to reveal the mechanism of pinocembrin in alleviating high glucose and free fatty acid-induced lipid accumulation in HepG2 cells. *Journal of Functional Foods*, 110, 105879.

Kheirollahzadeh, F., Eftekhari, E., Ghollasi, M., & Behzadi, P. (2022). Anti-hyperglycemic effects of *Eryngium billardierei F*. Delaroche extract on insulin-resistance HepG2 cells *in vitro*. *Molecular Biology Reports*, 49(5), 3401-3411.

Mazibuko, M., Ghazi, T., & Chuturgoon, A. (2024). Patulin alters alpha-adrenergic receptor signalling and induces epigenetic modifications in the kidneys of C57BL/6 mice. *Archives of Toxicology*, 1-10.

Montaigne, D., Butruille, L., and Staels, B. (2021). PPAR control of metabolism and cardiovascular functions. *Nature Reviews Cardiology*, 18(12), 809-823.

Liu, X., Zhang, J., Li, Y., Sun, L., Xiao, Y., Gao, W., & Zhang, Z. (2019). Mogroside derivatives exert hypoglycemics effects by decreasing blood glucose level in HepG2 cells and alleviates insulin resistance in T2DM rats. *Journal of Functional Foods*, 63, 103566.

Nnadi, C. O., Onoja, S. O., Ezeh, G. C., Kipi, C. B., Ezeja, M. L., Udem, S. C., ... and Asuzu, I. U. (2020). Antioxidant and antidiabetic potentials of a dimethoxylated flavone obtained from *Helianthus annuus* L. Leaf extract. *Pakistan Journal of Pharmacology*, 37(2), 59-69.

Odeyemi, S., & Dewar, J. (2019). *In vitro* antidiabetic activity affecting glucose uptake in hepg2 cells following their exposure to extracts of *Lauridia tetragona* (Lf) RH Archer. *Processes*, 8(1), 33.

Palomer, X., Barroso, E., Pizarro-Delgado, J., Peña, L., Botteri, G., Zarei, M., ... & Vázquez-Carrera, M. (2018). PPARβ/δ: A key therapeutic target in metabolic disorders. *International Journal Of Molecular Sciences*, 19(3), 913.

Rehman, A., Saeed, A., Kanwal, R., Ahmad, S., and Changazi, S. H. (2021). Therapeutic effect of sunflower seeds and flax seeds on diabetes. *Cureus*, 13(8).

Richmond, K., Williams, S., Mann, J., Brown, R., and Chisholm, A. (2013). Markers of cardiovascular risk in postmenopausal women with type 2 diabetes are improved by the daily consumption of almonds or sunflower kernels: a feeding study. *International Scholarly Research Notices*, 2013.

Saeed, N. A. H., Israa, H. H., and Ghasemian, A. (2022). *Helianthus annuus* seed hydro-alcoholic extract chemical composition and effects on body weight and blood parameters among Iraqi patients suffering from type 2 diabetes mellitus. *Journal of Advanced Biomedical Sciences*, 12(2), 223-228.

Tong, Y., Xu, S., Huang, L., and Chen, C. (2022). Obesity and insulin resistance: Pathophysiology and treatment. *Drug Discovery Today*, 27(3), 822-830.

Varshney, R., Mishra, R., Das, N., Sircar, D., and Roy, P. (2019). A comparative analysis of various flavonoids in the regulation of obesity and diabetes: An *in vitro* and *in vivo* study. *Journal of Functional Foods*, 59, 194-205.

Xie, Z., Gao, G., Wang, H., Li, E., Yuan, Y., Xu, J., ... and Chen, H. (2020). Dehydroabietic acid alleviates high fat diet-induced insulin resistance and hepatic steatosis through dual activation of PPAR-γ and PPAR-α. *Biomedicine and Pharmacotherapy*, 127, 110155.

Yang, Z., Huang, W., Zhang, J., Xie, M., & Wang, X. (2019). Baicalein improves glucose metabolism in insulin resistant HepG2 cells. *European Journal of Pharmacology*, 854, 187-193.

Chapter Six

General discussion, conclusion and recommendations.

1. General discussion

The global burden of type 2 diabetes (T2DM) is alarming: over 460 million people worldwide live with T2DM, accounting for at least 6.28% of the world's population, meaning that for every 100,000 people, 6059 individuals are diabetic (Abdul *et al*., 2020). The International diabetes federation (IDF) reported a staggering 24 million diabetic cases (adults) in Africa attributable majorly (90%) to T2DM. Concerningly, the World Health Organization (WHO) shows that only 36% of Africa countries are equipped with essential medicines for chronic illnesses such as diabetes (NCD, 2023).

T2DM is usually characterized by onset of insulin resistance in tissues and/or, the inability of the pancreatic β--cells to secrete insulin (Galicia-Garcia et al., 2020). With the lack of proper management or medical intervention, T2DM may lead to a cascade of health complications such as neuropathy, nephropathy, retinopathy, cardiopathy, interference with wound-healing associated with high susceptibility to infections (amputation of limbs in extreme circumstances) and dental issues (Dowarah and Singh, 2020). At present, available therapeutic measures include intravenous insulin supplementation, and most popularly oral antidiabetics such as the first line metformin (biguanides), thiazolidines, sulfonylureas, alpha-glucosidase inhibitors and dipeptidyl peptidase IV (DPP-4) inhibitors (Artasensi *et al*., 2020). Despite these management options, long-term use of oral antidiabetic drugs is often accompanied with nausea, diarrhoea, fatigue, gastrointestinal (GI) irritation, hepatotoxicity, mouth ulcers and potential heart failure (Bereda, 2022). Additionally, these drugs are often not readily accessible in resource-limited settings. Hence, bioprospection for antidiabetic therapeutics with minimal side effects, readily accessible and affordable in the management of T2DM is essential.

Plants and their products have long served a key role in medicine due to their phytoconstituents with characteristic health benefits (Egbuna *et al*., 2021). Approximately more than 400 plant species have been reported to possess antidiabetic properties (Ansari *et al*., 2022). Particularly in traditional medicine, plants play a vital role due to their relatively wide accessibility and also the limited access and financial means to allopathic medicine. The common sunflower "*Helianthus annuus* L." seeds due to its high nutritional profile and phytochemicals is one such plant. While the antidiabetic efficacy of sunflower seeds has been increasingly reported (Saeed *et al* 2022; Nnadi *et al.,* 2020 and Cheenam and Leena, 2016), there is limited information on its exact mechanism of action to date. Hence, this project explored the antidiabetic potential of

six cultivars of sunflower seeds commonly consumed in South Africa, establishing their possible mechanisms of action.

The study employed a two-pronged approach to evaluate the antidiabetic potential of the six cultivars (AGSUN 5101 CLP, 5103 CLP, 5106 CLP, 5108 CLP, 5270 and 8251), combining *in silico* screening with concluding cell-based validation. Primarily, metabolomic analysis identified the key metabolites present in these cultivars. The identified metabolites were then screened *in silico* against six enzymes known to be critical in the development and complications of T2DM. The computational analyses including molecular docking and molecular dynamics (MD) simulation, not only established the probable antidiabetic efficacy of sunflower seeds but also pinpointed specific lead metabolites potentially responsible for this effect while elucidating the potential mechanisms of these lead metabolites against the targeted enzymes. Simultaneously, the metabolomics data provided the foundation for a subsequent investigation using network pharmacology, molecular docking, MD simulations, and gene expression analysis. This integrated approach lent scientific credence to the potential metabolic signalling pathways by which sunflower seeds might influence T2DM management.

i. Metabolomics profiling of sunflower seeds

The primary objective of this section was to establish a foundation for subsequent studies by creating a comprehensive metabolomic profile of the six sunflower seed cultivars (AGSUN 5101 CLP, 5103 CLP, 5106 CLP, 5108 CLP, 5270, and 8251). Utilizing liquid chromatography - mass spectrometry (LC-MS) and gas chromatography - mass spectrometry (GC-MS) chromatography, the successful identification of a diverse range of metabolites, including phenolic compounds (LC-MS) and volatile compounds (GC-MS) was achieved as presented in Chapter three**.** GC-MS analysis revealed a total of 50 unique compounds belonging to various chemical classes (organic acids, alkanes, alcohols, terpenes, heterocyclic compounds, and hydrocarbons), while LC-MS analysis identified 44 phenolic compounds in all six cultivars. The classes of compounds observed in the six sunflower cultivars in this study are consistent with prior studies who also identified them in sunflower (do Nascimento *et al* ., 2023; Garcés *et al*., 2023; Bobiş *et al*., 2021; Mota *et al*., 2021 and Gai *et al*., 2020). Notably, the findings that all six cultivars had the same metabolites at similar retention times with negligible differences in the abundance of these compounds means that these cultivars share a similar metabolite profile, with minor variance in concentrations of these metabolites. This observation

is in contradiction with a prior study by Andrade *et al* (2021) that investigated two inbred line of sunflower's (B59 and B71) response to water-deficient stress, revealing both inbred lines to have distinct metabolite profiles. Despite this remarkable similarity amongst the cultivars in this current study, the PLS-DA distinguishing the six cultivars, highlighted subtle yet statistically significant differences in their chemical profiles. Contributing most significantly to the observed chemical profile variations within the six cultivars are 14 key metabolites namely, ginderdiol, strophanthobioase, gein, methyl acetate, chlorogenic acid, 1-(((3-Nitrobenzyl)oxy)methylpyridine-1-ium chloride, casacaroside C, 2-Deoxyryanodol, Dracunculifoside F, formononetin 7-(6"-malonylglucoside), tricin 5-glucoside, tryptohanate, 1-O-caffeoylglucose and Granatumin C as identified by VIP (Variable Importance in Projection). Subsequently, the 94 profiled metabolites from the six cultivars of sunflower were subjected for further *in silico* studies to evaluate their potential antidiabetic action.

ii. *In silico* bioprospection of sunflowers seed metabolites as potential antidiabetic drug candidate against enzymes implicated in T2DM and its pathogenesis

Metabolomic analysis of sunflower seeds revealed their potential antidiabetic properties and mechanisms of action. Six key enzymes involved in T2DM pathogenesis and complications were investigated: alpha-amylase (AAMY), alpha-glucosidase (AGLU), aldose reductase (AR), dipeptidyl peptidase-4 (DPP-4), protein tyrosine phosphatase 1B (PTP1B), and sorbitol dehydrogenase (SDH). *In-silico* analysis identified SON I, GRA C, and SAC A as lead metabolites with inhibitory potential against the carbohydrate-digesting enzymes AAMY and AGLU. These findings suggest that sunflower seed consumption might help manage post-prandial hyperglycaemia, a hallmark of T2DM, by delaying starch breakdown and subsequent glucose absorption. This is consistent with previous research by Ahmed et al. (2022), which identified apigenin-7-O-glucoside as the lead amongst 123 compounds present in betel leaves as a potent inhibitor of both AAMY and AGLU. The metabolomics and MD simulation study also explored the potential of sunflower seed metabolites to inhibit enzymes in the polyol pathway (AR and SDH), a pathway linked to T2DM complications like neuropathy and retinopathy. PLT and SAC A was identified as potential inhibitors of AR and SDH, respectively. By inhibiting these enzymes, it may be possible to prevent the accumulation of sorbitol, a toxic sugar alcohol that contributes to nerve damage and vision problems in T2DM patients. The findings of this analysis are consistent with previous research that explored the

suppression of the polyol pathway enzymes for the treatment of T2DM complications (Imran *et al*., 2022). Additionally, this study demonstrated the potential of sunflower seed metabolites to inhibit DPP-4 and PTP1B. PYR, in particular, exhibited inhibitory activity against DPP-4, which could promote the incretin effect and increase GLP-1 and GIP levels, leading to improved insulin secretion. This aligns with previous research by Paul *et al*. (2021), which identified butirosin as a DPP-4 inhibitor through MD simulations. Furthermore, CGA, a sunflower seed metabolite, may enhance insulin sensitivity by inhibiting PTP1B, a negative regulator of insulin signalling. This finding is consistent with a recent study by Ojo *et al.* (2023), which explored Allium sativum L-derived compounds as potential PTP1B inhibitors for T2DM management.

By elucidating the potential mechanisms through which sunflower seed metabolites interact with key enzymes involved in carbohydrate digestion, the polyol pathway, and insulin signalling, this study provides a strong foundation for further exploring the antidiabetic potential of sunflower seeds. This comprehensive analysis not only highlights the therapeutic potential of sunflower seeds but also identifies specific metabolites, such as SON I, SAC A, PYR, and CGA, as potential inhibitors of AAMY, AGLU, AR, DPP-4, and PTP1B. Future research, including *in vitro* and *in vivo* studies, is essential to validate these *in silico* findings and assess the effectiveness of sunflower seeds in managing type 2 diabetes mellitus.

iii. Network pharmacology and molecular dynamic simulation analysis of sunflower seed metabolites as potential antidiabetics

This study employed a complementary therapeutic strategy using network pharmacology analysis to explore the potential antidiabetic mechanisms of sunflower seeds. Unlike the targeted approach in objective two, network pharmacology identifies potential therapeutic targets based on the overall metabolite profile. Network pharmacology analysis revealed the PPAR signalling pathway as a key metabolic pathway implicated in the antidiabetic effects of sunflower seeds. This implies that the metabolites of sunflower seeds may enhance the augmentation of PPAR pathway promoting glucose metabolism and improved insulin sensitivity. Within this pathway, nine target genes were identified as directly interacting with a significant number (34 out of 84) of the identified sunflower seed metabolites. *MMP1* and

PPARA emerged as the most prominent genes, demonstrating interactions with the majority of these metabolites implicated in the antidiabetic effects of sunflower seeds The results of this analysis align with a previous study by Oh *et al.* (2020), which also implicated activation of the PPAR signalling pathway for antidiabetic effects associated with *Sorghum bicolor* metabolites. Hence, this analysis successfully screened sunflower seed metabolites for their therapeutic potential and mechanism of action against T2DM.

iv. *In vitro* validation of sunflower seed metabolites as antidiabetics through augmentation of *MMP1* and *PPARA*

Lastly, the *in vitro* analysis in insulin-resistant (IR) HepG2 cells validated the findings of the network pharmacology study, confirming the rationale behind the antidiabetic activity of the sunflower seed cultivars. AGSUN 5103 CLP, AGSUN 8251 and AGSUN 5101 CLP showed promising antidiabetic activity through its glucose-lowering action and upregulation of key targets *MMP1* and *PPARA* within the PPAR pathway. Notably, AGSUN 5101 CLP demonstrated superior therapeutic potential by enhancing PPAR signalling, improving insulin resistance, and maintaining glucose homeostasis. These results corroborate the findings of Zhou *et al*. (2021) that observed chrysin (flavone) exhibit potential antidiabetic activity in IR-HepG2 through modulation of the AMPK/PI3K/AKT signalling pathway to improve insulin sensitivity.

v. Sunflower seeds as therapeutics against T2DM

The combined findings from all the objectives of this project strongly support the antidiabetic activity of the six investigated sunflower seed cultivars and identified a multiple mechanism of action that contribute to their antidiabetic properties. The seeds appear to exert their antidiabetic effects through a combination of enzyme inhibition and modulation of insulin sensitivity and improved glucose metabolism via the PPAR signalling pathway. The enzyme inhibition properties of sunflower seeds suggest multiple potential mechanisms of action. Firstly, the anti-hyperglycaemic effects by inhibiting enzymes like AAMY and AGLU is suggestive that post-prandial hyperglycaemia can be manged by the seeds. Secondly, inhibition of polyol pathway enzymes (AR and SDH) may also contribute to managing or preventing

diabetic complications related to hyperglycaemia-induced damage. Thirdly, promoting incretin hormone action: inhibiting DPP-4 allows incretin hormones to function more effectively, promoting insulin secretion and improving glycaemic control. Lastly, inhibition of PTP1B, could prevent the negative regulation of the insulin signalling pathway, promoting insulin sensitivity. These diverse enzyme inhibitory effects, coupled with the insulin-sensitizing capabilities mediated through PPAR pathway activation, suggests a multifaceted approach by sunflower seed extracts in combating T2DM.

Intriguingly, both network pharmacology analysis **(**chapter four) and the targeted enzyme inhibition (chapter three) studies identified "chlorogenic acid" (CGA) and **"**4α,6S,7α)-6α-[6-O-(4-Hydroxybenzoyl)-β-D-glucopyranosyloxy]-7β-methyloctahydrocyclopenta[c]pyran-1-one)" (PYR) referred as 'HGM" in chapter four as potential lead compounds. CGA displayed agonistic and inhibitory activity for *MMP1* (potentially contributing to insulin sensitivity) and PTP1B (potentially regulating glucose metabolism), respectively, while PYR emerged as a promising inhibitor of DPP-4 and strong activator of *PPARA*, potentially enhancing incretin and insulin-sensitizing action. The high abundance of CGA (49.70 - 43.23%) across all cultivars, compared to the lower abundance of PYR (0.36 – 0.21%), suggests that CGA might be a major contributor to the overall antidiabetic effect (Chapter three). However, the *in vitro* studies in Chapter five revealed cultivar-specific variations in antidiabetic activity, indicating that the interplay of multiple metabolites might be responsible for the observed effects.

2. Conclusions and recommendations

In conclusion, this study successfully achieved its objectives, providing compelling evidence for the antidiabetic potential of sunflower seeds. Objective one presented in chapter three, successfully established the metabolite profiles for each cultivar, revealing a high degree of overall similarity, with all the six cultivars sharing the same 94 metabolites. However, PLS-DA and VIP analysis revealed statistically significant, albeit subtle differences in the cultivars' chemical profiles driven by variations in the abundance of specific phenolics. Subsequently, for the first time, the effects of these six cultivars AGSUN 5270, 8251, 5101 CLP, 5103 CLP, 5106 CLP and 5108 CLP on six target enzymes (objective two) and their ability to activate the PPAR signalling pathway, a key player in glucose metabolism was evaluated (objective three).

Specifically, objective two (presented in chapter three) identified the lead metabolites of sunflower seed namely, Sonchuside I against alpha-amylase and aldose reductase, Sacranoside against alpha-glucosidase and sorbitol dehydrogenase, and lastly 4α,6S,7α)-6α-[6-O-(4-Hydroxybenzoyl)-β-D-glucopyranosyloxy]-7β-methyloctahydrocyclopenta[c]pyran-1-one), and chlorogenic acid against dipeptidyl peptidase 4 and protein tyrosine phosphatase 1B, respectively as potential inhibitors. This was on the basis of favourable structural properties of the ligand-protein complexes and affinity of the enzyme for each respective lead metabolites through molecular docking and molecular dynamics simulation studies. In addition to identifying lead metabolites of sunflower seeds, the potential mechanisms of action of the metabolites including anti-hyperglycaemic activity (alpha-amylase and alpha-glucosidase inhibitors), promotion of incretin hormones (DPP-4 inhibitor), insulin sensitizing action (PTP1B inhibitor) and lastly, alleviation of T2DM complications such as diabetic retinopathy (aldose reductase and sorbitol dehydrogenase inhibitors) were deciphered.

Objective three (chapter four) on the other hand, employed a poly-pharmacology approach and identified several signalling pathways with the PPAR signalling pathway being the most significant through which sunflower seeds may potentially exhibit its antidiabetic action on the basis of its profiled metabolites. Particularly through augmentation of key genes *MMP1* and *PPARA* within the signalling pathway, which were stimulated by the lead metabolites 1-O-Caffeoylglucose and 4α,6S,7α)-6α-[6-O-(4-Hydroxybenzoyl)-β-D-glucopyranosyloxy]-7β-methyloctahydrocyclopenta[c]pyran-1-one)), respectively as revealed by the MD simulation. Ultimately this activity may potentially exert antidiabetic action through increasing insulin sensitivity and promoting fatty acid oxidation.

Finally, objective four (chapter five) validated the findings of objective three (chapter three) *in vitro* in insulin resistant HepG2 cells. The observed effects on cell viability, glucose consumption, and upregulation of *PPARA* and *MMP1* within the PPAR pathway suggest a multifaceted approach by sunflower seed cultivars, especially AGSUN 8251, AGSUN 5103 CLP and AGSUN 5101 CLP in regulating blood sugar levels. Taken together, the findings in this study hold significant promise for the development of novel dietary interventions or therapeutic strategies for T2DM management. Particularly noteworthy is AGSUN 5101 CLP, which emerged as a promising candidate based on its superior glucose-lowering effects and PPAR pathway activation.

While this study provides compelling evidence for the antidiabetic potential of sunflower seed extracts, further research is necessary to fully elucidate and explore their therapeutic applications. A key limitation is the reliance on the *in vitro* cell line model (HepG2). While cell lines offer valuable insights into cellular mechanisms, they may not fully capture the complex interactions occurring in the human body. Future *in vivo* studies using animal models with T2DM are crucial to assess the efficacy and safety of these seeds. Additionally, this project strictly focused on the PPAR signalling pathway as a potential target hub for insulin sensitization. Hence, it is recommended that the other pathways recognized in the study should also be further explored for sunflower seeds' antidiabetic activity. Also, *in vitro* validation studies could be conducted to confirm the observed enzyme inhibitory activities (objective three) of the identified compounds against profiled enzymes. These studies could also explore potential differences in inhibitory activity between the various sunflower seed cultivars, providing insights into cultivar-specific effects.

Based on these limitations, future studies may explore *in vitro* investigations focused on isolated lead metabolites and whole extract of the cultivars. The lead metabolite analysis will allow testing of the identified lead compounds in their pure form against the investigated enzymes to offer a direct assessment of their inhibitory potential. This approach will confirm whether these specific metabolites are indeed responsible for the predicted enzyme inhibition. Analysis of extracts of the cultivars can inform the antidiabetic activity of sunflower seed across different cultivars through insights into the potential synergistic effects of various metabolites present in the natural mixture. This analysis can then be compared with the activity of isolated metabolites to determine if a synergistic effect enhances their overall antidiabetic efficacy. Additionally, comparing the activity across different cultivars can reveal variations in their antidiabetic potential due to differences in metabolite composition. By combining these two approaches, a more comprehensive understanding of the antidiabetic activity of sunflower seeds can be established. Isolated metabolite analysis also be able to confirm individual enzyme inhibitory effects, while whole-cultivar analysis will shed light on potential synergistic interactions and cultivar-specific variations. This integrated approach will ultimately provide valuable information for identifying the most promising sunflower seed-derived antidiabetic agents for further therapeutic development. Hence, future research exploring the complete spectrum of mechanisms by which these sunflower seed cultivars and the profiled lead metabolites exert their antidiabetic effects may provide further insights regarding sunflower

seeds antidiabetic action. Additionally, further investigations are warranted to elucidate the specific roles of other potentially involved pathways and validate the observed enzyme inhibitory activities of the identified lead compounds. Noteworthily, by building upon these findings, future research can pave the way for the translation of this knowledge into clinically relevant applications for T2DM management.

References

Abdul Basith Khan, M., Hashim, M. J., King, J. K., Govender, R. D., Mustafa, H., and Al Kaabi, J. (2020). Epidemiology of type 2 diabetes—global burden of disease and forecasted trends. *Journal of Epidemiology and Global Health*, 10(1), 107-111.

Ahmed, S., Ali, M. C., Ruma, R. A., Mahmud, S., Paul, G. K., Saleh, M. A., ... & Islam, M. R. (2022). Molecular docking and dynamics simulation of natural compounds from betel leaves (*Piper betle* L.) for investigating the potential inhibition of alpha-amylase and alpha-glucosidase of type 2 diabetes. *Molecules*, 27(14), 4526.

Ansari, P., Akther, S., Hannan, J. M. A., Seidel, V., Nujat, N. J., and Abdel-Wahab, Y. H. (2022). Pharmacologically active phytomolecules isolated from traditional antidiabetic plants and their therapeutic role for the management of diabetes mellitus. *Molecules*, *27*(13), 4278.

Artasensi, A., Pedretti, A., Vistoli, G., and Fumagalli, L. (2020). Type 2 diabetes mellitus: a review of multi-target drugs. *Molecules*, *25*(8), 1987.

Bereda, G. (2022). Oral Antidiabetic Medications: Technical Notes. *Journal of Diabetic Nephropathy and Diabetes Management*, *2*(1), 1-10.

Bobiş, O., Bonta, V., Cornea-Cipcigan, M., Nayik, G. A., and Dezmirean, D. S. (2021). Bioactive molecules for discriminating *Robinia* and *Helianthus* honey: High-performance liquid chromatography–electron spray ionization–mass spectrometry polyphenolic profile and physicochemical determinations. *Molecules*, *26*(15), 4433.

Cheenam, B., and Leena, P. (2016). Effects of sunflower seeds on fasting blood glucose in diabetes mellitus type 2 patients. *Journal of Chemical and Pharmaceutical Research*, *8*(4), 1211-1217.

Dirir, A. M., Daou, M., Yousef, A. F., and Yousef, L. F. (2022). A review of alpha-glucosidase inhibitors from plants as potential candidates for the treatment of type-2 diabetes. *Phytochemistry Reviews*, 21(4), 1049-1079.

do Nascimento, T. P., Ladeira, K. C., Bezerra, F. D. S., Santos, M. C. B., de Souza, T. S. P., Cameron, L. C., ... and Koblitz, M. G. B. (2023). Metabolomic analysis and ecofriendly enrichment of sunflower meal extract. *Journal of the Science of Food and Agriculture*, *103*(3), 1161-1171.

Dowarah, J., and Singh, V. P. (2020). Anti-diabetic drugs recent approaches and advancements. *Bioorganic and Medicinal Chemistry*, *28*(5), 115263.

Egbuna, C., Awuchi, C. G., Kushwaha, G., Rudrapal, M., Patrick-Iwuanyanwu, K. C., Singh, O., ... and Chikwendu, C. J. (2021). Bioactive compounds effective against type 2 diabetes mellitus: a systematic review. *Current Topics in Medicinal Chemistry*, *21*(12), 1067-1095.

Gai, F., Karamać, M., Janiak, M. A., Amarowicz, R., and Peiretti, P. G. (2020). Sunflower (*Helianthus annuus* L.) plants at various growth stages subjected to extraction - Comparison of the antioxidant activity and phenolic profile. *Antioxidants*, *9*(6), 535.

Galicia-Garcia, U., Benito-Vicente, A., Jebari, S., Larrea-Sebal, A., Siddiqi, H., Uribe, K. B., ... and Martín, C. (2020). Pathophysiology of type 2 diabetes mellitus. *International Journal of Molecular Sciences*, *21*(17), 6275.

Garcés, R., de Andrés-Gil, C., Venegas-Calerón, M., Martínez-Force, E., Moreno-Pérez, A. J., and Salas, J. J. (2023). Characterization of sunflower seed and oil wax ester composition by GC/MS, a final evaluation. *LWT*, *173*, 114365.

Imran, A., Shehzad, M. T., Shah, S. J. A., Laws, M., Al-Adhami, T., Rahman, K. M., ... & Iqbal, J. (2022). Development, molecular docking, and in silico ADME evaluation of selective ALR2 inhibitors for the treatment of diabetic complications via suppression of the polyol pathway. *ACS omega*, 7(30), 26425-26436.

Kaur, N., Kumar, V., Nayak, S. K., Wadhwa, P., Kaur, P., and Sahu, S. K. (2021). Alpha-amylase as molecular target for treatment of diabetes mellitus: A comprehensive review. *Chemical Biology and Drug Design*, *98*(4), 539-560.

Montaigne, D., Butruille, L., and Staels, B. (2021). PPAR control of metabolism and cardiovascular functions. *Nature Reviews Cardiology*, *18*(12), 809-823.

Mota, M. F. S., Waktola, H. D., Nolvachai, Y., and Marriott, P. J. (2021). Gas chromatography–mass spectrometry for characterisation, assessment of quality and authentication of seed and vegetable oils. *TrAC Trends in Analytical Chemistry*, *138*, 116238.

Nnadi, C. O., Onoja, S. O., Ezeh, G. C., Kipi, C. B., Ezeja, M. L., Udem, S. C., ... and Asuzu, I. U. (2020). Antioxidant and antidiabetic potentials of a dimethoxylated flavone obtained from *Helianthus annuus* L. Leaf extract. *Pakistan Journal of Pharmacology*, *37*(2), 59-69.

Non-Communicable Diseases (NCD). (2023). Diabetes, a silent killer in Africa. *World Health Organization.*

Oh, K. K., Adnan, M., & Cho, D. H. (2020). Network pharmacology of bioactives from *Sorghum bicolor* with targets related to diabetes mellitus. *PLoS One*, 15(12), e0240873.

Ojo, O. A., Adegboyega, A. E., Taiwo, O. A., Olowosoke, C. B., Johnson, G. I., Umedum, N. L., ... & Johnson, T. O. (2023). Lead optimization of *Allium sativum* L. compounds for PTP1B inhibition in diabetes treatment: *in silico* molecular docking and dynamics simulation. *Journal of Biomolecular Structure and Dynamics*, 1-15.

Paul, R. K., Nath, V., & Kumar, V. (2021). Structure based virtual screening of natural compounds and molecular dynamics simulation: Butirosin as Dipeptidyl peptidase (DPP-IV) inhibitor. *Biocatalysis and Agricultural Biotechnology*, 35, 102042.

Rocha, S., Corvo, M. L., Fernandes, E., and Freitas, M. (2021). The emerging target protein tyrosine phosphatase 1B (PTP1B) for type 2 diabetes mellitus management. *Journal of Diabetes and Clinical Research*, *3*(4), 99-105.

Saeed, N. A. H., Israa, H. H., and Ghasemian, A. (2022). *Helianthus annuus* seed hydro-alcoholic extract chemical composition and effects on body weight and blood parameters among Iraqi patients suffering from type 2 diabetes mellitus. *Journal of Advanced Biomedical Sciences*, *12*(2), 223-228.

Yang, B. B., Hong, Z. W., Zhang, Z., Yu, W., Song, T., Zhu, L. L., ... and Dai, Y. T. (2019). Epalrestat, an aldose reductase inhibitor, restores erectile function in streptozocin-induced diabetic rats. *International Journal of Impotence Research*, *31*(2), 97-104.

Yin, R., Xu, Y., Wang, X., Yang, L., and Zhao, D. (2022). Role of dipeptidyl peptidase 4 inhibitors in antidiabetic treatment. *Molecules*, *27*(10), 3055.

Zhou, Y. J., Xu, N., Zhang, X. C., Zhu, Y. Y., Liu, S. W., & Chang, Y. N. (2021). Chrysin improves glucose and lipid metabolism disorders by regulating the AMPK/PI3K/AKT signaling pathway in insulin-resistant HepG2 cells and HFD/STZ-induced C57BL/6J mice. *Journal of Agricultural and Food Chemistry*, 69(20), 5618-5627.